

THE PRECURSOR FOR NERVE GROWTH FACTOR AND INNERVATION IN THYROID CANCER



THE UNIVERSITY OF
NEWCASTLE
AUSTRALIA

Christopher William Rowe

BSc (Med) MBBS (Hons1) FRACP

A thesis submitted in fulfillment of the requirements for the degree of
Doctor of Philosophy in Medicine.

School of Medicine and Public Health, University of Newcastle, Australia

November 2019

This research was supported by an
Australian Government Research Training Program Scholarship

The discovery of the growth response elicited by a soluble tumoural agent revealed the receptivity of developing nerve cells to hitherto unknown humoral factors, and in this way opened a new area of investigation.

Professor Dr. Rita Levi-Montalcini, Nobel Lecture, 1986.

DECLARATION

STATEMENT OF ORIGINALITY

I hereby certify that the work embodied in the thesis is my own work, conducted under normal supervision. The thesis contains no material which has been accepted, or is being examined, for the award of any other degree or diploma in any university or other tertiary institution and, to the best of my knowledge and belief, contains no material previously published or written by another person, except where due reference has been made. I give consent to the final version of my thesis being made available worldwide when deposited in the University's Digital Repository, subject to the provisions of the Copyright Act 1968 and any approved embargo.

THESIS BY PUBLICATION

I hereby certify that this thesis is in the form of a series of papers. I have included as part of this thesis a written declaration from each co-author, endorsed in writing by the Faculty Assistant Dean (Research Training), attesting to my contribution to any jointly authored papers.

Christopher Rowe

University of Newcastle, Australia

November 2019

ABSTRACT

The precursor for nerve growth factor (proNGF) has recently been shown to be expressed in thyroid cancer, suggesting that neurotrophins and nerves may contribute to thyroid malignancy. Nerves and neurotrophins are emerging as important mediators of cancer initiation and progression, and may represent new biomarkers or therapeutic targets.

It was first hypothesized that proNGF may be a diagnostic biomarker for thyroid cancer, either in serum or solubilised thyroid-biopsy material, in patients with benign and malignant nodular thyroid disease. ProNGF was detected in a minority of specimens, but there was no correlation with thyroid malignancy. However, serum proNGF correlated with hyperthyroidism, a relationship that is supported by animal data.

It was then considered whether proNGF could have a functional role in thyroid cancer, examining first the evidence for innervation of thyroid cancer. Nerve density in papillary thyroid cancers was found to be twofold higher than in benign thyroid (12 nerves/cm² [IQR 7-21] vs 6 nerves/cm² [IQR: 3-10], $p=0.001$). Most nerves were of the adrenergic subtype. Nerve density in papillary thyroid cancers was positively associated with extrathyroidal invasion ($p<0.001$). Nerves in the thyroid cancer microenvironment expressed the neurotrophin receptor TrkA, as did a subset of primary thyroid cancers. Whilst proNGF expression in thyroid cancer was again demonstrated, it was not shown to be associated with neo-innervation ($p=0.07$), although this relationship warrants further exploration in light of the near-significant result. ProNGF was shown to be expressed in thyroid cancer nodal metastases, which correlated with expression in paired primary tumours, although it did not correlate with markers of aggressiveness or high risk features.

The key finding of increased nerve density in the papillary subtype of thyroid cancer suggests that nerves may have biological relevance in thyroid cancer and invites further study. The presence of neurotrophin receptors in thyroid cancer raises the possibility that nerve-cancer crosstalk may be mediated by neurotrophins, however this relationship remains incompletely understood. This work establishes that proNGF is not a diagnostic biomarker for thyroid cancer in serum or biopsy material.

ACKNOWLEDGEMENTS

As I reflect on the enormous privilege that it has been to study and learn, I feel a deep sense of gratitude for this opportunity, and the burden of responsibility that comes with great opportunity.

To my supervisors, who have become friends and colleagues through this journey – thank you for your patient willingness to listen, to correct, and to guide.

To the organisations that have supported this research – Hunter New England Local Health District (through its Clinical Research Fellowship program and the Health Research and Translation Centre); the Hunter Cancer Research Alliance; Avant Mutual Group; NSW Health Pathology Teaching and Research; the Commonwealth Government of Australia’s Research Training Program; and the Faculty of Health at the University of Newcastle – thank you for your investment in the next generation of clinician-scientists.

To my colleagues in the Department of Diabetes and Endocrinology, and the Thyroid Cancer Multidisciplinary Team, both at John Hunter Hospital; and at Newcastle Endocrinology – thank you for your welcome, for your support of this work, and your friendship.

To my colleagues at the Cancer Neurobiology group at the University of Newcastle, and at the Mothers and Babies Research Centre at the Hunter Medical Research Institute – I have a deep respect for your dedication and skill. Thank you for sharing your enthusiasm and your knowledge so willingly.

To my parents, James and Sally – you modelled inquisitive thinking, persistence, the power of words, and the value of study; both at the family table, and in your lives – thank you for your love and support.

To my family, Rebecca, Evelyn, Bethany and Joshua – you remind me of what is truly important, and teach me the most valuable lessons of all – thank you.

PUBLICATIONS INCLUDED IN THESIS

Rowe CW, Boelaert K, Smith R. (2019) **Thyroid cancer during pregnancy and lactation.** In: Kovacs and Deal [Ed] Maternal-fetal and neonatal endocrinology. Elsevier. <https://doi.org/10.1016/B978-0-12-814823-5.00020-9> [Published].

Rowe CW, Faulkner S, Paul JW, Tolosa JM, Gedye C, Bendinelli C, Wynne K, McGrath S, Attia J, Smith R, Hondermarck H. (2019) **The precursor for nerve growth factor (proNGF) is not a serum or biopsy-rinse biomarker for thyroid cancer diagnosis.** BMC Endocrine Disorders. <https://doi.org/10.1186/s12902-019-0457-1> [Published]

Rowe CW, Dill T, Griffin N, Jobling P, Faulkner S, King S, Smith R, Hondermarck H. (2019) **Innervation of papillary thyroid cancer and its association with extra-thyroidal invasion.** Scientific Reports <https://doi.org/10.1038/s41598-020-58425-5> [Published].

Faulkner S, Jobling P, Rowe CW, Rodriguez-Oliveira S, Roselli S, Thorne R, Oldmeadow C, Attia Jiang J, Zhang X, Walker M, Hondermarck H. (2017) **Neurotrophin Receptors TrkA, p75NTR and Sortilin are Increased and Targetable in Thyroid Cancer.** American Journal of Pathology <https://doi.org/10.1016/j.ajpath.2017.09.008> [Published].

Rowe CW, Dill T, Faulkner S, Gedye C, Paul JW, Tolosa JM, Jones M, King S, Smith R, Hondermarck H. **The precursor for nerve growth factor (proNGF) in thyroid cancer lymph node metastases: correlation with primary tumour and pathological variables.** International Journal of Molecular Sciences <https://doi.org/10.3390/ijms20235924> [Published].

Rowe CW, Paul J, Gedye C, Tolosa J, Bendinelli C, McGrath S & Smith, R. (2017) **Targeting the TSH receptor in thyroid cancer.** Endocrine-Related Cancer. <https://doi.org/10.1530/ERC-17-0010> [Published].

A candidate contribution statement for each publication is included in the following pages.

By signing below I confirm that Christopher Rowe contributed to the paper/publication entitled:

Rowe CW, Boelaert K, Smith R. **Thyroid cancer during pregnancy and lactation**. In: Kovacs and Deal [Ed] Maternal-fetal and neonatal endocrinology. Elsevier 2019.
<https://doi.org/10.1016/B978-0-12-814823-5.00020-9>

Christopher Rowe's contribution to this paper was:

1. Lead in conception of the manuscript and drafting of methodology
2. Lead in literature search, review and critical appraisal of the literature
3. Lead in drafting manuscript, tables and figures
4. Lead in responding to reviewers

Author

Signature

Date

Christopher Rowe

12/08/2019

Kristien Boelaert

13/08/2019

Roger Smith

12/08/2019

24/10/19

Faculty Assistant Dean Research Training

By signing below I confirm that Christopher Rowe contributed to the paper/publication entitled:

Rowe CW, Faulkner S, Paul JW, Tolosa JM, Gedye C, Bendinelli C, Wynne K, McGrath S, Attia J, Smith R, Hondermarck H. The precursor for nerve growth factor (proNGF) is not a serum or biopsy-rinse biomarker for thyroid cancer diagnosis. BMC Endocrine Disorders (under review at time of document signing)

Christopher Rowe's contribution to this paper was:

1. Lead in conception and experimental design
2. Lead in performing experiments and analysing data
3. Lead in drafting manuscript, tables and figures
4. Lead in responding to reviewers.

<u>Author</u>	<u>Signature</u>
Christopher Rowe	30/08/2019
Sam Faulkner	30/08/2019
Jonathan Paul	30/08/2019
Jorge Tolosa	30/08/2019
Craig Gedye	30/08/2019
Cino Bendinelli	30/08/2019
Katie Wynne	30/08/2019
Shaun McGrath	30/08/2019
John Attia	30/08/2019
Roger Smith	30/08/2019
Hubert Hondermarck	30/08/2019

24/10/19

Faculty Assistant Dean Research Training

Christopher Rowe - November 2019

viii

By signing below I confirm that Christopher Rowe contributed to the paper/publication entitled:

Rowe CW, Dill T, Griffin N, Jobling P, Paul J, Faulkner S, King S, Smith R, Hondermarck H. Autonomic nerve density is increased in papillary thyroid cancers (PTC), and is associated with extra-thyroidal extension. Scientific Reports (under review at time of document signing).

Christopher Rowe's contribution to this paper was:

1. Lead in conception and experimental design
2. Lead in performing experiments and analysing data
3. Lead in drafting manuscript, tables and figures
4. Lead in responding to reviewers.

<u>Author</u>	<u>Signature</u>	<u>Date</u>
Christopher Rowe		16/08/2019
Tony Dill		16/08/2019
Nathan Griffin		16/08/2019
Phil Jobling		16/08/2019
Sam Faulkner		16/08/2019
Jonathan Paul		16/08/2019
Simon King		16/08/2019
Roger Smith		16/08/2019
Hubert Hondermarck		16/08/2019

<hr/>	<u>24/10/19</u>
<i>Faculty Assistant Dean Research Training</i>	

By signing below I confirm that Christopher Rowe contributed to the paper/publication entitled:

Faulkner S, Jobling P, Rowe CW, Rodriguez-Oliveira S, Roselli S, Thorne R, Oldmeadow C, Attia Jiang J, Zhang X, Walker M, Hondermarck H. (2017) Neurotrophin Receptors TrkA, p75NTR and Sortilin are Increased and Targetable in Thyroid Cancer. American Journal of Pathology <https://doi.org/10.1016/j.ajpath.2017.09.008>

Christopher Rowe's contribution to this paper was:

1. Contribution to review of experimental methodology and results
2. Lead in developing pathway for, and obtaining of, human tissue collection
3. Contribution to experimental work (Western blots of thyroid tissue)
4. Contribution to interpretation of results
5. Contribution to writing of manuscript

<u>Author</u>	<u>Signature</u>	<u>Date</u>
Sam Faulkner		09/10/18
Phillip Jobling		10.10.18
Christopher Rowe		2/10/18
Sonia Rodrigues Oliveira		08/02/19
Severine Roselli		31/01/19
Rick Thorne		31/01/19
Christopher Oldmeadow		15/10/19
John Attia		15/10/18
Xu-Dong Zhang		
Marjorie Walker		2/11/18
Hubert Hondermarck		02/10/2018
Faculty Assistant Dean Research Training		24/10/19

By signing below I confirm that Christopher Rowe contributed to the paper/publication entitled:

Rowe CW, Dill T, Faulkner S, Gedye C, Paul JW, Tolosa JM, Jones M, King S, Smith R, Hondermarck H. **The precursor for nerve growth factor (proNGF) is expressed in thyroid cancer metastases.** Int J Mol Sci (under review at time of document signing)

Christopher Rowe's contribution to this paper was:

1. Lead in conception and experimental design
2. Lead in performing experiments and analysing data
3. Lead in drafting manuscript, tables and figures
4. Lead in responding to reviewers.

<u>Author</u>	<u>Signature</u>	<u>Date</u>
Christopher Rowe		30/08/2019
Tony Dill		30/08/2019
Sam Faulkner		30/08/2019
Craig Gedye		30/08/2019
Jonathan Paul		30/08/2019
Jorge Tolosa		30/08/2019
Mark Jones		30/08/2019
Simon King		30/08/2019
Roger Smith		30/08/2019
Hubert Hondermarck		30/08/2019



Faculty Assistant Dean Research Training

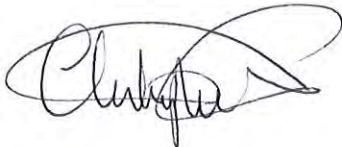




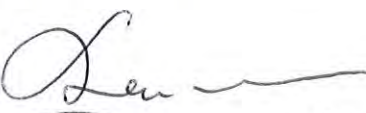

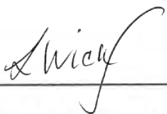
24/10/19

By signing below I confirm that Christopher Rowe contributed to the paper/publication entitled:

Rowe CW, Paul J, Geyde C, Tolosa J, Bendinelli C, McGrath S & Smith, R. (2017)
Targeting the TSH receptor in thyroid cancer. Endocrine-Related Cancer.
<https://doi.org/10.1530/ERC-17-0010>

Christopher Rowe's contribution to this paper was:

1. Lead in conception of the manuscript and drafting of methodology
2. Lead in literature search, review and critical appraisal of the literature
3. Lead in drafting manuscript, tables and figures
4. Lead in responding to reviewers

<u>Author</u>	<u>Signature</u>	<u>Date</u>
Christopher Rowe		5/4/19
Jonathan Paul		5/4/19
Craig Gedyde		13/09/2019
Jorge Tolosa		5/4/19
Cino Bendinelli		5/9/19
Shaun McGrath		2/9/2019
Roger Smith		2/9/2019
		24/10/19

Faculty Assistant Dean Research Training

NON-THESIS PUBLICATIONS COMPLETED DURING CANDIDATURE

Publications in peer-reviewed journals

Rowe CW, Murray K, Woods A, Gupta S, Smith R, Wynne K. (2016) **Metastatic Thyroid Cancer in Pregnancy: Risk and Uncertainty**. Endocrinology Diabetes & Metabolism Case Reports. <https://doi.org/10.1530/EDM-16-0071>

Rowe CW, Bendinelli C, McGrath S. (2016) **Charting a Course through the CEAs: Diagnosis and Management of Medullary Thyroid Cancer**. Clinical Endocrinology (Oxf). <http://dx.doi.org/10.1016/j.diabres.2017.06.022>

Rowe CW, Haider AS, Viswanathan D, Jones M, Attia J, Wynne K, Acharya S. (2017) **Insulin resistance correlates with maculopathy and severity of retinopathy in young adults with Type 1 Diabetes Mellitus**. Diabetes Research and Clinical Practice. <https://doi.org/10.1111/cen.13114>

Rowe CW, Arthurs S, O'Neill CJ, Hawthorne J, Carroll R, Wynne K, Bendinelli C. (2018) **High-dose cholecalciferol to prevent post-thyroidectomy hypocalcaemia: a randomized double-blind placebo-controlled trial**. Clinical Endocrinology. <https://doi.org/10.1111/cen.13897>

Gao F, Griffin N, Faulkner S, Rowe CW, Williams L, Roselli S, Thorne R, Ferdoushi A, Jobling P, Walker M and Hondermarck H. (2018) **The neurotrophic tyrosine kinase receptor TrkA and its ligand NGF are increased in squamous cell carcinomas of the lung**. Scientific Reports. <https://doi.org/10.1038/s41598-018-26408-2>

Rowe CW, Putt E, Brentnall O, Allabyrne J, Gebuehr A, Woods A, Wynne K. (2018) **An intravenous insulin protocol designed for pregnancy reduces neonatal hypoglycaemia following betamethasone administration in women with gestational diabetes**. Diabetic Medicine. <https://doi.org/10.1111/dme.13864>

Marlow A, Rowe CW, Anderson D, Wynne K, King B, Howley P, Smart C. (2019) **Young children, adolescent girls and women with type 1 diabetes are more overweight and obese than reference populations, and this is associated with increased cardiovascular risk factors**. Diabetic Medicine. <https://doi.org/10.1111/dme.14133>

Conference presentations - oral

Rowe CW Tolosa, JM, Faulkner S, Paul J, Gedye C, McGrath S, Smith R, Hondermarck H. (2017) **The precursor for nerve growth factor (proNGF) is detectable in the rinse of fine needle aspiration biopsy of thyroid cancer.** World Congress of Thyroid Cancer, Boston, United States of America.

Rowe CW, Dill T, Faulkner S, Griffin N, Jobling P, King S, Gedye C, Tolosa JT, Paul J, Smith R, Hondermarck H. (2018) **Increased autonomic nerve density around papillary thyroid cancers and cancers that metastasize.** Endocrine Society of Australia Annual Scientific Meeting, Melbourne, Australia.

Hawthorne J, Rowe CW, Arthurs S, O'Neill CJ, Carroll R, Wynne K, Bendinelli C. (2018) **High-dose pre-thyroidectomy cholecalciferol reduces post-operative hypocalcaemia when stratified by PTH status: a randomized, placebo-controlled trial.** Endocrine Society of Australia Annual Scientific Meeting, Adelaide, Australia.

Rowe CW, Putt E, Brentnall O, Gebuehr A, Allabyrne J, Woods A, Wynne K (2018) **An intravenous insulin protocol designed for pregnancy reduces neonatal hypoglycaemia after betamethasone administration in women with gestational diabetes.** Society for Endocrinology BES. Glasgow, United Kingdom.

Rowe CW, Dill T, Clarke M, Paul J, Gedye C, King S, Hondermarck H. (2018) **A methodology for validating automated digital whole-slide analysis of immunohistochemical biomarkers using open source software (QuPath).** Australian Society for Medical Research Satellite Symposium. Newcastle, Australia.

Faulkner S, Rowe CW, Gao F, Griffin N, Walker M, Denham J, Jobling P, Hondermarck H. (2018) **Nerve dependence in cancer.** Hunter Cancer Symposium, Newcastle, Australia.

Blefari N, Rowe CW, Carroll R, Weigner J, Bendinelli C, O'Neill CJ. (2019) **Long term quality of life outcomes in thyroid cancer survivors.** Royal Australasian College of Surgeons Annual Scientific Congress. Bangkok, Thailand.

Rowe CW (2019) **A validated insulin infusion protocol to reduce neonatal hypoglycaemia following betamethasone.** Australasian Diabetes in Pregnancy Society Annual Scientific Meeting. Sydney, Australia.

Rowe CW, Boelaert K, Colley S, Ballard M, Pracey P, Giblet N, Sharma N. (2019)
Integrated thyroid nodule risk stratification using BTA U (ultrasound) and Thy (cytology): outcomes at a large tertiary centre. Asia-Oceania-Thyroid Association
Annual Scientific Meeting, Sydney, Australia.

Conference presentations - poster

Rowe CW, King S, Tolosa JM, Paul J, Gedye C, Smith R. (2017) **Overexpression of the Sodium-Iodide Symporter in thyroid cancer co-existing with Graves' disease.** Endocrine Society of Australia Annual Scientific Meeting, Perth, Australia.

Croker E, Tan HLE, Rowe CW. (2017) **Diabetic ketoacidosis (DKA) in patients on maintenance dialysis: case series and literature review.** Australian Diabetes Society Annual Scientific Meeting, Perth, Australia.

Croker E, Chew CYM, Weigner J, Tan HLE, Bendinelli C, McGrath S, Rowe CW. (2018) **The whole is greater than the sum of its parts: synthesised triple-assessment of thyroid nodules optimises pre-operative risk-stratification.** Endocrine Society of Australia Annual Scientific Meeting, Adelaide, Australia.

Kuehn J, Rowe CW, Amico F, Ward A, Bendinelli C. (2018) **Management of an intrathyroidal cystic parathyroid gland with post-traumatic haemorrhagic transformation causing acute airway compromise.** Endocrine Society of Australia Annual Scientific Meeting. Adelaide, Australia.

Rowe CW, Delbridge M, Brown K, Watkins B, Addley J, Wynne K. (2019) **An insulin infusion designed for pregnancy provides comparable glycaemic control following betamethasone in women with gestational and pre-existing diabetes, although hypoglycaemia is more common in pre-existing diabetes.** Australasian Diabetes in Pregnancy Society Annual Scientific Meeting. Sydney, Australia.

Rowe CW, Woods A, Wynne K. (2019) **Transient extreme insulin resistance in pregnancy following betamethasone administration managed with high-dose intravenous insulin: case series and literature review.** Australasian Diabetes in Pregnancy Society Annual Scientific Meeting. Sydney, Australia.

Blefari ND, Rowe CW, Weigner J, Carroll R, Bendinelli C, O'Neill C. (2019) **Quality Of Life After Thyroid Surgery Is Similar In Patients With Thyroid Cancer And Benign Disease.** American Thyroid Association Annual Scientific Meeting. Chicago, United States of America.

SUPERVISORS

Laureate Professor Roger Smith

Professor of Endocrinology

School of Medicine and Public Health, University of Newcastle, Australia.

Professor Hubert Hondermarck

Professor of Medical Biochemistry

School of Biomedical Sciences and Pharmacy, University of Newcastle, Australia.

Dr Jonathan Paul

Lecturer

School of Medicine and Public Health, University of Newcastle, Australia.

Conjoint Associate Professor Craig Gedye

Conjoint Associate Professor of Medical Oncology

School of Biomedical Sciences and Pharmacy, University of Newcastle, Australia.

Dr Jorge Tolosa

Research Officer

School of Medicine and Public Health, University of Newcastle, Australia.

CONTENTS

1 OVERVIEW	1
1.1 INTRODUCTION	2
1.2 AIMS OF THIS STUDY.....	2
1.3 ORGANISATION OF THESIS	2
2 LITERATURE REVIEW	4
2.1 THYROID PHYSIOLOGY AND PATHOLOGY	5
2.1.1 <i>Normal thyroid development and function</i>	5
2.1.2 <i>Diseases of the thyroid gland</i>	7
2.1.3 <i>Thyroid cancer: clinical presentation and significance</i>	9
2.2 REVIEW: THYROID CANCER DURING PREGNANCY AND LACTATION	9
2.2.1 <i>Preface</i>	9
2.3 INNERVATION OF THE THYROID	23
2.3.1 <i>Introduction</i>	23
2.3.2 <i>Anatomy of thyroid innervation</i>	23
2.3.3 <i>Adrenergic (sympathetic) innervation and function</i>	24
2.3.4 <i>Cholinergic (parasympathetic) innervation and function</i>	25
2.3.5 <i>Evidence for innervation of thyroid cancer</i>	26
2.3.6 <i>Relevance for proposed research</i>	27
2.4 THE PRECURSOR FOR NERVE GROWTH FACTOR IN PHYSIOLOGY AND CANCER	27
2.4.1 <i>Physiology of the precursor for nerve growth factor</i>	27
2.4.2 <i>Role of the precursor for nerve growth factor in malignancy</i>	30
2.4.3 <i>Role of the precursor for nerve growth factor in thyroid cancer</i>	32
2.4.4 <i>Relevance for proposed research</i>	35
2.5 BIOMARKERS FOR DIAGNOSIS OF THYROID CANCER	35
2.5.1 <i>Clinical need</i>	35
2.5.2 <i>Blood-based diagnostic biomarkers</i>	37
2.5.3 <i>Biopsy-based diagnostic biomarkers</i>	38
2.5.4 <i>Relevance for proposed research</i>	39
3 THE PRECURSOR FOR NERVE GROWTH FACTOR (PRONGF) IS NOT A SERUM OR BIOPSY-RINSE BIOMARKER FOR THYROID CANCER DIAGNOSIS.....	40
3.1 PREFACE	41

4 INNERVATION OF PAPILLARY THYROID CANCER AND ITS ASSOCIATION WITH EXTRA-THYROIDAL INVASION.	55
4.1 PREFACE	56
5 NEUROTROPHIN RECEPTORS TRKA, P75-NTR AND SORTILIN ARE INCREASED AND TARGETABLE IN THYROID CANCER	71
5.1 PREFACE	72
6 THE PRECURSOR FOR NERVE GROWTH FACTOR IN THYROID CANCER LYMPH NODE METASTASES: CORRELATION WITH PRIMARY TUMOUR AND PATHOLOGICAL VARIABLES.....	89
6.1 PREFACE	90
7 TARGETING THE TSH RECEPTOR IN THYROID CANCER.....	104
7.1 PREFACE	105
8 GENERAL DISCUSSION.....	118
8.1 INTRODUCTION	119
8.2 THYROID AUTONOMIC DENERVATION	120
8.3 NERVES AS BIOMARKERS OF CANCER AGGRESSIVENESS	122
8.4 NEUROTROPHIN RECEPTORS AS THERAPEUTIC TARGETS.....	123
8.5 CONCLUSION	125
9 REFERENCES.....	126
10 APPENDICES.....	134
10.1 ADDITIONAL PUBLICATIONS COMPLETED DURING CANDIDATURE	135
10.2 PERMISSIONS TO INCLUDE PUBLISHED PAPERS IN THESIS.....	189
10.3 PERMISSIONS TO REPRODUCE FIGURES IN THESIS	196

LIST OF ABBREVIATIONS AND ACRONYMS

A

AJCC American Joint Cancer Committee

ANOVA Analysis of Variance

ATA American Thyroid Association

ATC Anaplastic thyroid cancer

AUROC Area under the receiver-operating characteristic curve

C

cAMP Cyclic adenosine monophosphate

CI Confidence Interval

CNS Central Nervous System

D

DAB 3,3'-Diaminobenzidine

DTC Differentiated thyroid cancer

E

ETE Extra-thyroidal extension

F

FNA Fine needle aspiration biopsy

FTC Follicular thyroid cancer

I

IgG Immunoglobulin G

IHC Immunohistochemistry

IgM Immunoglobulin M

M

MTC Medullary thyroid cancer

mRNA Messenger Ribonucleic acid

MW Molecular weight

N

NGF Nerve Growth Factor

NT Neurotrophin

P

P75^{NTR} p75 Neurotrophin receptor

PBS Phosphate buffered saline

PCR Polymerase chain reaction

PGP9.5 Protein gene product 9.5

PI Protease inhibitor

PTC Papillary Thyroid Cancer

R

ROC Receiver Operating Characteristic

RNA Ribonucleic acid

RTK Receptor tyrosine kinase

S

siRNA Small/short interfering RNA

SORT Sortilin

T

TGCA The Cancer Genome Atlas

TMA Tissue Microarray

Trk Tropomyosin-related kinase

TSH Thyroid stimulating hormone (thyrotropin)

1 OVERVIEW

1.1 Introduction

This thesis examines the link between nerves, nerve growth factors, and malignancy of the thyroid gland. A growing body of evidence supports the role of nerves and nerve growth factors in development and progression of several cancers, including prostate cancer, gastric cancer and breast cancer. Further, recent findings have suggested that the precursor of nerve growth factor (proNGF) is expressed in thyroid cancers, but not in benign thyroid tissue, suggesting a potential role of nerve-cancer crosstalk in thyroid oncogenesis. However, nothing further is known about this relationship.

Accurate diagnosis of thyroid cancer is a significant public health issue due to the frequency of thyroid nodules (present in 1 in 3 individuals by ultrasound screening). Current tests to distinguish benign thyroid nodules from thyroid cancers require highly specialized interpretation (neck ultrasound and cytopathology) and often result in diagnostic uncertainty, leading to anxiety for clinicians and patients, and driving the search for more accurate diagnostic biomarkers. Secondly, many thyroid cancers are indolent and require less intensive treatment; however current tests do not accurately distinguish indolent from aggressive tumours. As such, clinicians lack the necessary information to guide patients to more aggressive or less aggressive treatment strategies, or to accurately counsel patients about risk of recurrence. Finally, a subset of thyroid cancers behave aggressively, and result in significant morbidity and mortality. New treatments are required for this group.

1.2 Aims of this study

This body of work investigates the overarching hypothesis that nerves and neurotrophins are associated with thyroid cancer initiation and progression, and may have utility as biomarkers and therapeutic targets. More specifically, this thesis examines innervation of thyroid cancer, and the specific role of proNGF in innervation and metastases of thyroid cancer, and for its potential utility as a diagnostic biomarker.

1.3 Organisation of thesis

This thesis is presented as a series of six scientific papers: two narrative reviews bookending four original research articles. Seven additional articles that were published in peer-reviewed journals during the course of this thesis, but not directly contributing to this body of work, are included in the Appendix.

Following this overview (Chapter 1), Chapter 2 presents an introduction to thyroid nodules and thyroid cancer, viewed through the lens of the pregnant woman, as recently published as a chapter in the textbook, *Maternal-Fetal and Neonatal Endocrinology* (Kovacs and Deal, Elsevier). Following this, the chapter reviews physiological innervation of the thyroid; the role of neurotrophins and their receptors in benign and malignant diseases; and the need for biomarkers in evaluation of thyroid malignancy, by way of specific introduction to the subsequent research papers.

Chapters 3 to 6 contain original research contributing to this thesis, presented as a series of four scientific manuscripts. Chapter 3 reports on the role of proNGF as a diagnostic biomarker for thyroid cancer in prospective cohort studies. In Chapter 4, the first evidence for thyroid cancer innervation is presented. Chapter 5 details mechanistic studies of neurotrophin receptor expression in thyroid cell lines and tissues, demonstrating that the neurotrophin receptor, Tropomyosin receptor kinase A (TrkA), is targetable in thyroid cancer. Chapter 6 presents whole-slide analysis of proNGF expression in a paired cohort of thyroid cancers and lymph node metastases.

Chapter 7 is the final publication contributing to this thesis. In continued pursuit of clinically relevant strategies for addressing thyroid cancer, Chapter 7 re-imagines the role of the thyroid stimulating hormone (TSH) receptor as a tissue-specific theranostic target for thyroid cancer.

To conclude, Chapter 8 discusses the significance of the presented research, and future directions are explored.

2 LITERATURE REVIEW

2.1 Thyroid physiology and pathology

2.1.1 Normal thyroid development and function

The thyroid gland anlage develops during the second embryonic week from median endoderm as a downgrowth from the tongue, descending caudally to its final location below the thyroid cartilage, and leaving a trailing thyroglossal duct which regresses by the fifth week, leaving the remnant pyramidal lobe.¹ Around this time, the developing thyroid is joined by cells derived from the ultimobranchial bodies in the fourth pharyngeal pouch, which fuse medially and form the tubercles of Zukerkandl.² These neural cells from the fourth pharyngeal pouch contain the calcitonin-secreting C-cells of neuroendocrine origin. By the 8th embryonic week, follicular structures are evident, which by the 12th week are able to concentrate iodine and synthesise the thyroid hormones, triiodothyronine (T3) and thyroxine (T4).

In adulthood, the thyroid lies anterior to the trachea in the lower neck, and is comprised almost exclusively of follicular epithelial cells surrounding colloidal lakes, supported by a thin stroma containing blood vessels, parafollicular C-cells, and nerves (Figure 1).

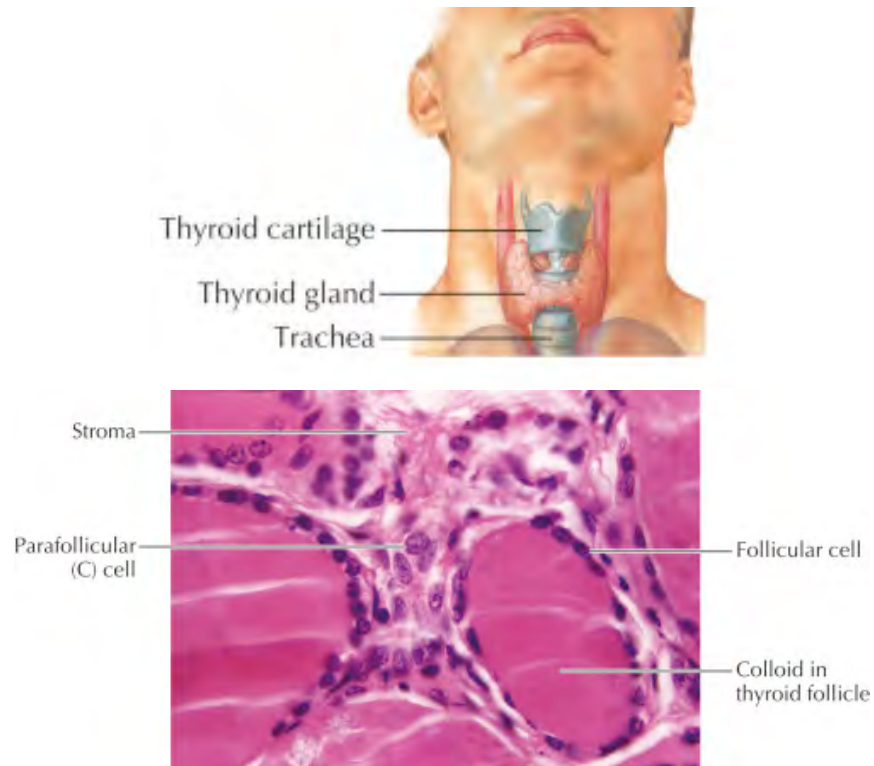


Figure 1: Normal thyroid anatomy. Top Panel: Location of thyroid in anterior neck. Bottom panel: Histological features of thyroid gland, showing thin follicular epithelium surrounding colloidal lakes. Between thyroid follicles are stromal cells including blood vessels, nerves and parafollicular C-cells. Source: Netter's Essential Physiology (Figures 28.1 and 28.2, reproduced with permission from Elsevier)

Morphologically, the thyroid is comprised of two lobes joined by a narrow isthmus, with a normal weight of 15-25 g. The thyroid is an exclusively endocrine organ, functioning to trap and concentrate iodine, which is utilised to synthesise T3 and T4, under regulation of pituitary-derived TSH, signalling via the 7-transmembrane domain G-protein coupled TSH receptor (Figure 2). T3 binds to nuclear receptors present in a wide variety of cells, controlling neural and somatic development in neonates and children, and metabolic activity in adults. C-cells predominantly secrete the peptide hormone, calcitonin, with a minor physiological role in calcium homeostasis; but also somatostatin.^{3,4}

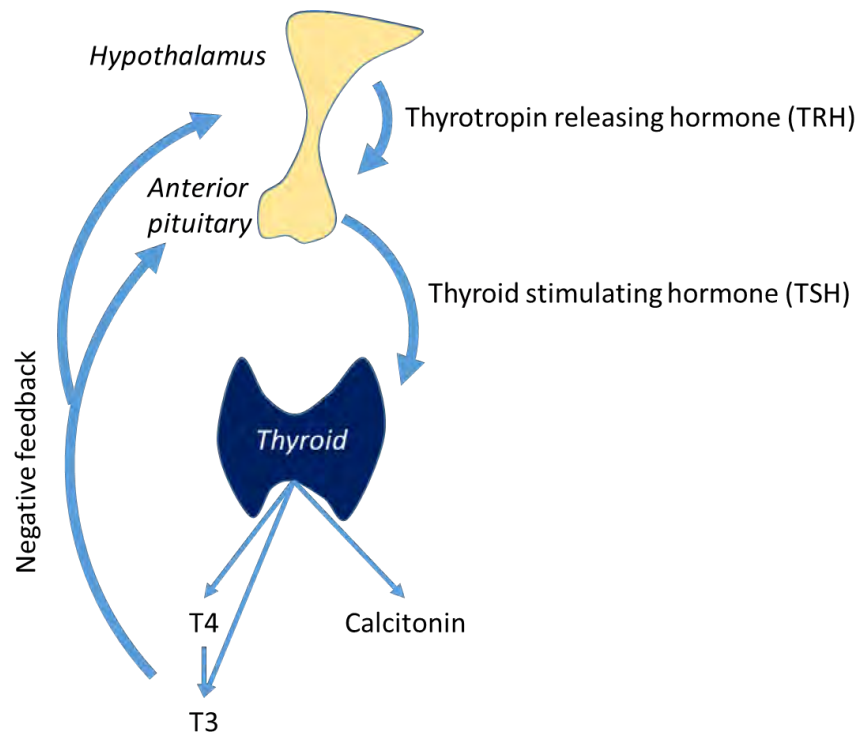


Figure 2: Thyroid hormone secretion.

2.1.2 Diseases of the thyroid gland

Diseases of endocrine glands can be broadly stratified into disorders of function (hormone secretion), or of structure (benign or malignant proliferation), as can be seen in Figure 3.

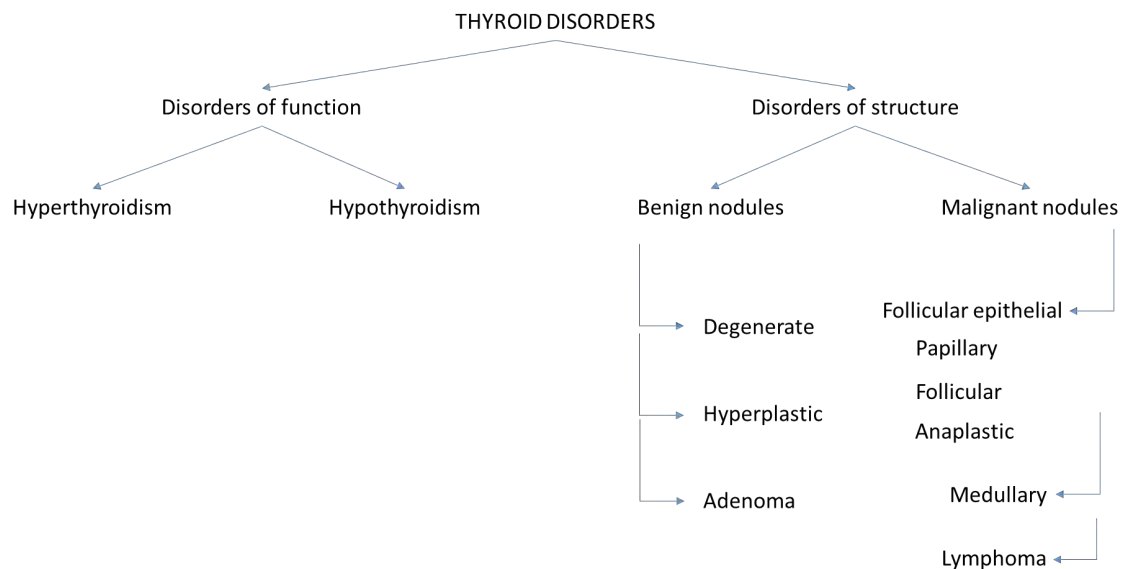


Figure 3: Schema of diseases of the thyroid gland

Functional thyroid disorders are due to overproduction or underproduction of thyroid hormone, and are common in adults, and are generally unrelated to malignancy.

The development of nodular lesions in the thyroid gland is a common finding, detectable by palpation in 2-6% of adults, and detected on imaging in 19–35% of randomly selected individuals.⁵ For reasons that remain poorly understood, thyroid nodules are more common in women, and increase in prevalence with age (see section 2.2).⁶ Many nodules show degenerative changes, seen by the accumulation of colloid in cysts containing blood and calcium, and may represent the end result of multiple cycles of proliferation and involution of the follicular epithelium over time.

Other nodules appear morphologically as densely packed follicular cells, and represent either hyperplasia or adenomas, which may be monoclonal or polyclonal in origin, and may either have increased or reduced production of thyroid hormone.⁷

Most thyroid nodules are benign, however, guidelines recommend the evaluation of all thyroid nodules for malignant potential.⁸ Autopsy studies show that the incidence of incidentally discovered differentiated thyroid cancer is high, between 4-11% in a meta-analysis of 35 studies.⁹ However, the incidence of clinically apparent thyroid cancer is much lower, with an estimated lifetime incidence in Australia of 1 in 85, suggesting that many thyroid cancers are indolent and remain subclinical throughout life.¹⁰

Therefore, due to the frequency of thyroid nodules, and the difficulty in distinguishing between indolent and significant malignant disease, the accurate diagnostic and

prognostic evaluation of thyroid nodules is of significant importance, affecting national health budgets and individual psychological health.

2.1.3 Thyroid cancer: clinical presentation and significance

Malignancy in the thyroid gland most commonly arises from the follicular epithelium and is termed differentiated thyroid cancer (DTC), presenting with the histological features of papillary (PTC) or follicular (FTC) subtypes. Uncommonly, an anaplastic thyroid cancer (ATC) variant, likely representing a poorly differentiated and aggressive form of a follicular-cell neoplasm, can present.

Thyroid tissue contains a small population of neural crest-derived C-cells, which secrete the hormone calcitonin, and are separate from the apparatus of thyroid hormone synthesis. Uncommonly, malignant transformation results in medullary thyroid cancer (MTC, <2% of thyroid cancers),¹¹ however, this is more common in patients with germline mutations in the Rearranged-in-Transfection (RET) proto-oncogene, as occurs in the familial cancer syndrome Multiple Endocrine Neoplasia-Type 2.

It is predicted that thyroid cancer will be the 11th most common cancer diagnosed in Australia in 2018, which is similar to worldwide incidence data.¹⁰

Thyroid cancer generally has a favourable prognosis, with overall 98% 10 year survival.¹¹ Whilst the survival for patients with early stage disease (AJCC 7th Edition TNM Stage I) is very high (>99%), those presenting with more advanced disease (AJCC TNM Stage II-IV) have significantly reduced 10 year survival (85% for Stage II, 75% for Stage III 37% for Stage IV).¹² Further, this summary statistic underestimates the morbidity of thyroid cancer. For patients who do not die from their disease, locoregional neck recurrence can cause significant morbidity and need for recurrent neck surgeries, radioactive iodine and regular follow up.

2.2 Review: Thyroid cancer during pregnancy and lactation

2.2.1 Preface

The below presented chapter is included in the recent textbook, Maternal-Fetal and Neonatal Endocrinology (Kovacs and Deal, editors). The setting of pregnancy provides an appropriate lens through which to examine the conundrum of nodular thyroid disease and thyroid cancer, both of which have a strong female preponderance. Through this publication, the reader is introduced to the key issues in the clinical

diagnosis and management of thyroid cancer, with particular focus on the challenge of timely diagnosis, the difficulties with prognosis, and the subgroup of patients who have a reduced prognosis due to advanced disease.

After this review, the remainder of Chapter 2 contains a focussed review of thyroid innervation, an introduction to neurotrophins and their receptors and a review of thyroid biomarkers, by way of introduction to the original research presented in Chapters 3 – 6.

Chapter 20

Thyroid cancer during pregnancy and lactation

Christopher W. Rowe^{*,†}, Kristien Boelaert[‡] and Roger Smith^{*,†}

^{*}Department of Endocrinology, John Hunter Hospital, Newcastle, NSW, Australia, [†]School of Medicine and Public Health, University of Newcastle, Newcastle, NSW, Australia, [‡]Institute of Metabolism and Systems Research, College of Medical and Dental Sciences, University of Birmingham, Birmingham, United Kingdom

Common clinical problems

- Thyroid nodules detected in pregnancy are common and require structured assessment, accounting for the unique circumstances of pregnancy.
- Survival from thyroid cancers diagnosed in pregnancy is similar to the nonpregnant population, although observational data may suggest an increased rate of locoregional recurrence.
- The timing of investigation of thyroid nodules, as well as consideration of surgery for thyroid cancer in pregnancy, should account for the stage of pregnancy and disease aggressiveness.
- A newly diagnosed, differentiated thyroid cancer without high risk features may often be managed conservatively during pregnancy, with surgery in the postpartum period.
- Active surveillance of papillary microcarcinomas in pregnancy is increasingly reported, but long-term-outcome data are lacking.
- Survivors of thyroid cancer should have specific prepregnancy counseling and intrapartum monitoring according to disease status, but they generally see favorable obstetric and oncologic outcomes.

20.1. INTRODUCTION

The detection of a thyroid nodule during pregnancy is a common clinical scenario, usually resulting in anxiety in both the woman and her physician. Two factors need to be considered in the assessment of a thyroid nodule: the presence of local symptoms due to mass effect, which occasionally necessitates removal if it compresses vital structures such as the trachea or great vessels; and the risk of malignancy. A third important factor—namely, whether the nodule is autonomously producing thyroid hormone—is unable to be assessed until the postpartum period due to the contraindication of scintigraphy during pregnancy. Any proposed treatment for a thyroid nodule must carefully balance the potential risks and benefits to both mother and developing fetus. We concur with the conclusions of Oduncu and colleagues that there is inevitable “maternal-fetal conflict” between the best care for the two patients, and thoughtful, patient-centered clinical reasoning is essential.¹

Malignancy of the thyroid gland usually arises from follicular epithelial cells, occurring in either a papillary thyroid cancer (PTC) or follicular thyroid cancer (FTC) pattern, and together, these are termed *differentiated thyroid cancer* (DTC). The rare, undifferentiated anaplastic thyroid cancer (ATC) is a highly aggressive subtype. Malignancy can also arise from the parafollicular, neuro-endocrine derived C-cells, termed *medullary thyroid cancer* (MTC). Infiltration of the

2 PART | B Maternal endocrine disorders during pregnancy and lactation

thyroid due to lymphoma or solid organ metastases is rare. In the absence of distant metastases, DTC has an excellent prognosis in women of childbearing age, with greater than 98% experiencing 10-year survival.²

20.2. EPIDEMIOLOGY OF NODULAR THYROID DISEASE AND THYROID CANCER

20.2.1 Nodular thyroid disease

For reasons that are still not well understood, thyroid nodules are more common in women and increase with age,³ a pattern that is observed across ethnicities and iodine-availability states.^{4–6} Increased exposure to female reproductive hormones is associated with increased nodularity. For example, later menopause, longer reproductive life, and multiparity are associated with increased thyroid nodules in a large community-based study from China.⁷ Multiparity is again associated with increased thyroid nodularity according to a study from Germany,⁸ and it may be exacerbated by iodine deficiency.⁶ Thyroid nodularity has also been associated with the presence of uterine fibroids.^{9,10} Current or previous oral contraceptive pill usage has been associated with reduced thyroid volume in a single study, although no difference in thyroid nodularity was found.¹¹

20.2.2 Thyroid cancer

Correlating with this pattern of increased thyroid nodularity, there is a strong female preponderance of thyroid cancer. Data from the U.S. National Cancer Institute Surveillance, Epidemiology, and End Results (SEER) Database shows an incidence of 21 cases per 100,000 females, compared to 7.1 per 100,000 males.¹² SEER data (Fig. 20.1) show that female preponderance is evident at puberty and that the female peak in incidence (ages 35–59 years) precedes the male peak in incidence (ages 65–75 years), corresponding with exposure to female reproductive hormones. There is no gender difference in incidence for ATC or MTC.

Despite these compelling epidemiological data, evidence linking reproductive-hormone exposure to thyroid cancer risk, examining factors such as age or pattern of menstrual cycle, menopause, or exogenous hormone therapy, is generally weak and heterogenous.¹³ However, reproductive history has a stronger link with DTC, particularly PTC risk, with some (but not all) studies finding a small or transient increase in risk of DTC following pregnancy compared to nulliparous women.¹³ Prolonged breastfeeding is associated with significant reductions in circulating estradiol levels and has been associated with reduced thyroid cancer risk in several studies.^{14,15}

20.2.3 Incidence of thyroid cancer in pregnancy

Thyroid cancer is the second-most-common solid organ malignancy complicating pregnancy (behind breast cancer), occurring in 14 in 100,000 births.¹⁶ Most of these cases represent a new diagnosis, usually of disease localized in the neck. Due to the increasing incidence of thyroid cancer and excellent prognosis,¹⁷ more survivors of thyroid cancer are presenting for obstetric management. For example, the prevalence of thyroid cancer among women in Taiwan (175 cases

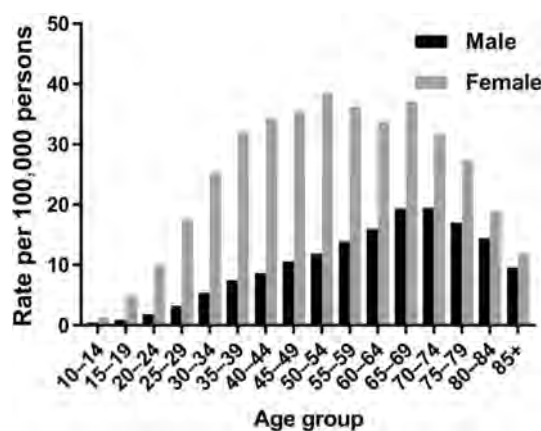


FIG. 20.1 Histogram showing age- and gender-specific incidence of thyroid cancer in the United States. Data source: SEER 18 (2010–2014). <https://seer.cancer.gov/faststats>.

per 100,000 women) is approximately ninefold higher than the incidence (18 cases per 100,000 women).¹⁸ Pregnancy in the setting of persistent structural disease is uncommon.

20.3. EFFECTS OF PREGNANCY ON THYROID NODULES

20.3.1 Effects of pregnancy hormones on thyroid follicular epithelium

Fig. 20.2 illustrates the known pregnancy-associated stimuli to the thyroid follicular cells.

The glycoprotein hormone human chorionic gonadotropin (hCG) is a heterodimer comprised of a common alpha-subunit shared with luteinizing hormone (LH), follicle-stimulating hormone (FSH), and thyroid-stimulating hormone (TSH), as well as a unique beta-subunit. This structural homology results in cross-stimulation of the seven-transmembrane domain G protein-coupled TSH receptor and contributes to the physiological suppression of endogenous TSH during the first trimester, gestational transient thyrotoxicosis, and stimulus for TSH receptor-mediated thyroid growth.¹⁹ An association between prolonged increase in TSH receptor-mediated signaling and subsequent risk of thyroid cancer has been demonstrated in several large observational studies, although the impact of shorter periods of increased TSH-receptor signaling is not known.²⁰

Driven by the strong epidemiological data linking female sex and nodular thyroid disease, the effect of estrogen on benign and malignant thyrocytes has been extensively studied in vitro and in animal models. Both benign and malignant thyrocytes express the estrogen receptors alpha and beta, and estrogen acts to stimulate growth of thyroid cells in culture.²¹ The G protein-coupled estrogen receptor 1 (GPER1), located on the endoplasmic reticulum, is overexpressed in thyroid cancers and may correlate with nodal metastases.²² Although less studied, progesterone receptors are also found in benign and malignant thyrocytes and may contribute to cell growth and gene transcription, although the magnitude of progesterone increase in pregnancy is around 10-fold lower than that of estradiol (Chapter 9).^{23, 24}

Although not a pregnancy hormone, the trace element iodine is essential for maternal and fetal thyroid function, and metabolic demands for iodine increase during pregnancy. Both conditions of iodine excess and iodine deficiency are associated with increased thyroid nodule formation.^{4, 25} Iodine requirements in pregnancy are approximately 250–300 mcg/day.²⁶

20.3.2 Physiology of thyroid nodules during pregnancy

Thyroid nodules are detected by ultrasound screening in 3%–21% of healthy pregnant women,^{8, 25, 27} although the majority are less than 1 cm in size.²⁵ Pregnancy has a small but significant effect on thyroid size and thyroid nodule growth. A prospective study of 221 Chinese women using serial thyroid ultrasound in pregnancy found that of the 34 women with nodules at baseline, 25/34 (74%) developed new nodules during pregnancy. Of women without nodules at baseline, 25/187 (11%) developed new nodules during pregnancy.²⁵ No nodule was suspicious for malignancy. A prospective study of 726 pregnant Belgian women found 20 of 726 women (3%) with nodules at baseline (identified

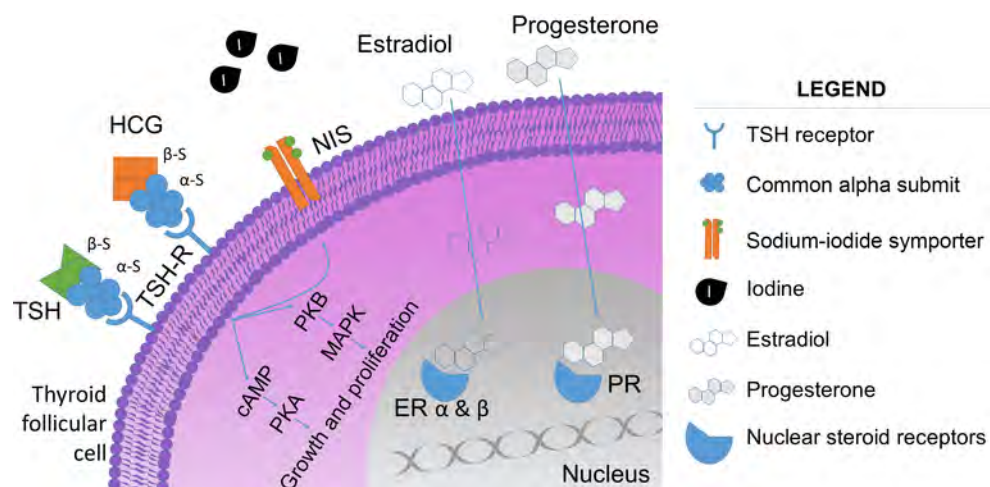


FIG. 20.2 Stimulatory signaling of pregnancy-associated factors on thyroid follicular epithelial cells.

4 PART | B Maternal endocrine disorders during pregnancy and lactation

using two-stage screening of palpation, and then ultrasound), with 12/20 having nodules double in size during pregnancy, and 4/20 women developing new nodules during pregnancy.²⁷

20.4. EVALUATION OF A NEWLY DISCOVERED THYROID NODULE IN PREGNANCY

As in the nonpregnant population, ultrasound-based screening for thyroid nodules in pregnancy is not recommended.²⁸ Hence, any thyroid nodule newly discovered in pregnancy should present either as an incidental finding or as a symptomatic/palpable lump.

The initial assessment of a thyroid lump should proceed as in a nonpregnant woman, with a goal of identifying lesions at high risk for malignancy. This assessment should include a thorough history, including risk factors for thyroid cancer, such as

- Familial syndromes of multiple endocrine neoplasia 2 (MEN2), familial PTC, Cowden's syndrome, familial adenomatous polyposis, and Carney complex
- Childhood neck irradiation, such as in treatment for prior head and neck cancers
- Early life exposure (< 18 years) to ionizing radiation

Clinical examination of the neck should characterize the lump, assess for symptoms due to mass-effect, and determine any cervical lymphadenopathy.

Although TSH and free thyroid hormones should be measured, their utility for risk stratification of thyroid nodules in pregnancy is limited by the contraindication of thyroid scintigraphy during pregnancy. Radioactive iodine readily crosses the placenta and can cause fetal hypothyroidism due to gland destruction if administered after fetal thyrogenesis in the 12th week of gestation. Further, exposure to gamma emissions from radioiodine being concentrated in the maternal bladder should be avoided. Thus, it is not possible to determine conclusively if a thyroid nodule is functional (and hence at very low risk of malignancy), or nonfunctional during pregnancy. Calcitonin is a sensitive serum biomarker for MTC,²⁹ although it has not been specifically validated in pregnant women and is generally not a recommended screening test in patients with thyroid nodules, either during or outside pregnancy. Further, calcitonin levels increase during normal pregnancy (see Chapter 5). CEA, also a sensitive biomarker of MTC, may rise slightly in normal pregnancy and should be interpreted cautiously.³⁰

The definitive risk stratification of a thyroid nodule uses thyroid/neck ultrasound using a high-frequency linear transducer, including detailed sonographic characterization of the nodule, and an assessment of the lateral neck for pathologically enlarged lymph nodes. Ultrasound-based risk-stratification systems for thyroid nodules have been published by the American Thyroid Association (ATA)³¹ and the American College of Radiology.³² Neck ultrasound is safe in pregnancy.

Based on this information, an initial risk stratification of malignancy risk can be performed, and the need for fine-needle aspiration biopsy (FNAB) determined. Indications for FNAB are identical to those in the nonpregnant population.³¹ Although FNAB is safe in all trimesters of pregnancy, careful consideration should be given to how this knowledge will be used. Several studies (reviewed next) have concluded that there is no impact on overall survival if surgery for a newly diagnosed DTC is deferred to the postpartum period, so a PTC with a typical ultrasound appearance and no pathological lymphadenopathy could be considered for deferred biopsy and surgery in the postpartum period. While the impact of pregnancy on MTC or ATC is unknown, given the more aggressive nature of these tumors, earlier surgery may be warranted, and cytological assessment of a sonographically concerning lesion during pregnancy may be useful. Patient preference is an important factor. This approach is consistent with published guidelines.³³

20.5. EFFECT OF PREGNANCY ON NEWLY DIAGNOSED THYROID CANCER

20.5.1 Impact on prognosis

Historically, outcome data for thyroid cancers diagnosed in pregnancy has been similar to the nonpregnant population, both in terms of recurrence and overall survival. These conclusions are based on data from retrospective studies from the United States over the period 1962–1999,^{34–36} with the most recent study (1991–1999) examining mortality only. Timing of surgery in these studies, either during pregnancy or postpartum, did not affect survival. While these studies draw on long follow-up periods, they are retrospective in nature and were conducted prior to the availability of now-standard tools

for monitoring and detecting recurrences, such as ultrasensitive thyroglobulin assays and high-resolution neck ultrasound.³³

Contrastingly, two recent retrospective studies from Italy,^{37, 38} recruiting patients diagnosed between 1995 and 2011, found that DTC diagnosed during pregnancy or within the first year postpartum may be associated with a higher risk of residual or recurrent disease. In the first study, Vannuchi and colleagues found that persistence/recurrence rates for women who were diagnosed with thyroid cancer in pregnancy or within 12 months postpartum were far higher (Group 2, 9/15, or 60%) than women with thyroid cancer diagnosed more than 12 months following pregnancy (Group 1, 2/47, about 4%) or never pregnant (Group 3, 8/61, about 13%).³⁷ However, an important confounder is that 11 of the 15 patients in Group 2 underwent surgery in the second trimester, and it is possible that a more cautious surgical approach prompted by pregnancy may have resulted in incomplete nodal clearance. In the second, larger study, Messuti and colleagues retrospectively stratified women less than 45 years into three groups: thyroid cancer diagnosed more than 2 years postpartum (Group 1, $n = 152$), thyroid cancer diagnosed during pregnancy or within 2 years (Group 2, $n = 38$), and nulliparous women (Group 3, $n = 150$).³⁸ Group 2 again had a higher incidence of persistent/recurrent disease in univariate analysis (11%, as opposed to 1% for Group 1 and 5% for Group 3, $p = 0.02$), although this difference was not observed in a multivariate model. The number of Group 2 patients who underwent thyroidectomy during pregnancy was not reported.

An Australian study over a similar period noted that DTC diagnosed in pregnancy or within 12 months postpartum had a larger size and a greater number of positive neck nodes than age- and sex-matched nonpregnant controls, although no difference in tumor micro-ribonucleic acid (microRNA) expression profiles between the two groups was noted.³⁹

A retrospective ultrasound study followed 19 patients with PTC diagnosed just prior to or in the early stages of pregnancy.⁴⁰ Among the findings, 13/19 tumors were < 1 cm in diameter and 3/19 showed evidence of involved lymph nodes. Over the course of pregnancy, increase in the tumor maximal diameter was noted in 16% of cases (3/19), and increase in tumor volume in 26% (5/19). Of the 3 patients with sonographically detected lymph nodes at diagnosis, 2 showed an increase in nodal size, although no new lymph nodes were observed and the extent of surgery was not altered. Further, 16/19 patients were managed surgically at a mean duration of 12 months following diagnosis, with either an ATA Excellent or ATA Indeterminate response to therapy after median follow-up of 54 months.

Overall, the available evidence suggests that DTC diagnosed in pregnancy has comparable overall survival to nonpregnant cohorts, whether surgery occurs during or after pregnancy. These data should reassure clinicians and patients that deferring surgery for a low-risk DTC until the postpartum period is a reasonable strategy. While it is possible that DTC diagnosed during pregnancy may be more likely to have local persistence or recurrence, appropriate surveillance will facilitate timely detection and management. Tumors with suspected high-risk features should be discussed in the context of an experienced multidisciplinary team for individualized management.

20.5.2 Timing of surgery

The decision of whether to proceed to thyroidectomy during pregnancy or to defer surgery until the postpartum period is largely based on expert opinion, as summarized in recent guidelines of the ATA.³³ In general, the presence of clinically aggressive features would prompt strong consideration of surgery during pregnancy, while their absence would lend support for a surveillance strategy, with surgery in the postpartum period. At present, specialized thyroid and neck ultrasound is the most useful tool to predict clinically aggressive DTC, and this should be performed at the initial assessment, and again by 24 weeks. Sonographic detection of lymph node metastases, or definite growth of the primary tumor, favor early surgery. MTC and ATC are considered more aggressive lesions by definition and early surgery should be strongly considered.

Repeat clinical and sonographic assessment of a suspicious thyroid nodule should occur prior to 24 weeks' gestation, to allow planning for thyroidectomy in the second trimester if required.

There is no optimal time for surgical management in the peripartum period. Surgery and anesthesia during pregnancy carry small but definite risks for the mother and fetus, which are minimized by elective operations in the second trimester. Conversely, surgery in the postpartum period may disrupt mother-child attachment and the establishment of breastfeeding, as well as placing increased stress on the family unit. Given the absence of evidence, patient-centered care that includes balanced discussion of various treatment options is appropriate.

20.5.3 Supportive management in pregnancy

TSH is an established growth factor for benign and malignant thyrocytes.¹⁹ While there are no studies examining the effect of supplemental levothyroxine to target lower TSH levels in thyroid cancers diagnosed during pregnancy, it is reasonable to establish a TSH target of the lower half of the pregnancy-specific reference range and administer levothyroxine if required to achieve this target.

We do not recommend restricting dietary iodine. Iodine is essential for fetal thyroid development, and maternal iodine requirements rise in pregnancy. Iodine deficiency in pregnancy is associated with development of maternal goiter, presumably in part through TSH-mediated stimulation of thyrocyte growth, and may contribute to increased nodularity as well.

20.5.4 Planning for radioiodine therapy

Serum thyroglobulin values in pregnancy may rise compared to prepregnancy levels, possibly due to maternal thyroid stimulation from hCG and estrogen, but they return to baseline levels within 1–6 months postpartum.^{41–43} We recommend waiting at least 6 weeks postpartum before assessing thyroglobulin status following pregnancy.

The indications for radioiodine therapy for either remnant ablation and adjuvant therapy have narrowed recently, such that fewer patients are requiring this treatment. This simplifies the initial management of the majority of women; however, a subset still will require radioiodine therapy based on risk stratification from recent guidelines.³¹

Radioiodine administration in the postpartum period presents unique medical and social challenges. Close contact with infants and children should be avoided for a minimum of 7 days after radioiodine therapy (the specific interval is determined by the administered dose and by the recommendations of the nuclear medicine physician).⁴⁴ Lactating mammary tissue overexpresses the sodium-iodide symporter and concentrates iodine,⁴⁵ and so to minimize radiation exposure to breast tissue, it is recommended that breastfeeding ceases at least 8 weeks prior to treatment with radioiodine therapy (ideally 3 months), and not be resumed for the current child to avoid radiation exposure to the child through breast milk.

If radioiodine therapy is required, the timing of therapy should be carefully considered, taking into account the risk of DTC progression, establishment of breastfeeding, and maternal-child bonding. A recent retrospective database study of over 9,000 patients with high-risk PTC (> 4 cm, nodal disease or grossly positive margins) found no impact on mortality (median survival 75 months) when radioiodine was administered early (within 3 months of surgery) compared to late (within 3–12 months), after adjustment for confounders.⁴⁶ In contrast, a smaller retrospective study of 235 ATA Low- and Intermediate-risk patients found a higher rate of persisting biochemical or structural disease (18.8% vs 4.3%) in patients with radioiodine therapy deferred longer than 3 months.⁴⁷

20.6. PRECONCEPTION COUNSELING OF WOMEN WITH A PRIOR HISTORY OF THYROID CANCER

Women of childbearing age with a prior history of thyroid cancer should be advised to seek preconception counseling. Periconception issues should be opportunistically addressed at regular follow-up appointments, both in primary and tertiary care.

Issues in preconception care

- Assessment of disease status: structural and biochemical
 - Potential impact of pregnancy on disease progress
 - Thyroxine dosing prior to, and following, conception
 - Impact of prior radioiodine therapy on timing of conception and future fertility
 - Use of pregnancy supplements that may interfere with thyroxine absorption
-

20.6.1 Establishment of disease status

The 2015 ATA guidelines for DTC provide a helpful framework for evaluating disease status in the period following initial treatment, accounting for the patient's response to therapy (Table 20.1).³¹ Different management considerations are relevant depending on a woman's prior treatment (total or hemithyroidectomy and whether radioiodine was administered), level of functional thyroid reserve (if hemithyroidectomy), and presence of any residual cancer. The presence of a microPTC under active surveillance represents a separate issue which is discussed next.

In patients with a past history of MTC, serum calcitonin and CEA are sensitive tumor markers and allow risk stratification of likelihood of structural disease.⁴⁸ No studies examine the impact of pregnancy on MTC.

20.6.2 Risk of recurrence

There is a theoretical risk that pregnancy may accelerate the recurrence or progression of previously treated DTC. Four key retrospective studies performed during the last 30 years are presented next.

Leboeuf and colleagues⁴³ evaluated 36 women with one or more pregnancies following therapy for DTC between 1997 and 2006, with pregnancy occurring a median of 4.3 years after DTC treatment. Only 44% of the cohort had neck imaging both before and after delivery, limiting the comparability of prepartum and postpartum assessments. Of the 3 women with structural disease prepartum, 1 had evidence of growth of a cervical lymph node metastasis during pregnancy. The 2 other women were noted to have new structural disease postpartum upon *imaging* that was not detected on *physical examination* prepartum. Further, 8/36 women had a > 20% rise in serum thyroglobulin following pregnancy, including 2 women with known structural disease, 1 with a new cervical lymphadenopathy, 3 with negative neck US, and 2 with negative physical examination.

Rosario and colleagues⁴⁹ reviewed 64 pregnancies following DTC, managed prior to 2006, with median time from treatment to conception being 2.4 years. All patients had no structural evidence of disease by neck ultrasound, either before or after pregnancy. The 49 patients with negative prepregnancy thyroglobulin remained negative postpartum. Eight patients with thyroglobulin 1–2 ng/mL did not show a rise in thyroglobulin postpartum.

Hirsch and colleagues⁵⁰ reviewed 63 women between 1992 and 2009 with pregnancy following PTC, with conception occurring a median of 5.1 years after initial treatment. They found that 5 of 6 women with documented structural disease prior to pregnancy demonstrated progression within 12 months postpartum (3 structural progressions and 2 biochemical progressions). All 5 women with biochemical-incomplete disease prior to conception did not have a rise in thyroglobulin postpartum. In 39 women with thyroglobulin < 0.9 ng/mL prior to pregnancy, no change was observed in thyroglobulin.

Rakhlin and colleagues reviewed 235 women between 1997 and 2015 with a term pregnancy following treatment for DTC, retrospectively stratified according to the 2015 "ATA Response to Therapy" criteria (Table 20.1).⁵¹ Of the 197 women without evidence of structural disease prepregnancy (comprising 148 ATA Excellent Response, 29 ATA

TABLE 20.1 2015 ATA risk stratification for DTC

2015 ATA response-to-therapy classification	Description
Excellent response	No clinical, biochemical, or structural evidence of persistent or recurrent thyroid cancer
Biochemical-incomplete response	Elevated serum thyroglobulin, or rising antithyroglobulin antibodies, in the absence of structural disease identifiable on imaging
Structural-incomplete response	Persistent or recurrent thyroid cancer visible upon imaging, either in neck or distant metastases
Indeterminate response	Nonspecific biochemical or structural findings that are not able to be classified as benign or malignant (includes stable/declining antithyroglobulin antibody levels without evidence of structural disease)

Note: Refer to ATA Guideline³¹ for full discussion of each class and qualifying criteria (table 13).

Tabulated from Haugen BR, Alexander EK, Bible KC, Doherty GM, Mandel SJ, Nikiforov YE, et al. 2015 American Thyroid Association Management Guidelines for adult patients with thyroid nodules and differentiated thyroid cancer: the American Thyroid Association Guidelines task force on thyroid nodules and differentiated thyroid cancer. *Thyroid* 2016;26(1):1–133.

8 PART | B Maternal endocrine disorders during pregnancy and lactation

Indeterminate, and 20 ATA Biochemical Incomplete), no structural disease was detected postpartum. However, 16/197 (8%) had a higher postpregnancy thyroglobulin than the prepregnancy value.

These data support the conclusion that women with an ATA Excellent response to therapy classification (that is, no evidence of disease structurally or biochemically) have minimal increased risk of DTC recurrence or progression in pregnancy and do not require additional monitoring during pregnancy.³³

Women with ATA Biochemical Incomplete or ATA Structural Incomplete disease may be at increased risk of disease progression from pregnancy. Risk and benefit discussions should involve the patient and be individualized. Women with known structural disease are discussed in further detail next.

20.6.3 Mitigating pregnancy-impacts of prior thyroid cancer treatment

20.6.3.1 *Levothyroxine supplementation*

All women require written advice for management of thyroid hormone replacement in the periconception period. Pregnancy increases requirements for thyroid hormone production, due in part to a rise in thyroid-binding globulin (see also Chapter 4). Additionally, adequate thyroid hormone is essential for fetal development and may reduce risk of early pregnancy loss. Women who were euthyroid in the nonpregnant state from a remaining hemithyroid may require supplemental levothyroxine due to insufficient functional thyroid reserve. Women dependent on exogenous levothyroxine due to total thyroidectomy should be instructed to increase their dose by 20%–40% as soon as conception occurs (our practice is to “double the dose” on 2 days of the week), with further adjustments based on monthly thyroid function testing for the first two trimesters.^{33, 52} Pregnancy multivitamins containing calcium or iron may inhibit absorption of levothyroxine, and patients should be instructed to take these at a time well away from levothyroxine (usually at night).⁵³ Women should be reassured that levothyroxine is safe to take in pregnancy to reduce risk of misinformed discontinuation at conception.⁵⁴

For most women, the individualized TSH target established prior to pregnancy will remain appropriate in the pregnant state, which is usually the lower half of the nonpregnant reference range. TSH suppression for women with persistent structural disease should be maintained in the pregnant state, as mild hyperthyroidism has not been shown to result in maternal or fetal complications.^{33, 55} However, overt thyrotoxicosis increases pregnancy risk.⁵⁶

20.6.3.2 *Radioiodine*

It is recommended that women avoid conception for 6 months following radioiodine therapy. This period is longer than the time required for radioiodine to totally decay (about 10 weeks, thus preventing fetal exposure to gamma emissions) and is recommended to allow the assessment of response to therapy and ensure that further treatments are not required in the following 15 months.⁵⁷ A longitudinal study enrolling 2,673 pregnancies did not show any increase in risk of pregnancy or neonatal complications in women treated with radioiodine.⁵⁸ A systematic review from 2008 confirmed these findings and reported no impact of radioiodine on fertility.⁵⁹ However, a recent prospective observational study of 30 premenopausal women receiving radioactive iodine (30–150 mCi) found a persistent decline in anti-Müllerian hormone (AMH) levels in 82% of women at 12 months following radioiodine therapy, which was associated with age, but not with dose of radioiodine.⁶⁰ There is some evidence of impaired testicular germ cell function following radioiodine, and men should be advised to avoid fathering children for 3–6 months after treatment.⁶¹

20.6.3.3 *Hypoparathyroidism*

Permanent surgical hypoparathyroidism is an uncommon long-term complication of neck surgery which requires active management during pregnancy. This condition is addressed in more detail in Chapter 21.

20.6.4 Surveillance and monitoring

Women with an ATA Excellent response to therapy do not require DTC-specific monitoring during pregnancy, but they should have a repeat thyroglobulin and thyroglobulin-antibody measurement at least 6 months postpartum as part of ongoing surveillance.

Women with ATA Biochemical Incomplete or ATA Indeterminate disease should have periodic monitoring during pregnancy, using thyroglobulin, thyroglobulin antibody, and neck ultrasound. Evidence of disease progression may

prompt an increase in the level of TSH suppression, or in rare cases, it can prompt expedited delivery. However there is no evidence to guide practice, and multidisciplinary decision-making is recommended.

20.6.4.1 Papillary thyroid microcarcinoma

Active surveillance of biopsy-proven papillary thyroid microcarcinoma (PMC; < 1 cm, no high-risk features) is an emerging management strategy, and three recent studies have evaluated the impact of pregnancy on its course. Shindo and colleagues followed 9 patients with PMC through pregnancy, noting that there was growth in size in 4/11 PMC (36%), compared to growth in 3/27 (11%) of nonpregnant controls.⁶² Ito and colleagues followed 50 pregnant patients with PMC and found growth of > 1 mm in 4 (8%), reduction in size in 1 (2%), and stable disease in the remaining 45 (90%). No lymph node metastases were observed.⁶³ Oh and colleagues followed 13 PMC patients through pregnancy, with 1 lesion showing significant growth.⁴⁰ Based on these studies, it appears reasonable to continue a strategy of active surveillance through pregnancy, monitored with serial maternal neck ultrasound; however, note that some microcarcinomas will grow during this period, and this may result in anxiety for the patient and clinicians. Further long-term follow-up data are required to guide practice in this area, as this remains an investigational strategy outside pregnancy, although supported by some recent guidelines.³¹

20.6.5 Germline RET mutations

Women either with syndromic MEN2 or known germline carriers of mutations in the REarranged during Transfection (RET) proto-oncogene should be offered prenatal counseling, regardless of a prior history of MTC, pheochromocytoma, or hyperparathyroidism. Mutations in RET in the mother, as well as in the fetus or child, can be stratified according to risk of early-onset MTC, which can inform management, including prophylactic thyroidectomy in early childhood for the most aggressive mutations.⁴⁸ Pheochromocytoma and hyperparathyroidism should be excluded prior to pregnancy in women with MEN2.

20.7. MANAGEMENT OF KNOWN RESIDUAL STRUCTURAL DISEASE IN PREGNANCY

A study of women with pregnancy in the setting of known structural disease retrospectively followed 38 women from a tertiary cancer center in the United States.⁵¹ They showed that 11/38 (29%) women demonstrated progression of known structural disease during pregnancy (5 with an increase in size of known abnormal lymph nodes, 3 with newly detected abnormal lymph nodes, and 1 with progression of known distant metastases). The authors subclassified 3 of these progressions as “clinically significant,” resulting in additional treatment within 12 months postpartum. The cohort included 10 women who had pulmonary metastases at diagnosis, 7 of whom had persistent structural disease prior to pregnancy. Disease progression was documented in 1 of these 10 cases.

These data suggest that pregnancy is a stimulatory environment for thyroid cancer, in keeping with epidemiological and in vitro data. However, the absolute magnitude of these effects appears small, and the majority of women with known structural disease can have a successful pregnancy without demonstrable impact on thyroid cancer status.

TSH suppression should be maintained in such cases, in keeping with prepregnancy targets. The effect of mild hyperthyroidism on pregnancy appears to be negligible. Anticipatory increases in levothyroxine in the first trimester, with monthly thyroid function tests, are required.

It is appropriate to monitor known neck disease with serial neck ultrasounds during pregnancy. Structural chest imaging with ionizing radiation should be avoided in pregnancy. If there are concerns regarding pulmonary function due to prior radioiodine exposure or widespread pulmonary metastases, serial lung function testing may provide some reassurance.

There are three tyrosine kinase inhibitors currently approved for the treatment of progressive or symptomatic metastatic thyroid cancer (lenvatinib, sorafenib, and cabozatenib). In animal studies using less than 10% of the recommended human dose, lenvatinib and sorafenib resulted in embryotoxicity, fetotoxicity, and teratogenicity in rats and rabbits.^{64, 65} No specific advice was provided for cabozatenib. Women of childbearing age should be advised to avoid pregnancy while on treatment with these agents. A single case of a woman with MEN2 and MTC treated with vandetanib up until 6 weeks gestation reported no adverse fetal outcomes.⁶⁶

20.8. CONCLUSION

Despite the conundrum of female preponderance of DTC remaining largely unexplained, effective treatment for thyroid cancer results in minimal long-term sequelae for the vast majority of women, including those who are pregnant or contemplating pregnancy. The increasing survivorship of young thyroid cancer patients, as well as the increased detection of thyroid nodules, mandates that pregnancy physicians are competent with the assessment and management of these conditions.

REFERENCES

1. F.S. Oduncu, R. Kimmig, H. Hepp, B. Emmerich, Cancer in pregnancy: maternal-fetal conflict, *J Cancer Res Clin Oncol* 129 (3) (2003) 133–146.
2. R.M. Tuttle, B. Haugen, N.D. Perrier, Updated American Joint Committee on cancer/tumor-node-metastasis staging system for differentiated and anaplastic thyroid cancer (eighth edition): what changed and why?, *Thyroid* 27 (6) (2017) 751–756.
3. C. Reiners, K. Wegscheider, H. Schicha, P. Theissen, R. Vaupel, R. Wrbitzky, et al., Prevalence of thyroid disorders in the working population of Germany: ultrasonography screening in 96,278 unselected employees, *Thyroid* 14 (11) (2004) 926–932.
4. J. Song, S.R. Zou, C.Y. Guo, J.J. Zang, Z.N. Zhu, M. Mi, et al., Prevalence of thyroid nodules and its relationship with iodine status in shanghai: a population-based study, *Biomed Environ Sci* 29 (6) (2016) 398–407.
5. B. Moifo, J.R. Moulion Tapouh, S. Dongmo Fomekong, F. Djomou, E. Manka'a Wankie, Ultrasonographic prevalence and characteristics of non-palpable thyroid incidentalomas in a hospital-based population in a sub-Saharan country, *BMC Med Imaging* 17 (1) (2017) 21.
6. N. Knudsen, P. Laurberg, H. Perrild, I. Bulow, L. Ovesen, T. Jorgensen, Risk factors for goiter and thyroid nodules, *Thyroid* 12 (10) (2002) 879–888.
7. K. Wang, Y. Yang, Y. Wu, J. Chen, D. Zhang, C. Liu, The association of menstrual and reproductive factors with thyroid nodules in Chinese women older than 40 years of age, *Endocrine* 48 (2) (2015) 603–614.
8. C.W. Struve, S. Haupt, S. Ohlen, Influence of frequency of previous pregnancies on the prevalence of thyroid nodules in women without clinical evidence of thyroid disease, *Thyroid* 3 (1) (1993) 7–9.
9. N. Spinos, G. Terzis, A. Crysanthopoulou, G. Adonakis, K.B. Markou, V. Vervita, et al., Increased frequency of thyroid nodules and breast fibroadenomas in women with uterine fibroids, *Thyroid* 17 (12) (2007) 1257–1259.
10. M.H. Kim, Y.R. Park, D.J. Lim, K.H. Yoon, M.I. Kang, B.Y. Cha, et al., The relationship between thyroid nodules and uterine fibroids, *Endocr J* 57 (7) (2010) 615–621.
11. N. Knudsen, I. Bulow, P. Laurberg, H. Perrild, L. Ovesen, T. Jorgensen, Low goitre prevalence among users of oral contraceptives in a population sample of 3712 women, *Clin Endocrinol* 57 (1) (2002) 71–76.
12. Thyroid cancer, National Cancer Institute, Bethesda, MD, 2016, [cited 2016 05/10/2016]; Available from: <http://seer.cancer.gov/statfacts/html/thyro.html>.
13. M. Moleti, G. Sturniolo, M. Di Mauro, M. Russo, F. Vermiglio, Female reproductive factors and differentiated thyroid cancer, *Front Endocrinol* 8 (2017) 111.
14. X. Yi, J. Zhu, X. Zhu, G.J. Liu, L. Wu, Breastfeeding and thyroid cancer risk in women: a dose-response meta-analysis of epidemiological studies, *Clin Nutr* 35 (5) (2016) 1039–1046.
15. H. Kim, K.Y. Kim, J.H. Baek, J. Jung, Are pregnancy, parity, menstruation and breastfeeding risk factors for thyroid cancer? Results from the Korea National Health and Nutrition Examination Survey, 2010–2015, *Clin Endocrinol* (2018).
16. L.H. Smith, B. Daniels, M.E. Allen, R. Cress, Cancer associated with obstetric delivery: results of linkage with the California cancer registry, *Am J Obstet Gynecol* 189 (4) (2003) 1128–1135.
17. H. Lim, S.S. Devesa, J.A. Sosa, D. Check, C.M. Kitahara, Trends in thyroid cancer incidence and mortality in the United States, 1974–2013, *JAMA* 317 (13) (2017) 1338–1348.
18. F.-C. Liu, H.-T. Lin, S.-F. Lin, C.-F. Kuo, T.-T. Chung, H.-P. Yu, Nationwide cohort study on the epidemiology and survival outcomes of thyroid cancer, *Oncotarget* 8 (45) (2017) 78429–78451.
19. C.W. Rowe, J. Paul, C. Geyde, J. Tolosa, C. Bendinelli, S. McGrath, et al., Targeting the TSH receptor in thyroid cancer, *Endocr Relat Cancer* 24 (2017) R191–R202.
20. H.R. Nieto, K. Boelaert, Thyroid stimulating hormone in thyroid cancer: does it matter?, *Endocr Relat Cancer* (2016).
21. M. Derwahl, D. Nicula, Estrogen and its role in thyroid cancer, *Endocr Relat Cancer* 21 (5) (2014) T273–T283.
22. L. Zhao, X.-Y. Zhu, R. Jiang, M. Xu, N. Wang, G.G. Chen, et al., Role of GPER1, EGFR and CXCR1 in differentiating between malignant follicular thyroid carcinoma and benign follicular thyroid adenoma, *Int J Clin Exp Pathol* 8 (9) (2015) 11236–11247.
23. G. Vannucchi, S. De Leo, M. Perrino, S. Rossi, D. Tosi, V. Cirello, et al., Impact of estrogen and progesterone receptor expression on the clinical and molecular features of papillary thyroid cancer, *Eur J Endocrinol* 173 (1) (2015) 29–36.
24. A.P.S. Bertoni, I.S. Brum, A.C. Hillebrand, T.W. Furlanetto, Progesterone upregulates gene expression in normal human thyroid follicular cells, *Int J Endocrinol* 2015 (2015), 864852.
25. A.W. Kung, M.T. Chau, T.T. Lao, S.C. Tam, L.C. Low, The effect of pregnancy on thyroid nodule formation, *J Clin Endocrinol Metab* 87 (3) (2002) 1010–1014.
26. F. Delange, Iodine requirements during pregnancy, lactation and the neonatal period and indicators of optimal iodine nutrition, *Public Health Nutr* 10 (12a) (2007) 1571–1580, (discussion 81–3).

27. D. Glinioer, M.F. Soto, P. Bourdoux, B. Lejeune, F. Delange, M. Lemone, et al., Pregnancy in patients with mild thyroid abnormalities: maternal and neonatal repercussions, *J Clin Endocrinol Metab* 73 (2) (1991) 421–427.
28. US Preventative Services Task Force, Screening for thyroid cancer: US preventive services task force recommendation statement, *JAMA* 317 (18) (2017) 1882–1887.
29. G. Costante, D. Meringolo, C. Durante, D. Bianchi, M. Nocera, S. Tumino, et al., Predictive value of serum calcitonin levels for preoperative diagnosis of medullary thyroid carcinoma in a cohort of 5817 consecutive patients with thyroid nodules, *J Clin Endocrinol Metab* 92 (2) (2007) 450–455.
30. S. Ercan, O. Kaymaz, N. Yucel, A. Orcun, Serum concentrations of CA 125, CA 15-3, CA 19-9 and CEA in normal pregnancy: a longitudinal study, *Arch Gynecol Obstet* 285 (3) (2012) 579–584.
31. B.R. Haugen, E.K. Alexander, K.C. Bible, G.M. Doherty, S.J. Mandel, Y.E. Nikiforov, et al., 2015 American Thyroid Association Management Guidelines for adult patients with thyroid nodules and differentiated thyroid cancer: the american thyroid association guidelines task force on thyroid nodules and differentiated thyroid cancer, *Thyroid* 26 (1) (2016) 1–133.
32. F.N. Tessler, W.D. Middleton, E.G. Grant, J.K. Hoang, L.L. Berland, S.A. Teehey, et al., ACR thyroid imaging, reporting and data system (TI-RADS): white paper of the ACR TI-RADS committee, *J Am Coll Radiol* 14 (5) (2017) 587–595.
33. E.K. Alexander, E.N. Pearce, G.A. Brent, R.S. Brown, H. Chen, C. Dosiou, et al., 2017 Guidelines of the american thyroid association for the diagnosis and management of thyroid disease during pregnancy and the postpartum, *Thyroid* 27 (3) (2017) 315–389.
34. M. Moosa, E.L. Mazzaferri, Outcome of differentiated thyroid cancer diagnosed in pregnant women, *J Clin Endocrinol Metab* 82 (9) (1997) 2862–2866.
35. S. Yasmeen, R. Cress, P.S. Romano, G. Xing, S. Berger-Chen, B. Danielsen, et al., Thyroid cancer in pregnancy, *Int J Gynaecol Obstet* 91 (1) (2005) 15–20.
36. F.S. Herzon, D.M. Morris, M.N. Segal, G. Rauch, T. Parnell, Coexistent thyroid cancer and pregnancy, *Arch Otolaryngol Head Neck Surg* 120 (11) (1994) 1191–1193.
37. G. Vannucchi, M. Perrino, S. Rossi, C. Colombo, L. Vicentini, D. Dazzi, et al., Clinical and molecular features of differentiated thyroid cancer diagnosed during pregnancy, *Eur J Endocrinol* 162 (1) (2010) 145–151.
38. I. Messuti, S. Corvisieri, F. Bardesono, I. Rapa, J. Giorcelli, R. Pellerito, et al., Impact of pregnancy on prognosis of differentiated thyroid cancer: clinical and molecular features, *Eur J Endocrinol* 170 (5) (2014) 659–666.
39. J.C. Lee, J.T. Zhao, R.J. Clifton-Bligh, A.J. Gill, J.S. Gundara, J. Ip, et al., Papillary thyroid carcinoma in pregnancy: a variant of the disease?, *Ann Surg Oncol* 19 (13) (2012) 4210–4216.
40. H.-S. Oh, W.G. Kim, S. Park, M. Kim, H. Kwon, M.J. Jeon, et al., Serial neck ultrasonographic evaluation of changes in papillary thyroid carcinoma during pregnancy, *Thyroid* 27 (6) (2017) 773–777.
41. S. Nakamura, S. Sakata, T. Komaki, N. Kojima, K. Kamikubo, S. Miyazaki, et al., Serum thyroglobulin concentration in normal pregnancy, *Endocrinol Jpn* 31 (6) (1984) 675–679.
42. N.G. Rasmussen, P.J. Hornnes, L. Hegedüs, U. Feldt-Rasmussen, Serum thyroglobulin during the menstrual cycle, during pregnancy, and post partum, *Acta Endocrinol* 121 (2) (1989) 168–173.
43. R. Leboeuf, L.E. Emerick, A.J. Martorella, R.M. Tuttle, Impact of pregnancy on serum thyroglobulin and detection of recurrent disease shortly after delivery in thyroid cancer survivors, *Thyroid* 17 (6) (2007) 543–547.
44. J.C. Sisson, J. Freitas, I.R. McDougall, L.T. Dauer, J.R. Hurley, J.D. Brierley, et al., Radiation safety in the treatment of patients with thyroid diseases by radioiodine 131I: practice recommendations of the American Thyroid Association, *Thyroid* 21 (4) (2011) 335–346.
45. F. Azizi, P. Smyth, Breastfeeding and maternal and infant iodine nutrition, *Clin Endocrinol* 70 (5) (2009) 803–809.
46. P. Suman, C.H. Wang, S.S. Abadin, R. Block, V. Raghavan, T.A. Moo-Young, et al., Timing of radioactive iodine therapy does not impact overall survival in high-risk papillary thyroid carcinoma, *Endocr Pract* 22 (7) (2016) 822–831.
47. H. Li, Y.Q. Zhang, C. Wang, X. Zhang, X. Li, Y.S. Lin, Delayed initial radioiodine therapy related to incomplete response in low- to intermediate-risk differentiated thyroid cancer, *Clin Endocrinol* (2018).
48. S.A. Wells Jr., S.L. Asa, H. Dralle, R. Elisei, D.B. Evans, R.F. Gagel, et al., Revised American Thyroid Association Guidelines for the management of medullary thyroid carcinoma, *Thyroid* 25 (6) (2015) 567–610.
49. P.W. Rosario, A.L. Barroso, S. Purisch, The effect of subsequent pregnancy on patients with thyroid carcinoma apparently free of the disease, *Thyroid* 17 (11) (2007) 1175–1176.
50. D. Hirsch, S. Levy, G. Tsvetov, R. Weinstein, A. Lifshitz, J. Singer, et al., Impact of pregnancy on outcome and prognosis of survivors of papillary thyroid cancer, *Thyroid* 20 (10) (2010) 1179–1185.
51. L. Rakhlin, S. Fish, R.M. Tuttle, Response to therapy status is an excellent predictor of pregnancy-associated structural disease progression in patients previously treated for differentiated thyroid cancer, *Thyroid* 27 (3) (2017) 396–401.
52. E.K. Alexander, E. Marqusee, J. Lawrence, P. Jarolim, G.A. Fischer, P.R. Larsen, Timing and magnitude of increases in levothyroxine requirements during pregnancy in women with hypothyroidism, *N Engl J Med* 351 (3) (2004) 241–249.
53. I. Zamfirescu, H.E. Carlson, Absorption of levothyroxine when coadministered with various calcium formulations, *Thyroid* 21 (5) (2011) 483–486.
54. C. Rowe, K. Murray, A. Woods, S. Gupta, R. Smith, K. Wynne, Metastatic thyroid cancer in pregnancy: risk and uncertainty, *Endocrinol Diabetes Metab Case Rep* (2016).
55. B.M. Casey, J.S. Dashe, C.E. Wells, D.D. McIntire, K.J. Leveno, F.G. Cunningham, Subclinical hyperthyroidism and pregnancy outcomes, *Obstet Gynecol* 107 (2 Pt 1) (2006) 337–341.
56. L.K. Millar, D.A. Wing, A.S. Leung, P.P. Koonings, M.N. Montoro, J.H. Mestman, Low birth weight and preeclampsia in pregnancies complicated by hyperthyroidism, *Obstet Gynecol* 84 (6) (1994) 946–949.

12 PART | B Maternal endocrine disorders during pregnancy and lactation

57. International Atomic Energy Agency, Radiation protection of pregnant women in nuclear medicine, International Atomic Energy Agency, 2018, [cited 2018 January]; Available from: <https://www.iaea.org/resources/rpop/health-professionals/nuclear-medicine/pregnant-women>.
58. J.P. Garsi, M. Schlumberger, C. Rubino, M. Ricard, M. Labbe, C. Ceccarelli, et al., Therapeutic administration of ¹³¹I for differentiated thyroid cancer: radiation dose to ovaries and outcome of pregnancies, *J Nucl Med* 49 (5) (2008) 845–852.
59. A.M. Sawka, D.C. Lakra, J. Lea, B. Alshehri, R.W. Tsang, J.D. Brierley, et al., A systematic review examining the effects of therapeutic radioactive iodine on ovarian function and future pregnancy in female thyroid cancer survivors, *Clin Endocrinol* 69 (3) (2008) 479–490.
60. I. Yaish, F. Azem, O. Gutfeld, Z. Silman, M. Serebro, O. Sharon, et al., A single radioactive iodine treatment has a deleterious effect on ovarian reserve in women with thyroid cancer: results of a prospective pilot study, *Thyroid* 28 (4) (2018) 522–527.
61. F. Pacini, M. Gasperi, L. Fugazzola, C. Ceccarelli, F. Lippi, R. Centoni, et al., Testicular function in patients with differentiated thyroid carcinoma treated with radioiodine, *J Nucl Med* 35 (9) (1994) 1418–1422.
62. H. Shindo, N. Amino, Y. Ito, M. Kihara, K. Kobayashi, A. Miya, et al., Papillary thyroid microcarcinoma might progress during pregnancy, *Thyroid* 24 (5) (2014) 840–844.
63. Y. Ito, A. Miyauchi, T. Kudo, H. Ota, K. Yoshioka, H. Oda, et al., Effects of pregnancy on papillary microcarcinomas of the thyroid re-evaluated in the entire patient series at Kuma Hospital, *Thyroid* 26 (1) (2015) 156–160.
64. U.S Food & Drug Administration, Lenvima prescribing information, FDA, 2015, Available from: https://www.accessdata.fda.gov/drugsatfda_docs/label/2016/208692s000lbl.pdf, Accessed 22 January 2018.
65. U.S Food & Drug Administration, Nexavar prescribing information, FDA, 2013, Available from: https://www.accessdata.fda.gov/drugsatfda_docs/label/2013/021923s016lbl.pdf, Accessed 22 January 2018.
66. N. Thomas, J. Glod, C. Derse-Anthony, E.L. Baple, N. Osborne, R. Sturley, et al., Pregnancy on vandetanib in metastatic medullary thyroid carcinoma associated with multiple endocrine neoplasia type 2B, *Clin Endocrinol* (2018).

2.3 Innervation of the thyroid

2.3.1 Introduction

As with most visceral organs, the thyroid receives autonomic innervation. However, most discussion of thyroid innervation in clinical thyroidology is concerned with techniques to avoid damage to the closely apposed recurrent laryngeal nerve during neck surgery (as see in Figure 4), as this nerve provides essential innervation of the vocal apparatus. Consequently, the potential role of functional innervation of the thyroid gland is rarely considered. Nonetheless, the rich autonomic innervation of the thyroid gland has demonstrable physiological effects.¹³ Fibres from both adrenergic and cholinergic neurones are demonstrated to terminate in close vicinity of thyroid follicles, suggesting that neural effects extend beyond mere control of vascular flow.¹⁴⁻¹⁶ This topic has been expertly reviewed by Ahren¹³, albeit three decades ago. Salient points, as well as new findings in the intervening 30 years, are discussed below. The key finding is that adrenergic innervation appears to have predominantly stimulatory effects on thyroid growth and hormone release, while cholinergic signalling is inhibitory to hormone secretion.

2.3.2 Anatomy of thyroid innervation

Adrenergic fibres enter the thyroid gland via plexuses on branches of the superior and inferior thyroidal arteries (Figure 4). These fibres are likely post-ganglionic, originating from synapses in the superior cervical ganglion. Additionally, at surgery, branching nerve fibres from the cervical sympathetic ganglia can be observed tracking into the recurrent or superior laryngeal nerves, before passing into the thyroid gland, sometimes termed the Sympathetic-Laryngeal nerve anastomotic branch.¹⁷ In a series of experiments in the mouse, Melander and colleagues showed that sympathetic nerve fibres had close anatomical relations with both arterioles and interfollicular spaces.¹⁸

Cholinergic fibres to the thyroid arise from the vagus nerve, with preganglionic fibres arising from the dorsal motor nucleus of vagus in the ipsilateral brainstem, and entering the thyroid gland through branches of the recurrent laryngeal and superior laryngeal nerves (Figure 4).

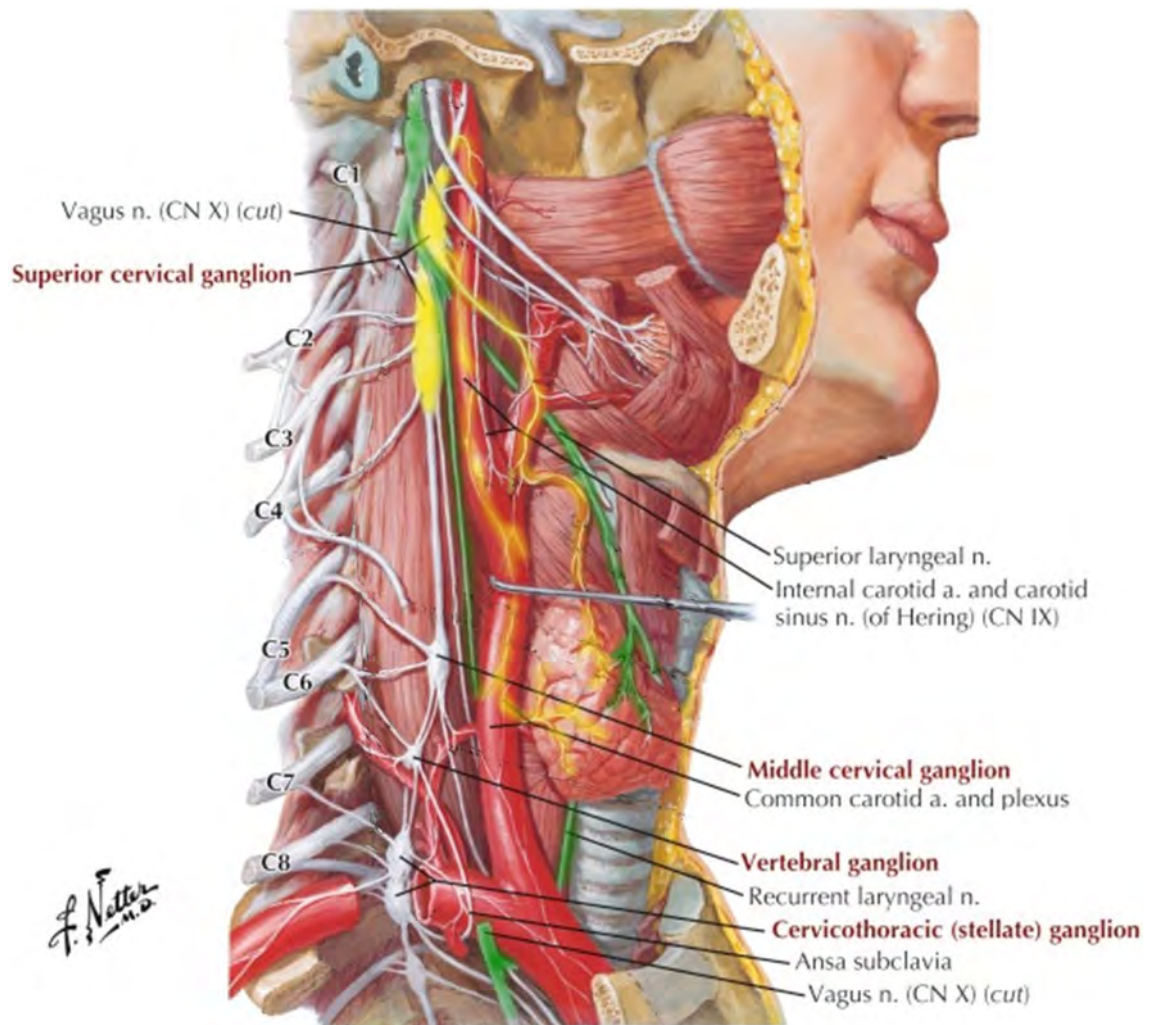


Figure 4: Autonomic Innervation of the thyroid. Adrenergic innervation (highlighted yellow) arises from the superior cervical ganglion, and enters the thyroid via superficial plexuses on blood vessels. Cholinergic innervation (highlighted green) arises from the superior laryngeal and inferior laryngeal nerves branching from the vagus nerve. Figure minimally adapted from Netter's Clinical Anatomy, 4th edition, Figure 8.68. © 2019 Elsevier. Used with permission.

2.3.3 Adrenergic (sympathetic) innervation and function

Studies examining the functional effects of adrenergic thyroid innervation either involve measuring response to administration of an adrenergic neurotransmitter; or through manipulation (either direct stimulation or destruction) of the superior cervical ganglion (Figure 4).

Adrenergic signalling has been shown to increase thyroid hormone secretion in animals. For example, in a TSH-suppressed environment, stimulation of the ipsilateral superior cervical ganglion resulted in increase in thyroid hormone synthesis, demonstrated by an

increase in intracellular colloid droplets in dependent follicles (a sign of increased activity of the follicular epithelium in thyroid hormone synthesis), and an increase in thyroid hormone release.¹⁹ These effects were reproduced by systemic administration of noradrenaline, and inhibited by the alpha-adrenoceptor antagonist, phentolamine; and were not reproduced by variations in arterial supply. These findings have been confirmed in other studies.¹³ Similarly, bilateral surgical sympathectomy (destruction of the superior cervical ganglion) in a 'normal-TSH' environment resulted in a reduction of hormone release from the thyroid.¹⁸ However, under conditions where thyrocytes are stimulated by TSH, adrenergic signalling may act to decrease thyroid hormone release, as noradrenaline may impair the increase in cyclic adenosine monophosphate (cAMP) that occurs in response to TSH stimulation, which may predominantly be mediated by alpha-adrenoceptors.¹³ Beta-adrenoceptor signalling retains stimulatory effects under basal or TSH-stimulated conditions, and is predominantly mediated by the beta-2 adrenoceptor subtype.^{20,21}

Adrenergic signalling may also be a positive regulator of thyroid growth. Unilateral pre-ganglionic denervation of the superior cervical ganglion of male rats resulted in reduced hemithyroid weight, and reduced hemithyroid uptake of iodine compared to the contralateral (control) lobe.²² Interestingly, effects were similar under conditions of basal TSH conditions, and with increased TSH stimulation (in response to oral propylthiouracil).

It is important to note that the technique of sympathetic denervation may confound experimental analysis. Ganglionectomy, in disrupting the post-ganglionic sympathetic innervation, may result in reactive 'denervation supersensitivity'^{22,23} and cause a paradoxical increase in adrenergic signalling. This mechanism may explain the conflicting results where ganglionectomy resulted in increase in thyroid hormone secretion in some studies.^{24,25}

2.3.4 Cholinergic (parasympathetic) innervation and function

Cholinergic signalling appears to be inhibitory to thyroid hormone secretion. Functional studies administering the cholinergic agonists acetylcholine or carbamylcholine have inhibited TSH-mediated thyroid hormone secretion, most likely by increased intracellular cAMP degradation following TSH stimulation.¹³ For example, in the mouse, carbamylcholine inhibited thyroid hormone release when injected under basal TSH

conditions, and when injected immediately prior to exogenous TSH stimulation, but not in a TSH-suppressed environment.¹⁴ Further, the administration of atropine (a cholinergic antagonist) significantly increased thyroid hormone secretion in response to TSH. Similarly, bilateral vagotomy in pigeons (reducing parasympathetic signalling) resulted in ultrastructural changes in follicular cells consistent with increased hormone production, and increased serum concentrations of T3, although T4 was reduced.²⁶

Contrastingly, bilateral ligation of the inferior laryngeal nerve in rats resulted in a decrease in thyroid weight, both in the presence and absence of TSH stimulation, suggesting a trophic role of cholinergic innervation in thyroid growth.²⁵ A reduction in circulating T4 was also observed.

2.3.5 Evidence for innervation of thyroid cancer

Interest in innervation of thyroid cancer is driven by compelling data from other solid organ malignancies, particularly prostate, gastric, breast and colorectal carcinomas,²⁷⁻³¹ showing that innervation of the tumour micro-environment has functional and prognostic significance. For example, in studies in humans, the presence of neo-neurogenesis (increased neural density) within colorectal carcinoma tissue was associated with a 50% reduction in overall survival, compared to patients with no neo-neurogenesis.³¹ In breast cancer, nerves were twice as likely to be detected within tumours that had metastasized to lymph nodes, compared to non-metastatic lesions.³⁰ In the prostate, the incidence of prostate cancer in men with spinal cord injuries (resulting in reduced descending innervation to the prostate) was reduced by 62% compared to men with intact autonomic signalling.³² The mechanism of nerve-dependence in prostate cancer may be via an angiogenic switch on blood vessels, whereby neo-neurogenesis drives neo-angiogenesis and tumour progression,²⁷ whereas in other tumour types these mechanisms are less clearly defined. In animal models, denervation of the gastric mucosa by vagotomy reduces the development of gastric tumours,²⁹ whilst chemical or surgical sympathectomy reduces growth of prostate tumours.²⁸

However, there are no data addressing the question of whether thyroid cancer is innervated, and whether this is of biological significance.

2.3.5.1 Inferences from perineural invasion

Perineural invasion (malignant cells either encasing or infiltrating nerves) is an established predictor of aggressive tumour biology in some cancers, including prostate carcinoma,³³ and squamous cell carcinoma of the head and neck.³⁴ However, perineural invasion is not an established risk factor in thyroid cancer, and is not routinely reported at histopathology. Perineural invasion is occasionally reported in thyroid cancer specimens (incidence of 1.8 % and 2% in two unrelated studies),^{35,36} providing supportive evidence for the presence of nerves in the vicinity of a minority of thyroid cancers.

The potential significance of perineural invasion in thyroid cancer can be inferred from study datasets investigating other hypotheses. In a cohort of 437 patients with lateral neck metastases (AJCC TNM stage N1b) at presentation of PTC, the incidence of histological perineural invasion in this high-risk cohort was 12.4%. This rate is 6-fold higher than the reported rates of perineural invasion observed in two other studies of lower risk thyroid cancer cohorts (1.8%, and 2%, discussed above);^{35,36} and was associated with lower rates of recurrence-free survival in univariate analysis (HR 3.1, 95%CI 1.3 – 7.8, $p=0.01$).³⁷ Similarly, an indication of the potential significance of perineural invasion is provided by a study of 678 cases of PTC, which found an association between perineural invasion and the established high-risk feature of lymphovascular invasion.³⁶ However, the comparison of rates of perineural invasion between studies is confounded by many factors, and dedicated studies are required.

2.3.6 Relevance for proposed research

These data confirm that the thyroid receives autonomic innervation. Adrenergic signalling is stimulatory to benign thyroid growth, and the secretion of thyroid hormones, while both adrenergic and cholinergic innervation may support normal thyroid homeostasis, as evidenced by gland atrophy following disruption to adrenergic or cholinergic innervation. However, it is not known whether thyroid tumours receive autonomic innervation, and whether this is of biological significance.

2.4 The precursor for nerve growth factor in physiology and cancer

2.4.1 Physiology of the precursor for nerve growth factor

Neurotrophins are a family of soluble proteins that function as growth factors for nerves, binding to cell surface receptors in the peripheral and central nervous system. Nerve

Growth Factor (NGF), the prototypical neurotrophin, was serendipitously identified in the laboratory of Cohen and Levi-Montalcini in 1951, where it was observed that mouse sarcoma tissue was able to attract nerve fibres from a chick embryo.³⁸ Since this time, several other neurotrophins have been identified, including brain-derived neurotrophic factor, neurotrophin 3 and neurotrophin 4/5.

NGF is a 120 amino acid protein encoded by the *NGF* gene on chromosome 1p13.³⁹ NGF is translated from its messenger RNA (mRNA) to form a 241 residue pro-hormone, which is cleaved by furins and matrix metalloproteinases (Figure 5).⁴⁰ This precursor for NGF (proNGF) was first detected in 1977, however, it was not until it was identified that the pro-domain was able to facilitate receptor binding and had unique physiological effects that it became the focus of study.⁴¹ A key difference from NGF is the ability of proNGF to co-stimulate a combined sortilin-p75^{NTR} complex,⁴² which may be a result of the pro-peptide contributing to a more stable tri-peptide conformation.⁴³

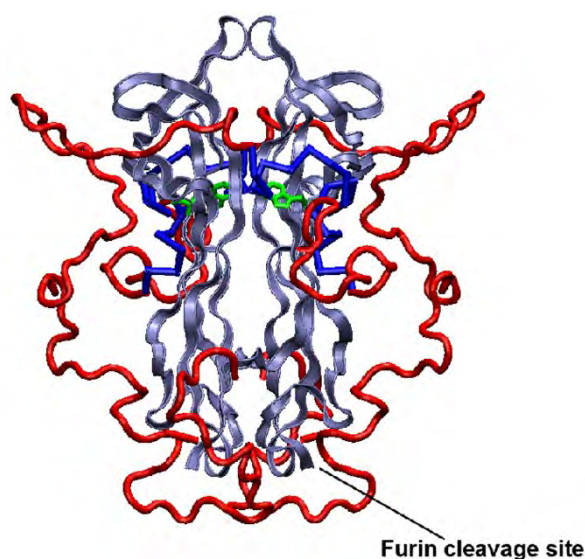


Figure 5. Structure of the precursor for nerve growth factor, showing the pro-domain (red), and the cleaved NGF molecule (blue). The furin cleavage site is shown. Figure reproduced from Paoletti *et al.*⁴⁴ with permission (CC BY 4.0)

NGF is a key driver of neuronal growth, survival and differentiation, mediated through the receptors p75^{NTR} and TrkA in both the central and peripheral nervous system (see Figure 6), although in benign tissues NGF does not cause cellular proliferation.⁴⁵ ProNGF is known to interact with three key cell-surface receptors: pan-neurotrophin receptor (p75^{NTR}, so named for its ability to bind all known neurotrophins and pro-neurotrophins);

Tropomyosin receptor kinase A (TrkA, also known as neurotrophic tyrosine kinase receptor type 1, NTRK1) and sortilin (also known as Neurotensin Receptor 3, NTSR3; or glycoprotein 110). The functional effects of pro/neurotrophin signaling are mediated by these ligand-receptor interactions, and vary from inducing neuronal survival and differentiation to driving neuronal apoptosis, depending on receptor expression (Figure 6).⁴⁶ Within the nervous system, proNGF functions to induce neuronal apoptosis and may provide a balance to the proliferative signals of NGF. ProNGF is secreted by cell targets of innervation under a number of physiological states, and is increased in the brain and cerebrospinal fluid of patients with neurodegenerative conditions, such as Alzheimer's disease and other tauopathies.⁴⁷⁻⁵⁰ Further, the pro/NGF pathway has been implicated in the mediation of pain syndromes in benign⁵¹⁻⁵³ and malignant conditions,⁵⁴ and may have a role in diabetes-associated nerve damage in the eye.⁵⁵

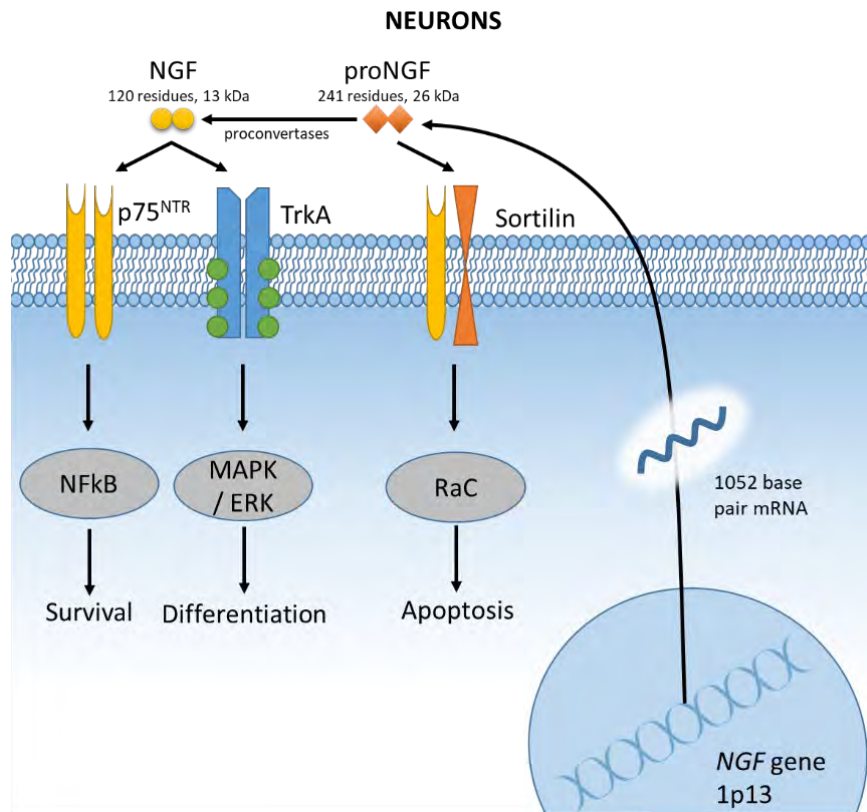


Figure 6: Physiological role of NGF and proNGF in neural tissue. Figure redrawn and adapted from Bradshaw *et al.*,⁴¹ including data from Aloe *et al.*⁴⁵

2.4.2 Role of the precursor for nerve growth factor in malignancy

As demonstrated in Figure 7, and in contrast to its effects in benign tissues (Figure 6), a different paradigm of neurotrophin-receptor crosstalk occurs in the cancer microenvironment, where the downstream effects of proNGF-receptor interactions result in pro-oncogenic signaling.

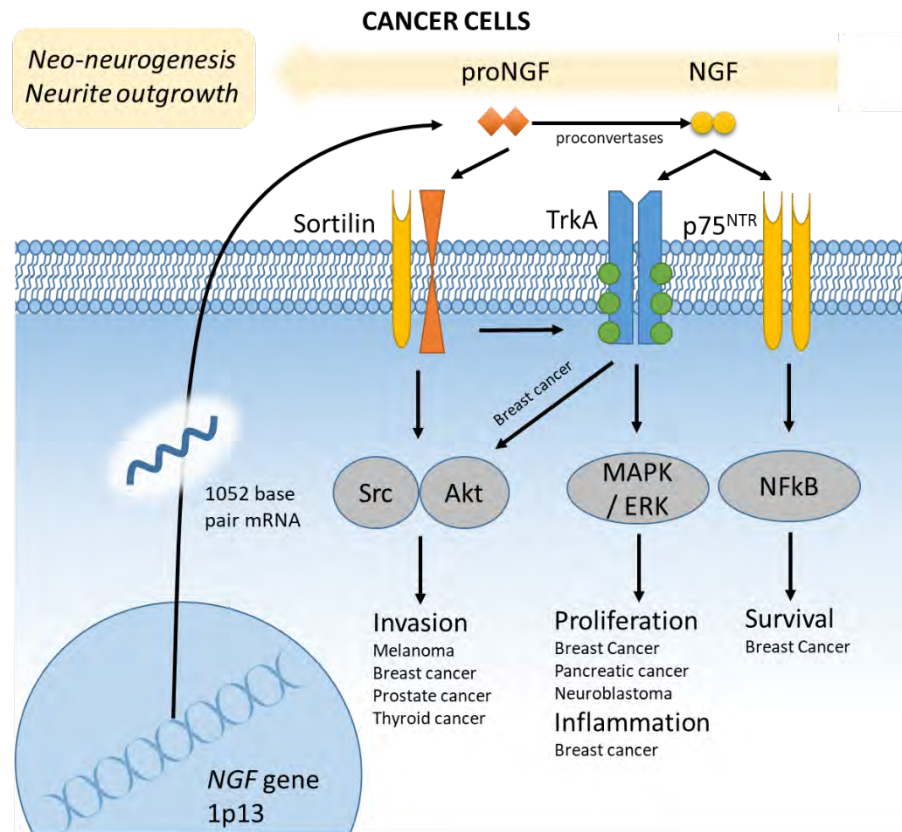


Figure 7: Post-receptor signaling of NGF and proNGF in malignant tissue. Figure redrawn and adapted from Bradshaw *et al.*,⁴¹ including data from Aloe *et al.*⁴⁵

These effects are most comprehensively described in breast cancer. Biologically active NGF is produced from breast cancer cells,⁵⁶ and both NGF and proNGF signaling promote self-renewal and growth of cancer stem cells.⁵⁷ The pro-oncogenic effect is mediated, at least in part, through neurotrophin receptors. For example, proNGF signaling, interacting through a sortilin-TrkA complex, has been associated with growth of breast cancer, and reduced patient survival.⁵⁸ In a separate study, autocrine proNGF signaling through TrkA and sortilin drives breast cancer cell invasion.⁵⁹ Knockdown of sortilin using siRNA impairs adhesion, migration and invasion on breast cancer cells *in vitro*,⁶⁰ while *in vivo*, NGF-p75^{NTR} signaling may drive de-differentiation, as shown through increased resistance of breast cancers to standard chemotherapy.⁶¹

In addition to breast cancer, data support a role for proNGF in other malignancies. In pancreatic cancer, proNGF protein expression is higher in malignant tissue than in surrounding benign or peritumoural tissues, and may have functional significance as proliferation, migration and invasion are all inhibited by proNGF siRNA knockdown *in vitro*.⁶² Benign prostatic epithelium synthesizes both proNGF and NGF, which are

biologically active, inducing growth of prostate tumour cells *in vitro*.⁶³ In prostate cancer, levels of proNGF protein expression in carcinoma correlate with histological markers of tumour aggressiveness in patient samples.⁶⁴ Melanoma, a neural crest-cell derived malignancy, is associated with growth through the pro/NGF pathway,⁶⁵ where NGF signaling drives transformation of melanocytes towards a bipotent precursor with higher growth potential.⁶⁶

As well as direct neurotrophin-receptor signaling driving proliferation and invasion, there is some evidence that neurotrophins mediate neo-neurogenesis (nerve formation) in the cancer microenvironment. For example, proNGF is able to directly stimulate outgrowth of neurites *in vitro*, perhaps through paracrine signaling or chemotaxis.⁶⁴ In breast cancer, NGF is associated with nerve fibre infiltration within the tumour microenvironment,³⁰ and breast cancer-derived NGF induces differentiation of embryonic neuronal precursors.⁵⁶

2.4.3 Role of the precursor for nerve growth factor in thyroid cancer

The role of proNGF in thyroid cancer is suggested by a single paper, where Faulkner *et al.* used immunohistochemistry to assess proNGF expression in benign and malignant thyroid tissue from commercial tissue-microarrays.⁶⁷ Strong immunostaining for proNGF was demonstrated in the cytoplasm of follicular cell-derived thyroid cancers (both papillary and follicular subtypes). In contrast, minimal proNGF protein was demonstrated in benign thyroid (Figure 8).

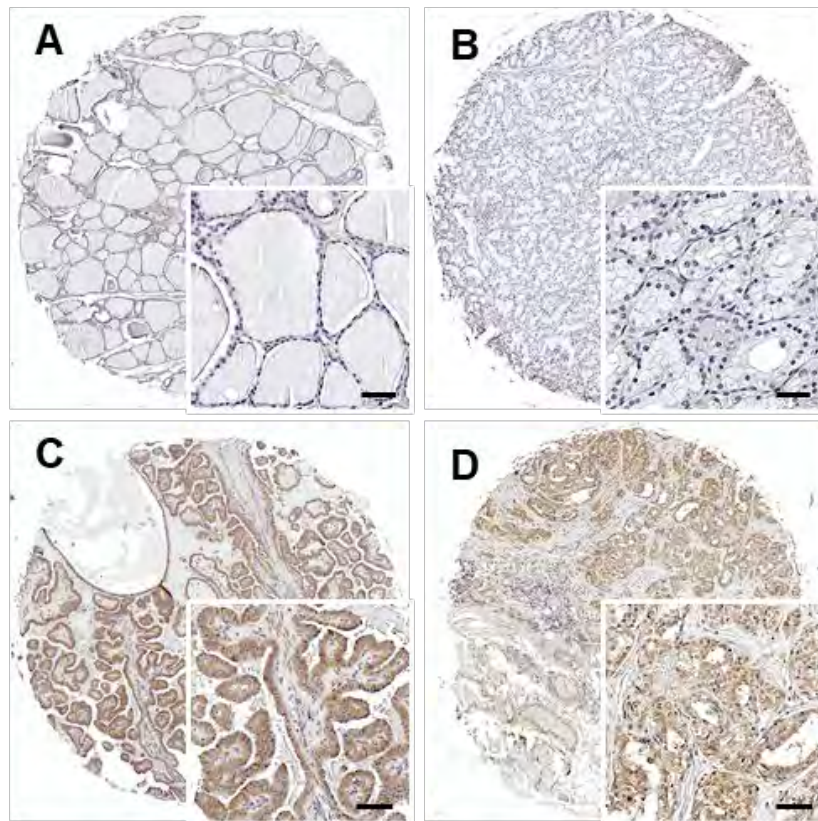


Figure 8: Immunohistochemistry for proNGF in benign and malignant thyroid tissue, demonstrating strong, specific labelling of the cytoplasm of malignant cells. Representative images are shown for (A) normal thyroid tissue, (B) adenoma, (C) papillary carcinoma and (D) follicular carcinoma. Scale 50 μ m. Reproduced from Faulkner *et al.*⁶⁷ with permission (CC BY 3.0).

As well as demonstrating a biological gradient between benign and malignant tissue (Figure 9A), the area under the receiver operating characteristic curve (AUROC) for ability of proNGF to discriminate between benign and malignant thyroid lesions was 0.95 (95% CI 0.85 – 0.96, $p < 0.0001$, Figure 9B), suggesting that proNGF may have a high discriminative ability as a biomarker for malignant thyroid lesions. Both NGF and proNGF are known to be secreted into the extracellular space,⁵⁹ and both have been detected in the serum of mice and humans,⁶⁸⁻⁷⁰ raising the possibility of detecting proNGF in serum or biopsy material.

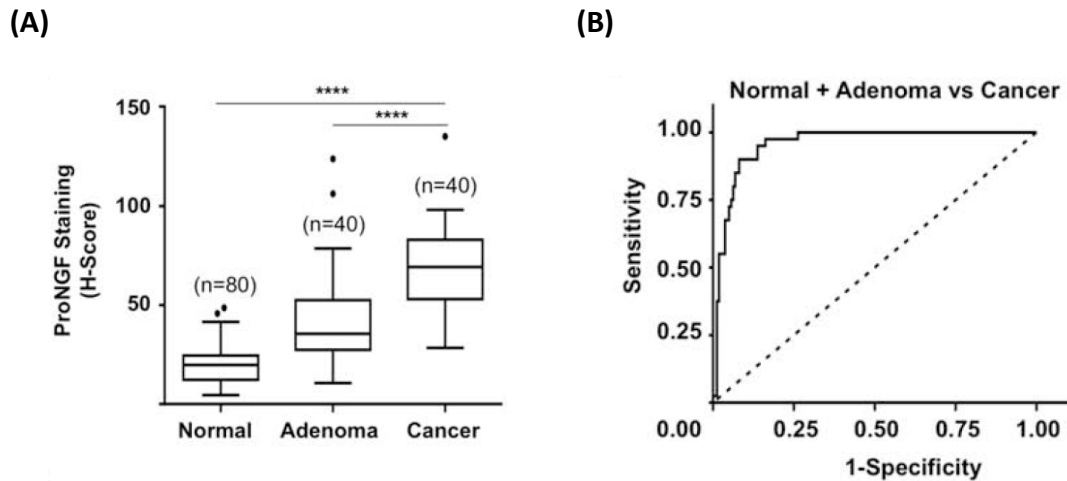


Figure 9: (A) Box and whisker plot quantifying proNGF expression in benign and malignant thyroid tissue (** $p < 0.0001$). (B) Receiver operating characteristic (ROC) curve for the ability of proNGF to discriminate between benign and malignant thyroid lesions. Reproduced from Faulkner *et al.*⁶⁷ with permission (CC BY 3.0).**

The biological plausibility for the role of proNGF-receptor signaling in thyroid cancer is supported by known genetic driver mutations in the TrkA signaling pathway. As previously outlined, TrkA is a receptor tyrosine kinase with downstream signaling via the RAS-BRAF-MEK-MAPK pathway (Figure 10).⁷¹ Increased proliferative signaling through this pathway appears to be a key driver of oncogenesis in thyroid tumours, as acquired mutations in TrkA, RET, RAS and BRAF are commonly found in PTC and FTC.⁷² Specifically, mutations in TrkA are sporadically acquired in up to 12% of papillary thyroid cancers.⁷³ Furthermore, TrkA is upregulated in some thyroid cancers.⁷⁴ Therefore, ligand-receptor interactions in this pathway are a plausible mechanism for proNGF mediated thyroid oncogenesis. However, the biological role of proNGF in thyroid cancer has not been elucidated.

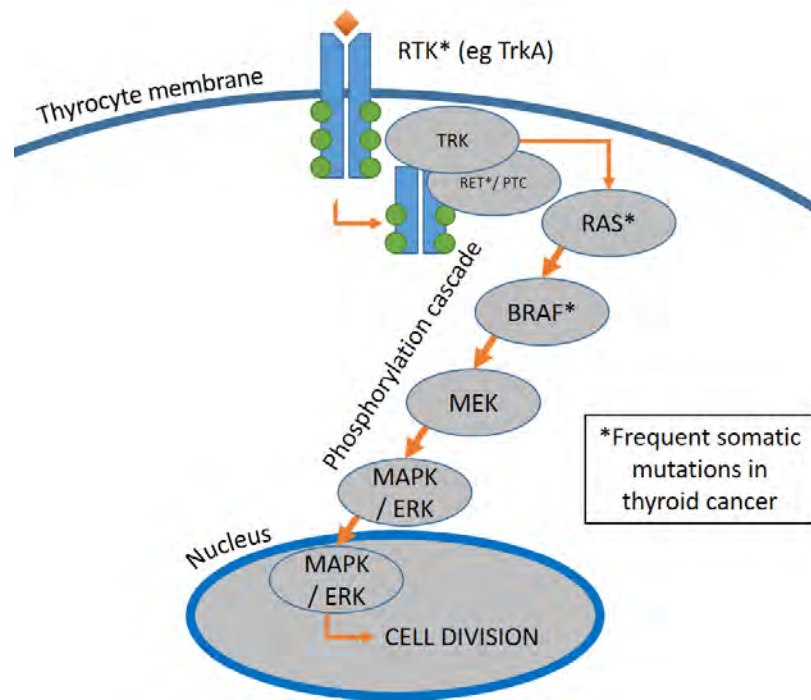


Figure 10: MAPK signalling pathway. RTK Receptor Tyrosine Kinase. Redrawn and adapted from Nikiforov *et al.*⁷¹

2.4.4 Relevance for proposed research

These data suggest the role of proNGF as a biomarker of thyroid cancer. However, these data also suggest that proNGF may have a role as a driver of thyroid cancer initiation or progression, both by inference from data from other cancers, as well as due to its unique over-expression in thyroid cancer cells. The mechanism by which proNGF exerts biological effects in thyroid cancer is not known, and it is not known whether thyroid cancer expresses receptors for neurotrophins, and whether these exert biological effects. These questions formed key hypotheses in this thesis.

2.5 Biomarkers for diagnosis of thyroid cancer

2.5.1 Clinical need

Current diagnostic tools are imperfect to determine whether thyroid nodules are benign or malignant. At present, best practice evaluation of thyroid nodules is to risk stratify clinically detected or incidentally discovered thyroid nodules for malignancy using thyroid ultrasound, with suspicious nodules proceeding to cytological assessment using fine-needle aspiration (FNA) biopsy.⁸ The frequency of each diagnostic category and the corresponding malignancy risk are both summarized in Table 1. As this table demonstrates, there is weak stratification of risk in the lower 4 categories of both the

Ultrasound (risk of malignancy 0 – 20%) and Cytology strata (risk of malignancy 0 – 30%), despite most nodules falling into these classifications (>75% of nodules for both risk scoring systems).

Table 1: Current best practice risk stratification for thyroid nodules using ultrasound and fine needle biopsy. FLUS: Follicular Lesion of Undetermined Significance. FN. Follicular neoplasm.

ATA 2016 Ultrasound Category	Frequency of Result ⁷⁵	Malignancy Risk & Recommended Action ⁸	Bethesda Biopsy Category	Frequency of Result ⁷⁶	Risk of Malignancy ⁷⁷
Benign	-	<1% No biopsy	Non-diagnostic	3%	1 – 4%
Very low suspicion	26%	<3% Biopsy >2cm	Benign	65%	0 – 3%
Low suspicion	38%	5 – 10% Biopsy >1.5cm	Atypia Undetermined Significance/FLUS	10%	5 – 30%
Intermediate suspicion	31%	10 – 20% Biopsy >1cm	Follicular neoplasm /Suspicious for FN	10%	10 – 30%
High Suspicion	4%	>70% Biopsy >1cm	Suspicious for malignancy	5%	60 – 75%
			Malignant	6%	97 – 99%

These data confirm that the majority (>95%) of thyroid nodules have <20% risk of malignancy, yet many still require an interventional procedure to evaluate. Additionally, 25% of biopsy results return an ‘indeterminate’ result, requiring further monitoring or surgical removal.⁷⁷ Further, a major issue with current diagnostic tests evaluating nodular thyroid disease is that both ultrasound and cytological interpretation are

subjective investigations that require a high level of operator expertise, and are resource intensive.⁸ Inexpensive, objective and reliable diagnostic biomarkers are required.

2.5.2 Blood-based diagnostic biomarkers

Sensitive and specific peptide-based serum biomarkers remain sought-after in clinical practice for both diagnosis and monitoring of cancers. Several solid-organ malignancies have established peptide-based biomarkers, which are useful in the diagnosis or prognosis of cancer. Examples include prostate specific antigen (PSA, prostate cancer), alpha-fetoprotein (AFP, testicular carcinoma and hepatocellular carcinoma), carcinoembryonic antigen (CEA) and CA19.9 (colorectal carcinoma).

Follicular cells of the thyroid uniquely synthesise the protein thyroglobulin, required in the production of thyroid hormone, and synthesis of this protein commonly persists following malignant transformation of thyroid follicular cells. Therefore, whilst thyroglobulin is not a useful diagnostic biomarker for thyroid cancer (as it is secreted by both benign and malignant follicular thyroid cells), it has established utility as a biomarker of recurrence in the follow up of patients who have had total thyroidectomy.⁸

Serum calcitonin, a specific peptide produced by the neuroendocrine thyroid tumour MTC, is an established sensitive serological biomarker for detection of MTC. Several large prospective studies have evaluated the efficacy of serum calcitonin in the evaluation of nodular thyroid disease.⁷⁸ Despite its high sensitivity and specificity, due to the rarity of MTC (approximately 50× less common than DTC) it remains controversial for use as a screening test as most positive results continue to be false positive, and recent clinical guidelines have failed to reach consensus on its use.⁸

In addition to peptide-based biomarkers, circulating tumour specific microRNAs (miRNA) or DNAs are under evaluation in many cancers, including thyroid cancer. In a recent review, Wojcicka *et al.* identified several possible candidate miRNAs that were identified in single studies, however, sensitivity ranges were 60 – 90%, while specificity was 57 – 88%.⁷⁹ Further, circulating tumour DNA has been shown in pilot studies to be an early marker of thyroid cancer recurrence,⁸⁰ although in small studies has not yet been shown useful in the assessment of thyroid nodules.⁸¹

However, there remains currently no serum biomarker in clinical practice for the diagnosis of DTC.

2.5.3 Biopsy-based diagnostic biomarkers

2.5.3.1 Protein

Needle rinse of FNA specimens is an established technique for detecting thyroglobulin (a ubiquitous thyroid-specific protein),⁸² which has utility in confirmation of metastatic thyroid lesions. Needle rinse calcitonin, as for serum, is sensitive and specific for the diagnosis of MTC and is a well-established technique for detecting this tumour type.⁸³ However, neither of these tests have utility in the most common clinical scenario of determining whether a thyroid nodule is benign or contains a DTC.

Although there are several established biomarkers for DTC by immunohistochemistry, including galectin-3 and cytokeratin-19, none exhibit sufficient sensitivity or specificity to be used in isolation or as a panel.^{84,85} Additionally, immunocytochemical analysis of thyroid biopsy specimens remains technically challenging due to small sample volumes and difficulty of standardization between laboratories. While proNGF may contribute usefully in the field of immunocytochemistry, its particular interest is as a secreted protein,⁵⁹ and its potential to be detected in serum or in needle wash fluid as a novel biomarker.

2.5.3.2 Gene panels

Genetic analysis of FNA material, either using a mRNA classifier system (measuring gene expression within the nodule) or extended next-generation sequencing (detecting the presence of point mutations or gene fusions) are available in some countries (although not Australia). These have been evaluated in the specific clinical setting of Bethesda Category 4 cytology (follicular lesion of undetermined significance).

Although a mutation panel of 7 genes (including BRAF, RAS, RET/PTC, PAX8/PPARc) has a reported specificity for malignancy of between 86 – 100%, a sensitivity as low as 44% when evaluating this cohort limits translational relevance.⁸ An extended gene expression classifier panel of 167 mRNAs has a reported sensitivity of up to 92%, and has been proposed as a possible “rule out” test, however, the low specificity of 48 – 53% again limits straightforward applicability.⁸ Whilst both tests are available commercially in the United States for over a decade, the lack of uptake more broadly speaks to the need for better biomarkers.

2.5.4 Relevance for proposed research

The discovery of objective biomarkers, either in blood or biopsy material, that reliably discriminate benign from malignant tissue would significantly improve the diagnostic efficiency of nodular thyroid disease. Whilst prognostic markers for thyroid cancer are established, diagnostic markers are wanting. Promising pilot data support the investigation of proNGF as a protein based biomarker in serum and biopsy material for the diagnosis of thyroid disease.

3 THE PRECURSOR FOR NERVE GROWTH FACTOR (PRoNGF) IS NOT A SERUM OR BIOPSY-RINSE BIOMARKER FOR THYROID CANCER DIAGNOSIS

3.1 Preface

This paper tests the hypothesis that proNGF is a discriminative biomarker for the diagnosis of thyroid cancer. This hypothesis is supported by prior data showing significant over-expression of proNGF in malignant thyroid tissue, and the detection of proNGF proteins and degradation products in serum and biological fluids in various conditions.

To test these hypotheses, two independent, but overlapping, cohort studies were established in Newcastle, Australia, to collect serum and biopsy samples from patients with benign and malignant thyroid diseases. The studies were sufficiently powered to provide pilot data on the diagnostic performance of proNGF in these media.


This paper is published in BMC Endocrine Disorders.

RESEARCH ARTICLE

Open Access



The precursor for nerve growth factor (proNGF) is not a serum or biopsy-rinse biomarker for thyroid cancer diagnosis

Christopher W. Rowe^{1,2,3*} , Sam Faulkner^{3,4}, Jonathan W. Paul^{1,3}, Jorge M. Tolosa^{1,3}, Craig Gedye^{3,4,5}, Cino Bendinelli^{1,6}, Katie Wynne^{1,2,3}, Shaun McGrath^{1,2}, John Attia^{1,3,7}, Roger Smith^{1,2,3} and Hubert Hondermarck^{3,4}

Abstract

Background: Nerves and neurotrophic growth factors are emerging promoters of cancer growth. The precursor for Nerve Growth Factor (proNGF) is overexpressed in thyroid cancer, but its potential role as a clinical biomarker has not been reported. Here we have examined the value of proNGF as a serum and biopsy-rinse biomarker for thyroid cancer diagnosis.

Methods: Patients presenting for thyroid surgery or biopsy were enrolled in separate cohorts examining serum ($n = 204$, including 46 cases of thyroid cancer) and biopsy-rinse specimens ($n = 188$, including 26 cases of thyroid cancer). ProNGF levels in clinical samples were analysed by ELISA. Univariate and multivariate statistical analyses were used to compare proNGF levels with malignancy status and clinicopathological parameters.

Results: ProNGF was not detected in the majority of serum samples (176/204, 86%) and the detection of proNGF was not associated with thyroid cancer diagnosis. In the few cases where proNGF was detected in the serum, thyroidectomy did not affect proNGF concentration, demonstrating that the thyroid was not the source of serum proNGF. Intriguingly, an association between hyperthyroidism and serum proNGF was observed (OR 3.3, 95% CI 1.6–8.7 $p = 0.02$). In biopsy-rinse, proNGF was detected in 73/188 (39%) cases, with no association between proNGF and thyroid cancer. However, a significant positive association between follicular lesions and biopsy-rinse proNGF was found (OR 3.3, 95% CI 1.2–8.7, $p = 0.02$).

Conclusions: ProNGF levels in serum and biopsy-rinse are not increased in thyroid cancer and therefore proNGF is not a clinical biomarker for this condition.

Keywords: Thyroid Cancer, proNGF, Biomarker, Serum, Biopsy-rinse

Background

Thyroid cancer is a common endocrine malignancy. In the United States, an average of 14 new cases per 100,000 person are diagnosed each year, with an annual increase in incidence of 3.6% since 1974 [1]. This rise is due to a combination of increased diagnosis of clinically indolent cancers, and a true but small increase in aggressive cases, with a corresponding small rise in incidence-based mortality [1]. Thus, the timely diagnosis of clinically significant

thyroid cancers is an important public health priority. These cancers must be distinguished from more common benign thyroid nodules, detected by ultrasound in 19–35% of adults [2]. At present, the diagnostic evaluation of nodular thyroid disease includes thyroid ultrasound and fine-needle aspiration (FNA) biopsy [3]. Importantly, no current technique can accurately predict clinically significant cancers from indolent thyroid cancers, as demonstrated by the “epidemic” of non-lethal papillary thyroid cancer in countries that have introduced neck ultrasound screening programs [4]. Therefore, blood-based and biopsy-based biomarkers are needed to refine the diagnosis and prognosis of thyroid cancers [5–7].

* Correspondence: Christopher.Rowe@hnehealth.nsw.gov.au

¹School of Medicine and Public Health, University of Newcastle, Newcastle, Australia

²Department of Endocrinology, John Hunter Hospital, Locked Bag 1 HMRC, Newcastle 2310, Australia

Full list of author information is available at the end of the article



© The Author(s). 2019 **Open Access** This article is distributed under the terms of the Creative Commons Attribution 4.0 International License (<http://creativecommons.org/licenses/by/4.0/>), which permits unrestricted use, distribution, and reproduction in any medium, provided you give appropriate credit to the original author(s) and the source, provide a link to the Creative Commons license, and indicate if changes were made. The Creative Commons Public Domain Dedication waiver (<http://creativecommons.org/publicdomain/zero/1.0/>) applies to the data made available in this article, unless otherwise stated.

Nerves and neurotrophic growth factors are emerging promoters of tumorigenesis and are increasingly regarded as potential biomarkers and therapeutic targets in oncology [8, 9]. The precursor for nerve growth factor (proNGF) has recently been shown to be overexpressed in thyroid cancer compared to benign thyroid tissues, suggesting utility as a discriminator in diagnostic testing [10]. ProNGF is a soluble 246 amino acid pro-peptide, transcribed from the nerve growth factor (*NGF*) gene on chromosome 1p13. ProNGF is cleaved into nerve growth factor (NGF) by tissue proconvertases such as furin and matrix metalloproteinases [11]. ProNGF has an established role in neural development in the foetus [12], and acts on neurons through interaction with specific NGF receptors to promote neural survival and differentiation, or apoptosis [11]. Interestingly, proNGF and its receptors have been associated with progression and aggressiveness of several cancers, including breast [13, 14], prostate [15], and melanoma [16]. In thyroid cancer, in addition to proNGF overexpression [10], the upregulation of proNGF/NGF receptors (the tyrosine kinase TrkA, the neurotrophin receptor p75^{NTR} and the pro-neurotrophin receptor sortilin) has been reported [17], suggesting a role for proNGF in thyroid carcinogenesis and a potential value as a diagnostic or prognostic biomarker.

In the present study, we hypothesized that the overexpression of proNGF may lead to an increased level of proNGF in the serum of patients with thyroid cancer, as compared with benign thyroid conditions, and might represent a useful biomarker for diagnosis and risk stratification of nodular thyroid disease. Further, we hypothesized that proNGF protein may also be detected in the needle-rinse of thyroid biopsy specimens, in a similar manner to the needle-rinse techniques used for assaying for thyroglobulin [18] and calcitonin [19]. Here we report the results of studies evaluating these hypotheses in nodular thyroid disease.

Methods

Patients and samples

This study was approved by the Hunter New England Local Health District Human Research Ethics Committee (HREC/16/HNE/247), and all participants provided written informed consent. To collect serum, we conducted a prospective nested cohort study, enrolling patients undergoing thyroid surgery or thyroid fine-needle aspiration biopsy for investigation or management of thyroid disease. To collect biopsy material, we conducted a prospective cohort study of patients referred for thyroid FNA biopsy at a single high-volume clinic.

In both cohorts, patients were followed after bio specimen collection to obtain a final diagnosis of their thyroid disease based on histopathology (surgical patients) or a

composite clinical assessment (clinical, ultrasound and FNA biopsy) for non-surgical patients. Relevant clinical data were extracted from the medical record to correlate levels of proNGF with age, sex, presence of hyperthyroidism (defined as thyroid stimulating hormone (TSH) level < 0.1 mIU/L), and thyroid histopathology.

Serum study

Prior to thyroid surgery or thyroid biopsy, serum was drawn into a serum separator tube (surgery-only patients) or plain serum tube (biopsy-first patients), centrifuged to separate, then aliquoted and frozen at -80 °C. Serum samples were assayed using a proNGF enzyme-linked immunosorbent assay (ELISA) (see below) on the first or second freeze-thaw cycle only. Samples were run in triplicate at 1:20 dilution (to minimize matrix effects, as recommended by the manufacturer), with positive results confirmed on a second plate; and run with an in-house quality control (QC) samples of serum spiked with recombinant human proNGF (Biosensis Pty Ltd., Adelaide, Australia). 4-parameter logistic regression curves were fit using GraphPad Prism (v7.0 California, USA). All results above the limit of detection of 0.05 ng/mL (a functional limit of 1 ng/mL allowing for 20x dilution) were reported as proNGF positive.

Biopsy rinse study

Consecutive consenting adults over 18 years with a thyroid nodule graded as 'Low-', 'Intermediate-' or 'High-risk', according to the Sonographic Pattern stratification of the 2015 American Thyroid Association [3], were prospectively enrolled. Each nodule was biopsied using a 25 g needle with capillary action technique. After expulsion of the cellular material for diagnostic cytopathology, the needle was rinsed with 0.5 mL phosphate-buffered saline at 4 °C with the addition of protease inhibitors (cOmplete Mini, Roche, Mannheim Germany, Catalogue number 046931590011, 1 tablet per 10 mL), with subsequent refrigerated centrifugation to pellet red blood cells and insoluble debris. The supernatant containing solubilised proteins was removed and stored at -80 °C prior to ELISA, performed without dilution in duplicate (due to constraints on sample volume) and analysed as above. This 'needle-rinse' technique is established as a sensitive method of detecting the thyroid-specific proteins thyroglobulin (an established biopsy-based tumour marker for metastatic thyroid cancer) [18] and calcitonin (an established biopsy-based tumour marker for medullary thyroid cancer) [19], and has the advantage of preserving cytological material for diagnostic purposes whilst potentially yielding additional information from the solubilised proteins. All results above the limit of detection of 0.05 ng/mL were reported as proNGF positive.

ProNGF ELISA validation

ProNGF was quantified using a human enzyme-linked immunosorbent assay kit (BEK-2226; Biosensis Pty Ltd., Adelaide, Australia), with wells coated with an antibody raised against the N-terminal precursor domain of human proNGF. Heterophilic antibody blockers were added as recommended by the manufacturer [20] to a final concentration of 38 µg/mL.

Performance of the proNGF ELISA was confirmed using spike and recovery and linearity of dilution experiments (Additional file 1: Table S1). A mean of 96% spike recovery was obtained (range 80–128%) when assayed in the presence of supplied heterophilic antibody blockers. Mean recovery of the in-house QC sample, which was assayed across all plates, was $98 \pm 22\%$ for serum, and $117 \pm 20\%$ for rinse. The between assay coefficient of variation was 20%, and the within-assay coefficient of variation (between wells) was $3.6 \pm 2.9\%$.

For serum, no difference in rates of proNGF detection were observed in samples collected in serum-separator (16% positive, $n = 95$) vs plain serum tubes (12% positive, $n = 109$) (unadjusted $p = 0.42$; adjusted for age, sex and thyroid hormone status $p = 0.79$), suggesting that proNGF is not sequestered in the gel layer of a serum separator tube. Additionally, no difference in levels of proNGF detection were observed in samples stored for more than 12 months (13%, $n = 117$), compared to less than 12 months (21%, $n = 87$) (unadjusted $p = 0.21$, adjusted for age, sex, thyroid cancer and hyperthyroidism $p = 0.79$), suggesting that endogenous proNGF is stable at -80°C for at least 12 months.

Statistical analysis

Power calculations were based on pilot data, using a power of 0.8 and two sided alpha of 0.05. For the serum study, to detect a 3-fold increase in proNGF levels in patients with cancer, above the background detection of proNGF cleavage products in 6–10% of healthy sera [21], 46 cases and 160 controls were required. For the biopsy study, the diagnostic performance of proNGF in histological specimens generated an area under the ROC curve of 0.94 [10]. Conservatively assuming that our tests generate an AUC ROC of 0.85, and that the minimum clinically significant value is 0.7, 28 cases with thyroid cancer and 124 benign nodules were required.

Between group comparisons were assessed categorically using the Pearson's Chi-square test, and continuously using the Wilcoxon Rank-Sum test, with multiple logistic regression to assess for potential interaction from clinical variables. Analyses were performed using the statistical software package Stata (version 14, Statacorp, Texas, USA).

Between 2014 and 2017, 204 patients with thyroid diseases were enrolled in the serum cohort (46 cases of

thyroid cancer and 158 cases of benign thyroid conditions); and between 2016 and 2018, 183 patients with 188 nodules were enrolled in the biopsy cohort (26 cases of thyroid cancer and 162 benign nodules). Demographic and clinical information regarding the two cohorts are presented in Table 1.

Results

Serum proNGF concentration is not associated with thyroid cancer

Overall, 176/204 (86%) of serum samples were negative for proNGF. In the remaining 14% of serum samples in which proNGF could be detected, median serum proNGF concentration was 6.2 ng/mL (IQR 4.2–12.4 ng/mL). With respect to the primary hypothesis, positive serum proNGF was detected in 6/46 (13%) cases of thyroid cancer, and in 22/158 (14%) benign samples ($p = 0.97$). The 6 positive results in the malignant group occurred in 5/36 papillary thyroid cancers and 1/8 follicular/hurthle-cell thyroid cancers (Additional file 2: Table S2). Median proNGF levels were not significantly different between benign and malignant cohorts (Table 2). Therefore proNGF is not a serum biomarker for thyroid cancer diagnosis.

Post-thyroidectomy sera (range 2–14 days post-operative) were available for analysis, with 11 cases positive for proNGF, and 20 cases negative for proNGF. Figure 1a shows 10/11 (91%) cases with detectable pre-operative proNGF (median 5.8 ng/mL, IQR 4.9–8.2) remained positive in the post-thyroidectomy sample (median 2.8 ng/mL, IQR 2.1–4.5). 18/20 (90%) cases with negative pre-operative proNGF had a concordant post-thyroidectomy sample. As the in-vitro serum half-life of proNGF was determined to be 90 min (Fig. 1b), our results suggest that the proNGF detected in the serum was not of thyroid origin.

Serum proNGF may be associated with hyperthyroidism

Analysis of serum proNGF data was undertaken in subgroups of hyperthyroidism, age and sex (Table 2). ProNGF was above 1 ng/mL in 9/28 (32%) of hyperthyroid cases, compared to 19/176 (11%) of euthyroid cases (Pearson's chi-square $p = 0.002$, Fig. 2a). ProNGF levels were higher in sera from patients who were hyperthyroid at the time of sampling (TSH $< 0.1\text{mIU/L}$) than in those who were euthyroid (proNGF interquartile range 0–1.76 ng/mL vs 0–0 ng/mL respectively, Wilcoxon Rank-Sum $p = 0.002$, Fig. 2b). No difference was observed in proNGF levels based on age or sex or follicular lesions. Multiple logistic regression was performed to assess the interaction of thyroid cancer, age, sex, follicular lesion and hyperthyroid status on serum proNGF levels (Table 2). The odds ratio for serum proNGF $> 1\text{ ng/mL}$ (compared to $\leq 1\text{ ng/mL}$, the assay limit of detection) in the presence of hyperthyroidism, holding other variables constant, was 3.3 (95% CI 1.6–

Table 1 Patient Demographics

	Serum study		Biopsy study	
<i>N</i>	204		188	
Female (<i>n</i> , %)	162 (79%)		153 (81%)	
Age, years (mean ± SD)	53 ± 16		55 ± 15	
TSH, mIU/L (mean ± SD)	1.1 ± 1.3		1.3 ± 0.88*	
TSH < 0.1 mIU/L (<i>n</i> , %)	28 (14%)		1 (1%)	
Nodule Diagnosis				
Thyroid cancer (<i>n</i> , %)	46 (24%)		26 (14%)	
Papillary	36		19	
Follicular/Hurthle carcinoma	8		5	
Anaplastic	1		2	
Medullary	1		0	
Benign nodule (<i>n</i> , %)	158 (76%)		162 (86%)	
Nodular goitre	109		139	
Follicular/Hurthle adenoma	13		15	
Graves'	25		1	
Lymphocytic	9		7	
Normal	2		0	
Diagnostic basis	Histology	Follow up	Histology	Follow up
Thyroid Cancer	46	0	25	1#
Benign nodule	82	74	41	121

*TSH data not available for 9 cases. #One patient with anaplastic cancer did not undergo thyroidectomy

Table 2 Serum proNGF levels, grouped by demographic and disease classification. Differences between groups are assessed using Pearson's Chi-Square test (binary classification at the 1 ng/mL limit of detection) and Wilcoxon Rank-Sum test (continuous)

Category	Serum proNGF (dichotomised)		Serum proNGF (continuous)		Multiple logistic regression*	
	<i>n</i> > 1 ng/mL/ <i>n</i> in group	<i>p</i> -value	Median (IQR)	<i>p</i> -value	OR (95% CI)	<i>p</i> -value
Overall	28/204 (14%)					
By malignancy status		0.88		0.97	1.0 (0.4–2.7)	0.98
-Thyroid cancer	6/46 (13%)		0 (0–0)			
-Benign thyroid diseases	22/158 (14%)		0 (0–0)			
By thyroid hormone status		0.002		0.002	3.3 (1.3–8.7)	0.02
-Hyperthyroid	9/28 (32%)		0 (0–1.74)			
-Euthyroid	19/176 (11%)		0 (0–0)			
By follicular lesion		0.93				
-Present	3/21 (14%)		0 (0–0)	0.80	1.1 (0.3–4.2)	0.88
-Absent	25/183 (14%)		0 (0–0)			
By age		0.20		0.11	1.0 (1.0–1.0)	0.18
-Age < 55	18/108 (17%)		0 (0–0)			
-Age \geq 55	10/96 (10%)		0 (0–0)			
By sex		0.53		0.54	0.7 (0.3–1.8)	0.44
-Female	21/162 (13%)		0 (0–0)			
-Male	7/42 (17%)		0 (0–0)			

Categorical variables evaluated with Pearson's Chi-square, and continuous variables with the Wilcoxon RankSum test. *Binary outcome variable is proNGF > 1 ng/mL, adjusting for age (continuous) presence of cancer, presence of hyperthyroidism, presence of follicular lesion, and female sex

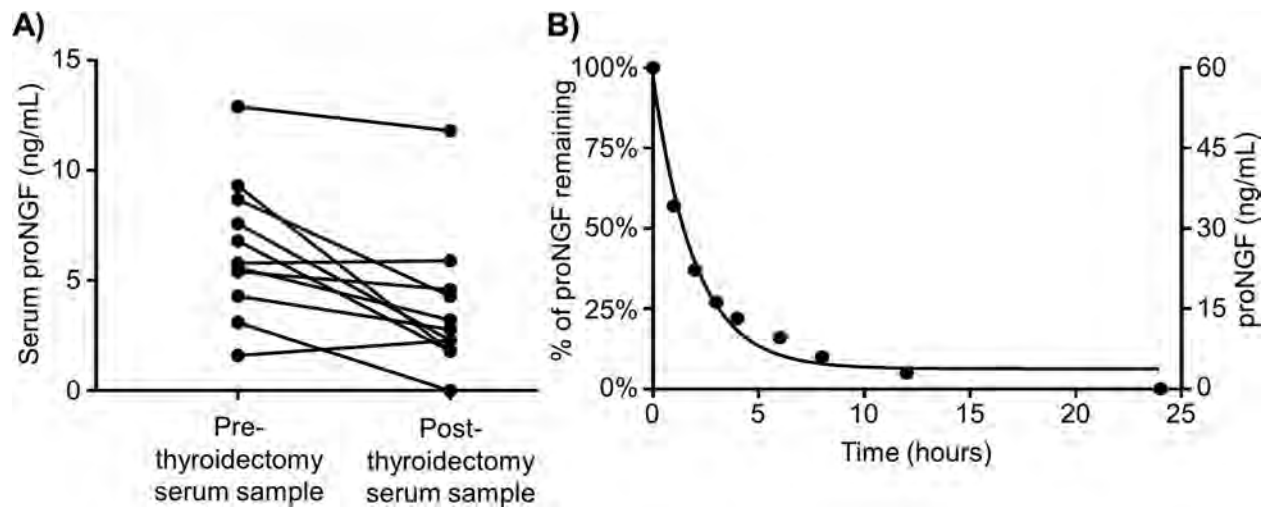


Fig. 1 ProNGF serum levels after thyroidectomy and half-life. **a** Change in serum proNGF following total thyroidectomy. Pre- and post-thyroidectomy serum samples were available for 11 cases where pre-operative serum proNGF was detectable. No significant difference was detected between pre- and post- thyroidectomy levels of proNGF. **b** ProNGF in vitro half-life. Aliquots of serum negative for proNGF was spiked with 20 ng/mL recombinant proNGF dissolved in Assay Diluent A (Biosensis, Australia) in a 1:1 ratio, then incubated at 37 °C for increments of 24 h, then assayed at 1:20 dilution with Heterophilic Blocking Antibody (BL-003-1000). An exponential decay curve was fitted, giving an estimated in-vitro half-life in serum of 1.5 h. Similar results were obtained using phosphate-buffered-saline as diluent

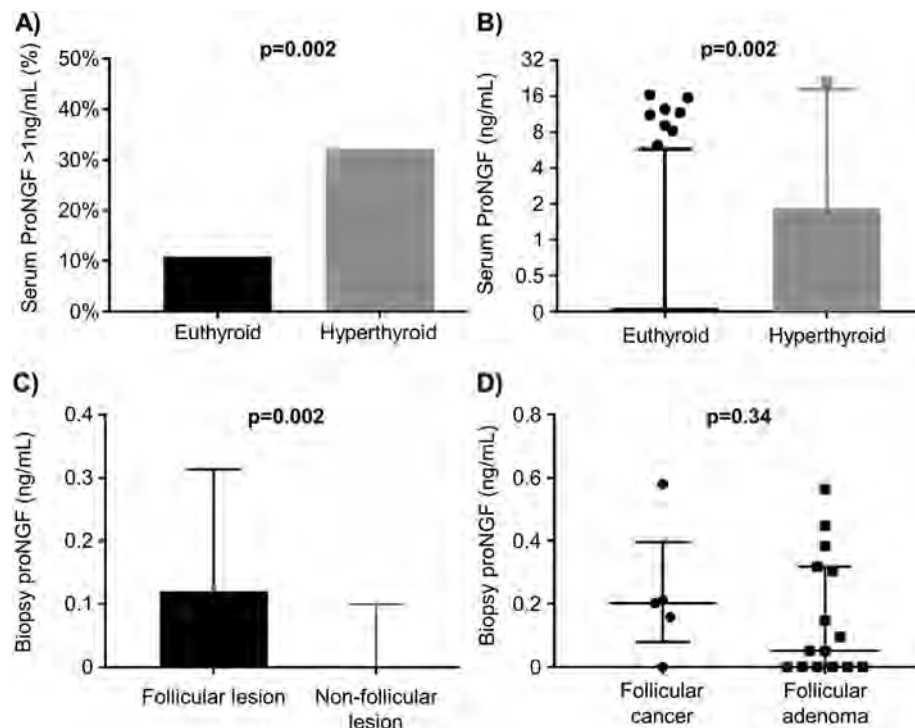


Fig. 2 Subgroup analysis of proNGF. **a** Bar graph showing detection of serum proNGF as a binary variable, stratified by hyperthyroid status. See Table 2 for details. **b** Box (interquartile range) and whisker (5–95% range) demonstrating detection of serum proNGF as a continuous variable, stratified by hyperthyroid status. See Table 2 for details. **c** Box (interquartile range) and whisker (5–95% range) graph showing concentration of proNGF in biopsy rinse, stratified the presence of follicular lesions. See Table 3 for details. **d** Scatter plot (with median and interquartile range overlaid) showing concentration of proNGF in biopsy-rinse, stratified by malignant status of follicular lesions. See Table 3 for details

8.7 $p = 0.02$). No association was found with the other parameters, and there was no confounding observed.

Biopsy rinse proNGF is not associated with thyroid cancer

Overall, 73/188 (39%) of biopsy-rinse specimens were positive for proNGF. Median proNGF concentration in positive samples was 0.15 ng/mL (IQR 0.1–0.2 ng/mL). With respect to the primary hypothesis, biopsy-rinse proNGF was detected in 12/26 (46%) nodules with thyroid cancer, and in 61/162 (38%) benign nodules ($p = 0.41$). The 12 positive results in the malignant group occurred in 7/19 papillary thyroid cancers (37%) and 4/5 follicular/Hurthle-cell thyroid cancers (80%). Median proNGF levels were not significantly different between benign and malignant thyroid nodules (Table 3). Individual patient characteristics for the 73 cases of detectable proNGF are presented in Additional file 3: Table S3.

Biopsy rinse proNGF may be associated with follicular lesions

Analysis of the biopsy-rinse proNGF cohort was undertaken in subgroups of age, sex and follicular lesions (including follicular adenoma, Hurthle cell adenoma, follicular carcinoma and Hurthle cell carcinoma) (Table 3). Insufficient patients were hyperthyroid at the time of biopsy (as hyperfunctioning nodules have a low risk of malignancy and are rarely biopsied) for analysis of this cohort by hyperthyroid status (see Table 1). ProNGF levels were higher from follicular lesions (median 0.12 vs 0 ng/mL, $p = 0.002$) compared to other nodules (Fig. 2c). However, proNGF was detected at similar rates in both benign (9/15, 60%) and malignant (4/5, 80%) follicular lesions, suggesting that

this is not a useful discriminative marker for follicular thyroid cancer ($p = 0.42$), and there was no difference in concentration of proNGF between benign and malignant follicular lesions (Fig. 2d, $p = 0.34$). Multiple logistic regression, dichotomizing biopsy proNGF at 0.05 ng/mL (negative/positive) as the dependent variable, and including model variables of age, sex, follicular lesion and malignant status, continued to demonstrate an association between proNGF and follicular lesions (odds ratio 3.3, 95% CI 1.2–8.7, $p = 0.02$), holding other parameters constant (Table 3). No other parameter showed significant association and there was no evidence of confounding.

Discussion

The over-diagnosis of clinically indolent thyroid cancer necessitates the development of biomarkers that better predict future disease aggressiveness to allow clinicians and patients to match treatment intensity with disease risk. An inexpensive protein-based biomarker in serum, or as an adjunct to needle biopsy, represents an attractive translational biomarker, and pilot data for proNGF suggested a possible utility for this protein in this role [10].

This present study, reporting proNGF evaluation in a large cohort of serum and biopsy material, found no difference in levels of proNGF between cases of thyroid cancer and other thyroid diseases. The study was adequately powered to detect clinically meaningful differences in proNGF levels. A smaller difference is unlikely to be clinically useful as a biomarker of thyroid malignancy. Therefore, the increased level of proNGF tissue expression in thyroid cancer previously observed [10] does not result in an increased proNGF concentration in

Table 3 Biopsy rinse proNGF levels, stratified by nodule diagnosis

Category	Biopsy-rinse proNGF (dichotomised)		Biopsy-rinse proNGF (continuous)		Multiple logistic regression*	
	$n > 0.05$ ng/mL/n in group	p -value	ng/mL Median (IQR)	p -value	OR (95% CI)	p -value
Overall	73/188 (39%)		0 (0–0.12)			
By malignancy status		0.41		0.11	1.3 (0.5–3.1)	0.57
-Thyroid cancer	12/26 (46%)		0 (0–0.20)			
-Benign nodule	61/162 (38%)		0 (0–0.10)			
By follicular lesion		0.01		0.002	3.3 (1.2–8.7)	0.02
-Present	13/20 (65%)		0.12 (0–0.31)			
-Absent	60/168 (36%)		0 (0–0.11)			
By age		0.61		0.82	1.0 (1.0–1.0)	0.87
-Age < 55	39/96 (41%)		0 (0–0.11)			
-Age ≥ 55	34/92 (37%)		0 (0–0.13)			
By sex		0.35		0.33	0.7 (0.2–2.3)	0.35
-Female	57/153 (37%)		0 (0–0.11)			
-Male	16/35 (46%)		0 (0–0.17)			

Categorical variables evaluated with Pearson's Chi-square, and continuous variables with the Wilcoxon RankSum test. *Binary outcome variable is proNGF > 0.05 ng/mL, adjusting for age (continuous) presence of cancer, presence of follicular lesion and female sex

the serum of thyroid cancer patients, or provide a sufficiently discriminatory level of proNGF in biopsy specimens, demonstrating that, based upon these data, serum and biopsy-rinse proNGF is not of clinical value for the diagnosis or prognosis of thyroid cancer.

A prior study has examined the presence of proNGF in sera of 20 patients with and without diabetic retinopathy, using Western blotting [22]. They found that a small subset of patients with diabetic retinopathy had detectable serum proNGF, although exact quantification was not possible due to the limitations of Western blot methodology. A study of 227 patients with autoimmune diseases measured LIP1 and LIP2 (short cleavage products of proNGF peptide) in serum using ELISA, with rates of positivity in control serum of 6 and 10% respectively. These findings are concordant with the present study [21]. Contrastingly, a recent study of 116 patients (77 with Parkinson's Disease and 39 healthy controls) detected serum proNGF using ELISA in all participants at a very low level, in the range of 0.085–0.122 ng/mL, 10–100 fold lower than detected in our study [23]. Together, these data and our study indicate generally low levels of proNGF in human sera across a variety of conditions. There were no prior data on the levels of proNGF in thyroid biopsy specimens.

The majority of patients with thyroid cancers included in both the serum and needle-rinse studies were diagnosed with the papillary subtype, and it is possible that other subtypes (follicular, medullary) may have different systemic expression patterns of proNGF. However, previous immunohistochemistry data demonstrated that the strongest overexpression of proNGF was in papillary cancers [10], so any positive signal would have been expected in this group. Medullary thyroid cancers, derived from neuro-endocrine parafollicular C-cells, may be more likely to secrete a neurotrophins such as proNGF [24, 25]. However, medullary tumors have established and highly sensitive serum biomarkers: calcitonin and carcino-embryonic antigen [26], and therefore the clinical utility of additional markers may have limited translational value.

Intriguingly, our study observed an association between serum proNGF and hyperthyroidism, which has not previously been described in humans. However, studies in mice have shown that administration of the thyroid hormones T4 or T3 increases synthesis of NGF in mouse submandibular glands and brain [27–31]. Black and colleagues [27] demonstrated increased *NGF* mRNA production in neonatal mouse salivary glands for 24–72 h following a single intravenous injection of thyroid hormone (triiodothyronine, T3). These previous animal studies and our present investigation suggest a thyroid-hormone regulated transcription of the *NGF* gene that may account for some of the cases of

detectable serum proNGF, although this observation requires validation in a larger cohort of hyperthyroid patients. We hypothesise that the detected proNGF is not of thyroidal origin, as it remained present in the serum of 91% of cases for which a paired post-thyroidectomy sample was available, but rather is likely to be secreted from an alternate site, such as salivary glands [32] under the regulation of thyroid hormone.

Conclusions

In conclusion, these data show that proNGF is not a useful clinical biomarker of thyroid malignancies. From a translational perspective, it is important to report data on both biomarkers that show promises as well as those that are not clinically useful. In addition, the association between proNGF and hyperthyroidism that we have observed warrants further investigation to better understand the molecular and/or functional relationship between proNGF and hyperthyroidism.

Supplementary information

Supplementary information accompanies this paper at <https://doi.org/10.1186/s12902-019-0457-1>.

Additional file 1: Table S1. (A-E): ProNGF ELISA Validation Experiments – Serum and Rinse. **A:** Effect of heterophilic antibody blockers (Ab) (BL-003-1000, Biosensis, Australia) on rate of positivity of serum proNGF levels. **B:** Spike and Recovery Experiments. **C:** Inter-plate Quality Control Samples **D:** Linearity of Dilution **E:** Linearity of Dilution of Biopsy Rinse Diluent.

Additional file 2: Table S2. Individual patient characteristics for cases with detectable serum proNGF.

Additional file 3: Table S3. Individual patient characteristics for cases with detectable biopsy proNGF. Age is presented as a range to preserve anonymity.

Abbreviations

ELISA: Enzyme-linked immunosorbent assay; FNA: Fine needle aspiration; NGF: Nerve growth factor; ProNGF: Precursor for nerve growth factor; QC: Quality control; TSH: Thyroid stimulating hormone

Acknowledgements

The authors acknowledge the assistance of Ms. Rosemary Carroll (Department of Surgery, John Hunter Hospital) with serum collection; Dr. Julie Weigner & Ms. Sharon Ling (NSW Health Pathology, Hunter) with biopsy preparation, and Ms. Catherine Fenwick (Newcastle Endocrinology) for assistance with recruitment.

Author's contributions

CR and HH conceived and conducted the study, analysed the data and drafted the manuscript, with contributions to study design and analysis from JA, and RS. SF, JP and JT contributed to ELISA optimisation. CB, KW and SM contributed to recruitment. CG contributed to interpretation. All authors have reviewed and approved the final manuscript.

Funding

This work was supported by a Hunter New England LHD Clinical Research Fellowship, and a Hunter Cancer Research Alliance Pilot Grant and an Australian Government Research Training Program Scholarship (to CR). None of the funding bodies had any role in the design of the study, or the collection, analysis, and interpretation of data, or in writing the manuscript.

Availability of data and materials

All data generated or analysed during this study are included in this published article [and its supplementary information files].

Ethics approval and consent to participate

This study was prospectively approved by the Hunter New England Local Health District Human Research Ethics Committee (HREC/16/HNE/247) and all participants provided written informed consent to participate.

Consent for publication

All participants provided written informed consent for study data to be published.

Competing interests

HH holds intellectual property for the use of proNGF as a diagnostic test in cancer. The other authors report nothing to disclose.

Author details

¹School of Medicine and Public Health, University of Newcastle, Newcastle, Australia. ²Department of Endocrinology, John Hunter Hospital, Locked Bag 1 HMRC, Newcastle 2310, Australia. ³Hunter Medical Research Institute, New Lambton Heights, Australia. ⁴School of Biomedical Sciences and Pharmacy, University of Newcastle, Newcastle, Australia. ⁵Department of Surgery, John Hunter Hospital, Newcastle, Australia. ⁶Department of Medical Oncology, Calvary Mater Newcastle, Waratah, Australia. ⁷Clinical Research Design, IT, and Statistical Support Unit, Hunter Medical Research Institute, Newcastle, Australia.

Received: 3 June 2019 Accepted: 13 November 2019

Published online: 27 November 2019

References

1. Lim H, Devesa SS, Sosa JA, Check D, Kitahara CM. Trends in thyroid Cancer incidence and mortality in the United States, 1974–2013. *JAMA*. 2017; 317(13):1338–48.
2. Dean DS, Gharib H. Epidemiology of thyroid nodules. *Best Pract Res Clin Endocrinol Metab*. 2008;22(6):901–11.
3. Haugen BR, Alexander EK, Bible KC, Doherty GM, Mandel SJ, Nikiforov YE, Pacini F, Randolph GW, Sawka AM, Schlumberger M, et al. 2015 American Thyroid Association management guidelines for adult patients with thyroid nodules and differentiated thyroid Cancer: the American Thyroid Association guidelines task force on thyroid nodules and differentiated thyroid Cancer. *Thyroid*. 2016;26(1):1–133.
4. Ahn HS, Kim HJ, Welch HG. Korea's thyroid-cancer "epidemic"—screening and overdiagnosis. *N Engl J Med*. 2014;371(19):1765–7.
5. Hu Y, Wang H, Chen E, Xu Z, Chen B, Lu G. Candidate microRNAs as biomarkers of thyroid carcinoma: a systematic review, meta-analysis, and experimental validation. *Cancer Med*. 2016;5(9):2602–14.
6. Nixon AM, Provatospoulou X, Kalogera E, Zografos GN, Gounaris A. Circulating thyroid cancer biomarkers: current limitations and future prospects. *Clin Endocrinol*. 2017;87(2):117–26.
7. Makki FM, Taylor SM, Shahnavaz A, Leslie A, Gallant J, Douglas S, Teh E, Trites J, Bullock M, Inglis K, et al. Serum biomarkers of papillary thyroid cancer. *J Otolaryngol Head Neck Surg*. 2013;42(1):16.
8. Griffin N, Faulkner S, Jobling P, Hondermarck H. Targeting neurotrophin signaling in cancer: the renaissance. *Pharmacol Res*. 2018;135:12–7.
9. Faulkner S, Jobling P, March B, Jiang CC, Hondermarck H. Tumor neurobiology and the war of nerves in Cancer. *Cancer Discov*. 2019; 9(6):702–10.
10. Faulkner S, Roselli S, Demont Y, Pundavela J, Choquet G, Leissner P, Oldmeadow C, Attia J, Walker MM, Hondermarck H. ProNGF is a potential diagnostic biomarker for thyroid cancer. *Oncotarget*. 2016;7:28488–97.
11. Hondermarck H. Neurotrophins and their receptors in breast cancer. *Cytokine Growth Factor Rev*. 2012;23(6):357–65.
12. Levi-Montalcini R. The nerve growth factor: thirty-five years later. *Biosci Rep*. 1987;7(9):681–99.
13. Tomellini E, Touil Y, Lagadec C, Julien S, Ostyn P, Ziental-Gelus N, Meignan S, Lengrand J, Adriaenssens E, Polakowska R, et al. Nerve growth factor and proNGF simultaneously promote symmetric self-renewal, quiescence, and

- epithelial to mesenchymal transition to enlarge the breast cancer stem cell compartment. *Stem Cells*. 2015;33(2):342–53.
14. Demont Y, Corbet C, Page A, Ataman-Onal Y, Choquet-Kastylevsky G, Flinaux I, Le Bourhis X, Toillon R-A, Bradshaw RA, Hondermarck H. Pro-nerve growth factor induces Autocrine stimulation of breast Cancer cell invasion through Tropomyosin-related kinase (a TrkA) and Sortilin protein. *J Biol Chem*. 2012;287(3):1923–31.
15. Pundavela J, Demont Y, Jobling P, Lincz LF, Roselli S, Thorne RF, Bond D, Bradshaw RA, Walker MM, Hondermarck H. ProNGF correlates with Gleason score and is a potential driver of nerve infiltration in prostate cancer. *Am J Pathol*. 2014;184(12):3156–62.
16. Truzzi F, Marconi A, Lotti R, Dallaglio K, French LE, Hempstead BL, Pincelli C. Neurotrophins and their receptors stimulate melanoma cell proliferation and migration. *J Invest Dermatol*. 2008;128(8):2031–40.
17. Faulkner S, Jobling P, Rowe CW, Rodrigues Oliveira SM, Roselli S, Thorne RF, Oldmeadow C, Attia J, Jiang CC, Zhang XD, et al. Neurotrophin receptors TrkA, p75(NTR), and Sortilin are increased and targetable in thyroid Cancer. *Am J Pathol*. 2018;188(1):229–41.
18. Moon JH, Kim YI, Lim JA, Choi HS, Cho SW, Kim KW, Park HJ, Paeng JC, Park YJ, Yi KH, et al. Thyroglobulin in washout fluid from lymph node fine-needle aspiration biopsy in papillary thyroid cancer: large-scale validation of the cutoff value to determine malignancy and evaluation of discrepant results. *J Clin Endocrinol Metab*. 2013;98(3):1061–8.
19. Kudo T, Miyauchi A, Ito Y, Takamura Y, Amino N, Hirokawa M. Diagnosis of medullary thyroid carcinoma by calcitonin measurement in fine-needle aspiration biopsy specimens. *Thyroid*. 2007;17(7):635–8.
20. Biosensis. BEK-2226 Human proNGF Rapid ELISA Kit. Adelaide, Australia: Biosensis Pty Ltd; 2015.
21. Dicou E. High levels of the proNGF peptides LIP1 and LIP2 in the serum and synovial fluid of rheumatoid arthritis patients: evidence for two new cytokines. *J Neuroimmunol*. 2008;194(1–2):143–6.
22. Mysona BA, Matragoon S, Stephens M, Mohamed IN, Farooq A, Bartasis ML, Fouda AY, Shanab AY, Espinosa-Heidmann DG, El-Remessy AB. Imbalance of the nerve growth factor and its precursor as a potential biomarker for diabetic retinopathy. *Biomed Res Int*. 2015;2015:571456.
23. Xu X-M, Dong M-X, Feng X, Liu Y, Pan J-X, Jia S-Y, Cao D, Wei Y-D. Decreased serum proNGF concentration in patients with Parkinson's disease. *Neurol Sci*. 2018;39(1):91–6.
24. Bigazzi M, Revoltella R, Aand SC, Vigneti E. High level of a nerve growth factor in the serum of a patient with medullary carcinoma of the thyroid gland. *Clin Endocrinol*. 1977;6(2):105–12.
25. Dicou E, Lee J, Brachet P. Synthesis of nerve growth factor mRNA and precursor protein in the thyroid and parathyroid glands of the rat. *Proc Natl Acad Sci U S A*. 1986;83(18):7084–8.
26. Costante G, Meringolo D, Durante C, Bianchi D, Nocera M, Tumino S, Crocetti U, Attard M, Maranghi M, Torlontano M, et al. Predictive value of serum calcitonin levels for preoperative diagnosis of medullary thyroid carcinoma in a cohort of 5817 consecutive patients with thyroid nodules. *J Clin Endocrinol Metab*. 2007;92(2):450–5.
27. Black MA, Pope L, Lefebvre FA, Lefebvre YA, Walker P. Thyroid hormones precociously increase nerve growth factor gene expression in the submandibular gland of neonatal mice. *Endocrinology*. 1992;130(4):2083–90.
28. Black MA, Lefebvre FA, Pope L, Lefebvre YA, Walker P. Thyroid hormone and androgen regulation of nerve growth factor gene expression in the mouse submandibular gland. *Mol Cell Endocrinol*. 1992;84(1–2):145–54.
29. Aloe L, Levi-Montalcini R. Comparative studies on testosterone and L-thyroxine effects on the synthesis of nerve growth factor in mouse submaxillary salivary glands. *Exp Cell Res*. 1980;125(1):15–22.
30. Walker P, Weichsel ME Jr, Hoath SB, Poland RE, Fisher DA. Effect of thyroxine, testosterone, and corticosterone on nerve growth factor (NGF) and epidermal growth factor (EGF) concentrations in adult female mouse submaxillary gland: dissociation of NGF and EGF responses. *Endocrinology*. 1981;109(2):582–7.
31. Walker P, Weil NL, Weichsel ME Jr, Fischer DA. Effect of thyroxine on nerve growth factor concentration in neonatal mouse brain. *Life Sci*. 1981;28(15–16):1777–87.
32. Nam JW, Chung JW, Kho HS, Chung SC, Kim YK. Nerve growth factor concentration in human saliva. *Oral Dis*. 2007;13(2):187–92.

Publisher's Note

Springer Nature remains neutral with regard to jurisdictional claims in published maps and institutional affiliations.

Additional Table 1 (A-E): ProNGF ELISA Validation Experiments – Serum and Rinse

1A: Effect of heterophilic blocking antibodies (Ab) (BL-003-1000, Biosensis, Australia) on rate of positivity of serum proNGF levels. No changes were observed in performance of the standard curve with presence or absence of blocking antibody (data not shown).

Disease category	Serum samples assayed (n)	% of samples positive		p-value
		No Heterophilic Blocking Ab	With Heterophilic Blocking Ab	
Thyroid cancer	20	45%	15%	0.04
Benign thyroid disease	20	30%	15%	0.25
No thyroid disease	18	44%	6%	0.006

1B: Spike and Recovery Experiments. 4 serum samples were assayed before and after a 2.5ng/mL spike (50ng/mL following adjustment for dilution) of recombinant proNGF (Biosensis, Australia) at 1:20 dilution, in the presence of Heterophilic Blocking Antibodies (BL-003-1000).

Sample	ProNGF (ng/mL)		% recovery of spike
	Pre-spike	Post-spike	
Sample A	2.7	66.7	128%
Sample B	0.0	47.8	96%
Sample C	0.1	41.0	82%
Sample D	0.0	40.1	80%
Mean			96%

1C: Inter-plate Quality Control Samples A quality-control solution (QC) was prepared by spiking 1:20 diluted proNGF-negative serum with 1.61ng/mL (32.15ng/mL after correction for dilution) recombinant proNGF with heterophilic blocking antibodies. Aliquots of the QC sample were included on each ELISA plate. Plate numbers reflect two different batches of ELISA plates.

Plate	1.1	1.2	1.3	1.4	1.5	1.6	2.1	2.2	2.3	2.4	2.5	Mean (SD)
proNGF (ng/mL)	39.9	31.9	34.5	41.4	41.1	29.3	20.1	29.0	29.5	18.6	32.2	31.6 ± 7.3
Percent Recovery	124%	99%	107%	129%	128%	91%	63%	90%	92%	58%	100%	98 ± 22%

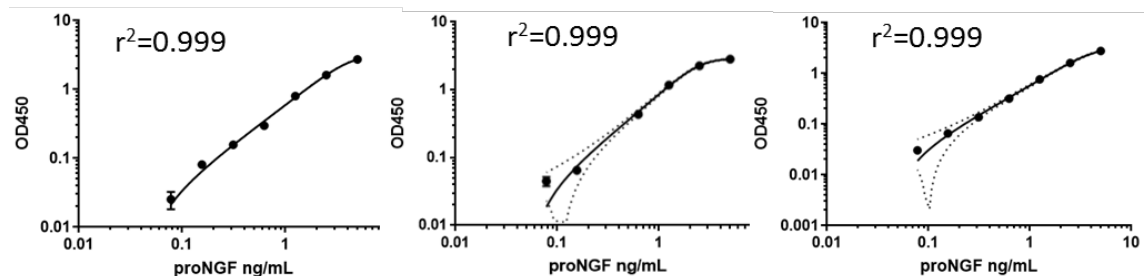
For the biopsy rinse, a similar QC solution was prepared by spiking 1.6ng/mL recombinant proNGF into phosphate buffered saline with the addition of protease inhibitors and heterophilic blocking antibodies (38µg/mL). Aliquots of the QC sample were included on each ELISA plate. Plate number represent different batches.

Plate	1.5	1.6	1.8	3.1	3.2	4.1	4.2	Mean (SD)
proNGF (ng/mL)	2.03	1.53	1.77	2.27	2.41	1.56	1.55	1.87 ± 0.34
Percent Recovery	127%	96%	111%	142%	151%	98%	97%	117 ± 20%

1D: Linearity of Dilution 3 serum samples positive for endogenous proNGF were assayed in serial dilution using Assay Diluent A (Biosensis, Australia) and Heterophilic Blocking Antibodies (BL-003-1000, Biosensis, Australia). The measured concentration at 1:20 dilution was defined as 100%. Reasonable linearity of dilution was observed. The zero values observed correspond to expected values below the limit of detection.

Sample	Endogenous ProNGF (ng/mL), corrected for dilution			
	1:10	1:20	1:40	1:80
Sample A	18.9 (109%)	17.3 (100%)	10.4 (60%)	14.6 (84%)
Sample B	2.6 (106%)	2.4 (100%)	0	0
Sample C	13.5 (124%)	10.9 (100%)	6.7 (62%)	0

1E: Linearity of Dilution of Biopsy Rinse Diluent In addition to the spike and recovery experiments performed above, a 1 in 2 dilution series from 5ng/mL was prepared as the standard curve for biopsy rinse specimens using the same phosphate-buffered saline with the addition of protease inhibitors and heterophilic antibody blockers that was used to prepare the biopsy rinse specimens. 4 parameter logistic regression curves are shown below for the first three ELISA plates, showing excellent linearity of dilution.



Additional Table 2: Individual patient characteristics for cases with detectable serum proNGF.

CASE	AGE	SEX	PRIMARY (SECONDARY) DIAGNOSIS	REASON FOR INVESTIGATION	SERUM PRONGF (ng/mL)		TSH (mIU/L)	BASIS OF DIAGNOSIS
					INITIAL	POST- OT		
10087	51-60	F	Graves'	Treatment of GD	8.7	4.3	<0.01	Histopath
10125	21-30	F	Graves'	Treatment of GD	4.3	2.8	<0.01	Histopath
10140	31-40	M	Graves'	Treatment of GD	12.9	11.8	<0.01	Histopath
10148	31-40	F	Graves'	Treatment of GD	1.6	2.3	<0.01	Histopath
10166	21-30	F	Graves'	Treatment of GD	5.4	4.6	<0.01	Histopath
10139	21-30	M	Graves'	Treatment of GD	1.0	.	0.01	Histopath
10318	61-70	F	Toxic MNG	Hyperthyroid	12.6	.	0.14	Histopath
10056	71-80	F	PTC	Recurrence	6	.	<0.01	Histopath
10208	21-30	F	PTC (8mm, 5mm)	Treatment of GD	2.2	.	<0.01	Histopath
10276	31-40	F	PTC (21mm)	Suspicious nodule	6.4	.	0.6	Histopath
10101	71-80	F	PTC (15mm) (FA)	Suspicious nodule	9.3	1.8	0.77	Histopath
10105	51-60	M	PTC (5mm) (MNG)	Compression	5.6	3.2	5.88	Histopath
10124	41-50	M	HCC (35mm) (FA)	Suspicious nodule	7.6	2.3	1.37	Histopath
10062	41-50	F	FA	Nodule	8	.	1.2	Histopath
10463	61-70	F	FA	Nodule	14.7	.	1.6	Biopsy + USS
10173	71-80	F	MNG	Compression	1.3	.	0.47	Histopath
10117	31-40	F	MNG	Compression	6.8	1.8	0.4	Histopath
10410	51-60	F	MNG	Compression	2.9	.	1.3	Histopath
10164	41-50	F	MNG	Compression	5.8	5.9	1.34	Histopath
10340	41-50	M	MNG	Nodule	3.4	.	1.66	Biopsy + USS
10116	51-60	M	MNG	Compression	3.1	0.7	2.7	Histopath
10465	41-50	F	MNG	Nodule	4.3	.	1.2	Biopsy + USS
10005	31-40	F	Benign nodule	Nodule	5.1	.	0.5	Biopsy + USS
10458	51-60	F	Benign nodule	Nodule	3.5	.	1.3	Biopsy + USS
10274	21-30	M	Benign nodule	Nodule	1.4	.	1.32	Biopsy + USS
10368	51-60	F	Benign nodule	Nodule	1.3	.	2.1	Biopsy + USS
10424	61-70	F	Benign nodule	Nodule	1.2	.	2.3	Biopsy + USS
10445	51-60	F	Normal	Completion HTx	8.7	.	0.66	Histopath

FA: Follicular adenoma. MNG: Multinodular Goitre. GD: Graves' Disease. PTC: Papillary thyroid cancer. FTC: Follicular thyroid cancer; HCC: Hurthle cell cancer. USS: Neck ultrasound. HTx: Hemithyroidectomy. Initial: Mean of 6 replicates performed over a minimum of 2 separate assays. Post-OT: post thyroidectomy sample (2-14 days)

Additional Table 3: Individual patient characteristics for cases with detectable biopsy proNGF.

CASE	AGE (years)	SEX	TSH (mIU/L)	PRONGF (ng/mL)	BETHESDA	NODULE DIAGNOSIS	BASIS OF Dx
10534	71-80	F	0.87	0.1	6	Anaplastic thyroid cancer	Biopsy and USS
10018	81-90	F	2.8	0.2	2	Follicular thyroid cancer	Histopath
10280	71-80	F	3	0.16	3	Follicular thyroid cancer	Histopath
10343	51-60	M	2.37	0.58	4	Follicular thyroid cancer	Histopath
10587	31-40	M	1.33	0.21	3	Follicular thyroid cancer	Histopath
10060	81-90	F	0.86	1.79	2	Papillary thyroid cancer	Histopath
10367	31-40	F	1.05	0.11	5	Papillary thyroid cancer	Histopath
10564	41-50	F	5.2	0.19	4	Papillary thyroid cancer	Histopath
10581	41-50	F	0.15	0.2	6	Papillary thyroid cancer	Histopath
10589	51-60	F	0.7	0.33	5	Papillary thyroid cancer	Histopath
10596	51-60	F	0.71	0.55	5	Papillary thyroid cancer	Histopath
10544	61-70	M	1.4	0.25	6	Papillary thyroid cancer	Histopath
10005	31-40	F	0.5	0.06	2	Benign nodule	Biopsy+USS
10368	61-70	F	2.1	0.05	2	Benign nodule	Biopsy+USS
10483	51-60	F	1.12	0.13	2	Benign nodule	Biopsy+USS
10486	51-60	F	1.06	0.15	2	Benign nodule	Biopsy+USS
10530	81-90	F	1	0.16	2	Benign nodule	Biopsy+USS
10531	61-70	F	1.9	0.15	2	Benign nodule	Biopsy+USS
10014	21-30	M	1.6	0.12	2	Benign nodule	Biopsy+USS
10502	81-90	M	1.83	0.1	2	Benign nodule	Biopsy+USS
10334	41-50	F	0.63	0.07	2	Benign nodule	Biopsy+USS
10402	41-50	F	2.2	0.15	2	Benign nodule	Biopsy+USS
10494	31-40	F	1.5	0.1	2	Benign nodule	Biopsy+USS
10504	21-30	F	.	0.08	2	Benign nodule	Biopsy+USS
10512	31-40	F	0.94	0.06	2	Benign nodule	Biopsy+USS
10524	71-80	F	0.72	0.1	2	Benign nodule	Biopsy+USS
10537	51-60	F	2.04	0.27	2	Benign nodule	Biopsy+USS
10547	31-40	F	2.9	0.16	2	Benign nodule	Biopsy+USS
10549	31-40	F	1	0.21	2	Benign nodule	Biopsy+USS
10550	61-70	F	0.6	0.09	2	Benign nodule	Biopsy+USS
10552	51-60	F	0.58	0.16	2	Benign nodule	Biopsy+USS
10553	71-80	F	1.5	0.32	2	Benign nodule	Biopsy+USS
10554	71-80	F	1.5	0.13	2	Benign nodule	Biopsy+USS
10555	51-60	F	2.86	0.12	2	Benign nodule	Biopsy+USS
10559	21-30	F	0.96	0.17	2	Benign nodule	Biopsy+USS
10560	41-50	F	2	0.11	2	Benign nodule	Biopsy+USS
10562	71-80	F	1.19	0.05	2	Benign nodule	Biopsy+USS
10565	51-60	F	2	0.24	2	Benign nodule	Biopsy+USS
10566	41-50	F	0.9	0.13	2	Benign nodule	Biopsy+USS
10569	71-80	F	2.6	0.21	2	Benign nodule	Biopsy+USS
10574	61-70	F	1.3	0.38	2	Benign nodule	Biopsy+USS

Chapter 3: ProNGF is not a serum or biopsy-rinse
biomarker for thyroid cancer diagnosis

10575	61-70	F	2.1	0.16	2	Benign nodule	Biopsy+USS
10578	61-70	F	1.07	0.05	2	Benign nodule	Biopsy+USS
10558	31-40	F	0.94	0.13	2	Benign nodule	Biopsy+USS
10558	31-40	F	0.94	0.09	2	Benign nodule	Biopsy+USS
10355	51-60	M	0.57	0.06	2	Benign nodule	Biopsy+USS
10404	61-70	M	1.2	0.05	2	Benign nodule	Biopsy+USS
10462	61-70	M	1.1	0.13	2	Benign nodule	Biopsy+USS
10499	41-50	M	0.3	0.05	2	Benign nodule	Biopsy+USS
10538	31-40	M	1.35	0.25	2	Benign nodule	Biopsy+USS
10568	61-70	M	0.72	0.3	2	Benign nodule	Biopsy+USS
10572	61-70	M	0.92	0.05	2	Benign nodule	Biopsy+USS
10573	31-40	M	0.25	0.19	2	Benign nodule	Biopsy+USS
10587	31-40	M	1.33	0.17	2	Benign nodule	Biopsy+USS
10012	31-40	F	0.2	0.11	2	Benign nodule	Histopath
10053	51-60	F	2.66	0.11	2	Benign nodule	Histopath
10366	41-50	F	1.1	0.18	2	Benign nodule	Histopath
10405	71-80	F	0.35	0.06	2	Benign nodule	Histopath
10463	61-70	F	.	0.09	3	Benign nodule	Histopath
10501	71-80	F	0.3	0.16	2	Benign nodule	Histopath
10521	51-60	F	2.04	0.65	4	Benign nodule	Histopath
10541	71-80	M	1.5	0.19	3	Benign nodule	Histopath
10423	11-20	F	.	0.05	2	Follicular adenoma	Histopath
10543	51-60	F	.	0.32	3	Follicular adenoma	Histopath
10576	31-40	F	1.5	0.38	3	Follicular adenoma	Histopath
10570	61-70	M	1.14	0.45	4	Hurthle cell adenoma	Biopsy+USS
10308	41-50	F	.	0.09	4	Hurthle cell adenoma	Histopath
10377	31-40	F	1.41	0.05	2	Hurthle cell adenoma	Histopath
10548	41-50	F	0.41	0.56	4	Hurthle cell adenoma	Histopath
10597	51-60	F	2.1	0.15	1	Hurthle cell adenoma	Histopath
10598	71-80	F	2.6	0.3	3	Hurthle cell adenoma	Histopath
10481	51-60	F	3.4	0.21	2	Lymphocytic thyroiditis	Histopath
10599	51-60	F	2.1	0.27	4	Lymphocytic thyroiditis	Histopath

USS: Neck ultrasound.

4 INNERVATION OF PAPILLARY THYROID CANCER AND ITS ASSOCIATION WITH EXTRA- THYROIDAL INVASION.

4.1 Preface

This paper examines the hypothesis that thyroid cancer is innervated. While innervation has been established for other solid organ malignancies, whether this occurs in thyroid cancer, or is of biological significance, is not known.

Determining whether thyroid cancer is innervated is a pre-requisite step for exploring deeper hypotheses of nerve-cancer crosstalk and nerve-mediated oncogenesis.

This work was conducted at our laboratories at the Hunter Medical Research Institute, drawing on collaborative resources from the Hunter Cancer Biobank and the John Hunter Hospital.

OPEN

Innervation of papillary thyroid cancer and its association with extra-thyroidal invasion

Christopher W. Rowe^{1,2,3*}, Tony Dill^{4,6}, Nathan Griffin^{3,5}, Phil Jobling⁵, Sam Faulkner^{3,5}, Jonathan W. Paul^{1,3}, Simon King⁴, Roger Smith^{1,2,3} & Hubert Hondermarck^{3,5}

Nerves are emerging regulators of cancer progression and in several malignancies innervation of the tumour microenvironment is associated with tumour aggressiveness. However, the innervation of thyroid cancer is unclear. Here, we investigated the presence of nerves in thyroid cancers and the potential associations with clinicopathological parameters. Nerves were detected by immunohistochemistry using the pan-neuronal marker PGP9.5 in whole-slide sections of papillary thyroid cancer (PTC) (n = 75), compared to follicular thyroid cancer (FTC) (n = 13), and benign thyroid tissues (n = 26). Nerves were detected in most normal thyroid tissues and thyroid cancers, but nerve density was increased in PTC (12 nerves/cm² [IQR 7–21]) compared to benign thyroid (6 nerves/cm² [IQR: 3–10]) (p = 0.001). In contrast, no increase in nerve density was observed in FTC. In multivariate analysis, nerve density correlated positively with extrathyroidal invasion (p < 0.001), and inversely with tumour size (p < 0.001). The majority of nerves were adrenergic, although cholinergic and peptidergic innervation was detected. Perineural invasion was present in 35% of PTC, and was independently associated with extrathyroidal invasion (p = 0.008). This is the first report of infiltration of nerves into the tumour microenvironment of thyroid cancer and its association with tumour aggressiveness. The role of nerves in thyroid cancer pathogenesis should be further investigated.

Emerging data show that many solid tumours are innervated and that nerves actively participate in cancer progression¹. Tumour denervation in prostate^{2,3}, gastric^{4,5} and pancreatic cancers^{6,7} reduces tumour growth and invasion; and the presence of nerves is associated with metastases and increased tumour grade. The stimulatory role of nerves appears to be related to the release of neurotransmitters (such as norepinephrine) by nerve endings in the tumour microenvironment, resulting in the activation of neurosignalling in both stromal and cancer cells and the promotion of tumour progression. For instance, adrenergic neurosignalling induced by sympathetic nerves stimulates an angio-metabolic switch in endothelial cells, while cholinergic neurosignalling has been shown to activate cancer stem cell growth^{4,5}. The growth of nerves in cancer is stimulated by the release of neurotrophic growth factors, such as nerve growth factor (NGF) from cancer cells^{5,6,8–10}, resulting in an increased nerve density in the tumour microenvironment. Together, nerves, as well as neurotrophic growth factors are increasingly regarded as potential biomarkers and therapeutic targets in cancer.

In thyroid cancer, the presence and potential significance of nerves in the tumour microenvironment has not been investigated. Although it is known that the normal thyroid follicular epithelium is infiltrated by adrenergic, cholinergic and peptidergic nerves^{11–14}, with nerve signalling causing measurable physiological effects on the secretion of thyroid hormone^{15,16} and on thyroid growth¹⁷, the presence and significance of nerves in thyroid cancer is unclear. Perineural invasion has rarely been described and appears to occur in only 2% of thyroid tumours¹⁸ but this may simply reflect the rarity of nerves in the thyroid cancer microenvironment.

In this study, we aimed to clarify the presence and quantity of nerves in the microenvironment of thyroid cancer. Nerves were detected in a cohort of thyroid cancers and benign thyroid tissues, and the association between

¹School of Medicine and Public Health, University of Newcastle, Callaghan, NSW, 2308, Australia. ²Department of Endocrinology, John Hunter Hospital, Locked Bag 1, Newcastle, NSW, 2310, Australia. ³Hunter Medical Research Institute, 1 Kookaburra Circuit, New Lambton Heights, 2305, NSW, Australia. ⁴Department of Anatomical Pathology, NSW Health Pathology (Hunter), Locked Bag 1, HMRC, Newcastle, NSW, 2310, Australia. ⁵School of Biomedical Sciences and Pharmacy, University of Newcastle, Callaghan, NSW, 2308, Australia. ⁶Present address: ACT Pathology, Canberra Health Services, ACT Government, Canberra Hospital, Canberra, ACT, Australia. *email: Christopher.Rowe@health.nsw.gov.au

	Benign thyroid	Thyroid Cancer	p
n	26	88	
Age (years)	56.4 ± 15.7	53.3 ± 18.6	0.45
Female gender (n, %)	18 (70%)	59 (67%)	0.83
TSH (mIU/L)*	0.95 ± 1.3	1.8 ± 1.2	0.94
Pathology (n, %)			
Papillary cancer		75 (85%)	
Follicular cancer		13 (16%)	
Normal thyroid	1 (4%)		
Multinodular	16 (62%)		
Follicular adenoma	9 (34%)		
Tumour characteristics			
Tumour size (cm)		2.5 ± 1.9	
Multifocality (n, %)		29 (33%)	
Extra-thyroidal invasion (n, %)		49 (56%)	
Microscopic		38/49	
Macroscopic		11/49	
Nodal metastases (n, %)		58 (66%)	

Table 1. Demographic and clinical characteristics of thyroid samples. *TSH data missing for 15 cases with thyroid cancer, and 2 cases with benign pathology.

innervation and clinicopathological parameters was investigated. The density of nerves was found to be increased in papillary thyroid cancer (PTC) compared to follicular thyroid cancers (FTC) and benign thyroid tissues. Interestingly, nerve density was positively associated with extra-thyroidal invasion.

Materials and Methods

Thyroid specimens. This study was prospectively approved by the Hunter New England Human Research Ethics Committee, who granted a waiver of consent for access to archival pathology material and approved the experimental protocol (HNE HREC 16/04/20/5.13). All study methodologies were carried out in accordance with relevant guidelines and regulations. Surgical resection specimens were processed and stored according to standard clinical and pathological procedures, then archived as formalin-fixed, paraffin-embedded blocks at a tertiary hospital pathology department (NSW Health Pathology, John Hunter Hospital, Lookout Road, New Lambton Heights, Australia). Archived blocks containing sections of lobes from thyroid cancers and benign thyroid pathology were obtained by electronic database search at a ratio of 4 cases of thyroid cancer for 1 benign control. 114 whole blocks of thyroid lobe specimens from 102 patients were included, comprising 26 cases of benign pathology, and 88 cases of thyroid cancer (PTC n = 75, FTC n = 13). 12 cases with malignant pathology in the ipsilateral lobe also had the contralateral lobe included in analysis due to separate pathology in the contralateral lobe (PTC [n = 4], follicular adenoma [n = 5] or multinodular change [n = 3]). No lobe was included twice. All histological samples were reviewed by an independent pathologist to confirm or revise the original diagnosis. Relevant clinical parameters were extracted from medical records.

Demographic and clinical characteristics of the included cases are presented in Table 1. Overall, patients with benign and malignant thyroid diseases were of a similar age (53.6 vs 56.4 years, $p = 0.50$), gender (70% vs 66% female, $p = 0.78$) and baseline thyroid function (TSH 0.95 vs 1.8 mIU/L $p = 0.21$).

Immunohistochemistry. Whole-slide sections (4 µm) were prepared from formalin-fixed paraffin-embedded blocks of benign and malignant thyroid tissue. Immunohistochemistry (IHC) for the pan-neuronal marker protein gene-product 9.5 (PGP9.5)¹⁹ was performed using the Ventana Discovery automated slide stainer (Roche Medical Systems, Tuscon, Az). The primary antibody was anti-rabbit polyclonal PGP9.5 antibody (catalogue number #Ab15503, Abcam, Cambridge, United Kingdom) at 1:600 dilution; previously validated in our laboratory^{10,20} and re-optimized for the automated platform. Negative controls were prepared using non-specific IgG isotype controls, and without addition of primary antibody (Supplementary Fig. S1), while positive controls were included on each slide. Antigen-retrieval was performed using Ribo-CC solution, (pH 6, Ventana, Roche), with secondary anti-rabbit HQ for 16 min at 37 °C (Ventana, Roche), and tertiary anti-HQ (Ventana, Roche) for 16 min at 37 °C. Manual counterstaining was performed using Mayer's hematoxylin for 10 sec and Scott's Tap Water for 30 sec, followed by dehydration, clearing and mounting. Staining of primary tumours for the precursor for nerve growth factor (proNGF) was performed using the automated Ventana platform and the anti-rabbit polyclonal proNGF antibody (Ab9040, Merck Millipore, Darmstadt, Germany) at a dilution of 1:350.

Subtyping of nerves was performed on a subgroup of thyroid cancers (n = 5) using antibodies against tyrosine hydroxylase (TH) for adrenergic (sympathetic) nerves (catalogue number #ab152, Abcam, Cambridge United Kingdom, 1:250 dilution); vesicular acetylcholine transporter (VACHT) for cholinergic (parasympathetic) nerves (catalogue number #ab62140, Abcam, 1:250 dilution) and anti-Substance P (SP) for peptidergic (sensory) nerves (catalogue number #ab14184, Abcam, 1:1000 dilution)²¹. Sections of innervated dermis and colonic mucosa were included as positive controls.

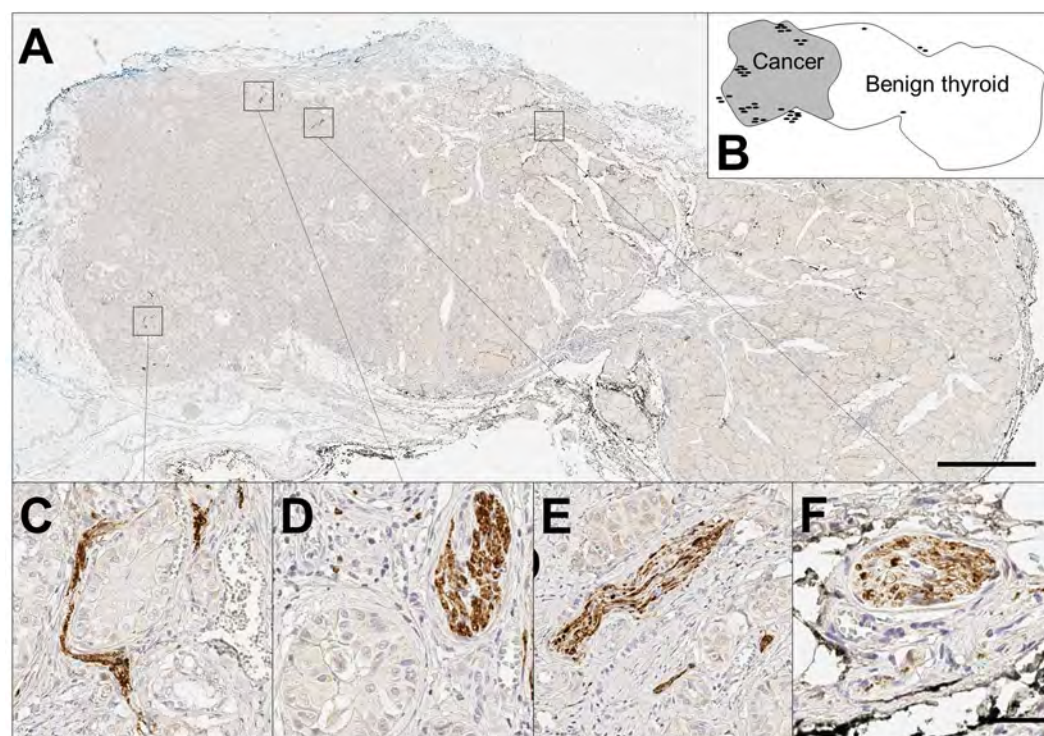


Figure 1. Nerves in benign and malignant thyroid tissues. (A) Low magnification ($0.5\times$) of papillary thyroid cancer (left) and adjacent benign thyroid (right), stained using immunohistochemistry for PGP9.5 (pan-neuronal marker) and counterstained with haematoxylin. Scale bar 2 mm. (B) Schematic of A, showing location of benign and malignant tissue and nerves. Each black oval represents a single nerve trunk in approximate location. In this particular section there were 38 nerves (of which 34 were in the cancer, and 4 within benign thyroid), and the section contains 1 cm^2 of thyroid tissue (including 0.32 cm^2 of cancer). This gives a density of 38 nerves per cm^2 of thyroid tissue; 108 cancer-associated nerves per cm^2 of cancer; and 6 nerves per cm^2 adjacent benign tissue. (C–F) High magnification ($20\times$), demonstrating nerve trunks (brown stain), surrounded by papillary thyroid cancer cells (C–E); or adjacent to the vascular bundle on edge of benign thyroid (F). Scale bar $50\text{ }\mu\text{m}$.

Digital quantification of nerve density. Prior to analysis, digitization of whole slides at $20\times$ magnification was performed using the Aperio AT2 scanner (Leica Biosystems, Victoria, Australia). Tissue was analyzed using QuPath (Queens University, Belfast)²². Nerves were counted if they met the following criteria: immunoreactivity (positive PGP9.5 staining), typical anatomical appearance, and 3 or more axons visualized (for example, see Fig. 1C–F). Nerves with fewer than 3 axons were discounted as they could not reliably be distinguished from non-specific staining. Each discrete nerve segment was counted separately. Nerve density is presented as nerves per cm^2 of thyroid tissue according to three parameters: (A) the number of thyroid-associated nerves (nerves within 1 mm of both benign and malignant thyroid tissue on a slide) divided by the total area of thyroid tissue present on the slide; (B) the number of cancer-associated nerves (nerves within 1 mm of intrathyroidal malignant cells) divided by the area of cancer present on the slide; and (C) the number of adjacent-benign associated nerves (thyroid-associated nerves present on a slide containing cancer, but $>1\text{ mm}$ from malignant cells) divided by the area of benign tissue adjacent to the cancer on the slide. Separation distances of 1 mm were chosen to reflect a plausible maximum biological distance for paracrine signaling. In addition, perineural invasion (defined as tumour cells circumferentially surrounding a nerve²³) was quantified for each case. Investigators were blinded to clinical and pathological characteristics of the included cases during slide analysis.

QuPath was further used to determine the intensity of cytoplasmic proNGF staining in cancer cells (quantified by h-score, an index between 0–300, calculated as the sum of $3\times\%$ of pixels with strong staining $+2\times\%$ of pixels with intermediate staining $+1\times\%$ of pixels with weak staining).

Statistical analysis. Group levels means and standard deviations (SD) are presented for parametric data, assessed with unpaired Student's t-tests; with medians and interquartile ranges (IQR) presented for non-parametric data, compared using Wilcoxon RankSum (unmatched pairs) or SignRank (matched pairs) tests. Distribution was assessed using histograms and q-q plots. Analysis of association between nerve density and clinical and pathological parameters was undertaken by fitting separate log-linear regression models with log-transformed nerve-density as the dependent variable, and including model variables of age, sex, tumour size, extra-thyroidal invasion, multifocality and the presence of lymph node metastases. Separate models were fitted for each nerve density measure. Categorical data was assessed using Pearson's Chi-square, with logistic regression

	Measure	n	Area of Tissue (cm ²)	Nerve Density (cm ²)	P value*
A	Thyroid section containing cancer	88	2.0 (1.5–2.6)	10.3 (5.9–20.2)	0.005*
	• Thyroid section containing PTC	75	1.9 (1.5–2.6)	12.4 (6.6–21.4)	0.0008*
	• Thyroid section containing FTC	13	2.6 (2.3–2.9)	3.4 (2.5–4.5)	ns*
	Exclusively-benign thyroid section	26	1.9 (1.6–2.3)	6.6 (2.8–9.7)	Reference
B	Region analysis (PTC only)				
	• PTC slide-region only	62	0.6 (0.2–1.2)	17.8 (8.0–41.2)	0.0008 [#]
	• Benign thyroid adjacent to PTC	62	0.7 (0.3–1.3)	9.6 [5.7–18.0]	0.027*

Table 2. Nerve density in benign and malignant thyroid tissue. Data are median (IQR). Wilcoxon Ranksum or SignRank test used. *Comparator is ‘Exclusively-benign thyroid section’. [#]Comparator is ‘Benign thyroid adjacent to PTC’. n = number of cases. ns = not significant.

models used to assess impact of potential confounding. Significance was assessed using a two-sided alpha of 0.05. All analyses were performed using Stata (version 14.2, Statacorp, College Station, Texas, USA).

Results

Nerve detection in thyroid cancer vs normal thyroid tissue. Using the pan-neuronal marker PGP9.5, nerves were detected in sections of PTC and FTC as well as benign thyroid tissues. Nerves were identified in 23/26 (88%) of exclusively-benign sections and 86/88 (98%) of sections containing malignant tissue, with nerves typically found in the periphery of the tumours (Fig. 1A,B) or invading deep inside the tumour (Fig. 1C–E), sometimes co-located in the neuro-vascular bundle (Fig. 1F).

Nerve density is increased in PTC compared to FTC and benign thyroid tissue. Nerve density was quantified and found to be higher in sections containing thyroid cancer (median 10.3 nerves per cm², IQR 5.9–20.2) than in sections containing exclusively-benign thyroid tissue (6.6 nerves per cm², IQR 2.8–9.7, $p = 0.005$, Table 2A). When stratified by cancer subtype, the increase in nerve density was found to be associated exclusively with PTC: 12.4 [6.6–21.4] nerves per cm² on sections containing PTC vs 6.6 [2.8–9.7] nerves per cm² on sections containing exclusively-benign thyroid, $p = 0.0008$. For FTC, no increase in nerve density was seen (Table 2A). To determine whether there was evidence of clustering of nerves around the cancer, a subset of 62 sections containing both benign and malignant tissue on the same section were analyzed (Table 2B). In PTC, nerve density was significantly higher in the tumour (17.8 [8.0–41.2] nerves per cm²) than the adjacent benign regions (9.6 [5.7–18.0] nerves per cm², $p = 0.0008$). However, nerve density in the benign tissue adjacent to PTC was also higher than nerve density in exclusively-benign thyroid tissue (9.6 [5.7–18.0] vs 6.6 [2.8–9.7] nerves per cm², $p = 0.03$).

Resection technique does not affect assessment of nerve density. Analysis was performed on a subgroup of exclusively-benign sections ($n = 19$) and PTC sections ($n = 13$) resected under identical surgical conditions of total thyroidectomy and without lymph node dissection to determine whether surgical methodology (hemithyroidectomy vs total thyroidectomy) or resection extent (presence or absence of simultaneous lymph node dissection) may be affecting the assessment of nerve density presented in Table 2. The pattern of increased nerve density in PTC compared to benign thyroid was confirmed (17.2 vs 6.6 nerves per cm² thyroid tissue respectively, $p = 0.002$), providing corroboration that the increase in nerve density observed around PTC is independent of the resection technique used (Supplementary Table S2). Further, using the full PTC and benign tissue dataset we constructed a log-linear regression model using nerve density per cm² thyroid tissue as the dependent variable, and including model variables of presence of cancer, type of thyroidectomy, and nodal clearance as binary variables. In the base model, the presence of cancer remained highly associated with nerve density ($p = 0.002$), and there was no material change in parameter estimates or significance ($p = 0.007$) when including model variables of operation type and nodal clearance (Supplementary Table S3).

The majority of nerves in PTC are of adrenergic nature. Using the pan-neuronal marker PGP9.5 labelling as a reference, nerve subtypes were identified using neuronal markers specific for adrenergic, cholinergic and peptidergic nerves in serial sections. Serial sections were immunostained for either TH, VACHT or SP, to identify adrenergic, cholinergic and peptidergic nerves respectively. Strong, specific co-staining with PGP9.5 and TH was observed in the majority of nerves (for example, see paired images in Fig. 2A,D and B,E), demonstrating a high proportion of adrenergic nerves in the tumour microenvironment. To quantify the proportion of adrenergic nerves, 4 medium-power fields (10× magnification) with PGP9.5 positive nerves were identified for each case ($n = 5$). Corresponding nerve labelling was counted for matched fields, yielding the percentage of sympathetic nerve staining. Using this method, 55/69 nerves (80%) showed strong concordant immunoreactivity for PGP9.5 and TH. Immunostaining for parasympathetic nerves (VACHT, paired images in Fig. 2C,F and G,I) and peptidergic nerves (Fig. 2H,K and I,L) was present, but markedly less compared to sympathetic staining and limited to a subset of axons within the nerves, rendering a precise quantification of nerve density difficult. In SP stained sections, co-staining of the adjacent cancer cells was also noted (Fig. 2K), which has been previously reported in gastric cancer²⁴.

Nerve density and perineural invasion in PTC are positively associated with extra-thyroidal invasion. Multiple log-linear regression models were used to assess the relationship between nerves and

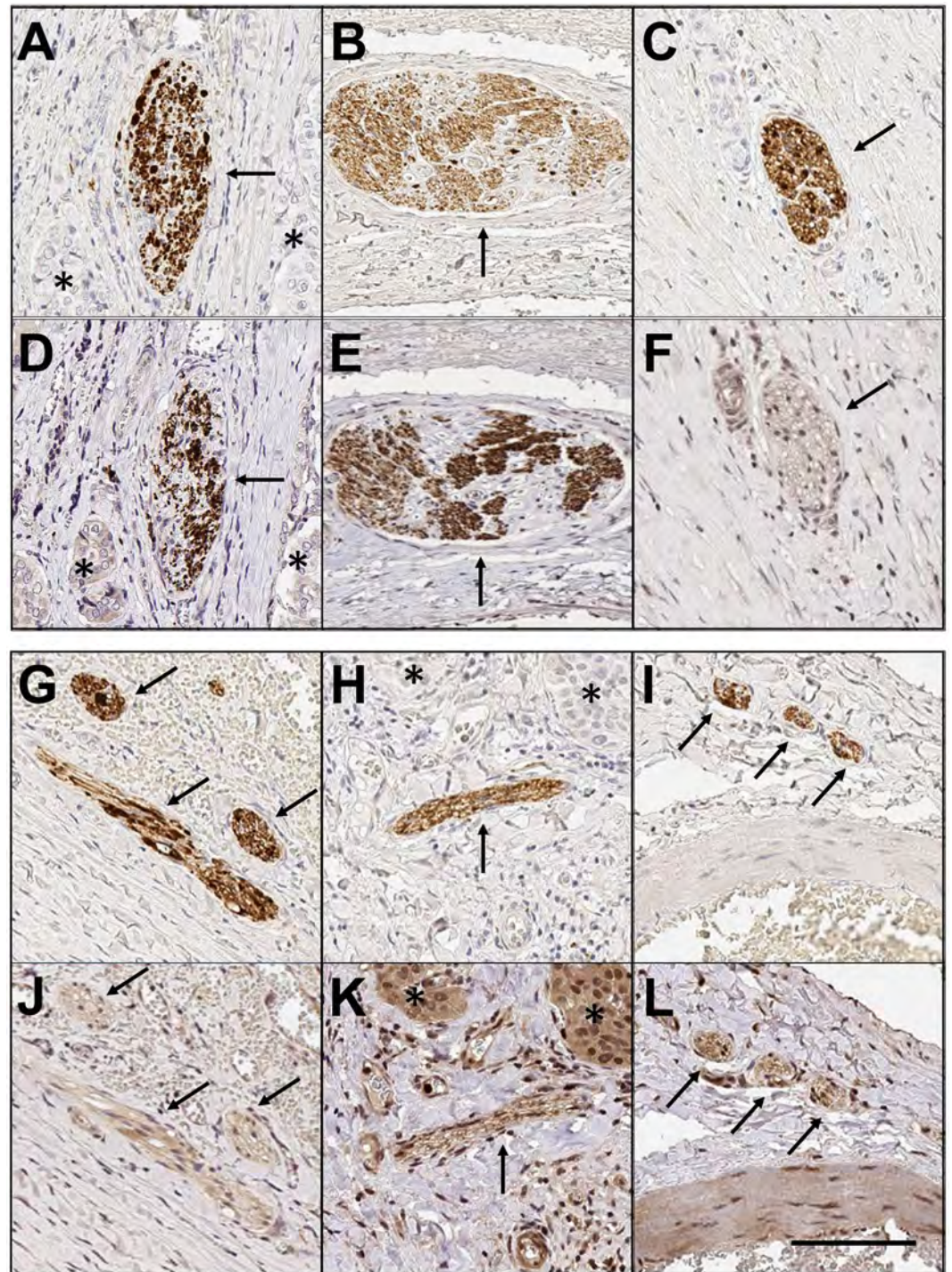


Figure 2. Subtyping of autonomic nerves. Paired images demonstrating serial sections through nerves in thyroid cancer, where the first image (A–C, G–I) shows a nerve immunolabelled with PGP9.5, and the second image (D–F, J–L) shows the same nerve labelled with a second neural immunostain. Pairs (A, D) and (B, E) show strong co-staining with PGP9.5 and Tyrosine Hydroxylase (adrenergic neuronal marker). Pairs (C, F) and (G, J) show co-staining between PGP9.5 and Vesicular acetylcholine transporter (VACHT, cholinergic neuronal marker). Pairs (H, K) and (I, L) show co-staining for PGP9.5 and Substance P (peptidergic neuronal marker). Note also the staining of some malignant cells with Substance P in panel (K). 10× magnification. Black arrows indicate labelled nerves. Stars indicate malignant cells (where present). Scale bar: 100 µm.

clinical parameters of PTC, using nerve density as the dependent variable, and including model variables of age, gender, tumour size (cm), presence of extra-thyroidal invasion (either microscopic or gross), presence of multifocality and presence of nodal metastases (Table 3). In both models, the presence of extra-thyroidal invasion had significant positive association with nerve density ($p < 0.001$). In contrast, tumour size was inversely associated

Model variable	Nerves per cm ² of thyroid tissue		Nerves per cm ² of PTC	
	Beta coefficient	p-value	Beta coefficient	p-value
Age	0 (0 to 0)	0.27	0 (0 to 0)	0.77
Sex	−0.2 (−0.7 to 0.3)	0.33	−0.2 (−0.7 to 0.3)	0.42
Tumour size (cm)	−0.3 (−0.5 to 0) −27% (−44 to −10%)	0.003	−0.5 (−0.8 to −0.4) −55% (−74 to −36%)	<0.0001
Extra-thyroidal invasion	0.8 (0.3 to 1.3) 123% (41 to 250%)	0.001	1.1 (0.6 to 1.6) 209% (87 to 411%)	<0.0001
Multifocality	0 (−0.4 to 0.5)	0.84	0 (0 to 0.2)	0.96
Nodal metastases	−0.1 (−0.6 to 0.4)	0.78	−0.3 (−0.8 to 0.3)	0.34
Intercept	3.3 (2.4 to 4.1)		3.9 (2.9 to 4.8)	

Table 3. Association between nerve density in PTCs and clinical/pathological parameters. Multiple log-linear regression of log-transformed nerve density and untransformed markers of cancer aggressiveness in PTCs. Coefficients (95% CI) are reported. Percentage change of the untransformed variable is co-reported (italics) for significant model variables, where each 1 unit increase in the model variable is associated with a percentage change in nerve density.

with nerve density ($p < 0.005$). No association with multifocality or nodal metastases was noted, and there was no evidence of confounding from age or gender. To confirm that the association between increased nerve density and extrathyroidal extension was not being caused by large tumours with gross extra-thyroidal extension resulting in encasement of nerves in the interstitial space, we repeated the regression model after excluding cases of PTC with gross extra-thyroidal extension ($n = 8$) (Supplementary Table S4). The association between nerves and extra-thyroidal invasion remained highly significant, with a 211% increase (95% CI 129 to 346%, $p = 0.004$) in nerve density in tumours with microscopic extra-thyroidal invasion, providing supportive evidence that the increase in nerve density is not an artefact of tumour growth.

We further explored the potential relationship between nerves and extra-thyroidal invasion in PTC by assessing perineural invasion, as either a continuous or dichotomized (present vs absent) variable. A total of 26/75 (35%) of PTC had evidence of perineural invasion, with a median 8 (IQR 3–13) involved nerves per section. On dichotomized univariate analysis, tumours with extra-thyroidal invasion were more likely to have evidence of perineural invasion (46%) than PTC without extra-thyroidal extension (22%, $p = 0.03$). There was no association between perineural invasion and tumour size, multifocality or nodal metastases. This relationship was then explored in a multiple logistic regression model, with presence of tumoural extra-thyroidal invasion as the dichotomized dependent variable, and including potential model variables of number of nerves with perineural invasion, age, gender, tumour size (cm), multifocality and presence of nodal metastases. In this model, the identification of each nerve with perineural invasion increased the odds of the tumour having extra-thyroidal invasion by 20% (odds ratio 1.2, 95%CI 1.05–1.38, $p = 0.008$). There was no evidence of confounding factors from other model variables. In this model, tumour size (OR 1.08, 95% CI 1.02–1.14, $p = 0.01$) was also associated with extrathyroidal invasion. The presence of tumour multifocality failed to reach a p -value < 0.05 (OR 3.09, 95%CI 0.93–10.2, $p = 0.06$).

Nerve density in PTC may be associated with proNGF expression. In light of previous data showing proNGF expression in thyroid cancers²¹, and given that in prostate cancer proNGF has been reported as a driver of nerve infiltration⁹, we examined whether there was an association between proNGF expression in primary thyroid tumours and nerve density. ProNGF expression was quantified in primary tumours ($n = 83$) using immunohistochemistry and h-score (staining intensity). Dichotomizing positive proNGF expression at a h-score of 25, 86% (71/83) of thyroid cancers expressed proNGF. Median proNGF h-score was 55 (IQR 33–78) for all tumours, and was not significantly different between papillary (56, IQR 39–78) and follicular (39, IQR 25–78, $p = 0.30$) subtypes. Tumours expressing proNGF showed a greater density of nerves than tumours with negative proNGF expression (Fig. 3), although statistical significance was limited ($p = 0.07$). There were a median 14.3 nerves per cm² thyroid cancer (IQR 6.0–36.8) associated with tumours expressing proNGF, compared to 10.3 (IQR 2.4–12.3) nerves per cm² associated with cancers without proNGF expression ($p = 0.07$).

Discussion

This paper clarifies the presence of nerves in thyroid cancer and demonstrates for the first time that nerve density is significantly higher in PTC compared to FTC and benign thyroid tissue. This relationship was robust, persisting when controlling for tumour size and other variables in multivariate models. Additionally, we have shown that these nerves were predominantly of adrenergic origin, although cholinergic and peptidergic nerves could also be occasionally detected; this is the first evidence for adrenergic nerves in PTC.

Tumour innervation has been established in several other malignancies²⁵. For example, adrenergic innervation is demonstrated in breast cancer, where nerves infiltrate the tumour microenvironment and are associated with lymph node invasion^{10,26}. In prostate cancer, both adrenergic and cholinergic nerves are present, and nerve density is increased inside and around prostate cancer compared to benign prostate, and correlates with more aggressive tumours^{2,27,28}. Prostate cancer cells can drive neuronal growth (axonogenesis) *in vitro*²⁷ and this neurotrophic effect is mediated through the release of proNGF^{9,27}. In gastric cancer, cholinergic innervation is necessary for tumourigenesis and is driven by NGF release from cancer cells^{4,5}. Increased nerve densities have also been found in the tumour microenvironment of colorectal²⁹ and pancreatic³⁰ carcinomas. Our data show a

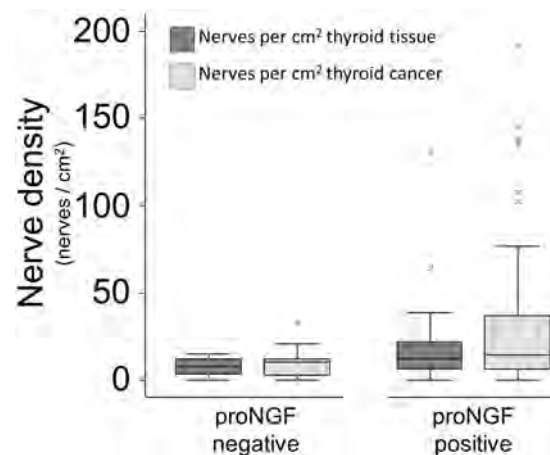


Figure 3. Nerve density in thyroid cancers, stratified by tumoural proNGF expression. Box (IQR) and whisker (5–95%) plot of nerve density, stratified by the presence or absence of proNGF expression in the primary tumour. Dark grey boxes compare density of nerves per cm² of thyroid lobe containing PTC or FTC (medians 8.5 vs 11.4, $p = 0.10$). Light grey boxes compare nerve density per cm² of PTC or FTC (medians 10.3 vs 14.3 $p = 0.07$).

robust positive association between nerves in PTC and extra-thyroidal invasion. Both the density of nerves, and the presence of perineural invasion, were associated with extra-thyroidal invasion in independent analyses. The finding that perineural invasion is associated with aggressive tumours is consistent with data from other cancers²³. Nerve density could therefore be used as a potential indication of PTC aggressiveness, and may assist with post-operative risk stratification of patients. However, further large scale clinicopathological investigations are warranted to confirm this hypothesis.

A further finding of our study is that nerve density in PTC may be associated with the expression of the neurotrophic factor proNGF by cancer cells, suggesting that proNGF could participate in the outgrowth of nerves in the tumour microenvironment and around the tumour. The role of proNGF/NGF in stimulating nerve outgrowth in the tumour microenvironment has already been described in prostate⁹, gastric⁵ and pancreatic⁶ cancers, where a NGF-adrenergic nerve feed-forward loop promotes nerve infiltration. Interestingly, the tyrosine kinase receptor TrkA, whose ligands include both NGF and proNGF, is expressed in nerves that have infiltrated the tumour microenvironment of thyroid cancer²⁰, suggesting the hypothesis that proNGF/NGF could stimulate nerve outgrowth via signalling through TrkA receptors in nerve terminals infiltrated in thyroid cancer.

The predominance of adrenergic nerves PTC suggests the possibility of adrenoceptor-mediated signalling, either as an angiogenic switch on endothelium, as seen in prostate cancer³, and/or via direct effects on cancer cells, including cancer stem cells, as described in pancreatic cancer^{6,7}. Functional alpha- and beta- adrenoceptors are present in benign thyroid tissue¹⁴, and adrenergic signalling is known to increase thyroid hormone production and mediate thyroid growth^{15,31–33}. Beta-adrenoceptors have been demonstrated in thyroid cancer, where they are over-expressed compared to benign thyroid^{34,35}. Therefore, similar to prostate and pancreatic cancers, the increased density of adrenergic nerves that we have detected in thyroid cancer could contribute to its progression and dissemination. The inverse association that we have observed between tumour size and nerve density also suggests that innervation may be important in the initiation of tumourigenesis, as described in gastric cancer⁴. Together, now that presence of nerves in thyroid cancer is clarified and given the association with extrathyroidal extension, further *in vitro* and *in vivo* animal experiments are warranted to explore the functional impact of nerves in thyroid cancer.

In conclusion, the demonstration that nerves are increased in PTC and correlate with extra-thyroidal invasion points to the potential clinical value of using nerve involvement as a biomarker of tumour aggressiveness in pathological analysis. In addition, these results suggest that similarly to prostate, gastric and pancreatic cancers, nerves may have a role in PTC progression.

Data availability

All data generated or analysed during this study are included in this published article (and its Supplementary Information files).

Received: 6 August 2019; Accepted: 13 January 2020;

Published online: 30 January 2020

References

1. Boilly, B., Faulkner, S., Jobling, P. & Hondermarck, H. Nerve dependence: from regeneration to cancer. *Cancer Cell* **31**, 342–354, <https://doi.org/10.1016/j.ccell.2017.02.005> (2017).
2. Magnon, C. *et al.* Autonomic nerve development contributes to prostate cancer progression. *Science* **341**, <https://doi.org/10.1126/science.1236361> (2013).
3. Zahalka, A. H. *et al.* Adrenergic nerves activate an angio-metabolic switch in prostate cancer. *Science* **358**, 321–326, <https://doi.org/10.1126/science.aah5072> (2017).

4. Zhao, C.-M. *et al.* Denervation suppresses gastric tumorigenesis. *Sci. Transl. Med.* **6**, 250ra115–250ra115, <https://doi.org/10.1126/scitranslmed.3009569> (2014).
5. Hayakawa, Y. *et al.* Nerve growth factor promotes gastric tumorigenesis through aberrant cholinergic signaling. *Cancer Cell* **31**, 21–34, <https://doi.org/10.1016/j.ccell.2016.11.005> (2017).
6. Renz, B. W. *et al.* beta2 adrenergic-neurotrophin feedforward loop promotes pancreatic cancer. *Cancer Cell* **33**, 75–90.e77, <https://doi.org/10.1016/j.ccell.2017.11.007> (2018).
7. Saloman, J. L. *et al.* Ablation of sensory neurons in a genetic model of pancreatic ductal adenocarcinoma slows initiation and progression of cancer. *Proc. Natl. Acad. Sci. USA* **113**, 3078–3083, <https://doi.org/10.1073/pnas.1512603113> (2016).
8. Griffin, N., Faulkner, S., Jobling, P. & Hondermarck, H. Targeting neurotrophin signaling in cancer: The renaissance. *Pharmacol. Res.* **135**, 12–17, <https://doi.org/10.1016/j.phrs.2018.07.019> (2018).
9. Pundavela, J. *et al.* ProNGF correlates with Gleason score and is a potential driver of nerve infiltration in prostate cancer. *Am. J. Pathol.* **184**, 3156–3162, <https://doi.org/10.1016/j.ajpath.2014.08.009> (2014).
10. Pundavela, J. *et al.* Nerve fibers infiltrate the tumor microenvironment and are associated with nerve growth factor production and lymph node invasion in breast cancer. *Mol. Oncol.* **9**, 1626–1635, <https://doi.org/10.1016/j.molonc.2015.05.001> (2015).
11. Melander, A. & Sundler, F. Presence and influence of cholinergic nerves in the mouse thyroid*. *Endocrinology* **105**, 7–9, <https://doi.org/10.1210/endo-105-1-7> (1979).
12. Van Sande, J., Dumont, J. E., Melander, A. & Sundler, F. Presence and influence of cholinergic nerves in the human thyroid. *J. Clin. Endocrinol. Metab.* **51**, 500–502, <https://doi.org/10.1210/jcem-51-3-500> (1980).
13. Melander, A. *et al.* Sympathetic innervation and noradrenaline content of normal human thyroid tissue from fetal, young, and elderly subjects. *J. Endocrinol. Invest.* **1**, 175–177, <https://doi.org/10.1007/bf03350368> (1978).
14. Ahren, B. Thyroid neuroendocrinology: neural regulation of thyroid hormone secretion. *Endocr Rev* **7**, 149–155, <https://doi.org/10.1210/edrv-7-2-149> (1986).
15. Melander, A., Nilsson, E. & Sundler, F. Sympathetic activation of thyroid hormone secretion in mice. *Endocrinology* **90**, 194–199, <https://doi.org/10.1210/endo-90-1-194> (1972).
16. Ishii, J., Shizume, K. & Okinaka, S. Effect of stimulation of the vagus nerve on the thyroidal release of ¹³¹I-labeled hormones. *Endocrinology* **82**, 7–16, <https://doi.org/10.1210/endo-82-1-7> (1968).
17. Romeo, H. E., Diaz, M. C., Ceppi, J., Zaninovich, A. A. & Cardinali, D. P. Effect of inferior laryngeal nerve section on thyroid function in rats. *Endocrinology* **122**, 2527–2532, <https://doi.org/10.1210/endo-122-6-2527> (1988).
18. Park, H. S. *et al.* Clinicopathologic characteristics and surgical outcomes of elderly patients with thyroid cancer. *Jpn. J. Clin. Oncol.* **44**, 1045–1051, <https://doi.org/10.1093/jjco/hyu132> (2014).
19. Thompson, R. J., Doran, J. F., Jackson, P., Dhillon, A. P. & Rode, J. PGP 9.5—a new marker for vertebrate neurons and neuroendocrine cells. *Brain Res.* **278**, 224–228 (1983).
20. Faulkner, S. *et al.* Neurotrophin receptors TrkA, P75(NTR), and sortilin are increased and targetable in thyroid cancer. *Am. J. Pathol.* **188**, 229–241, <https://doi.org/10.1016/j.ajpath.2017.09.008> (2018).
21. Faulkner, S. *et al.* ProNGF is a potential diagnostic biomarker for thyroid cancer. *Oncotarget* **7**, 28488–28497, <https://doi.org/10.18632/oncotarget.8652> (2016).
22. Bankhead, P. *et al.* QuPath: Open source software for digital pathology image analysis. *Sci. Rep.* **7**, 16878, <https://doi.org/10.1038/s41598-017-17204-5> (2017).
23. Liebig, C., Ayala, G., Wilks, J. A., Berger, D. H. & Albo, D. Perineural invasion in cancer: a review of the literature. *Cancer* **115**, 3379–3391, <https://doi.org/10.1002/cncr.24396> (2009).
24. Munoz, M., Rosso, M., Carranza, A. & Covenas, R. Increased nuclear localization of substance P in human gastric tumor cells. *Acta Histochem.* **119**, 337–342, <https://doi.org/10.1016/j.acthis.2017.03.003> (2017).
25. Faulkner, S., Jobling, P., March, B., Jiang, C. C. & Hondermarck, H. Tumor neurobiology and the war of nerves in cancer. *Cancer Discov.* <https://doi.org/10.1158/2159-8290.cd-18-1398> (2019).
26. Austin, M., Elliott, L., Nicolaou, N., Grabowska, A. & Hulse, R. P. Breast cancer induced nociceptor aberrant growth and collateral sensory axonal branching. *Oncotarget* **8**, 76606–76621, <https://doi.org/10.18632/oncotarget.20609> (2017).
27. Ayala, G. E. *et al.* Cancer-related axonogenesis and neurogenesis in prostate cancer. *Clin. Cancer Res.* **14**, 7593–7603, <https://doi.org/10.1158/1078-0432.Ccr-08-1164> (2008).
28. Bründl, J. *et al.* Computerized quantification and planimetry of prostatic capsular nerves in relation to adjacent prostate cancer foci. *Eur. Urol.* **65**, 802–808, <https://doi.org/10.1016/j.eururo.2013.04.043> (2014).
29. Albo, D. *et al.* Neurogenesis in colorectal cancer is a marker of aggressive tumor behavior and poor outcomes. *Cancer* **117**, 4834–4845, <https://doi.org/10.1002/cncr.26117> (2011).
30. Ceyhan, G. O. *et al.* Nerve growth factor and artemin are paracrine mediators of pancreatic neuropathy in pancreatic adenocarcinoma. *Ann. Surg.* **251**, 923–931, <https://doi.org/10.1097/SLA.0b013e3181d974d4> (2010).
31. Melander, A., Ranklev, E., Sundler, F. & Westgren, U. Beta2-adrenergic stimulation of thyroid hormone secretion. *Endocrinology* **97**, 332–336 (1975).
32. Ahren, B. & Rerup, C. Effects of beta-adrenoceptor agonists and antagonists on thyroid hormone secretion. *Eur. J. Pharmacol.* **88**, 383–387 (1983).
33. Young, J. B., Bürgi-Saville, M. E., Bürgi, U. & Landsberg, L. Sympathetic nervous system activity in rat thyroid: potential role in goitrogenesis. *Am. J. Physiol.-Endoc. M.* **288**, E861–E867, <https://doi.org/10.1152/ajpendo.00292.2004> (2005).
34. Rains, S. L., Amaya, C. N. & Bryan, B. A. Beta-adrenergic receptors are expressed across diverse cancers. *Oncoscience* **4**, 95–105, <https://doi.org/10.18632/oncoscience.357> (2017).
35. Ling, L., Haraguchi, K., Ohta, K., Endo, T. & Onaya, T. Beta 2-adrenergic receptor mRNA is overexpressed in neoplastic human thyroid tissues. *Endocrinology* **130**, 547–549, <https://doi.org/10.1210/endo.130.1.1309349> (1992).

Acknowledgements

This work was supported by a Hunter New England Local Health District Clinical Research Fellowship, a Hunter Cancer Research Alliance Pilot grant, and an Australian Government Research Training Program Scholarship (to CR). The authors would like to thank Dr. Anna Price (NSW Health Pathology, Hunter); Megan Clarke (Hunter Cancer Biobank); Dr. Jorge Tolosa (Hunter Medical Research Institute) and Dr. Craig Gedye (Department of Medical Oncology, Calvary Mater Newcastle) for invaluable support.

Author contributions

C.R. and H.H. conceived and conducted the study, analyzed the data and drafted the manuscript, with contributions to study design and analysis from T.D., N.G., P.J., S.F., J.W.P., S.K. and R.S. All authors have reviewed and approved the final manuscript.

Competing interests

The authors declare no competing interests.

Additional information

Supplementary information is available for this paper at <https://doi.org/10.1038/s41598-020-58425-5>.

Correspondence and requests for materials should be addressed to C.W.R.

Reprints and permissions information is available at www.nature.com/reprints.

Publisher's note Springer Nature remains neutral with regard to jurisdictional claims in published maps and institutional affiliations.



Open Access This article is licensed under a Creative Commons Attribution 4.0 International License, which permits use, sharing, adaptation, distribution and reproduction in any medium or format, as long as you give appropriate credit to the original author(s) and the source, provide a link to the Creative Commons license, and indicate if changes were made. The images or other third party material in this article are included in the article's Creative Commons license, unless indicated otherwise in a credit line to the material. If material is not included in the article's Creative Commons license and your intended use is not permitted by statutory regulation or exceeds the permitted use, you will need to obtain permission directly from the copyright holder. To view a copy of this license, visit <http://creativecommons.org/licenses/by/4.0/>.

© The Author(s) 2020

Supplementary Information for:

Innervation of papillary thyroid cancer and its association with extra-thyroidal invasion.

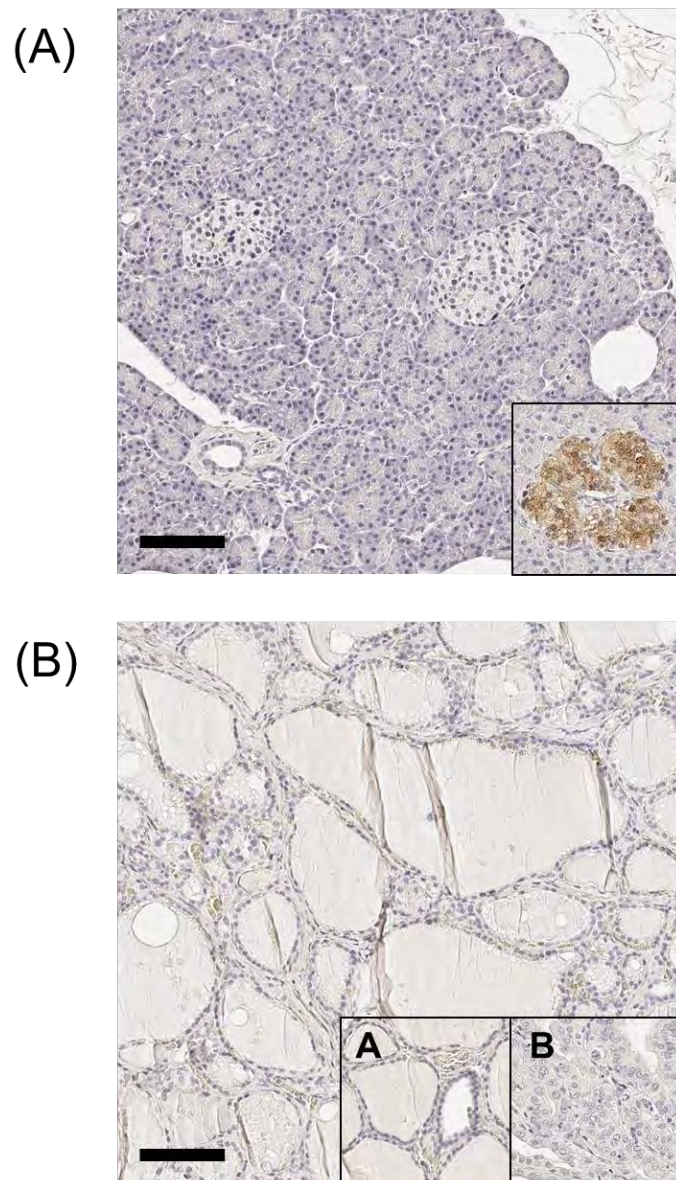
Christopher W Rowe^{1,2,3}, Tony Dill^{4*}, Nathan Griffin^{3,5}, Phil Jobling⁵, Sam Faulkner^{3,5}, Jonathan W Paul^{1,3}, Simon King⁴, Roger Smith^{1,2,3} and Hubert Hondermarck^{3,5}

Supplementary Figure S1

Negative controls for anti-PGP9.5 antibody (Abcam, catalogue number Ab15503). Immunostaining was performed without addition of primary antibody (shown). Scale bar: 100 μ m. Negative controls with substitution of the secondary antibody for non-specific IgG isotype controls were similar (not show).

(A): Section of human pancreas, 10 \times magnification. Islets of Langerhans are known positive controls for PGP9.5. Without addition of primary antibody, there is no staining of Islets, and no non-specific staining. Inset: Positive staining of Islet of Langerhans following addition of primary antibody.

(B): Human thyroid, 10 \times magnification. Without addition of primary antibody, there is no non-specific staining of thyroid follicular epithelium. Inset (A) shows normal thyroid following addition of correct primary antibody, demonstrating expected negative staining of thyroid follicular epithelium, allowing for straightforward identification of labelled nerves (See Figure 1 and 2). Inset (B) shows papillary thyroid cancer following addition of primary antibody, again showing absence of non-specific staining.



Supplementary Table S2: Subgroup analysis of nerve density around papillary thyroid cancers and benign thyroid tissue, resected under identical surgical conditions of total thyroidectomy and without lymph node dissection.

	Benign thyroid	Papillary cancer	<i>p-value</i>
Number of sections	19	13	
Age	54.3 ± 15.5	49.4 ± 20.9	0.44
Female gender (n, %)	15 (78%)	9 (69%)	0.53
TSH (mIU/L)^	0.73 ± 0.91	0.84 ± 0.62	0.64
Benign pathology			
Nodular goitre	11		
Follicular adenoma	8		
<i>Total number of nerves</i>	<i>11 (3 - 21)</i>	<i>23 (15 - 28)</i>	<i>0.048</i>
Total area of thyroid tissue (cm ²)	1.8 (1.7 – 2.3)	1.4 (0.9 – 1.9)	0.10
<i>Nerves per cm² of thyroid tissue</i>	<i>6.6 (2.9 – 9.8)</i>	<i>17.2 (11.2 – 18.8)</i>	<i>0.002</i>

Data are median (IQR). *Mann-Whitney test, using benign thyroid tissue as comparator. ^ TSH data missing for 2 benign cases and 1 malignant case.

Supplementary Table S3: Multiple log-linear regression of nerve density (dependent variable), including model variables of presence of cancer, type of operation (hemithyroidectomy = 0; total thyroidectomy = 1), and lymph node dissection (performed = 1) on the full cohort of benign thyroid tissue and papillary thyroid cancer. Inclusion of additional model variables around operation type did not change the overall parameter estimates or significance of the association between nerve density and thyroid cancer

Base model	Beta coefficient (95% CI)	<i>p</i>-value
Cancer present	0.69 (0.27 to 1.11)	0.002
Exploratory model		
Cancer present	0.67 (0.18 to 1.14)	0.007
Total thyroidectomy	0.50 (0.01 to 0.99)	0.05
Lymph node dissection	0.09 (-0.34 to 0.51)	0.69

Supplementary Table S4: Association between nerve density in PTCs and clinical/pathological parameters after excluding cases with gross extra-thyroidal invasion (n=8 with PTC and gross ETE excluded)

Model variable	Nerves per cm ² of thyroid tissue		Nerves per cm ² of PTC	
	Beta coefficient	<i>p-value</i>	Beta coefficient	<i>p-value</i>
Age	0 (0 to 0)	<i>0.45</i>	0 (0 to 0)	<i>0.86</i>
Sex	-0.3 (-0.8 to 0.2)	<i>0.26</i>	-0.2 (-0.8 to 0.3)	<i>0.42</i>
Tumor size (cm)	-0.3 (-0.5 to 0) -25% (-49% to 0%)	<i>0.05</i>	-0.6 (-0.9 to 0.0) -62% (-89% to -34%)	<i><0.0001</i>
Extra-thyroidal invasion	0.75 (0.3 to 1.2) 211% (129% to 346%)	<i>0.004</i>	1.0 (0.4 to 1.5) 261% (149% to 458%)	<i>0.001</i>
Multifocality	0.1 (-0.4 to 0.5)	<i>0.75</i>	0 (-0.4 to 0.6)	<i>0.70</i>
Nodal metastases	0 (-0.5 to 0.5)	<i>0.96</i>	-0.2 (-0.8 to 0.4)	<i>0.48</i>
Intercept	3.1 (2.1 to 4.0)		3.9 (2.8 to 5.0)	

Multiple log-linear regression of log-transformed nerve density and untransformed markers of cancer aggressiveness in PTCs. Coefficients (95% CI) are reported. Percentage change of the untransformed variable is co-reported (*italics*) for significant model variables, where each 1 unit increase in the model variable is associated with a percentage change in nerve density.

5 NEUROTROPHIN RECEPTORS

TrkA, P75-NTR AND SORTILIN

ARE INCREASED AND TARGETABLE

IN THYROID CANCER

5.1 Preface

While it has been established that proNGF has increased expression in differentiated thyroid carcinomas, the functional significance is not known. As highlighted in the previous paper, it is possible that proNGF may interact with receptors on nerves to drive neo-innervation of thyroid cancer. However, proNGF derived from thyroid cancer cells may have local paracrine actions via specific receptors expressed on thyroid cancer cells. ProNGF is known to interact with the cell surface receptors sortilin and TrkA, which have been shown to be expressed in some cancers. However, it is not known whether these, or other neurotrophin receptors, are expressed by malignant thyrocytes.

This paper examines expression of neurotrophin receptors, TrkA and sortilin, and the pan-neurotrophin receptor, p75^{NTR}, in malignant thyroid tissue, both in histological specimens and thyroid cancer cell lines.



TUMORIGENESIS AND NEOPLASTIC PROGRESSION

Neurotrophin Receptors TrkA, p75^{NTR}, and Sortilin Are Increased and Targetable in Thyroid Cancer



Sam Faulkner,^{*†} Philip Jobling,^{*†} Christopher W. Rowe,^{†‡§} S.M. Rodrigues Oliveira,^{*†} Severine Roselli,^{*†} Rick F. Thorne,[†] Christopher Oldmeadow,^{†¶} John Attia,^{†‡} Chen Chen Jiang,^{†‡} Xu Dong Zhang,^{*†} Marjorie M. Walker,^{†‡||} and Hubert Hondermarck^{*†}

From the School of Biomedical Sciences & Pharmacy,^{*} Faculty of Health and Medicine, the Hunter Medical Research Institute,[†] the School of Mathematical and Physical Sciences,[¶] Faculty of Science and Information Technology, and the School of Medicine & Public Health,[‡] Faculty of Health and Medicine, University of Newcastle, Callaghan, New South Wales; and the Departments of Endocrinology[§] and Anatomical Pathology,^{||} John Hunter Hospital, Callaghan, New South Wales, Australia

Accepted for publication
September 21, 2017.

Address correspondence to
Hubert Hondermarck, Ph.D.,
School of Biomedical Sciences
& Pharmacy, University of
Newcastle, Life Sciences
Building, Callaghan, NSW
2308, Australia. E-mail:
[hubert.hondermarck@
newcastle.edu.au](mailto:hubert.hondermarck@newcastle.edu.au).

Neurotrophin receptors are emerging targets in oncology, but their clinicopathologic significance in thyroid cancer is unclear. In this study, the neurotrophin tyrosine receptor kinase TrkA (also called NTRK1), the common neurotrophin receptor p75^{NTR}, and the proneurotrophin receptor sortilin were analyzed with immunohistochemistry in a cohort of thyroid cancers ($n = 128$) and compared with adenomas and normal thyroid tissues ($n = 62$). TrkA was detected in 20% of thyroid cancers, compared with none of the benign samples ($P = 0.0007$). TrkA expression was independent of histologic subtypes but associated with lymph node metastasis ($P = 0.0148$), suggesting the involvement of TrkA in tumor invasiveness. Nerves in the tumor microenvironment were positive for TrkA. p75^{NTR} was overexpressed in anaplastic thyroid cancers compared with papillary and follicular subtypes ($P < 0.0001$). Sortilin was overexpressed in thyroid cancers compared with benign thyroid tissues ($P < 0.0001$). Neurotrophin receptor expression was confirmed in a panel of thyroid cancer cell lines at the mRNA and protein levels. Functional investigations using the anaplastic thyroid cancer cell line CAL-62 found that siRNA against TrkA, p75^{NTR}, and sortilin decreased cell survival and cell migration through decreased SRC and ERK activation. Together, these data reveal TrkA, p75^{NTR}, and sortilin as potential therapeutic targets in thyroid cancer. (*Am J Pathol* 2018; 188: 229–241; <https://doi.org/10.1016/j.ajpath.2017.09.008>)

Thyroid cancer is the most common endocrine malignant tumor. Most tumors are derived from thyroid follicular epithelial cells, including papillary thyroid carcinoma (PTC), follicular thyroid carcinoma (FTC), and undifferentiated anaplastic thyroid carcinoma (ATC), whereas medullary thyroid carcinoma (MTC) is derived from neuroendocrine parafollicular cells. Worldwide, the incidence of thyroid cancer is increasing.¹ In part, this is explained by increased detection of indolent disease,² and there is a need for improved diagnostic strategies for clinically significant carcinomas.³ However, recent data have indicated an increase in mortality during the past 3 decades for patients diagnosed with advanced thyroid cancer, suggesting not only a true increase in incidence but also the need for novel treatment strategies for this subgroup.⁴ In particular, ATC, the most lethal histologic subtype, carries a

high mortality rate, with median survival of <1 year after diagnosis.⁵ Thus, the identification of new targets for the diagnosis and treatment of clinically significant thyroid cancer is essential.

Neurotrophin receptors are known to be overexpressed in some human cancers, where they participate in the stimulation of tumor growth and dissemination.^{6,7} In particular, recent data have indicated the crucial stimulatory impact of nerve growth factor (NGF) in gastric⁸ and pancreatic cancer,⁹ where targeting NGF resulted in a strong reduction of tumor growth and metastasis. In thyroid cancer, the overexpression of the precursor for NGF (proNGF) has been

Supported by the University of Newcastle (Australia) and the Hunter Cancer Research Alliance.

Disclosures: None declared.

found, suggesting a role in pathogenesis.¹⁰ However, the status of NGF/proNGF receptors in thyroid tissue is not clear. ProNGF binds to a complex between the membrane protein sortilin and the neurotrophin receptor p75^{NTR}, initiating various signaling pathways, including NF-κB, RhoA, and JNK.¹¹ In addition, proNGF has also been found to activate the neurotrophin tyrosine receptor kinase 1 (NTRK1 or TrkA).¹¹ In thyroid cancer, the expression of sortilin has never been reported, and although p75^{NTR}¹² and TrkA¹³ are expressed, their clinicopathologic significance is not defined.

In this study, we found the increased expression of TrkA, p75^{NTR}, and sortilin in a cohort of thyroid cancers compared with benign thyroid tissues (adenomas and normal thyroid tissues). Furthermore, *in vitro* experiments revealed that targeting these neurotrophin receptors resulted in a decreased growth and invasion of ATC cells, suggesting a potential utility as therapeutic targets.

Materials and Methods

Thyroid Tissue Samples

High-density tumor microarrays (TH801, TH641, TH8010) were obtained from US Biomax Inc. (Rockville, MD) and included 128 thyroid cancers (79 PTCs, 27 FTCs, 12 ATCs, 10 other subtypes), 6 adenomas, and 56 normal thyroid tissues. The other subtypes were follicular papillary carcinomas ($n = 6$), sarcomatoid carcinomas ($n = 1$), and MTCs ($n = 3$). Within the 27 cases of FTC, 3 cases were characterized as poorly differentiated, and 5 were characterized as moderately differentiated. The following information was available: patient age and sex, histologic subtype, tumor size, lymph node status, and stage. US Biomax Inc. quality controls are described as follows. Each single tissue spot on every array slide is individually examined by pathologists certified according to World Health Organization published standardizations of diagnosis, classification, and pathologic grade. Each specimen collected was consented to by both hospital and individual. Discrete legal consent was obtained, and the rights to hold research uses for any purpose or further commercialized uses were waived. The study was approved by the Human Research Ethics Committee of the University of Newcastle, Australia.

Immunohistochemistry and Digital Quantification

Immunohistochemistry and digital quantification of staining intensities were performed as previously described.¹⁰ Antibodies against TrkA (1/200 dilution, catalog number 2508; Cell Signaling Technology, Danvers, MA), p75^{NTR} (1/400 dilution, catalog number 4201; Cell Signaling Technology), sortilin (0.8 μg/mL, catalog number ANT-009; Alomone Labs, Jerusalem, Israel), or PGP9.5 (1/200 dilution, catalog number ab15503; Abcam, Cambridge, United Kingdom)

were applied. Negative controls with a rabbit monoclonal antibody IgG Isotype Control (DA1E, catalog number 3900; Cell Signaling Technology) were also performed (Supplemental Figure S1A). The specificity of the antibodies used for immunohistochemistry was assessed using Western blot analysis in a panel of thyroid tumor tissue samples (Supplemental Figure S1B). Thyroid tumor samples included one FTC and three PTCs. Specificity was also confirmed in the PC-12 cell line, which is known to express neurotrophin receptors (Supplemental Figure S1C). TrkA, p75^{NTR}, and sortilin were all found to be expressed at their expected molecular weights (140 kDa for TrkA, 75 kDa for p75^{NTR}, and 100 kDa for sortilin) in both the thyroid tumor tissue samples (Supplemental Figure S1B) and PC-12 cells (Supplemental Figure S1C). For quantification of p75^{NTR} and sortilin staining intensity, pixel intensity values were used to determine the h-scores for each core (index calculated as the sum of $3 \times$ percentage of pixels with strong staining + $2 \times$ percentage of pixels with intermediate staining + $1 \times$ percentage of pixels with weak staining). Staining intensities were categorized as negative (h-score < 25), low (h-score of 25 to 100), or high (h-score > 100). For TrkA, because of the limited proportion of cells that tested positive for TrkA, it was not possible to calculate a representative h-score; therefore, positivity versus negativity for TrkA staining was recorded. For statistical analyses, staining intensities for p75^{NTR}, sortilin, and positivity or negativity for TrkA, were compared with clinicopathologic parameters: normal versus malignant, patient age and sex, histologic type, tumor size, lymph node status, stage, and grade. Simple unadjusted associations with pathologic variables were performed using a χ^2 test with SAS statistical software version 9.4 (SAS Institute, Cary, NC).

Cell Culture

Thyroid cancer cell lines CAL-62 (ATC), BCPAP (PTC), and ML-1 (MTC) were purchased from DSMZ (Braunschweig, Germany), which uses STR verification of cell line authenticity. The TPC-1 (PTC) cell line was obtained from Dr. Mareel's laboratory (University of Gent, Gent, Belgium). The 8505c (ATC) cell line was a generous gift from Prof. Alfred Lam (Griffith University, Queensland, Australia). TPC-1 cell authenticity was validated using the GenePrint 10 System (catalog number B9510, Promega, Madison WI). PC-12 cells were obtained from Prof. Ralph A. Bradshaw (University of California, San Francisco, CA). All cell lines were maintained in RPMI-1640 with 10% (v/v) fetal calf serum (FCS) (JRH Biosciences, Lenexa, KS) and 2 mmol/L L-glutamine in a humidified incubator at 37°C with 5% (v/v) CO₂. Routine *Mycoplasma* testing was performed using the MycoAlert *Mycoplasma* Detection Kit (catalog number LT07-118; Lonza, Basel, Switzerland). Cells were not maintained in culture for longer than 3 months to ensure passage number remained fit for purpose.

Preparation of Conditioned Media

Conditioned media was prepared as previously described.¹⁴ Briefly, 5×10^6 cells were seeded per T-75 cm² culture flask and grown in 10 mL of serum free media for 24 hours. The collected medium was centrifuged ($800 \times g$ for 5 minutes at 4°C) and the supernatant was concentrated and desalted using 10-kDa cut-off Amicon Ultra-15 filtration unit (catalog number UFC900324; Merck Millipore, Darmstadt, Germany) for 30 minutes ($4000 \times g$, 4°C). The recovered concentrate was stored at -80°C.

Protein Extraction and Western Blotting

Protein extraction from cell lines and Western blotting experiments were performed as previously described.¹⁵ For protein extraction from thyroid tumors, thyroid tumor tissue samples (obtained from the biobank of the Department of Endocrinology, John Hunter Hospital, Newcastle, Australia) were snap frozen with liquid nitrogen, crushed using a mortar and pestle, and transferred to individual 1.5 mL Precellys CK28 Lysing Tubes (catalog number KT03961-1-007.2; Bertin Technologies, Montigny-le Bretonneux, France). Samples were lysed on ice using 1 mL of SDS extraction buffer (2% SDS, 1% IGEPAL, 0.5% sodium deoxycholate, 50 mmol/L Tris pH 7.5, 5 mmol/L EDTA). Complete mini-protease inhibitor cocktail tablets (catalog number 4693124001; Roche, Basel, Switzerland) and PhosSTOP phosphatase inhibitor tablets (catalog number 4906837001; Roche) were also used. Samples were homogenized in a Precellys 24 Homogenizer (Bertin Technologies) at $1500 \times g$ (6×30 seconds intervals). Finally, samples were centrifuged at $16,000 \times g$ for 15 minutes at 4°C, and the supernatant was extracted and stored at -80°C. Anti-TrkA (catalog number ANT018; Alomone Labs), anti-p75^{NTR} (catalog number sc-6188; Santa Cruz Biotechnology, Dallas, TX), and anti-sortilin (catalog number ANT009; Alomone Labs) antibodies were used at a dilution of 1:500. Anti-proNGF (catalog number ab9040; Merck Millipore) and anti-NGF (catalog number sc-548; Santa Cruz Biotechnology) antibodies were used at a dilution of 1:200. β -Actin detection (1/5000 dilution, catalog number A2066; Sigma-Aldrich, St. Louis, MO) was used as the equal loading control. Antibodies from Cell Signaling Technology were used to assess cellular signaling pathways: anti-phospho-TrkA (anti-p-TrkA) (Tyr490, catalog number 9141), anti-Src (catalog number 2100), anti-phospho-Src (anti-p-Src) (Tyr416, catalog number 2101), anti-Erk1/2 (catalog number 9107), and anti-phospho-Erk1/2 (anti-p-Erk1/2) (Thr202/Tyr204, catalog number 4370).

Real-Time RT-PCR

Total RNA was isolated from thyroid cancer cell lines using the illustra RNAspin Mini RNA Isolation Kit (catalog number

25-0500-70; GE Healthcare Life Sciences, Little Chalfont, UK). Reverse transcription was performed with 1 μ g of total RNA using the iScript cDNA Synthesis Kit (catalog number 1708890; Bio-Rad Laboratories Inc., Hercules, CA). Real-time PCR was performed using 2 μ L of 1/10 cDNA using iTaq Universal SYBR Green Supermix (catalog number 172-5120; Bio-Rad Laboratories Inc.). The primers used were as follows: sortilin primers were Quantitect Primer Assay QT00073318 (Qiagen, Venlo, Netherlands); p75^{NTR} primers were 5'-ACGG CTACTACCAGGATGAG-3' (forward) and 5'-TGGCCTCG TCGGAATACGTG-3' (reverse) (Sigma-Aldrich); TrkA primers were Quantitect Primer Assay QT00054110 (Qiagen); primers used for the reference gene *GAPDH* were 5'-CAC-CAGGGCTGCTTTTAACCTCTGTA-3' (forward) and 5'-CCTTGACGGTGCCATGGAATTTG-3' (reverse) (Sigma-Aldrich). PCR was performed in a ABI7500 Real-Time PCR System (Applied Biosystems, Thermo Fisher Scientific, Waltham, MA) using the following conditions: 95°C for 10 minutes, 40 cycles of 95°C for 15 seconds, and 60°C for 60 seconds followed by a continuous Melt curve from 65°C to 95°C. Data were analyzed using the ABI7500 Real-Time software version 2.3 (Applied Biosystems, Thermo Fisher Scientific). Relative expression was obtained using the $2^{-\Delta\Delta C_t}$ method.

Transfection with siRNA

ATC cell lines CAL-62 and 8505c were transfected for 72 hours with 15 nmol/L of siRNA using lipofectamine RNAi-MAX (catalog number 13778150; Life Technologies, Carlsbad, CA), according to the manufacturer's recommendations. Cells were seeded in 6-well plates and transfected 24 hours later with siRNA against TrkA (siTrkA, CGAGAACCCA-CAAUACUUCAGUGAT, catalog number SR303249; OriGene Technologies Inc., Rockville, MD), p75^{NTR} (siP75^{NTR}, GGAAUUGACUUCGACUGUGACCUGT, catalog number SR303174; OriGene Technologies Inc.), and sortilin (siSort, CUCUGCUGUUAACACCACC[dT][dT]; Sigma-Aldrich) as well as a commercially available siRNA control sequence: MISSION siRNA Universal negative control 1 (catalog number SIC001; Sigma-Aldrich). The efficiency of TrkA, p75^{NTR}, and sortilin knockdown was assessed using Western blot analysis at 24, 48, and 72 hours after transfection, using anti-TrkA (catalog number ANT018; Alomone Labs), anti-p75^{NTR} (catalog number sc-6188; Santa Cruz Biotechnology), and anti-sortilin (catalog number ANT009; Alomone Labs) antibodies, respectively. β -Actin (catalog number A2066; Sigma-Aldrich) was used as an equal loading control.

Cell Growth and Apoptosis Assay

A total of 7×10^5 ATC cells (CAL-62 and 8505c) were seeded in 2 mL of culture medium (RPMI containing 10% FCS and 2 mmol/L L-glutamine) on 6-well plates and were allowed to adhere overnight in a humidified incubator at 37°C and 5% CO₂. Cells were transfected the following day with siTrkA, siP75^{NTR}, siSort, a combination of the three

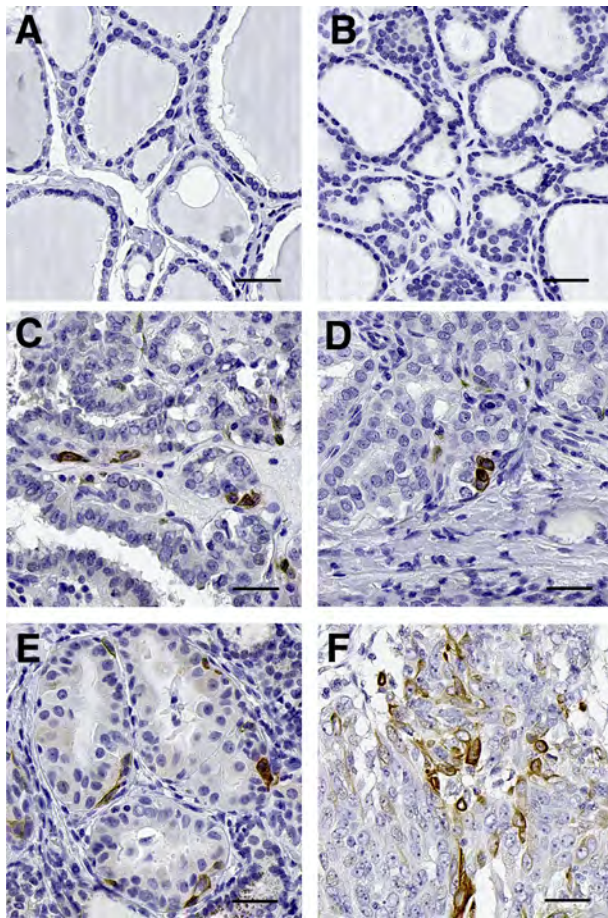


Figure 1 TrkA expression in thyroid cancers. **A–F:** TrkA immunostaining was performed on a cohort of thyroid cancers, adenomas, and normal thyroid tissues. TrkA is not observed in normal thyroid tissues (**A**) or adenomas (**B**). In contrast, TrkA staining is found in papillary thyroid carcinoma (**C** and **D**), follicular thyroid carcinoma (**E**), and anaplastic thyroid carcinoma (**F**) histologic subtypes. Only a small proportion of cancer cells are positive for TrkA. Recording of TrkA positivity is reported in Table 1. $n = 128$ thyroid cancers, 6 adenomas, and 56 normal thyroid tissues. Scale bars: 50 μ m. Original magnification, $\times 400$.

siRNAs (siCombo), or control siRNA (siCont). Images were obtained after 72 hours, and viable cell number was counted using Trypan Blue with a hemocytometer. For assessing apoptosis, 1×10^6 cells were incubated with 100 μ L of Muse Annexin V and Dead Cell Reagent (catalog number MCH100105; Merck Millipore, Darmstadt, Germany) for 20 minutes at room temperature as per the manufacturer's instructions. The Muse Cell Analyzer (Merck Millipore) was used to determine apoptosis, and the statistics obtained revealed the percentages of the cells represented by alive, apoptotic, and dead populations.

Cell Migration and Wound-Healing Assay

A total of 5×10^5 ATC cells (CAL-62 and 8505c) were seeded on 6-well plates in complete growth medium (RPMI containing 10% FCS and 2 mmol/L L-glutamine) and were allowed to adhere overnight in a humidified incubator at

37°C and 5% CO₂. Cells were transfected the following day with siTrkA, siP75^{NTR}, siSort, a combination of the three siRNAs (siCombo), or control siRNA (siCont). After 72 hours, during which the cells were allowed to grow to confluence, the cell monolayer was scratched with a 200- μ L pipette tip, rinsed three times with phosphate-buffered saline to remove floating cellular debris, and replaced with media that contained 0.1% (v/v) FCS. The wound area that resulted from the scratch was monitored using the JuLI Stage automated cell imaging system (NanoEnTek Inc., Seoul, Korea). Images were taken automatically every 5 hours during a 20-hour postscratch period. Results are shown as the percentage reduction of the wound area, measured using ImageJ version 1.60_20 (NIH, Bethesda, MD; <http://imagej.nih.gov/ij>).

Cell Invasion Assay

Cell invasion assays were performed on CAL-62 and 8505c ATC cells using the QCM ECMatrix Cell Invasion Assay (catalog number ECM554; Merck Millipore), which is made up of 24-well plates and contains upper invasion chamber inserts with 8- μ m pore size membranes. The extracellular matrix layer was rehydrated with 300 μ L of prewarmed serum free media for 30 minutes at room temperature. Cells were loaded into the invasion chamber insert using 2×10^5 siRNA transfected cells (72 hours after transfection with siTrkA, siP75^{NTR}, siSort, siCombo, and siCont.) in 250 μ L of media that contained 0.1% (v/v) FCS. Five hundred microliters of media, in the presence of a chemoattractant (10% FCS), was added to the lower chamber. After a 20-hour incubation period, the upper invasion chamber inserts were rinsed with phosphate-buffered saline, and cells at the upper surface of the membranes were gently scraped and removed. Invading cells were dislodged by placing the invasion chambers in 225 μ L of pre-warmed cell detachment buffer before being stained by CyQuant GR Dye (1:75 with $4\times$ lysis buffer) for 15 minutes. Two hundred microliters of the mixture from each sample was transferred to a black 96-well plate (catalog number CLS3792-100; Sigma-Aldrich), and the fluorescence was recorded at 480/520 nm using a FLUOstar OPTIMA fluorescence plate reader (BMG Labtech, Durham, NC). Samples without cells but containing cell detachment buffer, lysis buffer, and CyQuant Dye were used as blanks, and background fluorescence was subtracted from all samples. The number of invading cells was determined by running a fluorescent cell dose standard curve.

Statistical Analysis for *in Vitro* Assays

For cell proliferation, apoptosis, and migration and invasion assays, each condition was performed at least in triplicate, and experiments were repeated on three separate occasions. Statistical analysis was conducted using the GraphPad Prism software version 6 (GraphPad Software Inc., La Jolla, CA). Cell proliferation, apoptosis, migration, and invasion assays

were analyzed using ordinary one-way analysis of variance. For assessing multiple comparisons, Dunnett's multiple comparisons test was used.

Results

The expression of TrkA, p75^{NTR}, and sortilin was analyzed by immunohistochemistry in a series of 128 thyroid cancers of various histologic types, six adenomas, and 55 normal thyroid tissues. In addition, these neurotrophin receptors were detected in thyroid cancer cells in culture, and the functional impact of their targeting using siRNA was investigated.

Gene Versus Protein Expression

We initially started with data mining of gene expression, using cBioportal,¹⁶ of thyroid data sets in The Cancer Genome Atlas database.¹⁷ The results indicated that mRNA

for TrkA, p75^{NTR}, and sortilin are overexpressed in 4%, 6%, and 1% of thyroid cancers, respectively. However, mRNA abundance in tumors does not reliably predict differences in protein levels.¹⁸ Therefore, we proceeded with analyzing protein expression.

TrkA Expression in Thyroid Cancers

TrkA staining was not observed in normal thyroid tissue or adenoma samples (Figure 1, A and B). In contrast, TrkA staining was observed in a proportion of PTC (Figure 1C), FTC (Figure 1D), MTC (Figure 1E), and ATC (Figure 1F) histologic subtypes. TrkA staining was observed in only a small proportion (5% to 10%) of cancer cells; hence, digital quantification with h-score calculation did not provide a meaningful comparison of staining intensities among samples. Therefore, TrkA staining was analyzed in terms of TrkA-positive versus TrkA-negative samples (Table 1).

Table 1 TrkA, p75^{NTR}, and Sortilin Expression in Thyroid Cancers and Associations with Clinicopathologic Parameters

	TrkA intensity			p75 ^{NTR} intensity				Sortilin intensity			
Parameter	Negative, Total (%)	Positive, Total (%)	<i>P</i> value	Negative, Total (%)	Low, Total (%)	High, Total (%)	<i>P</i> value	Negative, Total (%)	Low, Total (%)	High, Total (%)	<i>P</i> value
Normal versus cancer			0.0007				< 0.0001				< 0.0001
Normal (<i>n</i> = 56)	56 (100)	0 (0)		6 (11)	49 (87)	1 (2)		56 (100)	0 (0)	0 (0)	
Adenoma (<i>n</i> = 6)	6 (100)	0 (0)		0 (0)	6 (100)	0 (0)		4 (67)	2 (33)	0 (0)	
Cancer (<i>n</i> = 128)	102 (80)	26 (20)		3 (2)	57 (45)	68 (53)		48 (38)	79 (61)	1 (1)	
Cancer histologic subtype			0.1020				< 0.0001				0.0415
Papillary (<i>n</i> = 79)	58 (73)	21 (27)		1 (1)	28 (36)	50 (63)		26 (33)	52 (66)	1 (1)	
Follicular (<i>n</i> = 27)	25 (93)	2 (7)		2 (7)	20 (74)	5 (19)		7 (26)	20 (74)	0 (0)	
Anaplastic (<i>n</i> = 12)	9 (75)	3 (25)		0 (0)	1 (8)	11 (92)		9 (75)	3 (25)	0 (0)	
Others (<i>n</i> = 10)	10 (100)	0 (0)		0 (0)	8 (80)	2 (20)		6 (60)	4 (40)	0 (0)	
Sex			1.0000				0.5750				0.8201
Female (<i>n</i> = 101)	80 (80)	21 (20)		3 (3)	46 (45)	52 (52)		37 (37)	63 (62)	1 (1)	
Male (<i>n</i> = 27)	22 (81)	5 (19)		0 (0)	11 (41)	16 (59)		11 (41)	16 (59)	0 (0)	
Age, years			0.3826				0.6287				0.4647
<50 (<i>n</i> = 74)	61 (82)	13 (18)		1 (1)	34 (46)	39 (53)		30 (41)	43 (58)	1 (1)	
≥50 (<i>n</i> = 54)	41 (76)	13 (24)		2 (3)	23 (42)	29 (55)		18 (33)	36 (67)	0 (0)	
Tumor size (T)			0.3686				0.4064				0.3686
T1 + T2 (<i>n</i> = 29)	24 (83)	5 (17)		2 (7)	13 (45)	14 (48)		5 (17)	24 (83)	0 (0)	
T3 + T4 (<i>n</i> = 59)	47 (80)	12 (20)		1 (2)	31 (53)	27 (45)		17 (29)	41 (69)	1 (2)	
Missing (<i>n</i> = 40)	31 (78)	9 (22)		0 (0)	13 (31)	27 (69)		26 (65)	14 (35)	0 (0)	
Lymph node (N)			0.0148				0.6772				0.8318
Negative (<i>n</i> = 68)	59 (87)	9 (13)		3 (5)	34 (50)	31 (45)		17 (25)	50 (73)	1 (2)	
Positive (<i>n</i> = 17)	10 (59)	7 (41)		0 (0)	9 (53)	8 (47)		5 (29)	12 (71)	0 (0)	
Missing (<i>n</i> = 43)	33 (77)	10 (23)		0 (0)	14 (31)	29 (69)		26 (60)	17 (40)	0 (0)	
Stage			0.5827				0.6381				0.4719
I + II (<i>n</i> = 54)	45 (83)	9 (17)		2 (4)	29 (53)	23 (43)		12 (22)	41 (76)	1 (2)	
III + IV (<i>n</i> = 35)	27 (77)	8 (23)		1 (3)	16 (44)	18 (53)		11 (31)	24 (69)	0 (0)	
Missing (<i>n</i> = 39)	30 (77)	9 (23)		0 (0)	12 (31)	27 (69)		25 (64)	14 (36)	0 (0)	

Immunohistochemical staining for each neurotrophin receptor was quantified. For TrkA, because only a small proportion of cancer cells were positive for TrkA, immunohistochemical staining in each sample was categorized only as negative versus positive. Representative images for TrkA staining are presented in Figure 1. For p75^{NTR} and sortilin, immunohistochemical staining in each sample was digitally quantified and categorized as negative (h-score <25), low staining (h-score of 25 to 100), or high staining (h-score >100). Representative images for p75^{NTR} and sortilin staining are presented in Figures 3 and 4, respectively. Statistically significant *P* values (*P* < 0.05, using the χ^2 test) are shown in bold.

TrkA positivity was found in 20% of thyroid cancers compared with none of the benign samples ($P = 0.0007$). An association was found between TrkA expression and lymph node metastases, with TrkA positivity observed in 41% of lymph node—positive cancers compared with only 13% of lymph node—negative cancers ($P = 0.0148$). There was no association between TrkA expression and other clinicopathologic parameters (sex, age, tumor size, and stage).

Some staining for TrkA also appears to be in endothelial and other stromal cells. In other models, endothelial cells¹⁹ and fibroblasts²⁰ have been reported to express TrkA; therefore, it is not unexpected to find some TrkA expression in stromal cells. Interestingly, TrkA expression was also detected in nerves present in thyroid cancers (Figure 2). The presence of nerves in the tumor microenvironment was validated using the neuronal marker PGP9.5 (Figure 2, A and E). TrkA staining was observed in nerves (Figure 2, B and F),

whereas p75^{NTR} (Figure 2C) and sortilin (Figure 2D) were not detected in serial tumor microarray cores.

p75^{NTR} Expression in Thyroid Cancers

Expression of p75^{NTR} was detected in most benign thyroid tissues and cancers (Figure 3, A–F). Digital quantification of p75^{NTR} staining intensities (Figure 3G) indicated a median combined h-score of 57.86 for benign thyroid tissue compared with 102.5 for thyroid malignant tumors. Within cancer histologic subtypes, p75^{NTR} was expressed at higher levels in ATC, with a median h-score of 130.60 ($P < 0.0001$) compared with 109.30 ($P < 0.0001$) and 76.82 ($P = 0.0054$) in PTC and FTC, respectively (Figure 3G). For analysis of the associations between p75^{NTR} expression and clinicopathologic parameters, p75^{NTR} staining intensities were categorized as negative (h-score <25), low (h-score of 25 to 100), or high (h-score >100). The frequency distribution of staining intensities (Table 1) indicated that most normal tissues, adenomas, and cancers were positive for p75^{NTR}, whereas only 0% to 2% of normal tissues and adenomas presented intense p75^{NTR} staining compared with 53% of cancers ($P < 0.0001$). By histologic subtypes, p75^{NTR} was expressed at higher levels in ATC, with high p75^{NTR} staining observed in 92% of ATC compared with 19% of FTC and 63% of PTC ($P < 0.0001$). There was no association between p75^{NTR} expression and sex, age, tumor size, lymph node invasion, and stage (Table 1).

Sortilin Expression in Thyroid Cancers

Sortilin was not detected in normal thyroid tissues (Figure 4A). In adenomas (Figure 4B), weak sortilin labeling was observed in epithelial cells of some tissue samples. Thyroid cancers were positive for sortilin, and the labeling was specifically observed in cancer cells (Figure 4, C–F). Digital quantification of staining intensities (Figure 4G) indicated that sortilin was higher in thyroid cancers compared with normal tissues and adenomas. Normal and adenoma thyroid tissues had a combined median h-score of 15.04 compared with 29.69 ($P < 0.0001$) and 40.80 ($P < 0.0001$) in the FTC and PTC cancer subtypes, respectively (Figure 4G). Sortilin expression in ATC yielded a median h-score of 24.11, which was not significantly different than benign thyroid tissues (normal and adenoma) (Figure 4G). For analysis of the association between sortilin expression and clinicopathologic parameters, sortilin staining intensities were categorized as negative (h-score <25), low (h-score of 25 to 100), or high (h-score >100). The frequency distribution of staining intensities (Table 1) indicated that 62% of thyroid cancers were positive for sortilin compared with 33% of adenomas and 0% of normal tissues ($P < 0.0001$). In terms of histologic subtypes, stronger sortilin staining was observed in FTC and PTC compared with ATC ($P = 0.0415$). There was no association between sortilin expression and other clinicopathologic parameters (sex, age, tumor size, lymph node invasion, and stage).

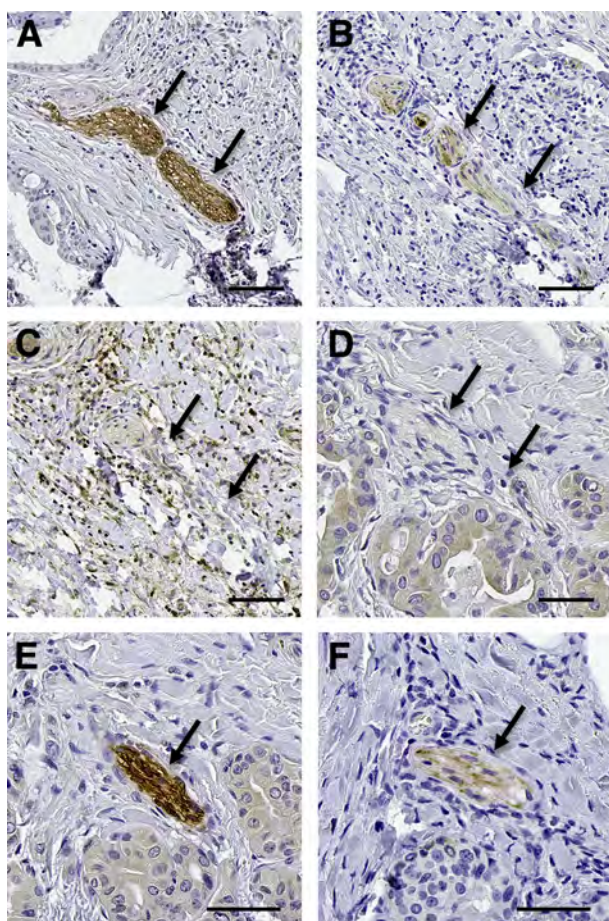


Figure 2 TrkA expression in nerves present in thyroid cancers. Immunohistochemical detection of the neuronal marker PGP9.5 was used to detect nerves in thyroid cancers, and the detection of TrkA, p75^{NTR}, and sortilin was performed in serial sections. **A:** Nerves stained for the neuronal marker PGP9.5. **B–D:** Serial sections for the detection of TrkA (**B**), p75^{NTR} (**C**), and sortilin (**D**) in the nerve shown in **A**. **E:** Another nerve stained for PGP9.5. **F:** TrkA staining observed in a serial section of the nerve shown in **E**. Arrows indicate the location of nerves. Scale bars: 50 μ m. Original magnification, $\times 400$.

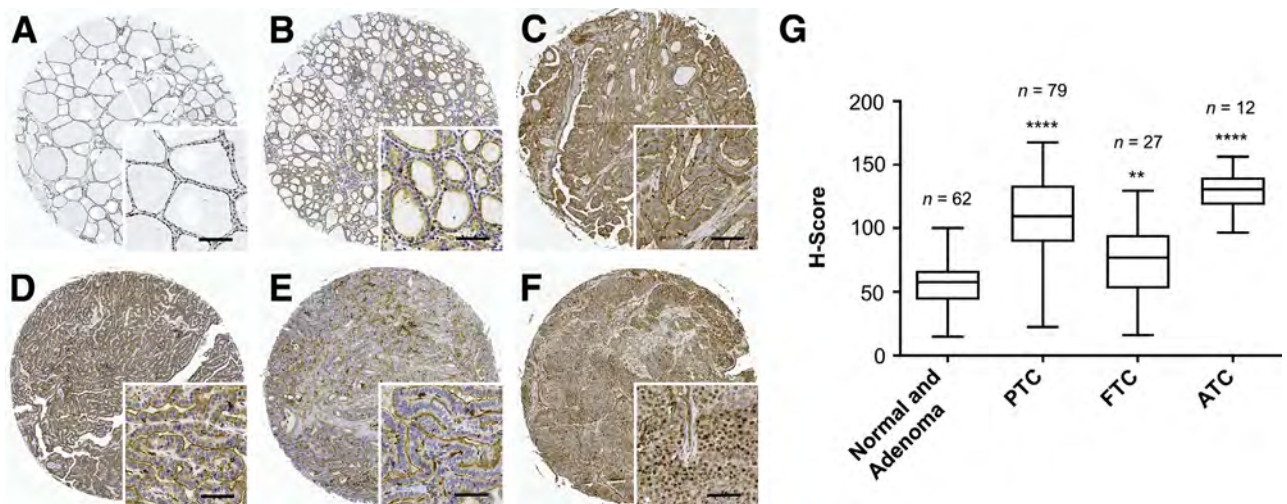


Figure 3 p75^{NTR} expression in thyroid cancers. **A–F:** Immunohistochemical detection of p75^{NTR} in thyroid cancers of various histologic types, adenomas, and normal thyroid tissues was performed. p75^{NTR} was found in epithelial cells of normal tissue (**A**), adenomas (**B**), and thyroid cancers of various histologic subtypes: papillary thyroid carcinoma (PTC) (**C** and **D**), follicular thyroid carcinoma (FTC) (**E**), and anaplastic thyroid carcinoma (ATC) (**F**). **Insets** show higher magnification. **G:** p75^{NTR} staining was quantified using the Halo image analysis platform; h-scores were calculated. p75^{NTR} staining intensities are significantly higher for ATC (median h-score = 130.60), PTC (median h-score = 109.30), and FTC (median h-score = 76.82) compared with normal and adenoma thyroid tissues combined (median h-score = 57.86). Data are expressed as means (horizontal line in center of box), 25th and 75th percentiles (box limits), and interquartile ranges (whiskers) (**G**). $n = 128$ thyroid cancers, 6 adenomas, and 56 normal thyroid tissues. $**P < 0.01$, $****P < 0.0001$ versus normal/adenoma tissue controls. Scale bars: 50 μm (**A–F**). Original magnification: $\times 50$ (**A–F**, main images); $\times 400$ (**insets**).

TrkA, p75^{NTR}, and Sortilin Expression in Thyroid Cancer Cell Lines

Real-time RT-PCR and Western blot analysis were used to detect TrkA, p75^{NTR}, and sortilin at the mRNA and protein levels in a series of thyroid cancer cell lines. The data

(Figure 5) indicate that the three receptors are expressed in the four tested cancer cell lines (CAL-62, ML-1, BCPAP, and TPC-1). All three receptors were detected at their expected theoretical molecular mass: 140 kDa for TrkA, 75 kDa for p75^{NTR}, and 100 kDa for sortilin. TrkA mRNA was present at higher levels in BCPAP, but again this difference

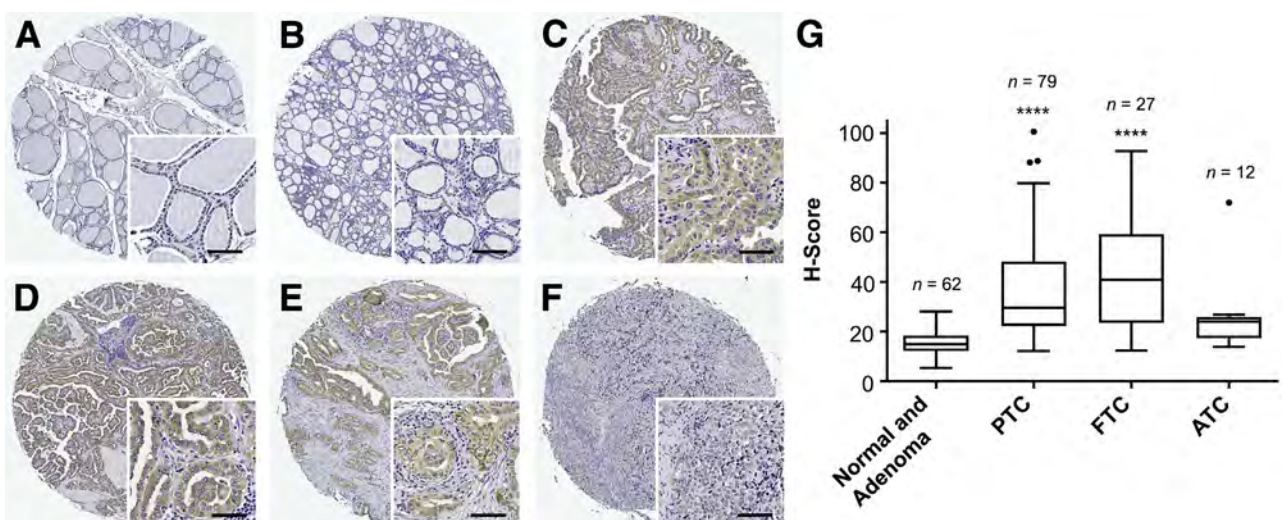


Figure 4 Sortilin expression in thyroid cancer versus normal thyroid tissue. **A–F:** Immunohistochemical detection of sortilin was performed on a cohort of thyroid cancers, adenomas, and normal thyroid tissues. Sortilin is not found in normal thyroid tissues (**A**) and in most adenomas (**B**). In contrast, sortilin staining is observed in cancer cells of papillary thyroid carcinoma (PTC) (**C** and **D**), follicular thyroid carcinoma (FTC) (**E**), and anaplastic thyroid carcinoma (ATC) (**F**). **Insets** show higher magnification. **G:** Sortilin staining was quantified using the Halo image analysis platform; h-scores were calculated. Sortilin staining intensities are significantly higher for PTC (median h-score = 29.69) and FTC (median h-score = 40.80) compared with normal and adenomas combined (median h-score = 15.04). Data are expressed as means (horizontal line in center of box), 25th and 75th percentiles (box limits), interquartile ranges (whiskers), and outliers (dots). $n = 128$ thyroid cancers, 6 adenomas, and 56 normal thyroid tissues. $****P < 0.0001$ versus normal/adenoma tissue controls. Scale bars: 50 μm (**A–F**). Original magnification: $\times 50$ (**A–F**, main images); $\times 400$ (**insets**).

was not found at the protein level, and all cell lines had comparable levels of TrkA. For p75^{NTR}, BCPAP cells expressed a higher level of mRNA than the other cell lines, but this difference was not found at the protein level, where p75^{NTR} appears similar among cell lines. For sortilin, the mRNA and protein levels were similar among cell lines. The protein expression of NGF and its precursor proNGF was also examined in two ATC cell lines, CAL-62 and 8505c (Supplemental Figure S2). NGF and proNGF were detected in protein extracts from both cell lines. Furthermore, the conditioned culture media obtained from CAL-62 and 8505c cells revealed that proNGF was secreted by CAL-62 and 8505c cells, whereas NGF was secreted only by 8505c cells. The concomitant expression of TrkA, p75^{NTR}, and sortilin with NGF and proNGF suggest the existence of an autocrine loop of stimulation in thyroid cancer cells.

Functional Impact of Targeting TrkA, p75^{NTR}, and Sortilin

In vitro assays were performed on the highly aggressive CAL-62 (Figure 6). Cells were transfected with siRNA directed against TrkA, p75^{NTR}, sortilin, and the impact on cell growth, apoptosis, migration, and invasion was assessed. The efficacy of the targeted siRNAs was determined using Western blot analysis at 24, 48, and 72 hours after transfection (Figure 6A). Sortilin protein expression was reduced after 24 hours and completely inhibited after 48

hours. However, maximal inhibition of TrkA and p75^{NTR} expression was achieved 72 hours after transfection, indicating that it was necessary to evaluate the effects of the siRNAs after 72 hours. The combination of the three siRNA (siCombo) against TrkA, p75^{NTR}, and sortilin similarly decreased the level of the three receptors 72 hours after transfection (Figure 6A).

Signaling Pathways

The effects of inhibiting TrkA, p75^{NTR}, and sortilin on various tumorigenic and metastatic-related signaling pathways were explored using Western blot analysis (Figure 6A). p-TrkA was markedly decreased in response to siTrkA, siP75^{NTR}, and siSort, suggesting that the activation of TrkA requires the presence of both p75^{NTR} and sortilin. Total ERK1/2 and p-ERK1/2 were comparable for siCont, siP75^{NTR}, and siSort; however, siTrkA resulted in a decreased level of p-ERK. Inhibition of TrkA, p75^{NTR}, and sortilin all reduced the level of p-SRC. Targeting all three receptors simultaneously mirrored data obtained when targeting each receptor alone; however, the observed effect was not potentiated (Figure 6A).

Cell Growth and Apoptosis

CAL-62 cell growth was analyzed at 72 hours after transfection, and the effects of siTrkA, siP75^{NTR}, siSort, and siCombo were compared with siCont-treated cells (Figure 6B). Treatment of cells with siTrkA, siP75^{NTR},

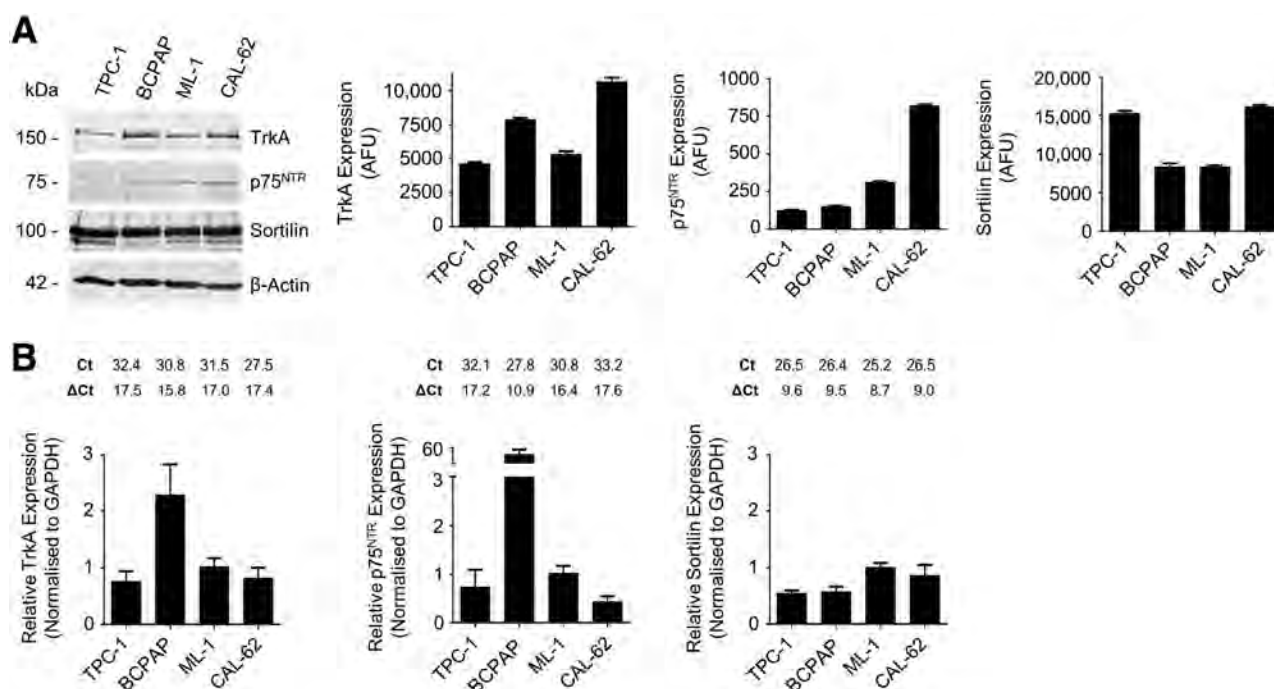


Figure 5 TrkA, p75^{NTR}, and sortilin expression in thyroid cancer cell lines. The levels of mRNA and protein for TrkA, p75^{NTR}, and sortilin were measured by real-time RT-PCR and Western blot analysis. **A:** Western blot analysis. TrkA, p75^{NTR}, and sortilin are detected at the expected molecular weight of 140, 75, and 100 kDa, respectively. Densitometric quantification indicates no significant differences among cell lines. β-Actin was used for normalization. **B:** Real-time RT-PCR. Relative quantification identifies mRNA for TrkA, p75^{NTR}, and sortilin at various levels among thyroid cancer cell lines. The value 1 represents the level obtained in ML-1 cells. mRNA levels were normalized with glyceraldehyde-3-phosphate dehydrogenase (GAPDH) as internal control. Cycle threshold (Ct) and ΔCt values are indicated. Data are representative of at least three independent experiments. AFU, arbitrary fluorescence unit.

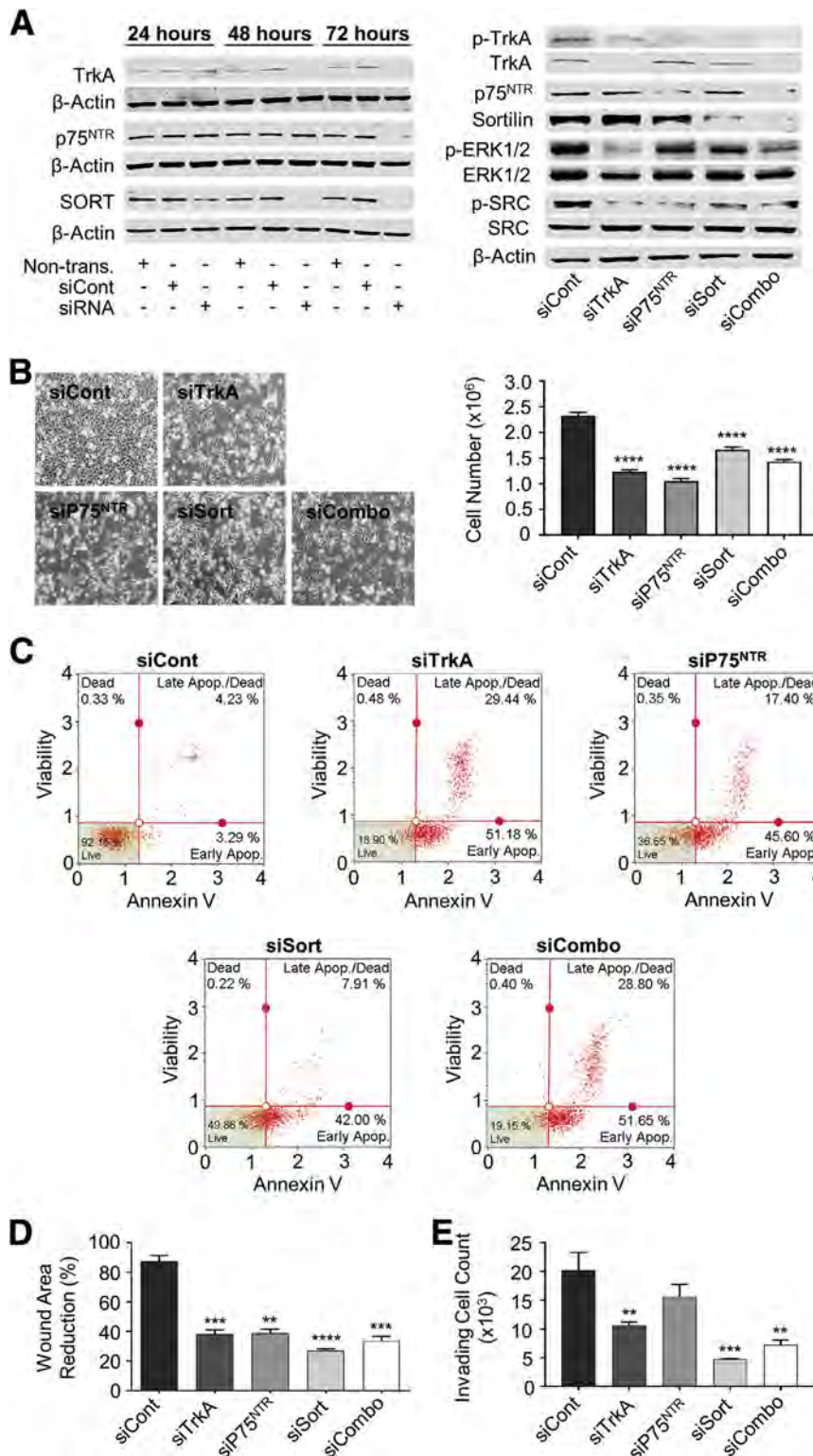


Figure 6 Impact of targeting TrkA, p75^{NTR}, and sortilin in the CAL-62 anaplastic thyroid cancer cell line. CAL-62 cells were transfected with siRNA against TrkA (siTrkA), p75^{NTR} (siP75^{NTR}), and sortilin (siSort), alone and in combination (siCombo), as well as with a universal negative control siRNA (siCont). **A:** Effect of siRNA on protein levels and cell signaling. The impact of siRNA transfection in inhibiting the protein level of TrkA, p75^{NTR}, and sortilin was measured by Western blot analysis 24, 48, and 72 hours after transfection. Non-transfected cells (nontrans.) were also analyzed. β-Actin protein expression was used as an equal loading control. TrkA protein level significantly decreases after 48 hours and further at 72 hours. p75^{NTR} protein level is inhibited after 72 hours. Sortilin is completely decreased after 48 and 72 hours. For cell signaling, siTrkA and siCombo decreased the level of phosphor-TrkA (p-TrkA), phosphor-ERK1/2 (p-ERK1/2), and phospho-SRC (p-SRC). siP75^{NTR} and siSort decrease p-ERK1/2 and p-SRC. **B:** Cell growth. The number of cells was measured by cell counting at 72 hours after transfection, and siRNA-treated cells were compared with siCont cells. siRNA against TrkA, p75^{NTR}, and sortilin, alone or combined (siCombo), all significantly inhibit cell growth. **C:** Apoptosis (Apop.). The proportion of apoptotic cells was measured in flow cytometry using Annexin V, and siRNA-treated cells were compared with siCont cells. siRNA against TrkA, p75^{NTR}, and sortilin, alone or in combination, all increase the percentage of apoptotic cells compared with siCont. The numbers indicate the percentages of the cells represented by alive, apoptotic, and dead populations. **D:** Cell migration. Scratching of the cell monolayer was performed 72 hours after transfection with siRNA, and reduction in gap area was measured 20 hours later. Targeting of all three receptors, alone and in combination (siCombo), resulted in the inhibition of wound scratch healing. **E:** Cell invasion. Transwell assays were set up 72 hours after siRNA transfection, and cells were allowed to invade for 20 hours. Only siSort and siTrkA, and siCombo significantly inhibited cancer cell invasion. Data are expressed as means ± SD (**B, D, and E**). Data are representative of at least three technical replicates, each consisting of at least three biological replicates. ****P* < 0.01, *****P* < 0.001, and ******P* < 0.0001 versus controls.

siSort, and siCombo all resulted in a reduction in CAL-62 cell number compared with siCont treated cells (*P* < 0.0001). To further elucidate the effects of targeting TrkA, p75^{NTR}, and sortilin, we determined the impact on apoptosis using Annexin V expression flow cytometry profiling (Figure 6C).

In comparison with siCont cells (7.5% apoptotic cells), the percentage of CAL-62 apoptotic cells increased after knockdown of TrkA (80.62%), p75^{NTR} (63%), and sortilin (49.9%). Simultaneous knockdown of all three receptors resulted in 80.4% of cells entering apoptosis (Figure 6C).

Cell Migration and Invasion

Cellular migration was assessed using a scratch wound healing assay, in which a scratch was made to a cell monolayer to create a wound area. The rate of closure was monitored and quantitated (Figure 6D). Transfection with siTrkA ($P = 0.0002$), siP75^{NTR} ($P = 0.0019$), siSort ($P < 0.0001$), and siCombo ($P = 0.0002$) all inhibited the migration of CAL-62 cells compared with siCont. The invasiveness of CAL-62 cells, in response to transfection with siRNA against TrkA, p75^{NTR}, and sortilin or the combination (siCombo), was assessed using a Transwell assay (Figure 6E). Invasion of CAL-62 cells was significantly inhibited by siTrkA ($P = 0.0085$), siSort ($P = 0.001$), and siCombo ($P = 0.0021$) compared with siCont cells. In contrast, knocking down p75^{NTR} expression did not significantly alter the invasion of CAL-62 cells ($P = 0.1268$).

The 8505c ATC cell line was also analyzed (Supplemental Figure S3). The impact of siRNA against the three receptors, alone or in combination, was studied following the same experimental procedures as for CAL-62. Similar results were obtained with 8505c cells compared with the CAL-62 cells, with respect to the decreased cell growth (Supplemental Figure S3B), apoptosis (Supplemental Figure S3C), migration (Supplemental Figure S3D), and invasion (Supplemental Figure S3E). In terms of cell signaling, similar decreased level of p-TrkA, ERK1/2, and SRC were obtained using siCombo, but the individual siRNAs had a less clear impact on signaling pathways (Supplemental Figure S3A), probably indicating a synergic effect of inhibiting the three receptors simultaneously. Interestingly, 8505c cells did not express the membrane receptor p75^{NTR} (Supplemental Figure S3A); thus, targeting this receptor with siRNA yielded similar results to that obtained with siCont cells. This finding highlights the specificity of the siRNA targeting in our experiment and points to a potential diversity of anaplastic cells in regard to neurotrophin receptor expression.

Discussion

New therapeutic strategies are required for treatment of thyroid cancers that do not respond to current treatment, in particular, ATC and metastatic differentiated thyroid cancer. We report that neurotrophin signaling may be an important component of tumor aggressiveness in ATC and differentiated thyroid carcinomas, which invites further examination as a potential drug target.

TrkA Expression and Targeting

This study found that TrkA protein expression is present in approximately 20% of thyroid cancers and is a marker of tumor aggressiveness, being associated with lymph node metastasis. Furthermore, targeting TrkA expression resulted in a decreased activation of SRC and ERK, ultimately

resulting in decreased thyroid cancer cell growth and invasion. TrkA participates in the stimulation of cancer cell invasion in several cancers,⁶ including those of the breast,^{21,22} prostate,^{23,24} and pancreas,^{23,25} and is increasingly being considered as a therapeutic target in oncology. In breast cancer, TrkA activation participates in cancer cell invasion,²¹ and in lung cancer, Trk inhibitors are in clinical trials.²⁶ The present data confirm the role of TrkA as an oncogenic protein and suggest a potential utility of targeting this pathway in thyroid cancer therapy.

In addition, TrkA expression was detected in the nerves present in the microenvironment of thyroid cancer. Although innervation of thyroid cancers has not been previously reported, using the neuronal marker PGP9.5, we found nerves in <5% of thyroid cancers (S.F., P.J., C.W.R., S.M.R.O., S.R., R.F.T., C.O., J.A., C.C.J., X.D.Z., M.M.W., H.H., unpublished data). This proportion of innervated tumors may be an underestimate because of the small sampling radius and depth of the tumor microarray cores. In developing neurons, TrkA activation results in the stimulation of various tyrosine kinase-induced signaling pathways, leading to neurite extension.¹¹ The thyroid gland is principally innervated by the autonomic nervous system, with parasympathetic nerves from the vagus and sympathetic nerves distributed from the sympathetic trunk, entering the gland along blood vessels.²⁷ Interestingly, the nerves observed in thyroid cancers were positive for TrkA but not for sortilin and p75^{NTR}. Given that NGF²⁸ and proNGF¹⁰ are expressed and released by thyroid cancer cells,¹⁰ it can be hypothesized that the activation of TrkA in nerves may lead to a stimulation of neurogenesis in the tumor microenvironment. NGF and TrkA are involved in perineural invasion in other cancers, as in pancreatic cancer,²⁹ and TrkA may play a similar role in thyroid cancer. In any case, the nerve-cancer cell crosstalk is increasingly regarded as a promoter of cancer progression,^{30,31} and the expression of TrkA in nerves suggests a potential association with neural infiltration in thyroid cancer.

p75^{NTR} Expression and Targeting

Although previous studies have found that p75^{NTR} is expressed in PTC and is associated with the presence of BRAF (V600E) mutations,¹² this study provides the first data that p75^{NTR} is expressed in normal thyroid tissue, although at a significantly lower level than in thyroid cancers. In addition, we found for the first time the expression of p75^{NTR} in FTC and ATC. p75^{NTR} is the common receptor for all neurotrophins and proneurotrophins.¹¹ It belongs to the tumor necrosis factor receptor gene family, and the proteins recruited by p75^{NTR} signaling are the tumor necrosis factor receptor-associated factor proteins followed by the activation of the NF-κB transcription factor. In addition, p75^{NTR} interacts with sortilin and TrkA and can modulate the tyrosine kinase activity of the latter on stimulation by neurotrophins.¹¹ Presumably because of its wide

range of interaction with various receptors and signaling, p75^{NTR} exhibits various biological activities in neurons, including the stimulation of survival or apoptosis, differentiation, and neurite outgrowth. In cancer, the same variety of effects are observed.³² p75^{NTR} acts as a tumor suppressor in gastric, bladder, and prostate cancers by blocking cell cycle progression and inducing apoptosis.^{33,34} In most other tumors, including melanoma,³⁵ glioma,³⁶ and breast cancer,³⁷ p75^{NTR} favors tumor development, in particular through the stimulation of the stem cell compartment.⁷ Interestingly, our data indicate that p75^{NTR} is overexpressed in most ATC. ATC has a poor survival rate (approximately 5% after 5 years), and at this stage there is no targeted treatment.⁵ Therefore, our data warrant future functional exploration to determine the interest of p75^{NTR} as a therapeutic target in thyroid cancer.

Sortilin Expression and Targeting

This study is the first report of sortilin expression in thyroid cancer. Sortilin is expressed in thyroid epithelial cells, where it contributes to the recycling of the thyroid hormone precursor thyroglobulin,³⁸ but its protein expression in thyroid cancer was previously unknown. Sortilin is a neuronal type 1 membrane protein, encoded by the *SORT1* gene.³⁹ It belongs to the vacuolar protein sorting 10 protein (VPS10P) family of receptors and is most abundantly expressed in the central and peripheral nervous systems. Initially described as neurotensin receptor 3, sortilin is more generally involved in sorting and trafficking of target proteins to distinct destinations.³⁹ It is a common binding partner of tyrosine kinase receptors, G-protein-coupled receptors, and ion channels, for which it facilitates ligand-induced signaling.³⁹ Sortilin has been identified as a co-receptor for proneurotrophins, including proNGF, in which it acts in a complex with the neurotrophin receptor p75^{NTR} to induce neuron apoptosis.⁴⁰ A few cancer cell lines express sortilin. In HT29 colon cancer cells, sortilin participates in the control of the growth-promoting activity induced by brain-derived growth factor through interacting with its tyrosine kinase receptor TrkB (NTRK2).⁴¹ In addition, sortilin mediates the release and transfer of exosomes in the A549 lung cancer cell line⁴² and regulates progranulin stimulatory activity of prostate cancer cells.⁴³ In melanoma cell lines, sortilin is a co-receptor for proNGF and acts in cooperation with the neurotrophin receptor p75^{NTR} to promote cancer cell invasion.³⁵ In breast cancer, sortilin expression is increased in invasive carcinomas compared with healthy tissues,¹⁵ and sortilin expression in the primary tumor is also associated with lymph node invasion.¹⁵ *In vitro*, sortilin participates in the proinvasive effect of proNGF in breast cancer cells.¹⁵ In the present study, similar to breast cancer, sortilin expression was increased in thyroid cancer compared with normal tissues and adenomas. This increased level of sortilin protein in thyroid cancers, compared with benign thyroid tissues,

suggested a potential role in the initiation and progression of the disease. Intriguingly, sortilin was expressed at higher levels in PTC and FTC compared with ATC. Sortilin is a ubiquitous receptor; its functions go beyond the sole control of cell growth and migration,³⁹ and this probably accounts for the fact that its expression is not strictly related to tumor aggressiveness in thyroid cancer. However, siRNA-targeting sortilin resulted in an inhibition of anaplastic thyroid cancer cell growth, migration, and invasion. Although the molecular mechanism of sortilin activity and its direct interacting signaling partners remain to be fully elucidated in thyroid cancer, our data suggest that targeting sortilin is a potential therapeutic strategy in thyroid cancer.

Conclusion

The present study found an increased level of TrkA, p75^{NTR}, and sortilin in thyroid cancers, which signals the potential value of these neurotrophin receptors as novel therapeutic targets. Further preclinical investigations *in vivo* are warranted to explore the therapeutic interest of targeting neurotrophin receptors in the different forms of thyroid cancers and particularly in ATCs, which are resistant to current treatment options. In addition, pain is a reported event in thyroid cancer, particularly in MTC and ATC.⁴⁴ Neurotrophins and their receptors have been well characterized as important mediators of pain initiation and maintenance,⁴⁵ and pharmacotherapies targeting the NGF/TrkA pathway are undergoing trials in the treatment of a variety of pain conditions,⁴⁶ including cancer.⁴⁷ Therefore, targeting neurotrophin receptors in ATC may potentially address the issue of pain, which also merits further attention.

Acknowledgments

We thank Sheridan Keene for excellent technical assistance and the Clinical Research Design, IT, and Statistical Support (CReditSS) Unit of the University of Newcastle (Callaghan, New South Wales, Australia). The 8505c (ATC) cell line was a generous gift from Prof. Alfred Lam (Griffith University, Queensland, Australia).

H.H. conceived and supervised the study and drafted the manuscript; S.F., S.R., and C.C.J. performed immunohistochemistry and quantified staining; tissue slide analyses and quantification were supervised by M.M.W. (histopathologist) and confirmed by R.F.T.; S.M.R.O. and P.J. performed nerve analysis; S.F. performed all cell culture experiments and prepared all figures and tables; C.W.R. and X.Z. provided clinical insights; J.A. and C.O. supervised statistical analyses; and all authors read and approved the final manuscript.

Supplemental Data

Supplemental material for this article can be found at <https://doi.org/10.1016/j.ajpath.2017.09.008>.

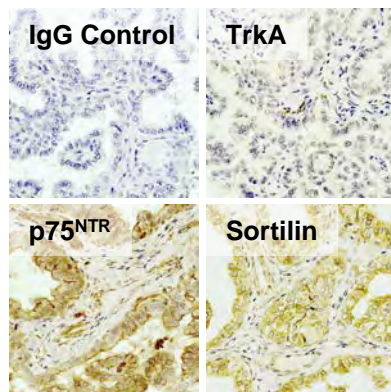
References

- Kitahara CM, Sosa JA: The changing incidence of thyroid cancer. *Nat Rev Endocrinol* 2016, 12:646–653
- Ahn HS, Kim HJ, Welch HG: Korea's thyroid-cancer "epidemic"—screening and overdiagnosis. *N Engl J Med* 2014, 371:1765–1767
- Cabanillas ME, McFadden DG, Durante C: Thyroid cancer. *Lancet* 2016, 388:2783–2795
- Lim H, Devesa SS, Sosa JA, Check D, Kitahara CM: Trends in thyroid cancer incidence and mortality in the United States, 1974-2013. *JAMA* 2017, 317:1338–1348
- Ranganath R, Shah MA, Shah AR: Anaplastic thyroid cancer. *Curr Opin Endocrinol Diabetes Obes* 2015, 22:387–391
- Demir IE, Tieftrunk E, Schorn S, Friess H, Ceyhan GO: Nerve growth factor & TrkA as novel therapeutic targets in cancer. *Biochim Biophys Acta* 2016, 1866:37–50
- Chopin V, Lagadec C, Toillon RA, Le Bourhis X: Neurotrophin signaling in cancer stem cells. *Cell Mol Life Sci* 2016, 73:1859–1870
- Hayakawa Y, Sakitani K, Konishi M, Asfaha S, Niikura R, Tomita H, Renz BW, Tailor Y, Macchini M, Middelhoff M, Jiang Z, Tanaka T, Dubeykovskaya ZA, Kim W, Chen X, Urbanska AM, Nagar K, Westphalen CB, Quante M, Lin CS, Gershon MD, Hara A, Zhao CM, Chen D, Worthley DL, Koike K, Wang TC: Nerve growth factor promotes gastric tumorigenesis through aberrant cholinergic signaling. *Cancer Cell* 2017, 31:21–34
- Lei Y, Tang L, Xie Y, Xianyu Y, Zhang L, Wang P, Hamada Y, Jiang K, Zheng W, Jiang X: Gold nanoclusters-assisted delivery of NGF siRNA for effective treatment of pancreatic cancer. *Nat Commun* 2017, 8:15130
- Faulkner S, Roselli S, Demont Y, Pundavela J, Choquet G, Leissner P, Oldmeadow C, Attia J, Walker MM, Hondermarck H: ProNGF is a potential diagnostic biomarker for thyroid cancer. *Oncotarget* 2016, 7:28488–28497
- Bradshaw RA, Pundavela J, Biarc J, Chalkley RJ, Burlingame AL, Hondermarck H: NGF and ProNGF: regulation of neuronal and neoplastic responses through receptor signaling. *Adv Biol Regul* 2015, 58:16–27
- Rocha AS, Risberg B, Magalhaes J, Trovisco V, de Castro IV, Lazarovici P, Soares P, Davidson B, Sobrinho-Simoes M: The p75 neurotrophin receptor is widely expressed in conventional papillary thyroid carcinoma. *Hum Pathol* 2006, 37:562–568
- Bevan S, Pal T, Greenberg CR, Green H, Wixey J, Bignell G, Narod SA, Foulkes WD, Stratton MR, Houlston RS: A comprehensive analysis of MNG1, TCO1, fPTC, PTEN, TSHR, and TRKA in familial nonmedullary thyroid cancer: confirmation of linkage to TCO1. *J Clin Endocrinol Metab* 2001, 86:3701–3704
- Pundavela J, Roselli S, Faulkner S, Attia J, Scott RJ, Thorne RF, Forbes JF, Bradshaw RA, Walker MM, Jobling P, Hondermarck H: Nerve fibers infiltrate the tumor microenvironment and are associated with nerve growth factor production and lymph node invasion in breast cancer. *Mol Oncol* 2015, 9:1626–1635
- Roselli S, Pundavela J, Demont Y, Faulkner S, Keene S, Attia J, Jiang CC, Zhang XD, Walker MM, Hondermarck H: Sortilin is associated with breast cancer aggressiveness and contributes to tumor cell adhesion and invasion. *Oncotarget* 2015, 6:10473–10486
- Cerami E, Gao J, Dogrusoz U, Gross BE, Sumer SO, Aksoy BA, Jacobsen A, Byrne CJ, Heuer ML, Larsson E, Antipin Y, Reva B, Goldberg AP, Sander C, Schultz N: The cBio cancer genomics portal: an open platform for exploring multidimensional cancer genomics data. *Cancer Discov* 2012, 2:401–404
- Cancer Genome Atlas Research Network, Weinstein JN, Collisson EA, Mills GB, Shaw KR, Ozenberger BA, Ellrott K, Shmulevich I, Sander C, Stuart JM: The Cancer Genome Atlas Pan-Cancer Analysis Project. *Nat Genet* 2013, 45:1113–1120
- Zhang B, Wang J, Wang X, Zhu J, Liu Q, Shi Z, Chambers MC, Zimmerman LJ, Shaddox KF, Kim S, Davies SR, Wang S, Wang P, Kinsinger CR, Rivers RC, Rodriguez H, Townsend RR, Ellis MJ, Carr SA, Tabb DL, Coffey RJ, Slebos RJ, Liebler DC, Nci C: Proteogenomic characterization of human colon and rectal cancer. *Nature* 2014, 513:382–387
- Romon R, Adriaenssens E, Lagadec C, Germain E, Hondermarck H, Le Bourhis X: Nerve growth factor promotes breast cancer angiogenesis by activating multiple pathways. *Mol Cancer* 2010, 9:157
- Palazzo E, Marconi A, Truzzi F, Dallaglio K, Petrachi T, Humbert P, Schnebert S, Perrier E, Dumas M, Pincelli C: Role of neurotrophins on dermal fibroblast survival and differentiation. *J Cell Physiol* 2012, 227:1017–1025
- Lagadec C, Meignan S, Adriaenssens E, Foveau B, Vanhecke E, Romon R, Toillon RA, Oxombre B, Hondermarck H, Le Bourhis X: TrkA overexpression enhances growth and metastasis of breast cancer cells. *Oncogene* 2009, 28:1960–1970
- Demont Y, Corbet C, Page A, Ataman-Onal Y, Choquet-Kastylevsky G, Fliniaux I, Le Bourhis X, Toillon RA, Bradshaw RA, Hondermarck H: Pro-nerve growth factor induces autocrine stimulation of breast cancer cell invasion through tropomyosin-related kinase A (TrkA) and sortilin protein. *J Biol Chem* 2012, 287:1923–1931
- Miknyoczki SJ, Wan W, Chang H, Dobrzanski P, Ruggeri BA, Dionne CA, Buchkovich K: The neurotrophin-trk receptor axes are critical for the growth and progression of human prostatic carcinoma and pancreatic ductal adenocarcinoma xenografts in nude mice. *Clin Cancer Res* 2002, 8:1924–1931
- Festuccia C, Muzi P, Gravina GL, Millimaggi D, Specia S, Dolo V, Ricevuto E, Vicentini C, Bologna M: Tyrosine kinase inhibitor CEP-701 blocks the NTRK1/NGF receptor and limits the invasive capability of prostate cancer cells in vitro. *Int J Oncol* 2007, 30:193–200
- Zhang Y, Dang C, Ma Q, Shimahara Y: Expression of nerve growth factor receptors and their prognostic value in human pancreatic cancer. *Oncol Rep* 2005, 14:161–171
- Vaishnavi A, Le AT, Doebele RC: TRKing down an old oncogene in a new era of targeted therapy. *Cancer Discov* 2015, 5:25–34
- Dumont J, Opitz R, Christophe D, Vassart G, Roger PP, Maenhaut C: Ontogeny, anatomy, metabolism and physiology of the thyroid. In *Endotext*. Edited by De Groot LJ, Beck-Peccoz P, Chrousos G, Dungan K, Grossman A, Hershman JM, Koch C, McLachlan R, New M, Rebar R, Singer F, Vinik A, Weickert MO. South Dartmouth, MA: MDTText.com, 2000
- van der Laan BF, Freeman JL, Asa SL: Expression of growth factors and growth factor receptors in normal and tumorous human thyroid tissues. *Thyroid* 1995, 5:67–73
- Bapat AA, Hostetter G, Von Hoff DD, Han H: Perineural invasion and associated pain in pancreatic cancer. *Nat Rev Cancer* 2011, 11:695–707
- Jobling P, Pundavela J, Oliveira SM, Roselli S, Walker MM, Hondermarck H: Nerve-cancer cell cross-talk: a novel promoter of tumor progression. *Cancer Res* 2015, 75:1777–1781
- Boilly B, Faulkner S, Jobling P, Hondermarck H: Nerve dependence: from regeneration to cancer. *Cancer Cell* 2017, 31:342–354
- Tomellini E, Touil Y, Lagadec C, Julien S, Ostyn P, Ziental-Gelus N, Meignan S, Lengrand J, Adriaenssens E, Polakowska R, Le Bourhis X: Nerve growth factor and proNGF simultaneously promote symmetric self-renewal, quiescence, and epithelial to mesenchymal transition to enlarge the breast cancer stem cell compartment. *Stem Cells* 2015, 33:342–353
- Jin H, Pan Y, Zhao L, Zhai H, Li X, Sun L, He L, Chen Y, Hong L, Du Y, Fan D: p75 neurotrophin receptor suppresses the proliferation of human gastric cancer cells. *Neoplasia* 2007, 9:471–478
- Khawaja F, Tabassum A, Allen J, Djakiew D: The p75(NTR) tumor suppressor induces cell cycle arrest facilitating caspase mediated apoptosis in prostate tumor cells. *Biochem Biophys Res Commun* 2006, 341:1184–1192
- Truzzi F, Marconi A, Lotti R, Dallaglio K, French LE, Hempstead BL, Pincelli C: Neurotrophins and their receptors stimulate melanoma cell proliferation and migration. *J Invest Dermatol* 2008, 128:2031–2040

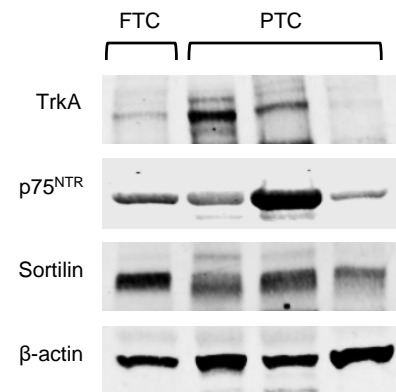
36. Johnston AL, Lun X, Rahn JJ, Liacini A, Wang L, Hamilton MG, Parney IF, Hempstead BL, Robbins SM, Forsyth PA, Senger DL: The p75 neurotrophin receptor is a central regulator of glioma invasion. *PLoS Biol* 2007, 5:e212
37. Vanhecke E, Adriaenssens E, Verbeke S, Meignan S, Germain E, Berteaux N, Nurcombe V, Le Bourhis X, Hondermarck H: Brain-derived neurotrophic factor and neurotrophin-4/5 are expressed in breast cancer and can be targeted to inhibit tumor cell survival. *Clin Cancer Res* 2011, 17:1741–1752
38. Botta R, Lisi S, Pinchera A, Giorgi F, Marcocci C, Taddei AR, Fausto AM, Bernardini N, Ippolito C, Mattii L, Persani L, de Filippis T, Calebiro D, Madsen P, Petersen CM, Marino M: Sortilin is a putative postendocytic receptor of thyroglobulin. *Endocrinology* 2009, 150:509–518
39. Nykjaer A, Willnow TE: Sortilin: a receptor to regulate neuronal viability and function. *Trends Neurosci* 2012, 35:261–270
40. Nykjaer A, Lee R, Teng KK, Jansen P, Madsen P, Nielsen MS, Jacobsen C, Kliemann M, Schwarz E, Willnow TE, Hempstead BL, Petersen CM: Sortilin is essential for proNGF-induced neuronal cell death. *Nature* 2004, 427:843–848
41. Akil H, Perraud A, Melin C, Jauberteau MO, Mathonnet M: Fine-tuning roles of endogenous brain-derived neurotrophic factor, TrkB and sortilin in colorectal cancer cell survival. *PLoS One* 2011, 6:e25097
42. Wilson CM, Naves T, Vincent F, Melloni B, Bonnaud F, Lalloue F, Jauberteau MO: Sortilin mediates the release and transfer of exosomes in concert with two tyrosine kinase receptors. *J Cell Sci* 2014, 127:3983–3997
43. Tanimoto R, Morcavallo A, Terracciano M, Xu SQ, Stefanello M, Buraschi S, Lu KG, Bagley DH, Gomella LG, Scotlandi K, Belfiore A, Iozzo RV, Morrione A: Sortilin regulates progranulin action in castration-resistant prostate cancer cells. *Endocrinology* 2015, 156:58–70
44. Chiacchio S, Lorenzoni A, Boni G, Rubello D, Elisei R, Mariani G: Anaplastic thyroid cancer: prevalence, diagnosis and treatment. *Minerva Endocrinol* 2008, 33:341–357
45. Pezet S, McMahon SB: Neurotrophins: mediators and modulators of pain. *Annu Rev Neurosci* 2006, 29:507–538
46. Chang DS, Hsu E, Hottinger DG, Cohen SP: Anti-nerve growth factor in pain management: current evidence. *J Pain Res* 2016, 9:373–383
47. Lam DK: Emerging factors in the progression of cancer-related pain. *Pain Manag* 2016, 6:487–496

Supp. Fig. S1

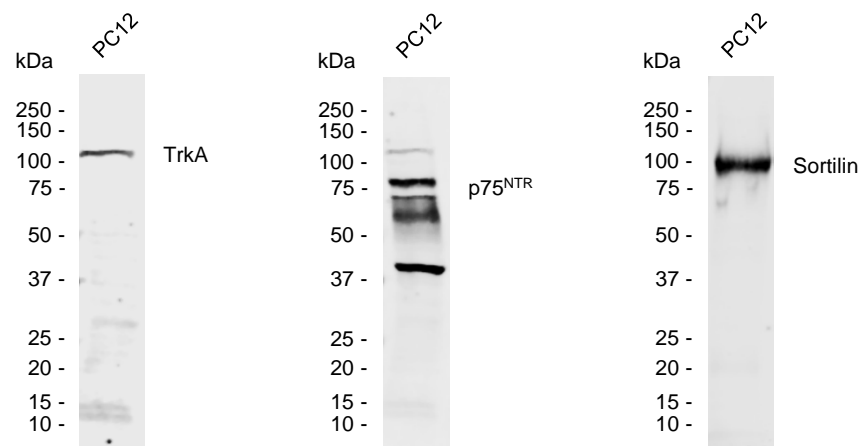
A



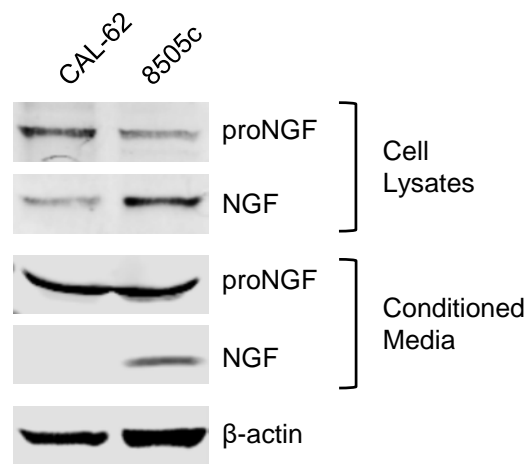
B

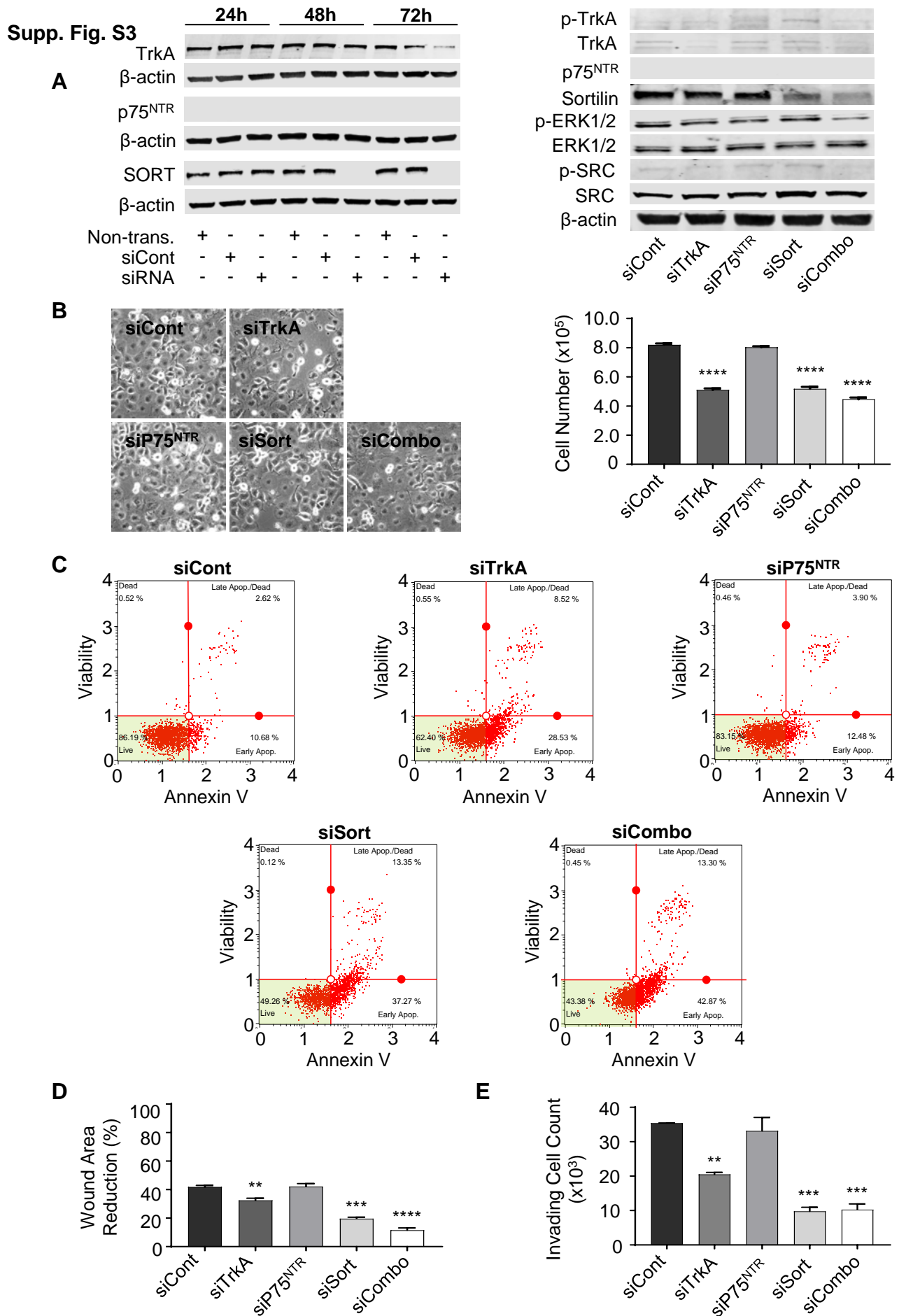


C



Supp. Fig. S2





6 THE PRECURSOR FOR NERVE GROWTH FACTOR IN THYROID CANCER LYMPH NODE METASTASES: CORRELATION WITH PRIMARY TUMOUR AND PATHOLOGICAL VARIABLES.

6.1 Preface

Previous work has established that proNGF is increased in thyroid cancers, based on tissue micro-arrays with limited clinicopathological correlation. Having established that thyroid cancer is innervated, we sought to confirm expression of proNGF in thyroid cancers using whole-slide analysis techniques, and correlate this more deeply with clinical and pathological information, which we were able to obtain from our collaboration with NSW Health Pathology (Hunter) and the John Hunter Hospital.

Using data linkage, we were able to identify archival specimens of thyroid cancer along with paired, resected lymph node metastases from the same patients. Using whole-slide analysis of these paired primary tumours and metastases, we were able to obtain a more complete picture of proNGF expression across different tumoural sites, and with deeper clinic-pathological integration.



Article

The Precursor for Nerve Growth Factor (proNGF) in Thyroid Cancer Lymph Node Metastases: Correlation with Primary Tumour and Pathological Variables

Christopher W. Rowe ^{1,2,3}, Tony Dill ⁴, Sam Faulkner ^{3,5} , Craig Gedye ^{5,6},
Jonathan W. Paul ^{1,3} , Jorge M. Tolosa ^{1,3}, Mark Jones ³ , Simon King ^{3,4},
Roger Smith ^{1,2,3} and Hubert Hondermarck ^{3,5,*}

¹ School of Medicine and Public Health, University of Newcastle, Callaghan 2308, Australia

² Department of Endocrinology, John Hunter Hospital, Newcastle 2310, Australia

³ Hunter Medical Research Institute, 1 Kookaburra Circuit, New Lambton Heights 2310, Australia

⁴ Department of Anatomical Pathology, NSW Health Pathology (Hunter), Newcastle 2310, Australia

⁵ School of Biomedical Sciences and Pharmacy, University of Newcastle, Callaghan 2308, Australia

⁶ Department of Medical Oncology, Calvary Mater Newcastle, Waratah 2298, Australia

* Correspondence: hubert.hondermarck@newcastle.edu.au

Received: 1 November 2019; Accepted: 24 November 2019; Published: 25 November 2019



Abstract: Metastases in thyroid cancer are associated with aggressive disease and increased patient morbidity, but the factors driving metastatic progression are unclear. The precursor for nerve growth factor (proNGF) is increased in primary thyroid cancers, but its expression or significance in metastases is not known. In this study, we analysed the expression of proNGF in a retrospective cohort of thyroid cancer lymph node metastases ($n = 56$), linked with corresponding primary tumours, by automated immunohistochemistry and digital quantification. Potential associations of proNGF immunostaining with clinical and pathological parameters were investigated. ProNGF staining intensity (defined by the median h-score) was significantly higher in lymph node metastases (h-score 94, interquartile range (IQR) 50–147) than in corresponding primary tumours (57, IQR 42–84) ($p = 0.002$). There was a correlation between proNGF expression in primary tumours and corresponding metastases, where there was a 0.68 (95% CI 0 to 1.2) increase in metastatic tumour h-score for each unit increase in the primary tumour h-score. However, larger tumours (both primary and metastatic) had lower proNGF expression. In a multivariate model, proNGF expression in nodal metastases was negatively correlated with lateral neck disease and being male. In conclusion, ProNGF is expressed in locoregional metastases of thyroid cancer and is higher in lymph node metastases than in primary tumours, but is not associated with high-risk clinical features.

Keywords: thyroid cancer; proNGF; neurotrophin; metastasis; nerves

1. Introduction

Thyroid cancer is the most common endocrine malignancy, with rising incidence [1]. Differentiated thyroid cancers arise from the thyroid follicular epithelium, and develop in either papillary or follicular growth patterns. The majority of differentiated thyroid cancers are localised within the thyroid in the early stages, and have an excellent prognosis if removed prior to the development of metastases, with >95% 10-year survival [2]. However, approximately 20% of thyroid cancers have metastases at diagnosis, usually loco-regionally within the lymph nodes of the neck or, less commonly, at distant sites such as lung and bone, and represent a more aggressive subset, with increased morbidity and mortality [2,3]. However, the size and location of metastases appears to be important in prognosis.

Microscopic deposits of cancer within the lymph nodes of the central compartment of the neck appear to have little prognostic significance, whilst larger nodal involvement, and the involvement of lymph nodes in the lateral compartment of the neck, increase the risk of local recurrence following treatment and are associated with reduced overall survival [4,5].

The precursor for nerve growth factor (proNGF) is a soluble protein of 246 amino acids, transcribed from the *NGF* gene on chromosome 1p13. ProNGF and NGF are involved in the survival, growth and differentiation of neurons in the central and peripheral nervous system [6]. Interestingly, increasing evidence reports the role of proNGF and NGF in stimulating cancer progression [7–10]. In thyroid cancer, ProNGF has been shown to be overexpressed in differentiated cancers of both papillary and follicular subtypes [11]. Based on prior data, we hypothesised that proNGF would be expressed in the metastases of thyroid cancer, and that expression of proNGF would correlate with tumour aggressiveness, which could suggest a role for proNGF as a prognostic biomarker for thyroid cancer aggressiveness, or may suggest a mechanistic target for future research.

Therefore, we designed and conducted a study to characterise the expression of proNGF in clinical specimens of thyroid cancer lymph node metastases, linked with analyses of the primary tumour, and correlated with clinical and pathological characteristics. The data show that proNGF is overexpressed in nodal metastases of thyroid cancers compared to corresponding primary tumours, but we found no correlation between proNGF expression in lymph node metastases and cancer aggressiveness.

2. Results

ProNGF expression was analysed by immunohistochemistry and digital quantification in a total of 112 whole-slide tissue sections from patients with thyroid cancer, corresponding to 56 lymph node metastases of thyroid cancer paired with primary tumours from the same patients. ProNGF intensity is presented as an h-score (a numeric scale between 0 and 300, with higher numbers representing greater immunostaining and protein expression). Demographic and clinical information for the included samples are presented in Table 1.

Table 1. Expression of proNGF in primary thyroid cancers and metastases, quantified by h-score of immunohistochemical staining.

	ProNGF Quantification (h-score)					
	<i>n</i>	Primary Tumour	<i>p</i> -Value	<i>n</i>	Nodal Metastasis	<i>p</i> -Value
Overall	56	57 (42–84)	0.96	56	94 (50–147)	0.002 ¹
Age						0.32
<55 years	34	58 (43–89)		34	95 (57–122)	
≥55 years	22	55 (32–77)		22	86 (46–123)	
Sex			0.20			0.85
Male	21	71 (46–100)		21	96 (46–148)	
Female	35	54 (40–71)		35	90 (51–146)	
Histopathology			0.36			0.11
Papillary	53	58 (43–89)		53	96 (51–148)	
Classical	27	54 (43–92)		27	106 (64–149)	
Follicular-variant	26	60 (46–89)		26	70 (49–130)	
Follicular	2	42 (23–60)		2	45 (30–60)	
Anaplastic	1	32		1	67	
Tumour size			0.02			
Primary <4 cm	48	62 (45–96)				
Primary ≥4 cm	8	38 (25–55)				
Total lymph node <3 cm				44	105 (57–149)	0.02
Total lymph node ≥3 cm				12	59 (44–64)	
Metastasis within node <2 mm				10	148 (94–175)	0.04
Metastasis within node ≥2 mm				46	82 (49–123)	

Table 1. Cont.

	n	Primary Tumour	ProNGF Quantification (h-score)		p-Value
			n	Nodal Metastasis	
Vascular invasion					0.32
Absent	35	56 (43–100)			
Present	21	58 (43–68)			
Extra-thyroidal extension					0.43
Absent	19	56 (45–106)			
Present	37	58 (40–75)			
AJCC TNM 8 Stage					0.005
I and II	46	63 (45–100)			
III and IV	10	38 (23–54)			
Nodal metastases (location)					0.004
Central neck only (N1a)			33	109 (64–152)	
Central + lateral neck (N1b)			23	60 (40–96)	
Timing of metastases					0.11
At time of primary tumour			49	99 (56–148)	
>6 months from primary			7	57 (46–96)	

The h-score is a digital quantification of immunohistochemistry intensity, with values ranging between 0 and 300, where higher values represent greater protein expression. Data are median (IQR), compared using the Mann-Whitney test. ¹ Comparison between Primary and Metastases. Other comparisons are within column.

2.1. Validation of Automated Scoring Algorithm (h-score)

Prior to proceeding with the analysis, the performance of the h-score (automated digital analysis) was confirmed by correlating with manual grading. Two operators who were blinded to the h-score independently assigned a manual score of proNGF immunohistochemical intensity of staining on a four-point scale (negative/weak/moderate/strong) on the full cohort of primary tumours ($n = 56$). The results are presented in Figure 1. Overall, there was an acceptable correlation between the manually assigned scores and the automated h-scores ($r^2 = 0.52$, $p < 0.0001$). The median h-scores for the five cases manually classified as “0: negative” were 23 (interquartile range 22–24).

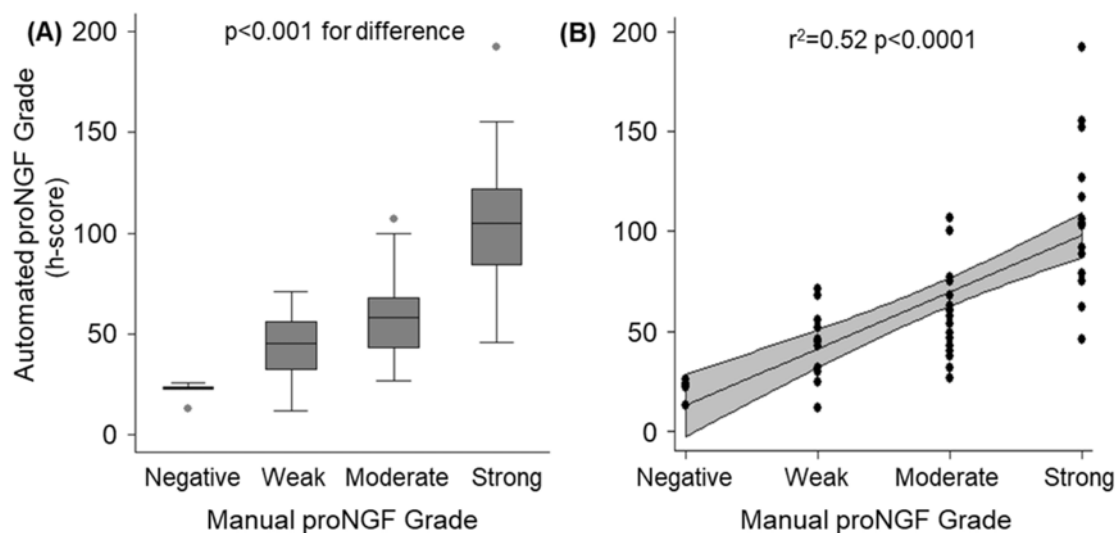


Figure 1. Validation of automated immunohistochemistry analysis (h-scores) compared to manual grading for the cohort of 56 primary tumours. (A): Box and whisker plot demonstrating distribution of automated h-scores, stratified by manual scores. Significant between-group differences were confirmed by ANOVA ($p < 0.001$). (B): Scatter-plot of individual automated h-scores (dots) over manual grading. The solid line represents the regression fit, with the grey band demonstrating the 95% CI of the regression line ($r^2 = 0.52$, $p < 0.0001$).

2.2. ProNGF Expression in Thyroid Cancer

ProNGF expression was detected in the majority of thyroid cancers and lymph node metastases (Table 1). It was found that 93% of sections from the papillary subtype and 75% from the follicular subtype expressed proNGF (positive expression was classified as h-score greater than 25, see Figure 1a for justification). An example of proNGF immunostaining is presented in Figure 2, showing a primary thyroid cancer and an adjacent lymph node metastasis, both expressing proNGF. ProNGF immunostaining was in the cytoplasm of cancer cells (Figures 2 and 3), which is the expected location for this protein to be expressed. Minimal staining of fibroblasts and adjacent stroma was noted (Figure 3a,f). Some specimens contained adjacent benign thyroid follicular cells, which generally had low expression of proNGF (Figure 2b). However, due to nonspecific uptake of DAB staining by colloid in the benign regions, the h-scores were not reliable.

The majority of primary tumours demonstrated uniform proNGF expression throughout the tumour; however, 25% showed a predominantly peripheral pattern of staining around the anatomical edge of the tumour (for example, Appendix B, Case 3). Peripheral immunostaining appeared to correlate with the biological properties of the tumour, as it was associated with the anatomical edge of the tumour rather than the cut edge of the pathology specimen, and was not caused by increased cellular density. Peripheral pattern staining did not correlate with the clinical or pathological parameters of the tumour.

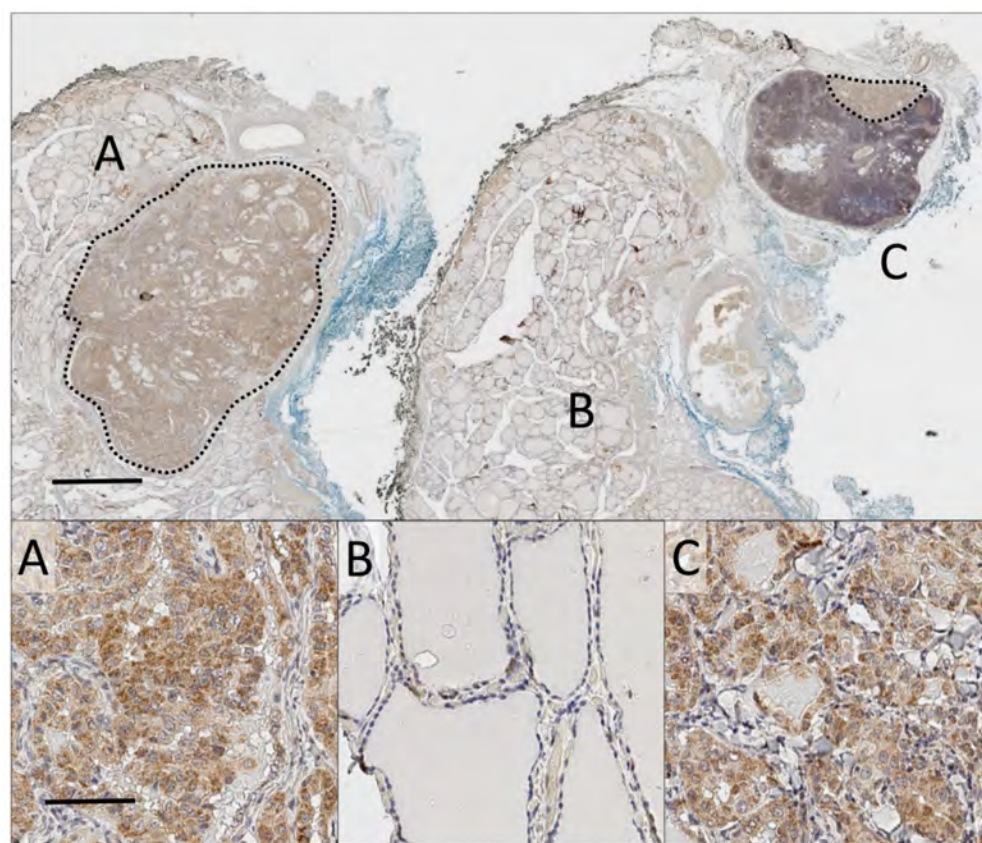


Figure 2. Whole-slide analysis of a primary thyroid cancer and corresponding thyroid cancer nodal metastasis. Main: Low magnification (0.5×) of whole-slide of proNGF immunostaining (DAB, brown), with haematoxylin nuclear counterstain (blue), of primary tumour and paired metastasis. Blue and black inking represent the anterior and tracheal borders of thyroid respectively. Scale bar 2mm. (A) 7 mm microPTC with staining for proNGF. (B) Adjacent normal thyroid tissue. (C) 2 mm lymph node micro-metastasis at upper edge of node, included in same anatomical block. Dotted lines demarcate tumour. Inset: 20× magnification of representative fields. Scale bar 50 μm.

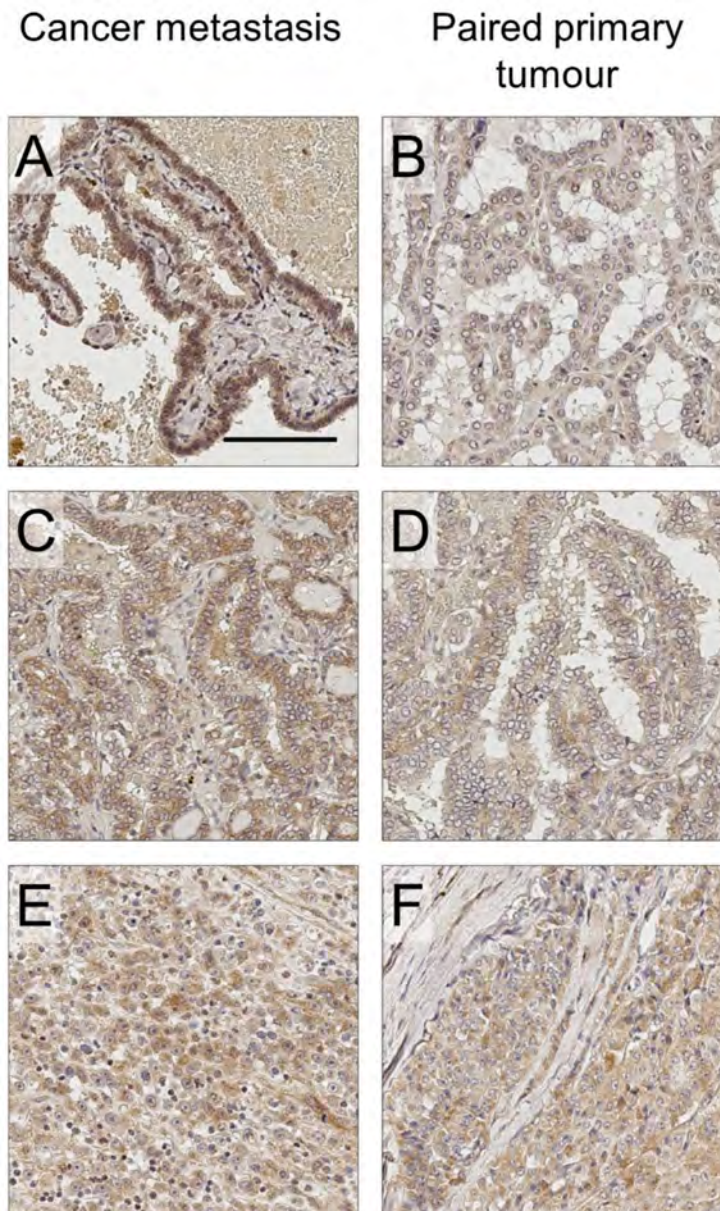


Figure 3. ProNGF immunostaining of thyroid cancer lymph node metastasis, compared with paired primary tumour. (A) Papillary thyroid cancer metastasis, h-score 148. (B) Primary tumour of A, h-score 56. (C) Papillary thyroid cancer metastasis, h-score 154. (D) Primary tumour of C, h-score 71. (E) Follicular thyroid cancer metastasis, h-score 60. (F) Primary tumour of F, h-score 60. Scale bar: 100 μ m. 20 \times magnification.

Considering all neoplastic tissues together (pooled analysis of primary and metastatic samples), papillary thyroid cancer had a trend towards higher expression of proNGF (Figure 4, median h-score 70, IQR 46–108) than follicular thyroid cancer (median h-score 30, IQR 23–60, $p = 0.07$ for difference). Within papillary thyroid cancers, there was no difference in proNGF expression between tumours expressing a classical architecture, as compared to those with follicular-variant histology (Table 1). One paired case of anaplastic thyroid cancer had low proNGF expression.

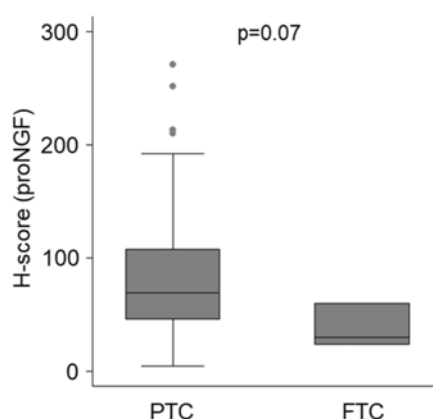


Figure 4. ProNGF immunostaining of thyroid cancer, stratified by histopathological subtype. Data for primary and metastatic lesions for PTC ($n = 106$) and FTC ($n = 4$) are combined. For analysis sub stratified by histopathological subtype, and by location of lesion, see Table 1.

2.3. ProNGF Expression in Lymph Node Metastases Positively Correlates with Primary Tumours

Median proNGF h-scores were higher in the nodal metastases (94, IQR 50–147), compared to the matched primary specimens (57, IQR 42–84, $p = 0.002$) (Table 1, Figure 5a). Quantile regression of metastatic h-scores on primary h-scores adjusted for age (≥ 55 years) and sex (male) confirmed this relationship, with an increase of 0.68 units in the median metastatic h-score for each unit increase in the primary score (95% CI 0 to 1.2, p -value = 0.009, Figure 5B). This pattern continued to be observed following a sensitivity analysis removing two outliers (median metastatic h-score increased 0.58 units (95% CI 0 to 0.9, $p = 0.05$) for each unit increase in the primary score). Finally, of the 56 metastases, 39 (69%) had higher expression of proNGF than the primary tumour (Figure 5c).

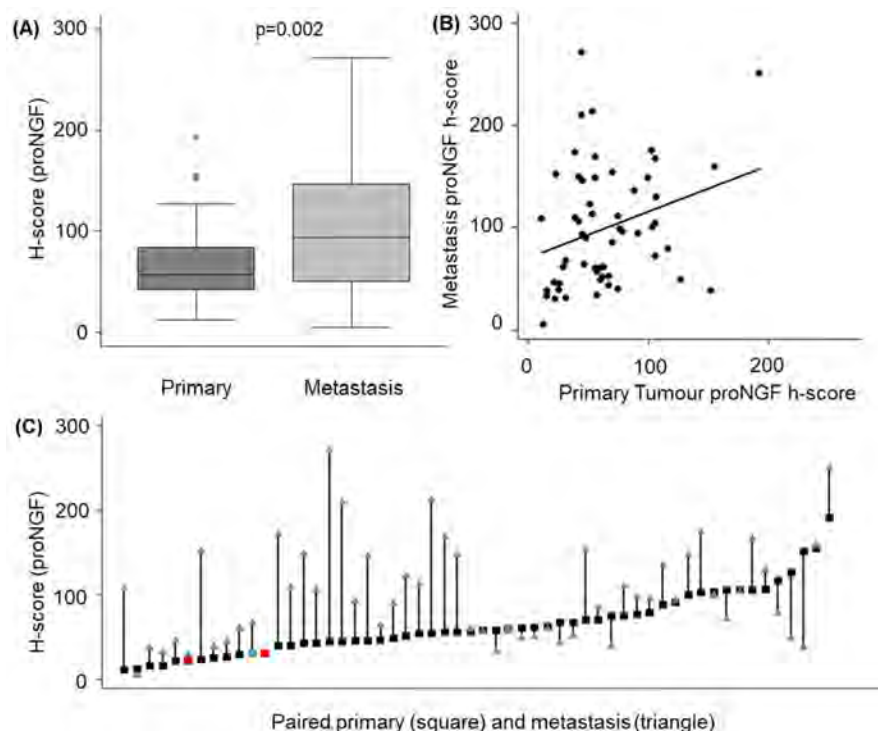


Figure 5. Quantification of proNGF staining in primary thyroid tumours vs lymph node metastases. (A) H-score for proNGF intensity in primary tumours and linked metastases. (B) Scatter plot showing correlation between h-score in primary and paired metastases (C) Individual data points for the 56 paired cases of primary tumour (squares, PTC = black, FTC = red, ATC = blue) and nodal metastases (triangle).

2.4. ProNGF Expression is not Associated with High Risk Clinical Features

A univariate analysis comparing proNGF expression to clinical and pathological variables was undertaken separately for primary tumours and metastases (Table 1). ProNGF expression in the primary tumour was inversely associated with tumour size and TNM stage ($p < 0.05$). In metastases, proNGF expression was inversely associated with the size of the involved lymph node, and with the location of the lymph node in the lateral neck. We then constructed an exploratory multivariate model to assess whether the characteristics of the primary tumours were associated with proNGF expression, which included covariates of age and gender (base model), and tumour size (≥ 4 cm), the presence of vascular invasion, the presence of extra-thyroidal extension and multifocality in the full model. The results are presented in Table 2. In the full model, the parameter estimate for the primary tumour h-score was similar to that of the model adjusting for age and gender alone, suggesting no evidence of confounding from any of the model variables (Table 2A). In the full model, none of the covariates were significantly associated with the h-score in the primary tumour.

Table 2. Multivariate analysis of association between h-score in primary or metastases and clinical/pathological parameters. Parameter estimates for linear quantile mixed models of association between median proNGF h-score and clinical/pathological parameters are presented. Separate models were fit for (A) primary tumours and (B) Lymph node metastasis. The estimate shows the difference in h-score associated with the parameter.

Parameter	Estimate (95% CI)	p-Value
(A) Primary Tumour:		
Age (≥ 55 years)	−6.1 (−35.9 to 23.7)	0.7
Sex (male)	−2.7 (−27.3 to 21.8)	0.8
Size (≥ 4 cm)	−9.1 (−28.8 to 10.6)	0.4
Extra-thyroidal extension	−14 (−29.0 to 1.0)	0.067
Vascular Invasion	−11.6 (−36.4 to 13.2)	0.4
Multi-focal	−1.7 (−19.1 to 15.7)	0.8
(B) Lymph node metastasis		
Age (≥ 55 years)	−13.8 (−32.5 to 4.9)	0.1
Sex (male)	−34.8 (−59.9 to −9.6)	0.008
Size (≥ 2 mm)	−29.1 (−65.34 to 7.2)	0.1
Location (lateral neck site, N1b)	−47.1 (−73.8 to −20.5)	0.001
Timing (> 6 months post primary)	−23.7 (−52 to 4.6)	0.1

A separate multivariate model was fit examining lymph node metastases, and including variables of covariates for age (≥ 55 years), sex, metastases size (≥ 2 mm), location (lateral neck) and timing of detection (> 6 months from primary); it identified significant effects for sex and neck site (Table 2B). Specifically, males had lower median proNGF h-scores (−35, 95% CI −60 to −10, p -value = 0.008), and the presence of lateral neck disease was associated with a −47 (95% CI −74 to −20, p -value < 0.001) change in the median proNGF h-score.

2.5. ProNGF Expression in Primary Tumours does not Predict Metastases

To determine whether proNGF expression in primary tumours was associated with metastatic potential, we compared the h-scores of primary tumours with metastases to a cohort of primary tumours without lymph node metastases ($n = 29$, comprising 18 PTC and 11 FTC, with mean age 57 years, 59% female and mean tumour size 25 mm). The median h-score in primary tumours without nodal metastases was 45 (IQR 26–68), compared to 57 (42–84) in tumours with metastases ($p = 0.16$). Similar results were obtained when comparing the PTC subgroup alone. Using a multiple logistic regression model to examine for potential confounding, with the presence or absence of locoregional metastases as the dependent variable, and including model variables of primary tumour proNGF h-score, age, gender, tumour size, the presence of extra-thyroidal extension and the presence of vascular

invasion, proNGF expression in primary tumours did not predict metastases (odds ratio 1.01, 95% CI 1.0 to 1.02, $p = 0.10$).

3. Discussion

Better knowledge of the characteristics of lymph node metastases of thyroid cancer is required to identify aggressive disease subsets that require additional treatments. Here, we report an increased expression of proNGF in thyroid cancer lymph node metastases, which correlated with expression in the primary tumour. However, we did not find that proNGF expression was able to predict the presence of these metastases, or that it correlated positively with tumour aggressiveness.

A key novel aspect of this study was the assessment of proNGF expression in lymph node deposits of thyroid cancer. ProNGF expression has never previously been reported in the metastases of any cancer, despite significant study of its biological effects in primary tumours of breast and prostate cancers [8,12]. This study identifies that proNGF is a biological feature of lymph node metastases of thyroid cancer. More importantly, by studying paired primary tumours and metastases, we were able to show a clear correlation between the biological behaviour of proNGF expression in the primary tumour and the metastases. Interestingly, although there was strong positive correlation between proNGF expression in the primary tumour and its linked metastases, we found that the degree of proNGF expression in the metastases was inversely associated with nodes located in the lateral neck (a site of higher-risk involvement), and with male gender.

This work provides important independent corroboration of the findings of a previous study of proNGF in thyroid cancer [11]. This current work confirms the pattern that the papillary subtype of thyroid cancer has higher levels of proNGF expression, as demonstrated previously. Further, this work confirms previous findings that proNGF expression in the primary tumour does not correlate with high risk clinical features. Table 2 shows that on multivariate analysis, there was no association between clinical or pathological risk-factors and proNGF expression. The observation that proNGF expression is lower in primary tumours harbouring high-risk features (seen on univariate analysis in Table 1) suggests that reduced proNGF expression could be a sign of early dedifferentiation. In the nervous system, proNGF/NGF expression is generally associated with neuronal differentiation [13], and it is plausible that in thyroid cancer, decreased expression of proNGF could similarly be associated with the dedifferentiation of cancer cells.

An important aspect of the study design was the use of whole-slide analyses of cases with a complete clinico-pathological dataset, as this provided a more complete picture of protein expression across the tumour. We found that although proNGF expression was mostly uniform across primary tumours, a subset of tumours expressed proNGF in a peripheral pattern. It is possible that expression of proNGF may be induced by factors in the tumour microenvironment, such as oxygen, or that proNGF is a component of actively growing cells preferentially located at the periphery of solid tumours; however, further functional investigation is warranted to understand the meaning of preferentially-peripheral expression of proNGF. Additional strengths of this study are the use of automated techniques for immunohistochemistry staining, and digital quantification of protein expression. Manual techniques for immunohistochemistry and biomarker quantification have inherent risks of inter-slide variability and inter-observer bias. The automated techniques used in this study were appropriately trained and validated, and hence, the comparison of differences in staining intensities between tissues, as undertaken here, was more robust.

The primary limitation of this study was the use of single modality immunohistochemistry to evaluate protein expression. However, risks of protein misidentification were minimised by using a well validated antibody against proNGF and appropriate controls. The specificity of proNGF targeting with the antibody used was confirmed against a monoclonal antibody in our previous study, as well as in Western blotting [11]. Minimal nonspecific staining was observed. An additional limitation was that this study included relatively few cases of follicular and anaplastic thyroid cancers and their metastases, and it is possible that these subgroups may exhibit different expression characteristics;

as such, cautious interpretation is required. However, the large number of paired papillary thyroid cancer metastases included in this study allows for a robust interpretation of this cohort.

On a broader perspective, proNGF may be of interest as a therapeutic target. In breast cancer, proNGF has been shown to stimulate cancer cell growth and dissemination [12,14], and in prostate cancer, proNGF expression is a driver of nerve infiltration in the tumour microenvironment [15] that is essential to tumour growth and dissemination [16]. The association between the presence of nerves, neurotrophic growth factor expression and cancer progression is an evolving field, with increasing recognition of the key role of nerve-derived factors in tumour progression [17]. Nerve-signalling has long been recognised as integral for tissue regeneration after injury, and it is hypothesised that similar mechanisms may promote neoplastic progression [17]. For example, denervation has been shown to reduce the incidence of gastric carcinoma [18] and basal cell carcinomas of the skin [19]. In animal models of prostate cancer, tumour progression in animal models is strongly inhibited after denervation [16,20]. Whether proNGF also contributes to thyroid cancer and the development of metastases should be experimentally explored both *in vitro* and *in vivo*.

In conclusion, this study demonstrates proNGF expression in lymph node metastases of thyroid cancer which correlates with expression in the primary tumour, suggesting an underlying biological link which warrants further investigation.

4. Materials and Methods

4.1. Patients and Samples

The Hunter New England Local Health District Human Research Ethics Committee prospectively approved this study, which included a waiver of consent for access to archival material (approval number HNE HREC 16/04/20/5.13, approved April 2016). Electronic records were searched to find lymph node metastases of thyroid cancer specimens during 2007–2017, where the original primary tumour was also available ($n = 56$). Clinical parameters were extracted from the medical record, and an independent pathologist reviewed all histological samples to confirm the diagnosis.

4.2. Immunohistochemistry

Sections (4 microns) were prepared from archival, formalin-fixed, paraffin-embedded tissue blocks immediately prior to staining. Immunohistochemistry was performed using the Ventana Discovery automated slide stainer (Roche Medical Systems, Tucson, AZ, USA). The primary antibody was an anti-rabbit polyclonal proNGF antibody (Ab9040, Merck Millipore, Darmstadt, Germany), which has been previously validated in our laboratory [11] and was reoptimised for automated tissue processing at a dilution of 1/350. Antigen-retrieval was performed using Ribo-CC solution, (pH 6, Ventana, Roche, North Ryde, NSW, Australia), with primary antibody incubation for 32 min, secondary anti-rabbit HQ for 16 min at 37 °C (Ventana, Roche, North Ryde, NSW, Australia) and tertiary anti-HQ (Ventana, Roche, North Ryde, NSW, Australia) for 16 min at 37 °C. Manual counterstaining was performed using Mayer's haematoxylin for 10 s and Scott's Tap Water for 30 s, followed by dehydration, clearing and mounting. Negative controls were prepared using nonspecific IgG isotype controls, and without the addition of primary antibody (Appendix A).

4.3. Digital Quantification

To quantify biomarker expression, whole slides were digitised at 20x magnification using an Aperio AT2 scanner (Leica Biosystems, Victoria, Australia). Two operators (CR and TD) manually graded a training image library of 20 cancers to obtain consensus. QuPath whole-slide digital image analysis software (Queens University, Belfast, UK) [21] was then optimised to quantify maximum cytoplasmic DAB staining. Initially, a cell detection algorithm was optimised to detect nuclear and cytoplasmic regions of malignant cells. DAB threshold values were then determined from histogram analyses of the training library. Finally, the training library was used to build a cell detection classifier (to exclude

fibroblasts, lymphocytes, erythrocytes and colloid) and optimise DAB thresholds to replicate the scoring in the training library. The classifier was then locked and batch-run on all slides. To minimise false positive cell detection and optimise processing time, tumour regions were manually defined. Areas of haemorrhage, dense stroma without malignant cells, dense lymphocytic infiltrate and folding artefacts were excluded. The intensity of DAB staining was quantified using a triple-threshold h-score for each tumour (calculated as the sum of $3 \times$ percentage of pixels with strong staining; $2 \times$ percentage of pixels with moderate staining and $1 \times$ percentage of pixels with weak staining). Examples of image analyses are shown in Appendix B. The quantification of intra-tumoural biomarker distribution in a peripheral or uniform pattern was performed by separately calculating h-score for the outer 1/3 and inner 1/3 of tumour. A peripheral > central pattern was defined as a peripheral: central h-score ratio >1, with an absolute difference in h-score >20 points. Uniformly positive was defined as total tumour h-score > 25 that did not meet the criteria for peripheral > central. Uniformly negative was defined as total tumour h-score \leq 25, irrespective of the peripheral: central ratio.

4.4. Statistical Analysis

A prior study showed that thyroid proNGF immunohistochemistry quantification by h-score was normally distributed with a standard deviation of 21 units [11]. To demonstrate a mean h-score difference of 25 units between groups, a minimum of 25 cases per group were required, with a power of 0.8 and two-sided alpha of 0.05.

We dichotomised age and tumour size based on thresholds in the 8th edition of the American Joint Cancer Committee TNM Staging System and tumour/node size, extra-thyroidal extension, node number and site on the 2015 American Thyroid Association guidelines [3]. We provide strata-level medians and interquartile ranges for h-scores across strata levels, compared using the Mann-Whitney test.

We modelled the association between h-scores and tumour types using linear quantile mixed models that include clinico-pathological covariates and account for within subject clustering. Using the paired tissue sections, we explored the association between the metastatic and primary tumour h-scores along with markers of aggressiveness using quantile regression. In instances where potentially influential points were identified, we excluded these observations and repeated the analyses to assess the sensitivity of parameter estimates. We provide point estimates, 95% confidence intervals and *p*-values for each of the model terms. All reference to significance assumes a 0.05 type-I error rate. All analyses were performed using Stata (version 14.1, Statacorp, Texas USA).

Author Contributions: Conceptualization, C.W.R. and H.H.; Data curation, C.W.R. and M.J.; Formal analysis, C.W.R., T.D., S.F., S.K. and H.H.; Funding acquisition, C.W.R. and H.H.; Investigation, S.K.; Methodology, C.W.R., T.D., S.F., J.W.P., J.M.T., S.K. and H.H.; Project administration, C.W.R.; Resources, R.S. and H.H.; Supervision, S.F., C.G., J.W.P., J.M.T., R.S. and H.H.; Validation, J.W.P., J.M.T., M.J. and H.H.; Writing—original draft, C.W.R. and H.H.; Writing—review & editing, C.W.R., T.D., S.F., C.G., J.W.P., J.M.T., M.J., S.K., R.S. and H.H.

Funding: This work was supported by a Hunter New England LHD Clinical Research Fellowship, a NSW Health Pathology (Hunter) Teaching and Research Committee Grant, a Hunter Cancer Research Alliance Pilot grant, and an Australian Government Research Training Program Scholarship (to CR).

Acknowledgments: The authors would like to thank Anna Price (NSW Health Pathology, Hunter), and Megan Clarke (Hunter Cancer Biobank) for invaluable support.

Conflicts of Interest: HH holds intellectual property for the use of proNGF as a diagnostic test in cancer. The other authors report nothing to disclose.

Abbreviations

AJCC	American Joint Committee on Cancer
DAB	3'3' diaminobenzidine
ProNGF	Precursor for nerve growth factor
TNM	Tumour, Nodes, Metastases Staging System

Appendix A

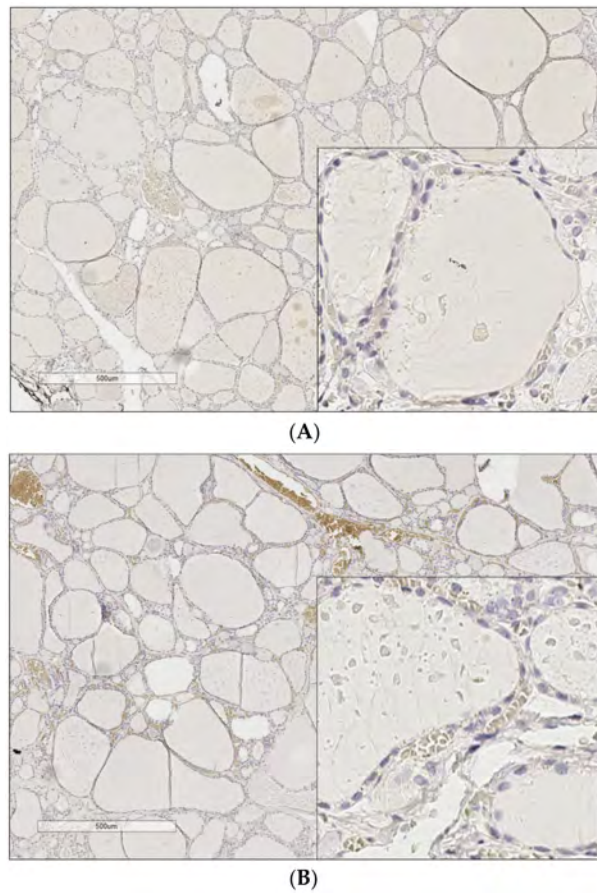


Figure A1. Negative Controls for proNGF staining. (A) IgG isotype control. Nonspecific IgG was added in place of the primary antibody. (B) Without primary antibody. Nonspecific brown staining is of red blood cells. For positive controls, see Faulkner et al. (2016) [5].

Appendix B

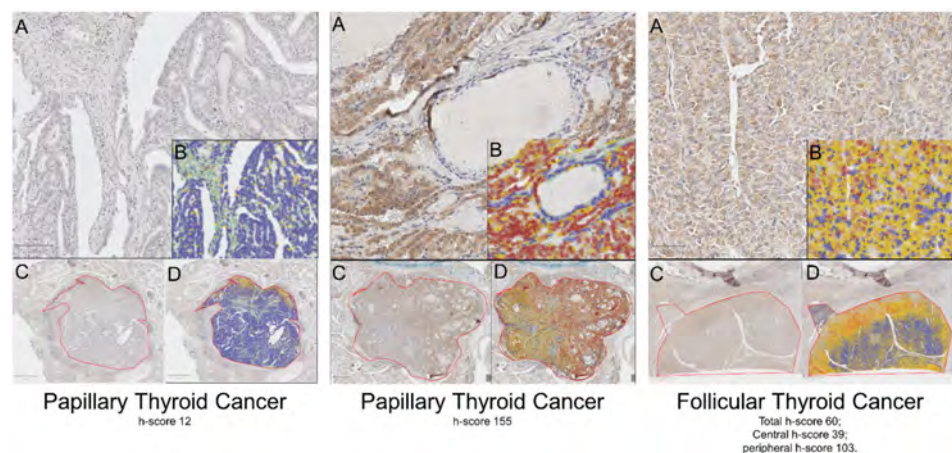
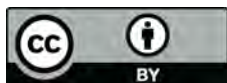


Figure A2. Examples of QuPath grading of cytoplasmic DAB intensity of three separate tumour cases. Each case has 4 separate panels presented (A–D). (A): High magnification (20×) image of immunohistochemistry staining of tumour. (B): QuPath markup of same region showing cell detection and classification. (C) Low magnification (4×) image of tumour, demarcated in red. (D): Low magnification image of tumour with QuPath markup. Markup: Green (stroma), Purple (immune cells), Blue (negative tumour cells).

References

1. Lim, H.; Devesa, S.S.; Sosa, J.A.; Check, D.; Kitahara, C.M. Trends in Thyroid Cancer Incidence and Mortality in the United States, 1974–2013. *JAMA* **2017**, *317*, 1338–1348. [[CrossRef](#)] [[PubMed](#)]
2. Sciuto, R.; Romano, L.; Rea, S.; Marandino, F.; Sperduti, I.; Maini, C.L. Natural history and clinical outcome of differentiated thyroid carcinoma: A retrospective analysis of 1503 patients treated at a single institution. *Ann. Oncol.* **2009**, *20*, 1728–1735. [[CrossRef](#)] [[PubMed](#)]
3. Haugen, B.R.; Alexander, E.K.; Bible, K.C.; Doherty, G.M.; Mandel, S.J.; Nikiforov, Y.E.; Pacini, F.; Randolph, G.W.; Sawka, A.M.; Schlumberger, M.; et al. 2015 American Thyroid Association Management Guidelines for Adult Patients with Thyroid Nodules and Differentiated Thyroid Cancer: The American Thyroid Association Guidelines Task Force on Thyroid Nodules and Differentiated Thyroid Cancer. *Thyroid* **2016**, *26*, 1–133. [[CrossRef](#)] [[PubMed](#)]
4. Randolph, G.W.; Duh, Q.Y.; Heller, K.S.; LiVolsi, V.A.; Mandel, S.J.; Steward, D.L.; Tufano, R.P.; Tuttle, R.M. American Thyroid Association Surgical Affairs Committee’s Taskforce on Thyroid Cancer Nodal Surgery. The prognostic significance of nodal metastases from papillary thyroid carcinoma can be stratified based on the size and number of metastatic lymph nodes, as well as the presence of extranodal extension. *Thyroid* **2012**, *22*, 1144–1152. [[PubMed](#)]
5. Sugitani, I.; Kasai, N.; Fujimoto, Y.; Yanagisawa, A. A novel classification system for patients with PTC: Addition of the new variables of large (3 cm or greater) nodal metastases and reclassification during the follow-up period. *Surgery* **2004**, *135*, 139–148. [[CrossRef](#)]
6. Hondermarck, H. Neurotrophins and their receptors in breast cancer. *Cytokine Growth Factor Rev.* **2012**, *23*, 357–365. [[CrossRef](#)]
7. Adriaenssens, E.; Vanhecke, E.; Saule, P.; Mougél, A.; Page, A.; Romon, R.; Nurcombe, V.; Le Bourhis, X.; Hondermarck, H. Nerve growth factor is a potential therapeutic target in breast cancer. *Cancer Res.* **2008**, *68*, 346–351. [[CrossRef](#)]
8. Pundavela, J.; Demont, Y.; Jobling, P.; Lincz, L.F.; Roselli, S.; Thorne, R.F.; Bond, D.; Bradshaw, R.A.; Walker, M.M.; Hondermarck, H. ProNGF correlates with Gleason score and is a potential driver of nerve infiltration in prostate cancer. *Am. J. Pathol.* **2014**, *184*, 3156–3162. [[CrossRef](#)]
9. Hayakawa, Y.; Sakitani, K.; Konishi, M.; Asfaha, S.; Niikura, R.; Tomita, H.; Renz, B.W.; Taylor, Y.; Macchini, M.; Middelhoff, M.; et al. Nerve Growth Factor Promotes Gastric Tumorigenesis through Aberrant Cholinergic Signaling. *Cancer Cell* **2017**, *31*, 21–34. [[CrossRef](#)]
10. Renz, B.W.; Takahashi, R.; Tanaka, T.; Macchini, M.; Hayakawa, Y.; Dantes, Z.; Maurer, H.C.; Chen, X.; Jiang, Z.; Westphalen, C.B.; et al. beta2 Adrenergic-Neurotrophin Feedforward Loop Promotes Pancreatic Cancer. *Cancer Cell* **2018**, *33*, 75–90. [[CrossRef](#)]
11. Faulkner, S.; Roselli, S.; Demont, Y.; Pundavela, J.; Choquet, G.; Leissner, P.; Oldmeadow, C.; Attia, J.; Walker, M.M.; Hondermarck, H. ProNGF is a potential diagnostic biomarker for thyroid cancer. *Oncotarget* **2016**, *7*, 28488–28497. [[CrossRef](#)] [[PubMed](#)]
12. Demont, Y.; Corbet, C.; Page, A.; Ataman-Önal, Y.; Choquet-Kastylevsky, G.; Fliniaux, I.; Le Bourhis, X.; Toillon, R.A.; Bradshaw, R.A.; Hondermarck, H. Pro-nerve Growth Factor Induces Autocrine Stimulation of Breast Cancer Cell Invasion through Tropomyosin-related Kinase A (TrkA) and Sortilin Protein. *J. Biol. Chem.* **2012**, *287*, 1923–1931. [[CrossRef](#)] [[PubMed](#)]
13. Bradshaw, R.A.; Pundavela, J.; Biarc, J.; Chalkley, R.J.; Burlingame, A.L.; Hondermarck, H. NGF and ProNGF: Regulation of neuronal and neoplastic responses through receptor signaling. *Adv. Biol. Regul.* **2015**, *58*, 16–27. [[CrossRef](#)] [[PubMed](#)]
14. Tomellini, E.; Touil, Y.; Lagadec, C.; Julien, S.; Ostyn, P.; Ziental-Gelus, N.; Meignan, S.; Lengrand, J.; Adriaenssens, E.; Polakowska, R.; et al. Nerve growth factor and proNGF simultaneously promote symmetric self-renewal, quiescence, and epithelial to mesenchymal transition to enlarge the breast cancer stem cell compartment. *Stem Cells* **2015**, *33*, 342–353. [[CrossRef](#)]
15. Pundavela, J.; Roselli, S.; Faulkner, S.; Attia, J.; Scott, R.J.; Thorne, R.F.; Forbes, J.F.; Bradshaw, R.A.; Walker, M.M.; Jobling, P.; et al. Nerve fibers infiltrate the tumor microenvironment and are associated with nerve growth factor production and lymph node invasion in breast cancer. *Mol. Oncol.* **2015**, *9*, 1626–1635. [[CrossRef](#)]

16. Magnon, C.; Hall, S.J.; Lin, J.; Xue, X.; Gerber, L.; Freedland, S.J.; Frenette, P.S. Autonomic Nerve Development Contributes to Prostate Cancer Progression. *Science* **2013**, *341*, 1236361. [[CrossRef](#)]
17. Boilly, B.; Faulkner, S.; Jobling, P.; Hondermarck, H. Nerve Dependence: From Regeneration to Cancer. *Cancer Cell* **2017**, *31*, 342–354. [[CrossRef](#)]
18. Zhao, C.-M.; Hayakawa, Y.; Kodama, Y.; Muthupalani, S.; Westphalen, C.B.; Andersen, G.T.; Flatberg, A.; Johannessen, H.; Friedman, R.A.; Renz, B.W.; et al. Denervation suppresses gastric tumorigenesis. *Sci. Transl. Med.* **2014**, *6*, 250ra115. [[CrossRef](#)]
19. Peterson, S.C.; Eberl, M.; Vagnozzi, A.N.; Belkadi, A.; Veniaminova, N.A.; Verhaegen, M.E.; Bichakjian, C.K.; Ward, N.L.; Dlugosz, A.A.; Wong, S.Y. Basal cell carcinoma preferentially arises from stem cells within hair follicle and mechanosensory niches. *Cell Stem Cell* **2015**, *16*, 400–412. [[CrossRef](#)]
20. Zahalka, A.H.; Arnal-Estape, A.; Maryanovich, M.; Nakahara, F.; Cruz, C.D.; Finley, L.W.S.; Frenette, P.S. Adrenergic nerves activate an angio-metabolic switch in prostate cancer. *Science* **2017**, *358*, 321–326. [[CrossRef](#)]
21. Bankhead, P.; Loughrey, M.B.; Fernandez, J.A.; Dombrowski, Y.; McArt, D.G.; Dunne, P.D.; McQuaid, S.; Gray, R.T.; Murray, L.J.; Coleman, H.G.; et al. QuPath: Open source software for digital pathology image analysis. *Sci. Rep.* **2017**, *7*, 16878. [[CrossRef](#)] [[PubMed](#)]



© 2019 by the authors. Licensee MDPI, Basel, Switzerland. This article is an open access article distributed under the terms and conditions of the Creative Commons Attribution (CC BY) license (<http://creativecommons.org/licenses/by/4.0/>).

7 TARGETING THE TSH RECEPTOR IN THYROID CANCER

7.1 Preface

Thus far, this thesis has examined the role of nerves and neurotrophins in the diagnosis and management of thyroid cancer. It has been identified that although the prognosis is favourable for many thyroid cancers, a significant proportion do not respond to initial therapy, and present with locoregional or distant recurrences. In this group, new modalities to localize and treat recurrence are required. The following paper examines the breadth of TSH receptor expression and signalling in thyroid cancer and explores the prospect of utilising the TSH receptor to as the foundation for new approaches to localize and treat recurrences.

Targeting the TSH receptor in thyroid cancer

Christopher W Rowe^{1,2,3}, Jonathan W Paul^{2,3}, Craig Gedye^{3,4,5}, Jorge M Tolosa^{2,3}, Cino Bendinelli^{2,6}, Shaun McGrath^{1,2} and Roger Smith^{1,2,3}

¹Department of Endocrinology, John Hunter Hospital, Newcastle, Australia

²School of Medicine and Public Health, University of Newcastle, Newcastle, Australia

³Hunter Medical Research Institute, Newcastle, New South Wales, Australia

⁴Department of Medical Oncology, Calvary Mater Newcastle, Waratah, Australia

⁵School of Biomedical Sciences and Pharmacy, University of Newcastle, Newcastle, Australia

⁶Department of Surgery, John Hunter Hospital, Newcastle, Australia

Correspondence
should be addressed
to C Rowe

Email

Christopher.Rowe@hnehealth.nsw.gov.au

Abstract

Recent advances in the arena of theranostics have necessitated a re-examining of previously established fields. The existing paradigm of therapeutic thyroid-stimulating hormone receptor (TSHR) targeting in the post-surgical management of differentiated thyroid cancer using levothyroxine and recombinant human thyroid-stimulating hormone (TSH) is well understood. However, in an era of personalized medicine, and with an increasing awareness of the risk profile of longstanding pharmacological hyperthyroidism, it is imperative clinicians understand the molecular basis and magnitude of benefit for individual patients. Furthermore, TSHR has been recently re-conceived as a selective target for residual metastatic thyroid cancer, with pilot data demonstrating effective targeting of nanoparticles to thyroid cancers using this receptor as a target. This review examines the evidence for TSHR signaling as an oncogenic pathway and assesses the evidence for ongoing TSHR expression in thyroid cancer metastases. Priorities for further research are highlighted.

Key Words

- thyroid cancer
- TSH receptor
- theranostics
- targeted therapy

Endocrine-Related Cancer
(2017) **24**, R191–R202

Introduction

The thyroid-stimulating hormone (TSH) receptor (TSHR) is a surface glycoprotein receptor, part of the leucine-rich repeat subfamily of G-protein-coupled receptors (LGR). It has been described as the ‘master switch’ in regulating thyroid growth, differentiation and thyroid hormone secretion, and is the antigenic target in Graves’ disease (Davies *et al.* 2005). TSHR is expressed on benign and malignant thyrocytes as the target receptor for TSH. In current clinical management of differentiated thyroid cancer (DTC), TSHR is therapeutically targeted to maximize radioiodine uptake into malignant thyrocytes by transiently upregulating the sodium–iodide symporter (NIS) through TSH stimulation, either endogenously

through thyroid hormone withdrawal or exogenously with recombinant human TSH (rhTSH) (Haugen *et al.* 2016). Additionally, proliferative signals to malignant thyrocytes mediated through the TSHR are therapeutically minimized by inducing pharmacologic hyperthyroidism, resulting in endogenous TSH suppression. Recent scientific advances suggest new strategies to target TSHR in thyroid cancers, either using selective small-molecule inhibitors of the TSHR to obviate the need for systemic hyperthyroidism or using the TSHR as a target to enhance the therapeutic index for drug delivery systems. This increased interest demands a critical appraisal of evidence for persistent TSHR expression in metastatic

Review	C W Rowe et al.	Targeting the TSH receptor in thyroid cancer	24:6	R192
--------	-----------------	--	------	------

Table 1 Data from studies of human extra-thyroidal tissue expression of TSHR.

Tissue	mRNA	Protein*	Functionality#	References
Adipose tissue	Y	Y	Y	Bell et al. (2000), Murakami et al. (2001), Gagnon et al. (2014)
Adrenal	Y	Y	–	Dutton et al. (1997)
Endometrium	Y	Y	–	Aghajanova et al. (2011)
Erythrocytes	–	Y	Y	Balzan et al. (2007)
Extra-ocular muscle, adipocytes	Y	Y	Y	Bahn et al. (1998), Vallyasevi et al. (1999)
Kidney	Y	Y	Y	Dutton et al. (1997), Sellitti et al. (2000)
Liver	Y	Y	Y	Zhang et al. (2009)
Lymphocytes	Y	Y	–	Chabaud and Lissitzky (1977), Coutelier et al. (1990)
Pituitary	Y	Y	–	Prummel et al. (2000), Theodoropoulou et al. (2000)
Hair follicles	Y	–	Y	Bodo et al. (2009)
Thymus	Y	Y	–	Murakami et al. (1996), Dutton et al. (1997)
Vascular smooth muscle	Y	Y	Y	Tian et al. (2014)

*Detected by immunohistochemistry, Western blot or ligand-binding assays. #Assessed by increased cyclic AMP production/p70 S6 kinase or Na/K ATPase in response to TSH stimulation *in vitro*.

–, not reported.

thyroid cancer. Herein, we review the evidence for TSHR signaling as a mitogenic pathway in thyroid cancers, assess the evidence for persistence of TSHR in advanced thyroid cancer and discuss new therapeutic strategies on the horizon.

Structure and distribution of TSHR

TSHR is a 764 amino acid 7-transmembrane domain receptor in the G-protein-coupled receptor superfamily. TSHR is encoded by the gene, thyroid-stimulating hormone receptor (*TSHR*), located on chromosome 14q31 and first cloned in 1989 (Parmentier et al. 1989). Although encoded by a single gene, the gene product undergoes post-translational cleavage into an extracellular A-subunit and a largely intracellular B-subunit linked by disulfide bonds, with the exclusion of a 50 amino acid C-peptide region (Rapoport & McLachlan 2016). The A-subunit contains multiple binding sites for TSH within a leucine-rich 'binding pocket', which undergoes conformational change after binding of TSH or stimulatory autoantibodies, resulting in receptor activation (Davies & Latif 2015).

TSHR is predominantly expressed on the basolateral membrane of thyroid follicular cells. Surface expression of TSHR is estimated at 5000 receptors per cell (Rees Smith et al. 1988). *TSHR* mRNA and protein have been detected in a variety of other human and animal tissues, including neural and immune tissues, ocular muscles and bone (Davies et al. 2002, Williams 2011, Bassett & Williams 2016). In particular, the role of TSHR expression in orbital preadipocytes and fibroblasts in the pathogenesis of Graves' ophthalmopathy has been extensively studied (Smith 2015), and there are animal data to support TSHR-mediated bone remodeling

(Abe et al. 2003, Ma et al. 2011). Human data regarding *TSHR* mRNA expression and protein production in extrathyroidal tissue are presented in Table 1. We are not aware of studies that quantify TSHR receptor density in extrathyroidal tissue. In most extrathyroidal tissues the physiologic role of the TSHR remains unclear (Williams 2011).

TSH as a growth factor for benign and malignant thyrocytes

TSH and intracellular growth signaling

As a glycoprotein receptor in the rhodopsin family, TSHR responds to ligand binding with activation of its coupled G protein. Activation of G α_s stimulates adenylate cyclase and activates the cyclic adenosine monophosphate (cAMP)/protein kinase A (PKA) pathway with well-established mitogenic effects, whereas G α_q stimulation results in the activation of protein kinase B and mitogen-activated protein kinase (MAPK) pathways (Morshed et al. 2009). The downstream effects are to increase the transcription of thyroid-specific genes, particularly controlling iodine uptake, synthesis of thyroglobulin and thyroperoxidase, with the end result of thyroid hormone production (Roger et al. 1988, Vassart & Dumont 1992, Bruno et al. 2005). The regulation of thyrocyte growth has been extensively studied using *in vitro* models; however, it is well recognized that human *in vivo* confirmation of any such model is paramount (Kimura et al. 2001).

Bruno and coworkers (Bruno et al. 2005) demonstrated *in vivo* in humans that TSH regulates the transcription of NIS (*SLC5A5*), thyroglobulin (*TG*), thyroperoxidase (*TPO*) and paired box 8 (*PAX8*) mRNA, but not *TSHR*, pendrin

(*SLC26A4*) or thyroid transcription factor 1 (*NKX2-1*). Importantly, they showed that absence of TSH due to suppression from exogenous hyperthyroidism does not reduce *TSHR* mRNA. These data support the observations by Shuppert and coworkers (Shuppert *et al.* 1996) from human tissues that *TSHR* mRNA is not reduced in the presence of chronic stimulation by thyroid-stimulating autoantibodies and from Maenhaut and coworkers (Maenhaut *et al.* 1992) in dogs, confirming not only that TSHR is important in thyrocyte growth but also that TSHR gene transcription stably continues both in the presence and absence of its ligand. This contrasts with *NIS* gene and protein expression, which are affected by cellular signaling from iodine and TSH (Dohán *et al.* 2003).

TSHR stimulation and thyroid growth

Human disease states of chronic TSH stimulation provide *in vivo* models of TSHR-mediated thyroid growth, as seen in TSH-secreting pituitary adenomas, and Graves' disease (where TSHR stimulation occurs by thyroid stimulatory immunoglobulins (TSI) binding to TSHR). Both conditions are characterized by pathological thyroid enlargement, seen in 77% and 93%, respectively (Hegedus *et al.* 1983, Beck-Peccoz *et al.* 2009). Additionally, chronic exposure to TSI has been associated with increased disease-specific mortality in thyroid cancer in some, but not all, studies (Belfiore *et al.* 1990, Pellegriti *et al.* 2013).

Recently, multiple large cohort studies have found that increased levels of serum TSH are associated with increased subsequent risk of thyroid cancer (Nieto & Boelaert 2016). The largest study, recruiting 10,178 patients presenting with nodular thyroid disease for fine needle aspiration (FNA) biopsy, found an increasing odds ratio for papillary thyroid cancer (PTC) with incremental increases of TSH within the reference range of 0.4–3.4 IU/L (Fiore *et al.* 2009). Both higher pathological stage of the primary tumor and the increased incidence of nodal metastases were significantly associated with higher baseline TSH levels. In this study, level of TSH, not autoantibody status, was shown to be an independent variable in predicting malignancy.

Further, several studies have now shown the importance of TSHR signaling as part of the oncogenic pathway, particularly in tumors containing mutations in B-Raf proto-oncogene (*BRAF*). Franco and coworkers (Franco *et al.* 2011) showed in mice that *BRAF*^{V600E} mutations were only oncogenic in the presence of a TSHR stimulatory pathway. This finding was confirmed by

Kim and coworkers (Kim *et al.* 2014) showing that TSH signaling overcomes senescence induced by *BRAF*^{V600E} mutations in cell culture. Similarly, Lu and coworkers (Lu *et al.* 2010) used a TSHR-knockout mouse model of follicular thyroid cancer (FTC) to show that TSHR-mediated growth signaling is required for thyroid cancer to metastasize, but only in the presence of additional oncogenic mutations.

Suppressed TSH and reduced progression of thyroid cancer

A correlation between a hyperthyroid state and reduced thyroid cancer growth was noted in the 1930s by the Australian surgeon Dunhill (1937). However, it was not until the 1950s that other surgeons, notably George Crile Jr, began to widely advocate the practice of levothyroxine therapy to reduce the size of thyroid cancer metastases (Hurley 2011). Subsequently, multiple large studies, including a meta-analysis (McGriff *et al.* 2002), have confirmed that levothyroxine-induced suppression of TSH is associated with reduced growth of thyroid cancers. Key studies are reviewed below.

Mazzaferri and Jhiang (1994) prospectively followed 1355 patients with treated DTC. After 30 years, the rate of recurrence for patients treated with levothyroxine was 30%, compared to 40% in untreated patients. Baseline characteristics of these subgroups, reasons for treatment and degree of suppression of TSH were not reported. Pujol and coworkers (Pujol *et al.* 1996) retrospectively compared a group of 18 patients with stable TSH <0.05 IU/L with a group of 15 patients with stable TSH >1 IU/L after thyroidectomy for DTC. Baseline characteristics were similar. Median relapse-free survival was twice as long in the suppressed TSH group (21.6 vs 9.3 years), with significantly fewer relapses over this period (1 vs 6 relapses). Cooper and coworkers (Cooper *et al.* 1998) followed 617 DTC patients from a thyroid cancer registry for median of 4.5 years, with patients grouped according to mean of measured TSH levels. In patients with advanced stage disease at diagnosis, greater TSH suppression was associated with higher rates of progression-free survival. Finally, Jonklaas and coworkers (Jonklaas *et al.* 2006) followed 2936 DTC patients from a multi-institutional registry. Patients with AJCC-TNM5 Stage 2 or higher disease had higher rates of overall survival with TSH levels below the reference range, with increased degrees of TSH suppression correlating with higher overall survival in Stages III and IV disease.

TSHR expression in *in vitro* models of thyroid cancer

Although cell lines have represented an attractive model for cancer research for decades, it is increasingly understood that due to mutation and selection pressures within culture media, these cells commonly dedifferentiate. Several independent analyses of commonly studied thyroid cancer cell lines confirm that these cell lines have largely ceased to express markers of thyrocyte differentiation, and more closely represent anaplastic thyroid cancers than DTC (Meireles *et al.* 2007, van Staveren *et al.* 2007, Pilli *et al.* 2009). This is particularly true of TSHR expression, which is downregulated early in monolayer culture due to disruption of follicular architecture and loss of apical-basal polarity (Williams & Wynford-Thomas 1997). In a recent review, Pilli and coworkers (Pilli *et al.* 2009) note that TSHR expression was not detected in any of a number of commonly studied cell lines. There are conflicting data regarding TSHR expression in the FTC-133 cell line (originating from a lymph node metastases of a differentiated human follicular thyroid cancer), with some authors demonstrating mRNA expression (D'Agostino *et al.* 2014) and TSH ligand binding (Paolino *et al.* 2014), which may represent heterogeneity within this cell line between laboratories. Additionally, there is conflicting evidence for TSHR expression in the BCPAP cell line

(derived from a poorly differentiated PTC) (Pilli *et al.* 2009, D'Agostino *et al.* 2014, Dotan *et al.* 2016). Similarly, PTC cells grown in thyrosphere culture lack expression of thyroid-specific proteins, and cells fail to produce cAMP in response to TSH stimulation (Malaguarnera *et al.* 2011, Giani *et al.* 2015). The cell line XTC-UC1, derived from a metastatic Hurthle cell carcinoma, appeared to retain TSHR expression as well as other markers of differentiation (Zielke *et al.* 1998, Meireles *et al.* 2007), however, is no longer widely available. Consequently, cells stably transfected with *TSHR* are commonly used for *in vitro* targeting studies where reliable TSHR expression is desired.

TSHR expression in primary thyroid tumors

After seminal work by Ichikawa and coworkers (Ichikawa *et al.* 1976), robust evidence obtained over four decades supports the continued expression of TSHR in the majority of DTC, based on studies using ligand binding, mRNA detection using Western blotting or PCR and protein immunohistochemistry (IHC) (Table 2). Although *TSHR* mRNA and/or protein can be detected in over 90% of PTC and FTC, the relative expression of TSHR in different tumors is highly variable, both in terms of pattern and intensity of staining by IHC, and in the semi-quantitative analysis of mRNA recovery (Table 3).

Table 2 Evidence for TSHR expression in primary thyroid tumors and metastases.

Study	Method	TSHR expression in primary tumors								TSHR expression in lymph node metastases*							
		PTC		FTC		ATC		MTC		PTC		FTC		ATC		MTC	
		<i>n</i>	%	<i>n</i>	%	<i>n</i>	%	<i>n</i>	%	<i>n</i>	%	<i>n</i>	%	<i>n</i>	%	<i>n</i>	%
Carayon <i>et al.</i> 1980	Ligand binding	6/6	100	2/4	50	0/4	0	0/4	0	5/5	100	6/7	86	0/1	0	0/1	0
Clark <i>et al.</i> 1983	Ligand binding	10/10	100	←	←	—	—	—	—	—	—	—	—	—	—	—	—
Brabant <i>et al.</i> 1991	mRNA	8/8	100	1/1	100	1/3	33	—	—	6/6	100	—	—	0/1	0	—	—
Ohta <i>et al.</i> 1991	mRNA	3/3	100	4/4	100	—	—	—	—	—	—	—	—	—	—	—	—
Hoang-Vu <i>et al.</i> 1992	mRNA	19/20	95	6/8	75	0/5	0	—	—	—	—	—	—	—	—	—	—
Shi <i>et al.</i> 1993	mRNA	13/20	65	2/2	100	1/3	33	—	—	—	—	—	—	—	—	—	—
Elisei <i>et al.</i> 1994	mRNA	16/16	100	2/2	100	0/2	0	3/6	50	4/4	100	—	—	—	—	0/1	0
Arturi <i>et al.</i> 1997	mRNA	—	—	—	—	—	—	—	—	23/23	100	3/3	100	—	—	—	—
Lazar <i>et al.</i> 1999	mRNA	38/38	100	5/5	100	—	—	—	—	—	—	—	—	—	—	—	—
Tanaka <i>et al.</i> 2000	mRNA	31/31	100	—	—	—	—	—	—	4/4	100	—	—	—	—	—	—
Park <i>et al.</i> 2000	mRNA	23/23	100	—	—	—	—	—	—	—	—	—	—	—	—	—	—
Wang <i>et al.</i> 2011	mRNA	31/32	97	←	←	—	—	—	—	—	—	—	—	—	—	—	—
Wang <i>et al.</i> 2011	IHC, frozen	32/32	100	←	←	—	—	—	—	—	—	—	—	—	—	—	—
Tanaka <i>et al.</i> 1997	IHC, frozen	21/21	100	2/2	100	—	—	—	—	—	—	—	—	—	—	—	—
Gerard <i>et al.</i> 2003	IHC, FFPE	16/16	100	14/14	100	—	—	—	—	1/1	100	2/2	100	—	—	—	—
Matsumoto <i>et al.</i> 2008	IHC, FFPE	23/23	100	←	←	0/8	0	—	—	—	—	—	—	—	—	—	—
So <i>et al.</i> 2012	IHC, FFPE	18/20	90	—	—	—	—	—	—	39/52	75	—	—	—	—	—	—
Lin <i>et al.</i> 2016	IHC	37/46	80	—	—	—	—	—	—	—	—	—	—	—	—	—	—
Liu <i>et al.</i> 2016	IHC	102/150	68	—	—	—	—	—	—	—	—	—	—	—	—	—	—

*Data from Elisei *et al.* included 2 local (non-lymph node) recurrences. Location of metastases was not reported by Tanaka *et al.* or Gerard *et al.*

←, data for PTC and FTC grouped together; dash, no data; FFPE, formalin fixed paraffin embedded; frozen: frozen tissue; IHC, immunohistochemistry.

Review	C W Rowe <i>et al.</i>	Targeting the TSH receptor in thyroid cancer	24:6	R195
--------	------------------------	--	------	------

Table 3 Relative expression of TSHR in primary and metastatic DTC.

			Tumoral TSHR expression relative to comparison tissue							
Author	Method	Comparison tissue	Increased	%	Similar	%	Reduced	%	Absent	%
Primary DTC										
Carayon <i>et al.</i> 1980	Ligand binding	Normal	1/10	10	2/10	20	5/10	50	2/10	20
Clark <i>et al.</i> 1983	Ligand binding	Normal	6/10	60	2/10	20	2/10	20	0/10	0
Brabant <i>et al.</i> 1991	mRNA, frozen	Normal	–	–	–	–	5/5	100	–	–
Shi <i>et al.</i> 1993	mRNA, frozen	MNG	0/22	0	4/22	18	9/22	41	9/22	41
Tanaka <i>et al.</i> 1997	IHC, frozen	Normal	4/21	19	7/21	33	10/21	48	0/21	0
Sheils <i>et al.</i> 1999	mRNA, FFPE	Normal	2/76	3	34/76	45	40/76	53	0/76	0
Matsumoto <i>et al.</i> 2008	IHC, FFPE	Normal	16/23	70	–	–	7/23	30	0/23	0
Wang <i>et al.</i> 2011	mRNA/IHC, FFPE	Relative	20/32	63	7/32	22	–	–	5/32	16
So <i>et al.</i> 2012	IHC, FFPE	Relative	7/20	35	9/20	45	1/20	5	2/20	20
Metastases of DTC										
Carayon <i>et al.</i> 1980	Ligand binding	Normal	0/14	0	2/14	14	9/14	64	3/14	21
So <i>et al.</i> 2012	IHC, FFPE	Primary tumour	23/52	44	24/52	46	5/52	10	0/52	0

–, no data reported; DTC, differentiated thyroid cancer; FFPE, formalin fixed, paraffin embedded; frozen, frozen tissue; IHC, immunohistochemistry; MNG, multinodular goiter; normal, normal thyroid tissue.

Sheils and Sweeney (1999) used PCR to semi-quantitatively study mRNA extracted from 90 formalin-fixed paraffin-embedded (FFPE) thyroid tumors, expressed as a ratio of *TSHR* mRNA to the housekeeping enzyme glyceraldehyde-3-phosphate dehydrogenase (*GAPDH*), and stratified by tumor type and degree of differentiation. Although *TSHR* mRNA was detected in all tumors, they found a significant positive correlation between degree of differentiation and *TSHR* expression (Fig. 1). Recovery of *TSHR* mRNA from medullary thyroid cancer (MTC) would not usually be expected given the neuroendocrine origin of these cells and could suggest contamination of samples from surrounding normal thyroid tissue; however, the finding is consistent with other studies suggesting MTC may in fact express the TSHR (Elisei *et al.* 1994).

Tanaka and coworkers (Tanaka *et al.* 1997) studied TSHR protein expression in 21 PTCs (18 well differentiated) and 2 FTCs (both well differentiated) using IHC. They compared receptor immunostaining intensity and distribution to surrounding thyroid tissue. They found that intensity of staining for TSHR was weaker in 43%, similar in 30% and increased in 17% of tumors, with TSHR intensity reported as homogenous in 57% and heterogenous in 43%. Tumors with weaker TSHR staining were more likely to have an aggressive clinical phenotype.

In most studies, no TSHR expression was detected in anaplastic thyroid cancer (ATC), which is consistent with the expected loss of differentiation in this phenotype (Table 2).

TSHR expression in thyroid cancer metastases

There is a paucity of data regarding TSHR expression in thyroid cancer metastases. As is evident from Tables 2 and 3, the majority of studies of *TSHR* mRNA expression or TSHR protein levels have focused on primary thyroid tumors, with several studies including occasional metastases in their cohort, almost exclusively from neck lymph nodes. The largest and only systematic study of TSHR expression in DTC metastases is from So and coworkers (So *et al.* 2012), who examined using immunohistochemistry, the specific instance of subclinical lymph node metastases from papillary microcarcinoma, using 20 primary tumors and 52 associated subclinical central compartment metastases. They demonstrated that in their cohort, 90% of primary tumors and 75% of metastatic nodes stained positive for TSHR, with concordance between primary

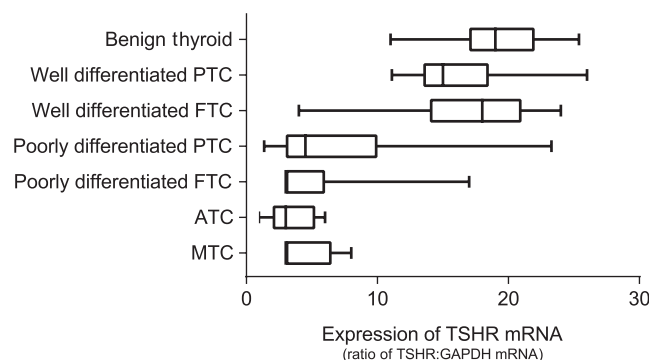


Figure 1 Box (25–75%) and whisker (5–95%) plot of *TSHR* mRNA expression by tumor type and differentiation. Redrawn with permission from data in Sheils and coworkers (Sheils *et al.* 1999). TSHR mRNA expressed as a ratio of the housekeeping gene *GAPDH*.

tumor and metastases demonstrated in 85% of cases. Intensity of staining was weaker in metastases than that in primary tumor in 44% of cases and similar or stronger in 56%.

Arturi and coworkers (Arturi *et al.* 1997) used RT-PCR to study FNAs of enlarged neck lymph nodes from 27 patients with predominant PTC. In the 26 aspirates with adequate samples, *TSHR* mRNA was detected in all specimens. No details of patient or tumor characteristics were provided.

Evidence for persistent functional TSHR expression in thyroid cancer metastases can be inferred from detecting increased thyroglobulin production in response to TSH stimulation, as it occurs in preparation for radioiodine ablation in the context of known residual disease after thyroidectomy. Lippi and coworkers (Lippi *et al.* 2001) studied 12 patients with metastatic or locally invasive FTC ($n=10$) or PTC ($n=2$). In the 9 patients for whom data are available, thyroglobulin rose by a median of 8.4-fold (range 1.3–29 \times) after TSH stimulation. Luster and coworkers (Luster *et al.* 2000) report radioiodine treatment in 11 patients with advanced recurrent or residual DTC. Nine of 11 patients had previous radioiodine therapy (median 5 treatments). Ten of 11 patients had a rise in thyroglobulin after treatment with rhTSH (median 2.4 \times baseline, range 1.2–59.1). Jarzab and coworkers (Jarzab *et al.* 2003) studied administration of rhTSH in 54 patients with either locoregional or distant metastatic DTC. Fifty patients had received prior radioiodine ablation. Median serum thyroglobulin concentration increased 3.8-fold from baseline to day 6 after rhTSH. Individual patient data were not reported.

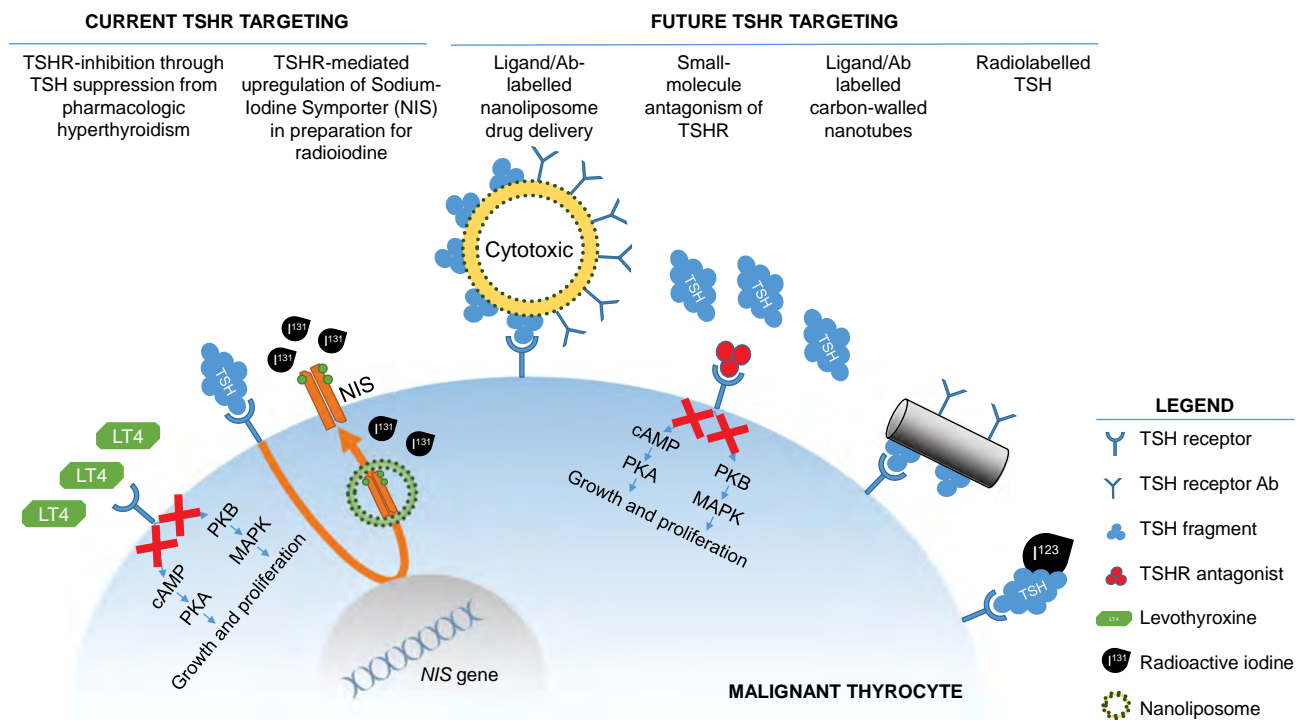
In a review of the 11 largest studies of rhTSH-assisted treatment of residual or recurrent DTC (124 patients), Luster and coworkers (Luster *et al.* 2005) found that serum thyroglobulin increased in response to rhTSH in at least 67% of patients for whom data were recorded. This figure is similar to the 75% prevalence of TSHR expression reported by So and coworkers (So *et al.* 2012) in papillary microcarcinoma and strongly suggests that TSHR expression is preserved in the majority of clinically significant DTC metastases and persists despite previous radioiodine exposure in the majority of cases. Importantly, this 67% is likely to underestimate actual TSHR expression in clinically significant metastases, both because these case series predominantly included patients with longstanding and advanced metastatic disease and because the surrogate outcome measure (thyroglobulin rise) relies on an intact multistep signaling cascade from TSHR to thyroglobulin production for a positive result.

Persistence of TSHR expression in the setting of loss of other differentiation markers

TSHR expression in DTC has been compared to the expression of other thyroïdal markers of differentiation. Several studies have found that TSHR expression closely parallels other markers of differentiation, such as thyroglobulin and thyroperoxidase (Hoang-Vu *et al.* 1992, Elisei *et al.* 1994, Park *et al.* 2000). However, evidence from a number of studies of resected thyroid tissue suggests that TSHR is more persistently expressed than other differentiation markers, including NIS and thyroglobulin proteins (Filetti *et al.* 1999, Lazar *et al.* 1999, Gerard *et al.* 2003), indicating not only that TSHR may remain an important signaling pathway for cellular growth but also its utility as a conserved therapeutic target. Further *in vivo* evidence of continued TSHR expression in the absence of NIS is provided by a study of 63 patients with metastatic DTC, and no radioactive iodine uptake on whole body scan, who underwent ^{18}F -fludeoxyglucose positron emission tomography (^{18}F -FDG-PET) both under basal conditions and after rhTSH stimulation (Leboulleux *et al.* 2009). This study found that the sensitivity of FDG-PET was significantly increased after rhTSH stimulation on a per lesion basis (95% vs 81%), suggesting that these lesions continued to express TSHR in the absence of the ability to concentrate radioiodine.

Current therapeutic targeting of TSHR in DTC

Firstly, as discussed previously, pharmacological TSH suppression with exogenous levothyroxine has been a mainstay of clinical DTC management for decades. However, the most recent guidelines of the American Thyroid Association now support a more individualized approach to TSH suppression, based on the likelihood of progressive residual disease and the risks associated with systemic hyperthyroidism (Haugen *et al.* 2016), better reflecting the paucity of evidence for benefit in low-risk patients. The long-term utility of TSH-suppressive therapy is limited in part by its tumorigenic, not tumoricidal, efficacy, although a survival benefit has been shown in high-risk patients (Jonklaas *et al.* 2006). However, in patients at lower risk of recurrence, the adverse effects of hyperthyroidism, including accelerated bone loss resulting in osteoporosis, and cardiac side effects, including atrial fibrillation, remain important caveats to universal therapy.

**Figure 2**

Schematic diagram outlining current and future theranostic targeting of TSHR in DTC. A full colour version of this figure is available at <http://dx.doi.org/10.1530/ERC-17-0010>.

Secondly, TSHR-mediated upregulation of NIS expression is routinely exploited in preparation for ablative radioiodine therapy, either with endogenous TSH stimulation by thyroxine withdrawal or pharmacologically with rhTSH. In clinical studies, expression of TSHR has been shown to correlate with the degree of iodine trapping (Edmonds *et al.* 1977), and with efficacy of ablation (Fallahi *et al.* 2012). Further, both positive and negative regulation of NIS mRNA in response to TSHR stimulation has been demonstrated in human thyroid cells (Saito *et al.* 1997, Bruno *et al.* 2005). Interestingly, TSHR stimulation also increases the sensitivity of ^{18}F -FDG-PET imaging in the detection of residual metastatic disease, again suggesting that TSHR stimulation increases mitotic activity and glucose utilization within malignant thyrocytes (Leboulleux *et al.* 2009).

Novel theranostic exploitation of TSHR

Thus far, key characteristics have been identified that establish the TSHR as an attractive therapeutic target in DTC, namely its pivotal role in growth signaling, and its persistence as an expressed surface protein until late stages of de-differentiation. Additionally, the relative specificity of TSHR as a marker on thyroid tissue makes

it an attractive potential target for novel theranostic and therapeutic agents. Over the last decade, there have been several exciting developments targeting TSHR in diagnosis or treatment of thyroid malignancies (Fig. 2).

TSHR as a theranostic target for drug delivery

New modalities for the localization and treatment of metastatic DTC are required, especially for tumors that are not cured by radioiodine. Although the majority of DTC has a favorable prognosis, up to 15% of cases do not respond completely to radioiodine ablation, including 4% that exhibit no tumor reduction or progressive disease (Sciuto *et al.* 2009). In cases that no longer concentrate radioiodine, the twin utility of radioiodine as a true theranostic agent (a modality with both diagnostic and therapeutic utility) is absent. Localization of recurrent disease is then reliant on structural imaging with ultrasound, computed tomography (CT) scan or ^{18}F -FDG-PET, which although sensitive, lacks the specificity of radioiodine avidity to confirm metastatic disease. Additionally, small molecule kinase inhibitors, which have surpassed traditional cytotoxics as first-line treatment for progressive radioiodine-resistant DTC, are cytostatic rather than tumoricidal, and thus, at best can prolong

progression-free survival rather than offer a chance of cure (Haugen *et al.* 2016). In addition, the toxicities of such agents preclude widespread use.

Late last century, Mayo Clinic Endocrinologist John Morris (1997) suggested that TSHR may be a suitable receptor for novel targeted therapies to thyroid cancers, although identified that 'no direct data toward this goal have appeared in the literature'. Although not widely cited, this article defines what has become an increasingly relevant and potentially transformative field.

An early publication by Signore's laboratory in Rome examined radiolabeled rhTSH (either with ^{123}I or ^{125}I) as a potential imaging tracer for detection of thyroid cancer metastases in a nude-mouse xenograft tumor model, demonstrating focal increase in activity at sites of tumor (Corsetti *et al.* 2004). A later study similarly examined $\text{Tc}^{99\text{m}}$ -labeled rhTSH injected into CD-1 xenograft mice, and a dog with PTC, and demonstrated focal uptake of radioisotope in TSHR-positive cells (Galli *et al.* 2014).

The field of theranostics in cancer therapy has rapidly expanded over the past decade, seeking the 'holy grail' of delivery of significant concentrations of drug to target tissues (either a chemotherapeutic agent or imaging tracer) with high specificity and minimal off-target effects, with the goals of increasing therapeutic index (Sercombe *et al.* 2015). Nanoliposomes offer a well-studied and attractive model for drug delivery and can deliver large payloads per particle. Organ-specific targeting and immune system evasion can be modulated by molecules embedded in the lipid bilayer (Sercombe *et al.* 2015).

Paolino and coworkers (Paolino *et al.* 2014) constructed nanoliposomes coated with fragments of TSH. They demonstrated competitive binding to TSHR *in vitro*, and 3-fold selectivity in localization to thyroid tissue in Wistar rats *in vivo*. TSHR-targeted nanoliposomes loaded with the chemotherapeutic agent gemcitabine had higher efficacy against the thyroid cancer cell line FTC-133 *in vitro* than non-targeted liposomal gemcitabine and free gemcitabine. Finally, in a xenograft model, TSHR-targeted gemcitabine nanoliposomes resulted in greater reduction of FTC-133 tumor mass over 15 days of therapy than non-targeted gemcitabine liposomes. A similar study the following year confirmed these results using cisplatin (Gao *et al.* 2015). These studies provide *in vivo* models to investigate the paradigm of TSHR-targeted theranostics, as liposomes can be readily adapted to deliver either a diagnostic or therapeutic load.

This paradigm was further extended by Dotan and coworkers (Dotan *et al.* 2016) using bio-affinity-functionalized carbon-walled nanotubes targeted

with either antibodies against TSHR or rhTSH. Such nanotubes are designed to convert electromagnetic energy to thermal energy, and thus, deliver a cytotoxic local thermal load when stimulated by an external near-infrared light source. *In vitro* data demonstrated specific cytotoxicity against TSHR-expressing cells from infrared-stimulated nanotubes targeted using two commercially available antibodies against TSHR compared to controls, with similar findings using TSH and rhTSH as targeting ligands. Targeting using rhTSH and TSH resulted in greater cytotoxicity than targeting using TSHR antibody. Although this study again provides *in vitro* evidence for TSHR as a specific theranostic target for thyrocytes, it is unique in suggesting a further method of localizing cytotoxicity using an external infrared light source. This additional external 'targeting' may eliminate off-target cytotoxicity that may be conferred from cytotoxic laden nanoliposomes through non-specific binding, clearance of liposomes in the reticulo-endothelial system or low-density binding to non-thyroidal TSHR.

Small-molecule antagonists of TSHR

Currently, inhibition of TSHR-mediated growth signaling is achieved by pharmacologic suppression of endogenous TSH, with resultant systemic hyperthyroidism. A better system would be a pharmacological antagonist of TSHR, permitting inhibition of thyroid cancer growth while avoiding systemic side effects that limit current widespread use of pharmacologically induced hyperthyroidism. Such small-molecule antagonists of TSHR have significant parallel interest in the treatment of Graves' disease, where stimulatory autoantibodies against TSHR induce marked hyperthyroidism. Davies and Latif (2015), in their recent appraisal of this issue, identify several molecules that have been trialed over the last decade. To date, however, no molecule has been able to achieve sufficient specificity *in vivo* to substantially inhibit TSHR signaling (inhibition of cAMP production in orbital fibroblasts was 50% in one study (Neumann *et al.* 2012)).

Areas for future research

The described advances suggest a future horizon of targeted therapies for thyroid cancer, where a patient's individual tumor characteristics, such as the surface expression of proteins, can be exploited for selective drug delivery. However, there remain significant obstacles to final clinical translation of these targeted therapies. Additionally, there are several fundamental questions regarding TSHR

targeting in metastatic DTC that remain unanswered. Firstly, although evidence for TSHR expression on DTC metastases is compelling, it is largely indirect. The density of TSHR expression on metastatic lesions is not well studied, and whether TSHR expression would be sufficient for binding of targeted ligands is not known. Secondly, although *TSHR* mRNA and TSHR protein have been detected in a variety of tissues, our knowledge of the functional significance of these extrathyroidal TSHR is still in its infancy. Indeed, the density of TSHR expression, and whether non-thyroidal TSHR would bind TSHR-targeted therapies in any significant quantity, would need to be carefully studied, especially in the setting of delivery of cytotoxic therapies. Finally, although there is much interest in redifferentiation therapies for thyroid cancer metastases to upregulate NIS expression, little is known about whether TSHR expression could be upregulated in DTC in a similar manner, and whether such therapies may enhance current or future treatments.

Conclusions

Although our understanding of the role of the TSHR as a target in thyroid cancer has progressed significantly since the astute clinical observations of the effects of levothyroxine on PTC in the 1930s, our therapeutic abilities to manipulate this system are largely unchanged over several decades. The era of personalized medicine and targeted therapy has cast new light on the TSHR as a potential theranostic target in metastatic DTC. Although promising advances have been made in the last decade, the TSHR invites further study and the possibility of new treatment paradigms for metastatic, radioiodine-resistant DTC.

Declaration of interest

The authors declare that there is no conflict of interest that could be perceived as prejudicing the impartiality of this review.

Funding

This research was supported by a Hunter New England Local Health District Clinical Research Fellowship, and an AVANT Clinical Research Scholarship (to C R).

References

- Abe E, Marians RC, Yu W, Wu X-B, Ando T, Li Y, Iqbal J, Eldeiry L, Rajendren G, Blair HC, et al. 2003 TSH is a negative regulator of skeletal remodeling. *Cell* **115** 151–162. (doi:10.1016/S0092-8674(03)00771-2)

- Aghajanova L, Stavreus-Evers A, Lindeberg M, Landgren B-M, Sparre LS & Hovatta O 2011 Thyroid-stimulating hormone receptor and thyroid hormone receptors are involved in human endometrial physiology. *Fertility and Sterility* **95** 230–237.e232.
- Arturi F, Russo D, Giuffrida D, Ippolito A, Perrotti N, Vigneri R & Filetti S 1997 Early diagnosis by genetic analysis of differentiated thyroid cancer metastases in small lymph nodes. *Journal of Clinical Endocrinology and Metabolism* **82** 1638–1641. (doi:10.1210/jcem.82.5.4062)
- Bahn RS, Dutton CM, Natt N, Joba W, Spitzweg C & Heufelder AE 1998 Thyrotropin receptor expression in Graves' orbital adipose/connective tissues: potential autoantigen in Graves' ophthalmopathy. *Journal of Clinical Endocrinology and Metabolism* **83** 998–1002. (doi:10.1210/jc.83.3.998)
- Balzan S, Nicolini G, Forini F, Boni G, Del Carratore R, Nicolini A, Carpi A & Iervasi G 2007 Presence of a functional TSH receptor on human erythrocytes. *Biomedical Pharmacotherapy* **61** 463–467. (doi:10.1016/j.biopha.2007.04.009)
- Bassett JH & Williams GR 2016 Role of thyroid hormones in skeletal development and bone maintenance. *Endocrine Reviews* **37** 135–187. (doi:10.1210/er.2015-1106)
- Beck-Peccoz P, Persani L, Mannavola D & Campi I 2009 Pituitary tumours: TSH-secreting adenomas. *Best Practice Research in Clinical Endocrinology and Metabolism* **23** 597–606. (doi:10.1016/j.beem.2009.05.006)
- Belfiore A, Garofalo MR, Giuffrida D, Runello F, Filetti S, Fiumara A, Ippolito O & Vigneri R 1990 Increased aggressiveness of thyroid cancer in patients with Graves' disease. *Journal of Clinical Endocrinology and Metabolism* **70** 830–835. (doi:10.1210/jcem-70-4-830)
- Bell A, Gagnon A, Grunder L, Parikh SJ, Smith TJ & Sorisky A 2000 Functional TSH receptor in human abdominal preadipocytes and orbital fibroblasts. *American Journal of Physiology* **279** C335–C340.
- Bodo E, Kromminga A, Biro T, Borbiro I, Gaspar E, Zmijewski MA, Van Beek N, Langbein L, Slominski AT & Paus R 2009 Human female hair follicles are a direct, nonclassical target for thyroid-stimulating hormone. *Journal of Investigative Dermatology* **129** 1126–1139. (doi:10.1038/jid.2008.361)
- Brabant G, Maenhaut C, Köhrle J, Scheumann G, Dralle H, Hoang-Vu C, Hesch RD, Von Zur Mühlen A, Vassart G & Dumont JE 1991 Human thyrotropin receptor gene: expression in thyroid tumors and correlation to markers of thyroid differentiation and dedifferentiation. *Molecular and Cellular Endocrinology* **82** R7–R12. (doi:10.1016/0303-7207(91)90018-N)
- Bruno R, Ferretti E, Tosi E, Arturi F, Giannasio P, Mattei T, Scipioni A, Presta I, Morisi R, Gulino A, et al. 2005 Modulation of thyroid-specific gene expression in normal and nodular human thyroid tissues from adults: an in vivo effect of thyrotropin. *Journal of Clinical Endocrinology and Metabolism* **90** 5692–5697. (doi:10.1210/jc.2005-0800)
- Carayon P, Thomas-Morvan C, Castanas E & Tubiana M 1980 Human thyroid cancer: membrane thyrotropin binding and adenylate cyclase activity. *Journal of Clinical Endocrinology and Metabolism* **51** 915–920. (doi:10.1210/jcem-51-4-915)
- Chabaud O & Lissitzky S 1977 Thyrotropin-specific binding to human peripheral blood monocytes and polymorphonuclear leukocytes. *Molecular and Cellular Endocrinology* **7** 79–87. (doi:10.1016/0303-7207(77)90077-6)
- Clark OH, Gerend PL, Goretzki P & Nissenson RA 1983 Characterization of the thyrotropin receptor-adenylate cyclase system in neoplastic human thyroid tissue. *Journal of Clinical Endocrinology and Metabolism* **57** 140–147. (doi:10.1210/jcem-57-1-140)
- Cooper DS, Specker B, Ho M, Sperling M, Ladenson PW, Ross DS, Ain KB, Bigos ST, Brierley JD, Haugen BR, et al. 1998 Thyrotropin suppression and disease progression in patients with differentiated thyroid cancer: results from the National Thyroid Cancer Treatment

- Cooperative Registry. *Thyroid* **8** 737–744. (doi:10.1089/thy.1998.8.737)
- Corsetti E, Chianelli M, Cornelissen B, Van De Wiele C, D'alessandria C, Slegers G, Mather SJ, Di Mario U, Filetti S, Scopinaro F, et al. 2004 Radioiodinated recombinant human TSH: a novel radiopharmaceutical for thyroid cancer metastases detection. *Cancer Biotherapy and Radiopharmaceuticals* **19** 57–63. (doi:10.1089/108497804773391685)
- Coutelier JP, Kehrl JH, Bellur SS, Kohn LD, Notkins AL & Prabhakar BS 1990 Binding and functional effects of thyroid stimulating hormone on human immune cells. *Journal of Clinical Immunology* **10** 204–210. (doi:10.1007/bf00918653)
- D'agostino M, Sponziello M, Puppini C, Celano M, Maggiasano V, Baldan F, Biffoni M, Bulotta S, Durante C, Filetti S, et al. 2014 Different expression of TSH receptor and NIS genes in thyroid cancer: role of epigenetics. *Journal of Molecular Endocrinology* **52** 121–131. (doi:10.1530/jme-13-0160)
- Davies T, Marians R & Latif R 2002 The TSH receptor reveals itself. *Journal of Clinical Investigation* **110** 161–164. (doi:10.1172/JCI0216234)
- Davies TF, Ando T, Lin RY, Tomer Y & Latif R 2005 Thyrotropin receptor-associated diseases: from adenomata to Graves disease. *Journal of Clinical Investigation* **115** 1972–1983. (doi:10.1172/JCI26031)
- Davies TF & Latif R 2015 Targeting the thyroid-stimulating hormone receptor with small molecule ligands and antibodies. *Expert Opinion on Therapeutic Targets* **19** 835–847. (doi:10.1517/14728222.2015.1018181)
- Dohán O, Vieja ADL, Paroder V, Riedel C, Artani M, Reed M, Ginter CS & Carrasco N 2003 The sodium/iodide symporter (NIS): characterization, regulation, and medical significance. *Endocrine Reviews* **24** 48–77. (doi:10.1210/er.2001-0029)
- Dotan I, Roche PJ, Paliouras M, Mitmaker EJ & Trifiro MA 2016 Engineering multi-walled carbon nanotube therapeutic bionanofluids to selectively target papillary thyroid cancer cells. *PLoS ONE* **11** e0149723. (doi:10.1371/journal.pone.0149723)
- Dunhill T 1937 The Lettsomian lectures. The surgery of the thyroid gland. *Transactions of the Medical Society of London* **60** 234–282.
- Dutton CM, Joba W, Spitzweg C, Heufelder AE & Bahn RS 1997 Thyrotropin receptor expression in adrenal, kidney, and thymus. *Thyroid* **7** 879–884.
- Edmonds CJ, Hayes S, Kermode JC & Thompson BD 1977 Measurement of serum TSH and thyroid hormones in the management of treatment of thyroid carcinoma with radioiodine. *British Journal of Radiology* **50** 799–807. (doi:10.1259/0007-1285-50-599-799)
- Elisei R, Pinchera A, Romei C, Gryczynska M, Pohl V, Maenhaut C, Fugazzola L & Pacini F 1994 Expression of thyrotropin receptor (TSH-R), thyroglobulin, thyroperoxidase, and calcitonin messenger ribonucleic acids in thyroid carcinomas: evidence of TSH-R gene transcript in medullary histotype. *Journal of Clinical Endocrinology and Metabolism* **78** 867–871. (doi:10.1210/jc.78.4.867)
- Fallahi B, Beiki D, Takavar A, Fard-Esfahani A, Gilani KA, Saghari M & Eftekhari M 2012 Low versus high radioiodine dose in postoperative ablation of residual thyroid tissue in patients with differentiated thyroid carcinoma: a large randomized clinical trial. *Nuclear Medicine Communications* **33** 275–282. (doi:10.1097/MNM.0b013e32834e306a)
- Filetti S, Bidart JM, Arturi F, Caillou B, Russo D & Schlumberger M 1999 Sodium/iodide symporter: a key transport system in thyroid cancer cell metabolism. *European Journal of Endocrinology* **141** 443–457. (doi:10.1530/eje.0.1410443)
- Fiore E, Rago T, Provenzale MA, Scutari M, Ugolini C, Basolo F, Di Coscio G, Berti P, Grasso L, Elisei R, et al. 2009 Lower levels of TSH are associated with a lower risk of papillary thyroid cancer in patients with thyroid nodular disease: thyroid autonomy may play a protective role. *Endocrine-Related Cancer* **16** 1251–1260. (doi:10.1677/ERC-09-0036)
- Franco AT, Malaguamera R, Refetoff S, Liao X-H, Lundsmith E, Kimura S, Pritchard C, Marais R, Davies TF, Weinstein LS, et al. 2011 Thyrotropin receptor signaling dependence of Braf-induced thyroid tumor initiation in mice. *PNAS* **108** 1615–1620. (doi:10.1073/pnas.1015557108)
- Gagnon A, Langille ML, Chaker S, Antunes TT, Durand J & Sorisky A 2014 TSH signaling pathways that regulate MCP-1 in human differentiated adipocytes. *Metabolism* **63** 812–821. (doi:10.1016/j.metabol.2014.02.015)
- Galli F, Manni I, Piaggio G, Balogh L, Weintraub BD, Szkudlinski MW, Fremont V, Dierckx RA & Signore A 2014 (99m)Tc-labeled-rhTSH analogue (TR1401) for imaging poorly differentiated metastatic thyroid cancer. *Thyroid* **24** 1297–1308. (doi:10.1089/thy.2013.0429)
- Gao X-J, Li A-Q, Zhang X, Liu P, Wang J-R & Cai X 2015 Thyroid-stimulating hormone (TSH)-armed polymer-lipid nanoparticles for the targeted delivery of cisplatin in thyroid cancers: therapeutic efficacy evaluation. *Royal Society of Chemistry Advances* **5** 106413–106420. (doi:10.1039/c5ra12588j)
- Gagnon A, Langille ML, Chaker S, Antunes TT, Durand J & Sorisky A 2014 TSH signaling pathways that regulate MCP-1 in human differentiated adipocytes. *Metabolism* **63** 812–821. (doi:10.1016/j.metabol.2014.02.015)
- Gerard AC, Daumerie C, Mestdagh C, Gohy S, De Burbure C, Costagliola S, Miot F, Nollevaux MC, Deneff JF, Rahier J, et al. 2003 Correlation between the loss of thyroglobulin iodination and the expression of thyroid-specific proteins involved in iodine metabolism in thyroid carcinomas. *Journal of Clinical Endocrinology and Metabolism* **88** 4977–4983. (doi:10.1210/jc.2003-030586)
- Giani F, Vella V, Nicolosi ML, Fierabracci A, Lotta S, Malaguamera R, Belfiore A, Vigneri R & Frasca F 2015 Thyrospheres from normal or malignant thyroid tissue have different biological, functional, and genetic features. *Journal of Clinical Endocrinology and Metabolism* **100** E1168–E1178. (doi:10.1210/jc.2014.4163)
- Haugen BR, Alexander EK, Bible KC, Doherty GM, Mandel SJ, Nikiforov YE, Pacini F, Randolph GW, Sawka AM, Schlumberger M, et al. 2016 2015 American Thyroid Association Management guidelines for adult patients with thyroid nodules and differentiated thyroid cancer: the American Thyroid Association guidelines task force on thyroid nodules and differentiated thyroid cancer. *Thyroid* **26** 1–133. (doi:10.1089/thy.2015.0020)
- Hegedus L, Hansen J & Karstrup S 1983 High incidence of normal thyroid gland volume in patients with Graves' disease. *Clinical Endocrinology* **19** 603–607. (doi:10.1111/j.1365-2265.1983.tb00037.x)
- Hoang-Vu C, Dralle H, Scheumann G, Maenhaut C, Horn R, Von Zur Muhlen A & Brabant G 1992 Gene expression of differentiation- and dedifferentiation markers in normal and malignant human thyroid tissues. *Experimental and Clinical Endocrinology* **100** 51–56. (doi:10.1055/s-0029-1211176)
- Hurley JR 2011 Historical note: TSH suppression for thyroid cancer. *Thyroid* **21** 1175–1176. (doi:10.1089/thy.2011.2111.com)
- Ichikawa Y, Saito E, Abe Y, Homma M & Muraki T 1976 Presence of TSH receptor in thyroid neoplasms. *Journal of Clinical Endocrinology and Metabolism* **42** 395–398. (doi:10.1210/jcem-42-2-395)
- Jarab B, Handkiewicz-Junak D, Roskosz J, Puch Z, Wygoda Z, Kukulska A, Jurecka-Lubieniecka B, Hasse-Lazar K, Turska M & Zajusz A 2003 Recombinant human TSH-aided radioiodine treatment of advanced differentiated thyroid carcinoma: a single-centre study of 54 patients. *European Journal of Nuclear Medicine and Molecular Imaging* **30** 1077–1086. (doi:10.1007/s00259-003-1190-5)
- Jonklaas J, Sarlis NJ, Litofsky D, Ain KB, Bigos ST, Brierley JD, Cooper DS, Haugen BR, Ladenson PW, Magner J, et al. 2006 Outcomes of patients with differentiated thyroid carcinoma following initial therapy. *Thyroid* **16** 1229–1242. (doi:10.1089/thy.2006.16.1229)
- Kim YH, Choi YW, Han JH, Lee J, Soh EY, Park SH, Kim J-H & Park TJ 2014 TSH Signaling overcomes B-RafV600E-induced senescence in papillary thyroid carcinogenesis through regulation of DUSP6. *Neoplasia* **16** 1107–1120. (doi:10.1016/j.neo.2014.10.005)
- Kimura T, Van Keymeulen A, Golstein J, Fusco A, Dumont JE & Roger PP 2001 Regulation of thyroid cell proliferation by TSH and other

- factors: a critical evaluation of in vitro models. *Endocrine Reviews* **22** 631–656. (doi:10.1210/edrv.22.5.0444)
- Lazar V, Bidart JM, Caillou B, Mahe C, Lacroix L, Filetti S & Schlumberger M 1999 Expression of the Na⁺/I⁻ symporter gene in human thyroid tumors: a comparison study with other thyroid-specific genes. *Journal of Clinical Endocrinology and Metabolism* **84** 3228–3234. (doi:10.1210/jc.84.9.3228)
- Leboulleux S, Schroeder PR, Busaidy NL, Auperin A, Corone C, Jacene HA, Ewertz ME, Bournaud C, Wahl RL, Sherman SI, et al. 2009 Assessment of the incremental value of recombinant thyrotropin stimulation before 2-[18F]-Fluoro-2-deoxy-D-glucose positron emission tomography/computed tomography imaging to localize residual differentiated thyroid cancer. *Journal of Clinical Endocrinology and Metabolism* **94** 1310–1316. (doi:10.1210/jc.2008-1747)
- Lin JD, Fu SS, Chen JY, Lee CH, Chau WK, Cheng CW, Wang YH, Lin YF, Fang WF & Tang KT 2016 Clinical manifestations and gene expression in patients with conventional papillary thyroid carcinoma carrying the BRAF(V600E) mutation and BRAF pseudogene. *Thyroid* **26** 691–704. (doi:10.1089/thy.2015.0044)
- Lippi F, Capezzone M, Angelini F, Taddei D, Molinaro E, Pinchera A & Pacini F 2001 Radioiodine treatment of metastatic differentiated thyroid cancer in patients on L-thyroxine, using recombinant human TSH. *European Journal of Endocrinology* **144** 5–11. (doi:10.1530/eje.0.1440005)
- Liu TR, Su X, Qiu WS, Chen WC, Men QQ, Zou L, Li ZQ, Fu XY & Yang AK 2016 Thyroid-stimulating hormone receptor affects metastasis and prognosis in papillary thyroid carcinoma. *European Review for Medical and Pharmacological Science* **20** 3582–3591.
- Lu C, Zhao L, Ying H, Willingham MC & Cheng SY 2010 Growth activation alone is not sufficient to cause metastatic thyroid cancer in a mouse model of follicular thyroid carcinoma. *Endocrinology* **151** 1929–1939. (doi:10.1210/en.2009-1017)
- Luster M, Lassmann M, Haenschel H, Michalowski U, Incerti C & Reiners C 2000 Use of recombinant human thyrotropin before radioiodine therapy in patients with advanced differentiated thyroid carcinoma. *Journal of Clinical Endocrinology and Metabolism* **85** 3640–3645. (doi:10.1210/jcem.85.10.6903)
- Luster M, Lippi F, Jarzab B, Perros P, Lassmann M, Reiners C & Pacini F 2005 rhTSH-aided radioiodine ablation and treatment of differentiated thyroid carcinoma: a comprehensive review. *Endocrine-Related Cancer* **12** 49–64. (doi:10.1677/erc.1.00830)
- Ma R, Morshed S, Latif R, Zaidi M & Davies TF 2011 The influence of thyroid-stimulating hormone and thyroid-stimulating hormone receptor antibodies on osteoclastogenesis. *Thyroid* **21** 897–906. (doi:10.1089/thy.2010.0457)
- Maenhaut C, Brabant G, Vassart G & Dumont JE 1992 In vitro and in vivo regulation of thyrotropin receptor mRNA levels in dog and human thyroid cells. *Journal of Biological Chemistry* **267** 3000–3007.
- Malaguarnera R, Frasca F, Garozzo A, Giani F, Pandini G, Vella V, Vigneri R & Belfiore A 2011 Insulin receptor isoforms and insulin-like growth factor receptor in human follicular cell precursors from papillary thyroid cancer and normal thyroid. *Journal of Clinical Endocrinology and Metabolism* **96** 766–774. (doi:10.1210/jc.2010-1255)
- Matsumoto H, Sakamoto A, Fujiwara M, Yano Y, Shishido-Hara Y, Fujioka Y & Kamma H 2008 Decreased expression of the thyroid-stimulating hormone receptor in poorly-differentiated carcinoma of the thyroid. *Oncology Reports* **19** 1405–1411. (doi:10.3892/ijmm.2012.1173)
- Mazzaferri EL & Jhiang SM 1994 Long-term impact of initial surgical and medical therapy on papillary and follicular thyroid cancer. *American Journal of Medicine* **97** 418–428. (doi:10.1016/0002-9343(94)90321-2)
- McGriff NJ, Csako G, Gourgoutis L, Lori CG, Pucino F & Sarlis NJ 2002 Effects of thyroid hormone suppression therapy on adverse clinical outcomes in thyroid cancer. *Annals of Medicine* **34** 554–564. (doi:10.1080/088538902321117760)
- Meireles AM, Preto A, Rocha AS, Rebocho AP, Maximo V, Pereira-Castro I, Moreira S, Feijao T, Botelho T, Marques R, et al. 2007 Molecular and genotypic characterization of human thyroid follicular cell carcinoma-derived cell lines. *Thyroid* **17** 707–715. (doi:10.1089/thy.2007.0097)
- Morris JC 1997 Structure and function of the TSH receptor: its suitability as a target for radiotherapy. *Thyroid* **7** 253–258. (doi:10.1089/thy.1997.7.253)
- Morshed SA, Latif R & Davies TF 2009 Characterization of thyrotropin receptor antibody-induced signaling cascades. *Endocrinology* **150** 519–529. (doi:10.1210/en.2008-0878)
- Murakami M, Hosoi Y, Negishi T, Kamiya Y, Miyashita K, Yamada M, Iriuchijima T, Yokoo H, Yoshida I, Tushima Y, et al. 1996 Thymic hyperplasia in patients with Graves' disease. Identification of thyrotropin receptors in human thymus. *Journal of Clinical Investigation* **98** 2228–2234. (doi:10.1172/jci119032)
- Murakami M, Kamiya Y, Morimura T, Araki O, Imamura M, Ogiwara T, Mizuma H & Mori M 2001 Thyrotropin receptors in brown adipose tissue: thyrotropin stimulates type II iodothyronine deiodinase and uncoupling protein-1 in brown adipocytes. *Endocrinology* **142** 1195–1201. (doi:10.1210/en.142.3.1195)
- Neumann S, Pope A, Geras-Raaka E, Raaka BM, Bahn RS & Gershengorn MC 2012 A drug-like antagonist inhibits thyrotropin receptor-mediated stimulation of cAMP production in Graves' orbital fibroblasts. *Thyroid* **22** 839–843. (doi:10.1089/thy.2011.0520)
- Nieto HR & Boelaert K 2016 Thyroid stimulating hormone in thyroid cancer: does it matter? *Endocrine-Related Cancer* **23** T109–T121. (doi:10.1530/ERC-16-0328)
- Ohta K, Endo T & Onaya T 1991 The mRNA levels of thyrotropin receptor, thyroglobulin and thyroid peroxidase in neoplastic human thyroid tissues. *Biochemical and Biophysical Research Communications* **174** 1148–1153. (doi:10.1016/0006-291X(91)91540-S)
- Paolino D, Cosco D, Gaspari M, Celano M, Wolfram J, Voce P, Puxeddu E, Filetti S, Celia C, Ferrari M, et al. 2014 Targeting the thyroid gland with thyroid-stimulating hormone (TSH)-nanoliposomes. *Biomaterials* **35** 7101–7109. (doi:10.1016/j.biomaterials.2014.04.088)
- Park HJ, Kim JY, Park KY, Gong G, Hong SJ & Ahn IM 2000 Expressions of human sodium iodide symporter mRNA in primary and metastatic papillary thyroid carcinomas. *Thyroid* **10** 211–217. (doi:10.1089/thy.2000.10.211)
- Parmentier M, Libert F, Maenhaut C, Lefort A, Gerard C, Perret J, Van Sande J, Dumont JE & Vassart G 1989 Molecular cloning of the thyrotropin receptor. *Science* **246** 1620–1622. (doi:10.1126/science.2556796)
- Pellegriti G, Mannarino C, Russo M, Terranova R, Marturano I, Vigneri R & Belfiore A 2013 Increased mortality in patients with differentiated thyroid cancer associated with Graves' disease. *Journal of Clinical Endocrinology and Metabolism* **98** 1014–1021. (doi:10.1210/jc.2012-2843)
- Pilli T, Prasad KV, Jayarama S, Pacini F & Prabhakar BS 2009 Potential utility and limitations of thyroid cancer cell lines as models for studying thyroid cancer. *Thyroid* **19** 1333–1342. (doi:10.1089/thy.2009.0195)
- Prummel MF, Brokken LJ, Meduri G, Misrahi M, Bakker O & Wiersinga WM 2000 Expression of the thyroid-stimulating hormone receptor in the folliculo-stellate cells of the human anterior pituitary. *Journal of Clinical Endocrinology and Metabolism* **85** 4347–4353. (doi:10.1210/jc.85.11.4347)
- Pujol P, Dares JP, Nsakala N, Baldet L, Bringer J & Jaffiol C 1996 Degree of thyrotropin suppression as a prognostic determinant in differentiated thyroid cancer. *Journal of Clinical Endocrinology and Metabolism* **81** 4318–4323. (doi:10.1210/jc.81.12.4318)
- Rapoport B & McLachlan SM 2016 TSH receptor cleavage into subunits and shedding of the A-Subunit; a molecular and clinical perspective. *Endocrine Reviews* **37** 114–134. (doi:10.1210/er.2015-1098)

- Rees Smith B, McLachlan SM & Furmaniak J 1988 Autoantibodies to the thyrotropin receptor. *Endocrine Reviews* **9** 106–121. (doi:10.1210/edrv-9-1-106)
- Roger P, Taton M, Van Sande J & Dumont J 1988 Mitogenic effects of thyrotropin and adenosine 3',5'-monophosphate in differentiated normal human thyroid cells in vitro. *Journal of Clinical Endocrinology and Metabolism* **66** 1158–1165. (doi:10.1210/jcem-66-6-1158)
- Saito T, Endo T, Kawaguchi A, Ikeda M, Nakazato M, Kogai T & Onaya T 1997 Increased expression of the Na⁺/I⁻ symporter in cultured human thyroid cells exposed to thyrotropin and in Graves' thyroid tissue. *Journal of Clinical Endocrinology and Metabolism* **82** 3331–3336. (doi:10.1210/endo.138.2.4918)
- Schuppert F, Deiters S, Rambusch E, Sierralta W, Dralle H & Von Zur Muhlen A 1996 TSH-receptor expression and human thyroid disease: relation to clinical, endocrine, and molecular thyroid parameters. *Thyroid* **6** 575–587. (doi:10.1089/thy.1996.6.575)
- Sciuto R, Romano L, Rea S, Marandino F, Sperduti I & Maini CL 2009 Natural history and clinical outcome of differentiated thyroid carcinoma: a retrospective analysis of 1503 patients treated at a single institution. *Annals of Oncology* **20** 1728–1735. (doi:10.1093/annonc/mdp050)
- Sellitti DF, Akamizu T, Doi SQ, Kim GH, Kariyil JT, Kopchik JJ & Koshiyama H 2000 Renal expression of two 'thyroid-specific' genes: thyrotropin receptor and thyroglobulin. *Experimental Nephrology* **8** 235–243. (doi:10.1159/000020674)
- Sercombe L, Veerati T, Moheimani F, Wu SY, Sood AK & Hua S 2015 Advances and challenges of liposome assisted drug delivery. *Frontiers in Pharmacology* **6** 286. (doi:10.3389/fphar.2015.00286)
- Sheils OM & Sweeney EC 1999 TSH receptor status of thyroid neoplasms – TaqMan RT-PCR analysis of archival material. *Journal of Pathology* **188** 87–92. (doi:10.1002/(SICI)1096-9896(199905)188:1<87::AID-PATH322>3.0.CO;2-5)
- Shi Y, Zou M & Farid NR 1993 Expression of thyrotrophin receptor gene in thyroid carcinoma is associated with a good prognosis. *Clinical Endocrinology* **39** 269–274. (doi:10.1111/j.1365-2265.1993.tb02365.x)
- Smith TJ 2015 TSH-receptor-expressing fibrocytes and thyroid-associated ophthalmopathy. *Nature Reviews Endocrinology* **11** 171–181. (doi:10.1038/nrendo.2014.226)
- So YK, Son YI, Baek CH, Jeong HS, Chung MK & Ko YH 2012 Expression of sodium-iodide symporter and TSH receptor in subclinical metastatic lymph nodes of papillary thyroid microcarcinoma. *Annals of Surgical Oncology* **19** 990–995. (doi:10.1245/s10434-011-2047-y)
- Tanaka K, Inoue H, Miki H, Masuda E, Kitaichi M, Komaki K, Uyama T & Monden Y 1997 Relationship between prognostic score and thyrotropin receptor (TSH-R) in papillary thyroid carcinoma: immunohistochemical detection of TSH-R. *British Journal of Cancer* **76** 594–599. (doi:10.1038/bjc.1997.431)
- Tanaka K, Otsuki T, Sonoo H, Yamamoto Y, Udagawa K, Kunisue H, Arime I, Yamamoto S, Kurebayashi J & Shimozuma K 2000 Semi-quantitative comparison of the differentiation markers and sodium iodide symporter messenger ribonucleic acids in papillary thyroid carcinomas using RT-PCR. *European Journal of Endocrinology* **142** 340–346. (doi:10.1530/eje.0.1420340)
- Theodoropoulou M, Arzberger T, Gruebler Y, Korali Z, Mortini P, Joba W, Heufelder A, Stalla G & Schaaf L 2000 Thyrotrophin receptor protein expression in normal and adenomatous human pituitary. *Journal of Endocrinology* **167** 7–13. (doi:10.1677/joe.0.1670007)
- Tian L, Ni J, Guo T, Liu J, Dang Y, Guo Q & Zhang L 2014 TSH stimulates the proliferation of vascular smooth muscle cells. *Endocrine* **46** 651–658. (doi:10.1007/s12020-013-0135-4)
- Valyasevi RW, Erickson DZ, Harteneck DA, Dutton CM, Heufelder AE, Jyonouchi SC & Bahn RS 1999 Differentiation of human orbital preadipocyte fibroblasts induces expression of functional thyrotropin receptor. *Journal of Clinical Endocrinology and Metabolism* **84** 2557–2562. (doi:10.1210/jc.84.7.2557)
- Van Staveren WCG, Solís DW, Delys L, Duprez L, Andry G, Franc B, Thomas G, Libert F, Dumont JE, Detours V, et al. 2007 Human thyroid tumor cell lines derived from different tumor types present a common dedifferentiated phenotype. *Cancer Research* **67** 8113–8120. (doi:10.1158/0008-5472.CAN-06-4026)
- Vassart G & Dumont JE 1992 The thyrotropin receptor and the regulation of thyrocyte function and growth. *Endocrine Reviews* **13** 596–611. (doi:10.1210/er.13.3.596)
- Wang ZF, Liu QJ, Liao SQ, Yang R, Ge T, He X, Tian CP & Liu W 2011 Expression and correlation of sodium/iodide symporter and thyroid stimulating hormone receptor in human thyroid carcinoma. *Tumori* **97** 540–546. (doi:10.1700/950.10410)
- Williams GR 2011 Extrathyroidal expression of TSH receptor. *Annals of Endocrinology* **72** 68–73. (doi:10.1016/j.ando.2011.03.006)
- Williams D & Wynford-Thomas D 1997 Human thyroid epithelial cells. In *Methods in Molecular Biology*. Totowa, NJ, USA: Humana Press, Inc.
- Zhang W, Tian LM, Han Y, Ma HY, Wang LC, Guo J, Gao L & Zhao JJ 2009 Presence of thyrotropin receptor in hepatocytes: not a case of illegitimate transcription. *Journal of Cellular and Molecular Medicine* **13** 4636–4642. (doi:10.1111/j.1582-4934.2008.00670.x)
- Zielke A, Tezelman S, Jossart GH, Wong M, Siperstein AE, Duh QY & Clark OH 1998 Establishment of a highly differentiated thyroid cancer cell line of Hurthle cell origin. *Thyroid* **8** 475–483. (doi:10.1089/thy.1998.8.475)

Received in final form 14 March 2017

Accepted 28 March 2017

Accepted Preprint published online 28 March 2017

8 GENERAL DISCUSSION

8.1 Introduction

This thesis set out to examine whether thyroid cancers are innervated, to determine the relationship between innervation, proNGF and its receptors in thyroid cancer, and to assess whether proNGF was a discriminatory biomarker of thyroid malignancy.

The key finding of this research, that nerve density is increased in thyroid cancer, is concordant with a large body of data from other malignancies demonstrating that nerves are present in the microenvironment of many solid organ malignancies, and are contributory to oncogenesis. As with any novel findings, it is important that these data are confirmed in large independent cohorts, and followed by functional studies to examine mechanisms of cross-talk between nerves and the cancer micro-environment that may lead to deeper understanding of cancer biology, and targeted therapies.

However, there are several clinically-translatable testable hypotheses that emerge from these data, and could be explored first in animal, then in human studies. Figure 11 provides a conceptual overview, which is further discussed in the following sections.

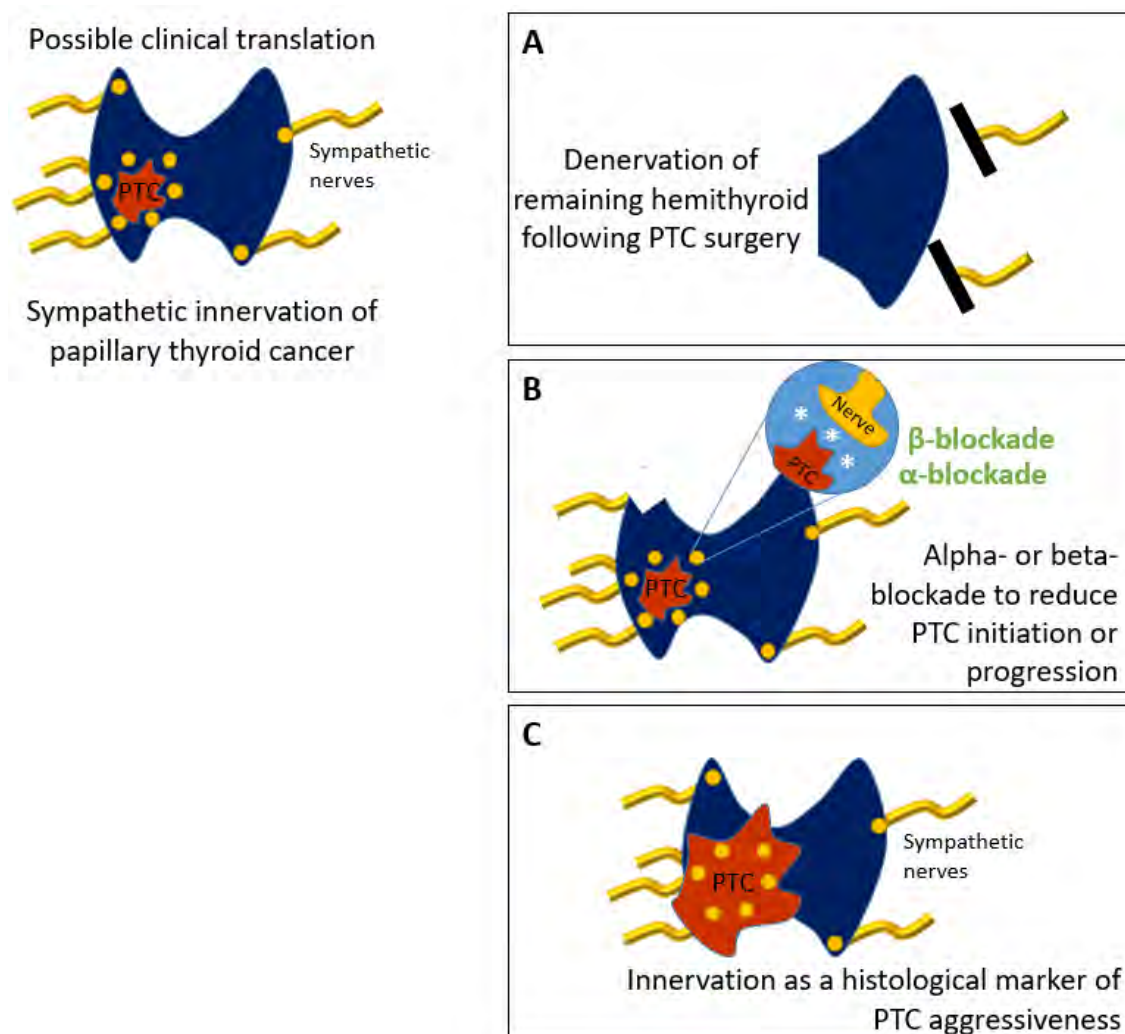


Figure 11: Future clinical translation of innervation of papillary thyroid cancer.

8.2 Thyroid autonomic denervation

Studies are required to examine whether autonomic denervation of the thyroid is able to reduce the development of papillary thyroid cancer in at-risk glands (Figure 11A). This is particularly translationally relevant due to the current clinical paradigm of selective hemithyroidectomy for thyroid cancer,⁸ which leaves a remaining unaffected hemithyroid that is at increased risk of development of a second thyroid cancer (Figure 11A). In fact, recent studies have confirmed that the most frequent site of recurrence of papillary thyroid carcinoma following hemithyroidectomy is in the contralateral lobe. For example, in patients who have undergone hemithyroidectomy for small PTC (mean size 0.8 ± 0.6 cm) and are followed for 5 years, over 70% of 'recurrences' of thyroid cancer occur in the contralateral lobe, rather than with local or distant metastases.^{86,87} Whether denervation of the remaining hemithyroid at the time of partial thyroidectomy

for cancer reduces the subsequent development of second thyroid malignancies should be tested.

Available evidence suggests that denervation of the thyroid gland may be a well-tolerated procedure. As reviewed in Chapter 2, thyroid autonomic innervation has a minor role in secretion of thyroid hormone, when compared to the dominant role of endocrine regulation that occurs through TSH (for example, see Figure 2). Therefore, interrupting the autonomic supply to the thyroid may have oncologic benefits, without materially affecting the physiological gland function, thereby minimising patient morbidity. Further, given the separate anatomical pathways for adrenergic and cholinergic innervation (see Figure 4), selective denervation targeting either the adrenergic or cholinergic nerves could be performed.

Autonomic denervation can be achieved through surgical ligation, however minimally invasive techniques have been developed to target sympathetic nerve plexus that travels on the external arterial surface to reach target organs (Figure 4). For example, selective sympathetic denervation of the renal arteries can be performed using devices with regulatory approval in clinical practice, such as an endovascular technique, with an acceptable safety profile (Figure 12).

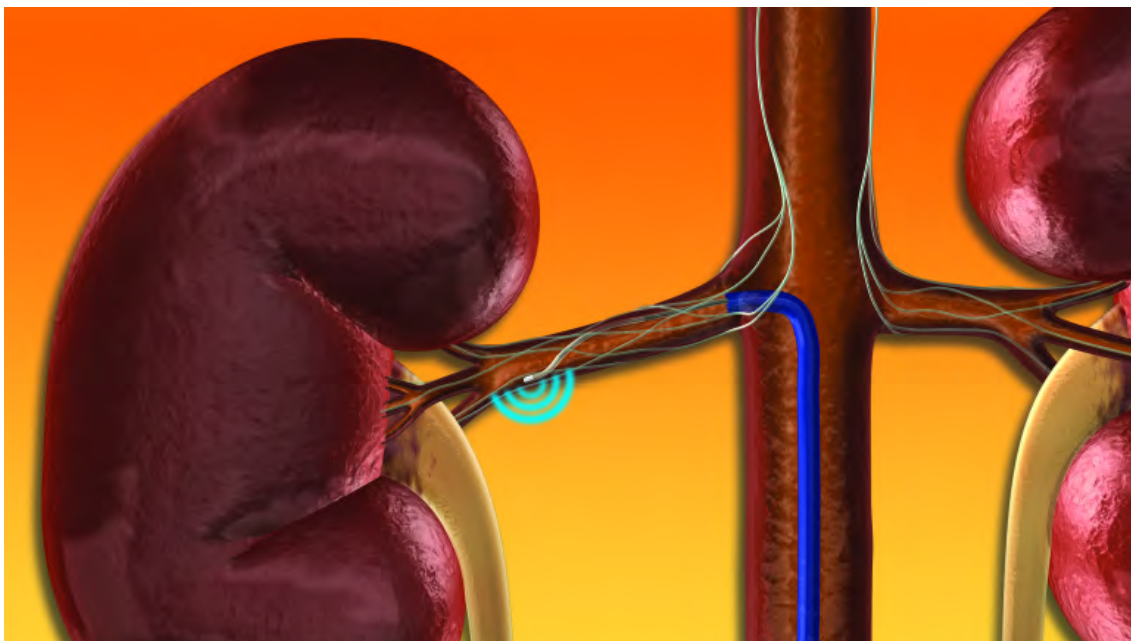


Figure 12: Schematic drawing of endovascular catheter-based device for sympathetic denervation of the renal arteries. Source: Medtronic Inc.

In addition to physical denervation, the role of pharmacological blockade of the adrenergic system (such as with α - or β -adrenergic blockers) in reducing the incidence of thyroid cancer, or reducing the recurrence or progression of known thyroid cancer, should be carefully explored (Figure 11B). Thyroid cancer cells have been shown to express β -adrenergic receptors,^{88,89} and *in vitro* studies have shown that propranolol is able to inhibit growth of thyroid cancer cells.⁹⁰ Two recent meta-analyses of large retrospective studies of the association between β -adrenergic blockade and overall cancer survival suggested a possible survival benefit from β -blockers in melanoma, ovarian cancer and pancreatic cancer.^{91,92} Data regarding thyroid cancer were not included in either analysis.

8.3 Nerves as biomarkers of cancer aggressiveness

Additionally, these data prompt consideration whether perineural invasion should be included in the histopathological reporting of thyroid cancers, as is routine in other malignancies, such as skin cancer (Figure 11C). This is clinically important, as current biomarkers to distinguish indolent from aggressive cancers are imperfect at selecting patients for appropriate therapy.

Larger validation studies examining the detection of true perineural invasion using routine pathological stains (such as haematoxylin and eosin) and correlating with

clinically relevant outcomes, such as recurrence and mortality, are the first extension from this work. Given that this thesis suggests that nerve density is correlated with extra-thyroidal invasion, and that TrkA receptors on nerves within thyroid cancers correlate with the presence of nodal metastases, it is plausible that the relationship between perineural invasion and prognosis is significant.

8.4 Neurotrophin receptors as therapeutic targets

In a different vein, the role of the receptors of neurotrophins in the progression of cancer is highlighted by this work, in particular, TrkA, which was shown to be expressed in 20% of thyroid cancers, and associated with metastases.

At present, two pharmacologic inhibitors of TrkA have been approved for use in humans: entrectinib (also inhibiting TrkB, TrkC, ALK and ROS1)⁹³ and larotrectinib (a highly selective Trk inhibitor).⁹⁴ In the largest trial to date, Drilon and colleagues recruited 55 patients with Trk-fusion positive cancers, including 5 patients with thyroid cancer.⁹⁴ In this trial, there was a durable response to larotrectinib seen in the majority of patients, including in all patients with thyroid cancer (see Figure 13). This thesis would support the expansion of therapeutic trials of TrkA inhibitors in the subset of thyroid cancers demonstrating upregulation of this receptor, in addition to the Trk-fusion cancers that have been studied.

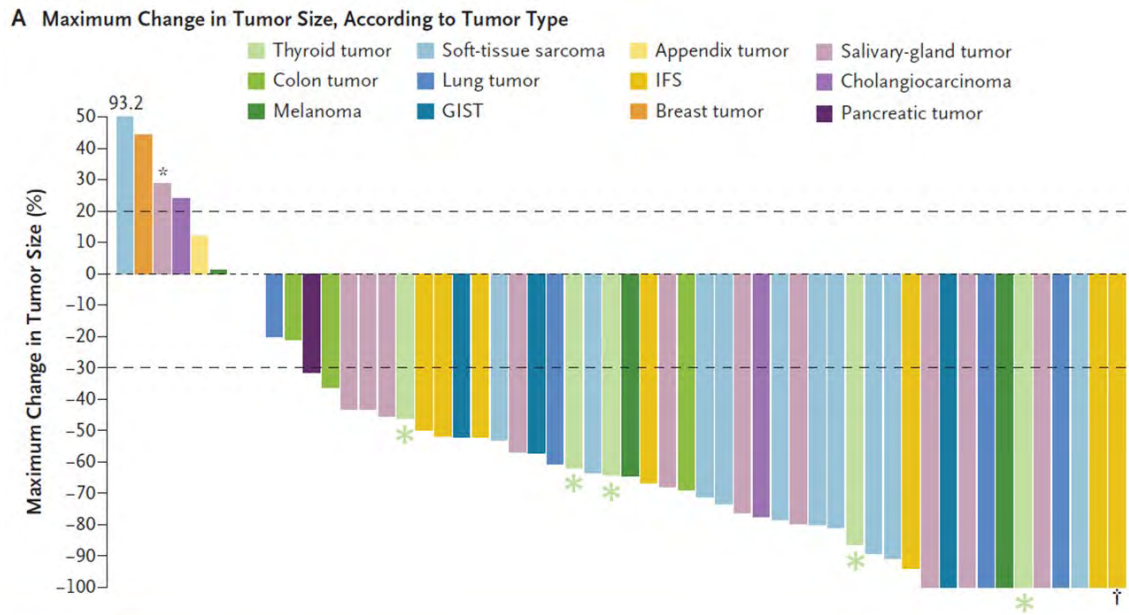


Figure 1. Efficacy.

Panel A shows a waterfall plot of the maximum change in tumor size, according to tumor type. One patient (asterisk) had a tropomyosin receptor kinase (TRK) solvent front resistance mutation (*NTRK3* G623R) at baseline owing to previous therapy. One patient (dagger) had a pathological complete response. Data for 1 patient are not shown; the patient had clinical deterioration and no tumor measurements after baseline were recorded. GIST denotes gastro-intestinal stromal tumor, and IFS infantile fibrosarcoma.

Figure 13: Response of TRK-fusion tumours to larotrectinib. All thyroid tumours (denoted with asterisks, added to original figure), had a >30% response. Reproduced with permission from (Drilon *et al.*, N Eng J Med 2018)⁹⁴, Copyright Massachusetts Medical Society.

Further, this thesis suggests that targeting TrkA expression may be of particular value in anaplastic thyroid cancer, which is an extremely aggressive subtype of thyroid cancer associated with a median overall survival of 4 months.⁹⁵ As reported in Chapter 5, TrkA was seen using immunohistochemistry in 25% of cases of anaplastic thyroid cancer, which was a similar overall proportion to that seen in PTC, and much greater than seen in FTC. These *in vitro* data showed that the highest expression of TrkA was seen in the anaplastic thyroid cancer cell line CAL-62, and the poorly differentiated PTC cell line BCPAP, as compared to more differentiated cell lines. Additionally, knockdown of TrkA expression in CAL-62 cells had a marked impact on cell growth, measured by wound reduction and invading cell assays.

The role of proNGF signalling in thyroid cancer, as in other cancers, remains incompletely understood, but it is possible that either proNGF or its cleavage product, NGF, are targetable molecules in cancer. Monoclonal antibodies against NGF are in clinical trials for their analgesic properties, although the potential role in oncological

outcomes is yet to be tested.⁹⁶ The use of targeted drug delivery systems, such as nanoliposomes targeted to the TSH receptor, may be an effective way of maximising the therapeutic index of cytotoxic or targeted biological therapies.

8.5 Conclusion

Seeded by the first experimental work in 1948 suggesting a soluble nerve growth factor secreted by tumours,³⁸ and strengthened by the Nobel prize in 1986, the field of cancer neurobiology is now firmly established, with both functional and outcome studies confirming the significance of tumour innervation for growth and prognosis for some cancers. Data within this thesis draw malignancy of the thyroid gland into the family of cancers that may be nerve-associated, and invite the deeper study that is already occurring in cancers of the prostate and breast (among others) to understand the mechanisms of nerve-cancer crosstalk that may open a new era of diagnostic and therapeutic modalities.

9 REFERENCES

The following references relate only to the non-published works of this thesis, contained in Chapter 2, parts 1 and 3, and Chapter 8. References cited in the scientific papers (Chapter 2, part 2, and chapters 3-7) are included as part of the published works in their respective chapters.

- 1 Maenhaut, C. *et al.* in *Endotext [Internet]* (ed Chrousos G De Groot LJ, Dungan K, et al.) (MDText.com, Inc., South Dartmouth (MA), 2015).
- 2 McMullen, T. P. W. & Delbridge, L. W. in *Endocrine Surgery: Principles and Practice* (eds Johnathan Hubbard, William B. Inabnet, & Chung-Yau Lo) Ch. Chapter 1, 3-16 (Springer London, 2009).
- 3 Kameda, Y., Oyama, H., Endoh, M. & Horino, M. Somatostatin immunoreactive C cells in thyroid glands from various mammalian species. *Anat. Rec.* **204**, 161-170, doi:10.1002/ar.1092040210 (1982).
- 4 Van Noorden, S., Polak, J. M. & Pearce, A. G. E. Single cellular origin of somatostatin and calcitonin in the rat thyroid gland. *Histochemistry* **53**, 243-247, doi:10.1007/bf00511079 (1977).
- 5 Dean, D. S. & Gharib, H. Epidemiology of thyroid nodules. *Best Pract. Res. Clin. Endocrinol. Metab.* **22**, 901-911, doi:10.1016/j.beem.2008.09.019 (2008).
- 6 Rowe, C., Boelaert, K. & Smith, R. in *Maternal, Fetal and Neonatal Endocrinology* (eds C. Kovacs & C. Deal) (Elsevier, 2019).
- 7 Apel, R. L. *et al.* Clonality of thyroid nodules in sporadic goiter. *Diagn. Mol. Pathol.* **4**, 113-121 (1995).
- 8 Haugen, B. R. *et al.* 2015 American Thyroid Association Management Guidelines for Adult Patients with Thyroid Nodules and Differentiated Thyroid Cancer: The American Thyroid Association Guidelines Task Force on Thyroid Nodules and Differentiated Thyroid Cancer. *Thyroid* **26**, 1-133, doi:10.1089/thy.2015.0020 (2016).
- 9 Furuya-Kanamori, L., Bell, K. J. L., Clark, J., Glasziou, P. & Doi, S. A. R. Prevalence of Differentiated Thyroid Cancer in Autopsy Studies Over Six Decades: A Meta-Analysis. *J. Clin. Oncol.* **34**, 3672-3679, doi:10.1200/jco.2016.67.7419 (2016).
- 10 Cancer Australia. *Thyroid cancer statistics*, <<https://thyroid-cancer.canceraustralia.gov.au/statistics>> (2018).
- 11 *Thyroid Cancer*, <<http://seer.cancer.gov/statfacts/html/thyro.html>> (2016).
- 12 Sciuto, R. *et al.* Natural history and clinical outcome of differentiated thyroid carcinoma: a retrospective analysis of 1503 patients treated at a single institution. *Ann. Oncol.* **20**, 1728-1735, doi:10.1093/annonc/mdp050 (2009).
- 13 Ahren, B. Thyroid neuroendocrinology: neural regulation of thyroid hormone secretion. *Endocr. Rev.* **7**, 149-155, doi:10.1210/edrv-7-2-149 (1986).
- 14 Melander, A. & Sundler, F. Presence and Influence of Cholinergic Nerves in the Mouse Thyroid*. *Endocrinology* **105**, 7-9, doi:10.1210/endo-105-1-7 (1979).
- 15 Van Sande, J., Dumont, J. E., Melander, A. & Sundler, F. Presence and influence of cholinergic nerves in the human thyroid. *J. Clin. Endocrinol. Metab.* **51**, 500-502, doi:10.1210/jcem-51-3-500 (1980).
- 16 Melander, A. *et al.* Sympathetic innervation and noradrenaline content of normal human thyroid tissue from fetal, young, and elderly subjects. *J. Endocrinol. Invest.* **1**, 175-177, doi:10.1007/bf03350368 (1978).

- 17 Delbridge, L. Total thyroidectomy: the evolution of surgical technique. *ANZ J. Surg.* **73**, 761-768 (2003).
- 18 Melander, A., Ericson, L. E., Sundler, F. & Ingbar, S. H. Sympathetic Innervation of the Mouse Thyroid and Its Significance in Thyroid Hormone Secretion. *Endocrinology* **94**, 959-966, doi:10.1210/endo-94-4-959 (1974).
- 19 Melander, A., Nilsson, E. & Sundler, F. Sympathetic Activation of Thyroid Hormone Secretion in Mice. *Endocrinology* **90**, 194-199, doi:10.1210/endo-90-1-194 (1972).
- 20 Melander, A., Ranklev, E., Sundler, F. & Westgren, U. Beta2-Adrenergic Stimulation of Thyroid Hormone Secretion. *Endocrinology* **97**, 332-336, doi:10.1210/endo-97-2-332 (1975).
- 21 Ahren, B. & Rerup, C. Effects of beta-adrenoceptor agonists and antagonists on thyroid hormone secretion. *Eur. J. Pharmacol.* **88**, 383-387, doi:10.1016/0014-2999(83)90590-3 (1983).
- 22 Young, J. B., Bürgi-Saville, M. E., Bürgi, U. & Landsberg, L. Sympathetic nervous system activity in rat thyroid: potential role in goitrogenesis. *American Journal of Physiology-Endocrinology and Metabolism* **288**, E861-E867, doi:10.1152/ajpendo.00292.2004 (2005).
- 23 Shibata, K., Takei, S., Kawai, T., Imaizumi, Y. & Watanabe, M. Decrease in neuronal uptake of noradrenaline simply explains the supersensitivity after sympathectomy in the rat iris dilator. *Jpn. J. Pharmacol.* **50**, 19-29, doi:10.1254/jjp.50.19 (1989).
- 24 CARDINALI, D. P. *et al.* Role of the Sympathetic Nervous System in the Control of the Goitrogenic Response in the Rat*. *Endocrinology* **109**, 2202-2207, doi:10.1210/endo-109-6-2202 (1981).
- 25 Romeo, H. E., Diaz, M. C., Ceppi, J., Zaninovich, A. A. & Cardinali, D. P. Effect of inferior laryngeal nerve section on thyroid function in rats. *Endocrinology* **122**, 2527-2532, doi:10.1210/endo-122-6-2527 (1988).
- 26 Pilo, B., John, T. M., Pemsingh, R. S. & George, J. C. Post-vagotomy changes in the ultrastructure of the thyroid gland and circulating levels of its hormones in the pigeon. *Cytobios* **41**, 175-180 (1984).
- 27 Zahalka, A. H. *et al.* Adrenergic nerves activate an angio-metabolic switch in prostate cancer. *Science* **358**, 321-326, doi:10.1126/science.aah5072 (2017).
- 28 Magnon, C. *et al.* Autonomic Nerve Development Contributes to Prostate Cancer Progression. *Science* **341**, 1236361, doi:10.1126/science.1236361 (2013).
- 29 Zhao, C.-M. *et al.* Denervation suppresses gastric tumorigenesis. *Sci. Transl. Med.* **6**, 250ra115-250ra115, doi:10.1126/scitranslmed.3009569 (2014).
- 30 Pundavela, J. *et al.* Nerve fibers infiltrate the tumor microenvironment and are associated with nerve growth factor production and lymph node invasion in breast cancer. *Mol. Oncol.* **9**, 1626-1635, doi:<https://doi.org/10.1016/j.molonc.2015.05.001> (2015).
- 31 Albo, D. *et al.* Neurogenesis in colorectal cancer is a marker of aggressive tumor behavior and poor outcomes. *Cancer* **117**, 4834-4845, doi:10.1002/cncr.26117 (2011).
- 32 Rutledge, A., Jobling, P., Walker, M. M., Denham, J. W. & Hondermarck, H. Spinal Cord Injuries and Nerve Dependence in Prostate Cancer. *Trends in Cancer* **3**, 812-815, doi:10.1016/j.trecan.2017.10.001 (2017).

- 33 Zareba, P. *et al.* Perineural Invasion and Risk of Lethal Prostate Cancer. *Cancer Epidemiology Biomarkers & Prevention* **26**, 719-726, doi:10.1158/1055-9965.Epi-16-0237 (2017).
- 34 Fagan, J. J. *et al.* Perineural Invasion in Squamous Cell Carcinoma of the Head and Neck. *Archives of Otolaryngology–Head & Neck Surgery* **124**, 637-640, doi:10.1001/archotol.124.6.637 (1998).
- 35 Park, H. S. *et al.* Clinicopathologic characteristics and surgical outcomes of elderly patients with thyroid cancer. *Jpn. J. Clin. Oncol.* **44**, 1045-1051, doi:10.1093/jjco/hyu132 (2014).
- 36 Sezer, A. *et al.* Relationship between lymphovascular invasion and clinicopathological features of papillary thyroid carcinoma. *Bosn. J. Basic Med. Sci.* **17**, 144-151, doi:10.17305/bjbms.2017.1924 (2017).
- 37 Lee, S. H. *et al.* Risk Factors for Recurrence After Treatment of N1b Papillary Thyroid Carcinoma. *Ann. Surg.* **269**, 966-971, doi:10.1097/sla.0000000000002710 (2018).
- 38 Levi-Montalcini, R. The nerve growth factor: thirty-five years later. *Biosci. Rep.* **7**, 681-699, doi:10.1007/bf01116861 (1987).
- 39 Hondermarck, H. Neurotrophins and their receptors in breast cancer. *Cytokine Growth Factor Rev.* **23**, 357-365, doi:10.1016/j.cytogfr.2012.06.004 (2012).
- 40 Seidah, N. G., Benjannet, S., Pareek, S., Chretien, M. & Murphy, R. A. Cellular processing of the neurotrophin precursors of NT3 and BDNF by the mammalian proprotein convertases. *FEBS Lett.* **379**, 247-250, doi:10.1016/0014-5793(95)01520-5 (1996).
- 41 Bradshaw, R. A. *et al.* NGF and ProNGF: Regulation of neuronal and neoplastic responses through receptor signaling. *Adv Biol Regul* **58**, 16-27, doi:10.1016/j.jbior.2014.11.003 (2015).
- 42 Nykjaer, A. *et al.* Sortilin is essential for proNGF-induced neuronal cell death. *Nature* **427**, 843-848, doi:10.1038/nature02319 (2004).
- 43 Kliemann, M. *et al.* The mature part of proNGF induces the structure of its pro-peptide. *FEBS Lett.* **566**, 207-212, doi:10.1016/j.febslet.2004.04.034 (2004).
- 44 Paoletti, F. *et al.* Conformational Plasticity of proNGF. *PLoS One* **6**, e22615, doi:10.1371/journal.pone.0022615 (2011).
- 45 Aloe, L., Rocco, M. L., Balzamino, B. O. & Micera, A. Nerve growth factor: role in growth, differentiation and controlling cancer cell development. *J. Exp. Clin. Cancer Res.* **35**, 116, doi:10.1186/s13046-016-0395-y (2016).
- 46 Masoudi, R. *et al.* Biological activity of nerve growth factor precursor is dependent upon relative levels of its receptors. *J. Biol. Chem.* **284**, 18424-18433, doi:10.1074/jbc.M109.007104 (2009).
- 47 Wang, Y. J. *et al.* Effects of proNGF on neuronal viability, neurite growth and amyloid-beta metabolism. *Neurotox. Res.* **17**, 257-267, doi:10.1007/s12640-009-9098-x (2010).
- 48 Counts, S. E. *et al.* Cerebrospinal Fluid proNGF: A Putative Biomarker for Early Alzheimer's Disease. *Curr Alzheimer Res* **13**, 800-808 (2016).
- 49 Peng, S., Wu, J., Mufson, E. J. & Fahnstock, M. Increased proNGF levels in subjects with mild cognitive impairment and mild Alzheimer disease. *J. Neuropathol. Exp. Neurol.* **63**, 641-649, doi:10.1093/jnen/63.6.641 (2004).
- 50 Belrose, J. C., Masoudi, R., Michalski, B. & Fahnstock, M. Increased pro-nerve growth factor and decreased brain-derived neurotrophic factor in non-

- Alzheimer's disease tauopathies. *Neurobiol. Aging* **35**, 926-933, doi:10.1016/j.neurobiolaging.2013.08.029 (2014).
- 51 von Loga, I. S. *et al.* Active immunisation targeting nerve growth factor attenuates chronic pain behaviour in murine osteoarthritis. *Ann. Rheum. Dis.* **78**, 672-675, doi:10.1136/annrheumdis-2018-214489 (2019).
- 52 da Silva, J. T., Evangelista, B. G., Venega, R. A. G., Seminowicz, D. A. & Chacur, M. Anti-NGF treatment can reduce chronic neuropathic pain by changing peripheral mediators and brain activity in rats. *Behav. Pharmacol.* **30**, 79-88, doi:10.1097/FBP.0000000000000422 (2019).
- 53 Monteleone, F. *et al.* Nerve growth factor is elevated in the CSF of patients with multiple sclerosis and central neuropathic pain. *J. Neuroimmunol.* **314**, 89-93, doi:10.1016/j.jneuroim.2017.11.012 (2018).
- 54 Slatkin, N. *et al.* Fulranumab as Adjunctive Therapy for Cancer-Related Pain: A Phase 2, Randomized, Double-Blind, Placebo-Controlled, Multicenter Study. *J. Pain* **20**, 440-452, doi:10.1016/j.jpain.2018.09.014 (2019).
- 55 Mysona, B. A. *et al.* Imbalance of the nerve growth factor and its precursor as a potential biomarker for diabetic retinopathy. *BioMed Res. Int.* **2015**, 571456, doi:10.1155/2015/571456 (2015).
- 56 Dolle, L., El Yazidi-Belkoura, I., Adriaenssens, E., Nurcombe, V. & Hondermarck, H. Nerve growth factor overexpression and autocrine loop in breast cancer cells. *Oncogene* **22**, 5592-5601, doi:10.1038/sj.onc.1206805 (2003).
- 57 Tomellini, E. *et al.* Nerve growth factor and proNGF simultaneously promote symmetric self-renewal, quiescence, and epithelial to mesenchymal transition to enlarge the breast cancer stem cell compartment. *Stem Cells* **33**, 342-353, doi:10.1002/stem.1849 (2015).
- 58 Leveque, R. *et al.* ProNGF increases breast tumor aggressiveness through functional association of TrkA with EphA2. *Cancer Lett.* **449**, 196-206, doi:10.1016/j.canlet.2019.02.019 (2019).
- 59 Demont, Y. *et al.* Pro-nerve Growth Factor Induces Autocrine Stimulation of Breast Cancer Cell Invasion through Tropomyosin-related Kinase A (TrkA) and Sortilin Protein. *J. Biol. Chem.* **287**, 1923-1931, doi:10.1074/jbc.M110.211714 (2012).
- 60 Roselli, S. *et al.* Sortilin is associated with breast cancer aggressiveness and contributes to tumor cell adhesion and invasion. *Oncotarget* **6**, 10473-10486, doi:10.18632/oncotarget.3401 (2015).
- 61 Chakravarthy, R., Mnich, K. & Gorman, A. M. Nerve growth factor (NGF)-mediated regulation of p75(NTR) expression contributes to chemotherapeutic resistance in triple negative breast cancer cells. *Biochem. Biophys. Res. Commun.* **478**, 1541-1547, doi:10.1016/j.bbrc.2016.08.149 (2016).
- 62 Xu, J. *et al.* ProNGF siRNA inhibits cell proliferation and invasion of pancreatic cancer cells and promotes anoikis. *Biomed. Pharmacother.* **111**, 1066-1073, doi:10.1016/j.biopha.2019.01.002 (2019).
- 63 Delsite, R. & Djakiew, D. Characterization of nerve growth factor precursor protein expression by human prostate stromal cells: a role in selective neurotrophin stimulation of prostate epithelial cell growth. *Prostate* **41**, 39-48 (1999).

- 64 Pundavela, J. *et al.* ProNGF correlates with Gleason score and is a potential driver of nerve infiltration in prostate cancer. *Am. J. Pathol.* **184**, 3156-3162, doi:10.1016/j.ajpath.2014.08.009 (2014).
- 65 Truzzi, F. *et al.* Neurotrophins and their receptors stimulate melanoma cell proliferation and migration. *J. Invest. Dermatol.* **128**, 2031-2040, doi:10.1038/jid.2008.21 (2008).
- 66 Kasemeier-Kulesa, J. C. *et al.* NGF reprograms metastatic melanoma to a bipotent glial-melanocyte neural crest-like precursor. *Biology open* **7**, doi:10.1242/bio.030817 (2018).
- 67 Faulkner, S. *et al.* ProNGF is a potential diagnostic biomarker for thyroid cancer. *Oncotarget* **7**, 28488-28497, doi:10.18632/oncotarget.8652 (2016).
- 68 Dicou, E. High levels of the proNGF peptides LIP1 and LIP2 in the serum and synovial fluid of rheumatoid arthritis patients: evidence for two new cytokines. *J. Neuroimmunol.* **194**, 143-146, doi:10.1016/j.jneuroim.2007.11.002 (2008).
- 69 Xu, J. B. *et al.* Serum nerve growth factor level indicates therapeutic efficacy of 125I seed implantation in advanced pancreatic adenocarcinoma. *Eur. Rev. Med. Pharmacol. Sci.* **19**, 3385-3390 (2015).
- 70 Bigazzi, M., Revoltella, R., Aand, S. C. & Vigneti, E. High level of a nerve growth factor in the serum of a patient with medullary carcinoma of the thyroid gland. *Clin. Endocrinol. (Oxf.)* **6**, 105-112, doi:10.1111/j.1365-2265.1977.tb02001.x (1977).
- 71 Nikiforov, Y. E. Thyroid Carcinoma: Molecular Pathways and Therapeutic Targets. *Modern pathology : an official journal of the United States and Canadian Academy of Pathology, Inc* **21**, S37-S43, doi:10.1038/modpathol.2008.10 (2008).
- 72 Kimura, E. T. *et al.* High prevalence of BRAF mutations in thyroid cancer: genetic evidence for constitutive activation of the RET/PTC-RAS-BRAF signaling pathway in papillary thyroid carcinoma. *Cancer Res.* **63**, 1454-1457 (2003).
- 73 Greco, A., Miranda, C. & Pierotti, M. A. Rearrangements of NTRK1 gene in papillary thyroid carcinoma. *Mol. Cell. Endocrinol.* **321**, 44-49, doi:10.1016/j.mce.2009.10.009 (2010).
- 74 Koizumi, H., Morita, M., Mikami, S., Shibayama, E. & Uchikoshi, T. Immunohistochemical analysis of TrkA neurotrophin receptor expression in human non-neuronal carcinomas. *Pathol. Int.* **48**, 93-101 (1998).
- 75 Tang A, Falciglia M, Yang H, Mark J & D, S. in *American Thyroid Association Annual Meeting* (Denver, Colorado, 2016).
- 76 Arul, P., Akshatha, C. & Masilamani, S. A study of malignancy rates in different diagnostic categories of the Bethesda system for reporting thyroid cytopathology: An institutional experience. *Biomed J* **38**, 517-522, doi:10.1016/j.bj.2015.08.001 (2015).
- 77 Cibas, E. S. & Ali, S. Z. The Bethesda System For Reporting Thyroid Cytopathology. *Am. J. Clin. Pathol.* **132**, 658-665, doi:10.1309/ajcpplwmi3jv4la (2009).
- 78 Costante, G. & Filetti, S. Early diagnosis of medullary thyroid carcinoma: is systematic calcitonin screening appropriate in patients with nodular thyroid disease? *Oncologist* **16**, 49-52, doi:10.1634/theoncologist.2010-0344 (2011).
- 79 Wojcicka, A., Kolanowska, M. & Jazdzewski, K. MECHANISMS IN ENDOCRINOLOGY: MicroRNA in diagnostics and therapy of thyroid cancer. *Eur. J. Endocrinol.* **174**, R89-98, doi:10.1530/eje-15-0647 (2016).

- 80 Allin, D. M. *et al.* Circulating tumour DNA is a potential biomarker for disease progression and response to targeted therapy in advanced thyroid cancer. *Eur. J. Cancer* **103**, 165-175, doi:10.1016/j.ejca.2018.08.013 (2018).
- 81 Lupo, M. *et al.* IS MEASUREMENT OF CIRCULATING TUMOR DNA OF DIAGNOSTIC USE IN PATIENTS WITH THYROID NODULES? *Endocr. Pract.* **24**, 453-459, doi:10.4158/ep-2017-0213 (2018).
- 82 Moon, J. H. *et al.* Thyroglobulin in washout fluid from lymph node fine-needle aspiration biopsy in papillary thyroid cancer: large-scale validation of the cutoff value to determine malignancy and evaluation of discrepant results. *J. Clin. Endocrinol. Metab.* **98**, 1061-1068, doi:10.1210/jc.2012-3291 (2013).
- 83 Trimboli, P. *et al.* Use of fine-needle aspirate calcitonin to detect medullary thyroid carcinoma: A systematic review. *Diagn. Cytopathol.* **44**, 45-51, doi:10.1002/dc.23375 (2016).
- 84 de Matos, L. L. *et al.* Expression of CK-19, galectin-3 and HBME-1 in the differentiation of thyroid lesions: systematic review and diagnostic meta-analysis. *Diagn. Pathol.* **7**, 97, doi:10.1186/1746-1596-7-97 (2012).
- 85 Rossi, E. D. *et al.* Diagnostic and prognostic value of immunocytochemistry and BRAF mutation analysis on liquid-based biopsies of thyroid neoplasms suspicious for carcinoma. *Eur. J. Endocrinol.* **168**, 853-859, doi:10.1530/eje-13-0023 (2013).
- 86 Cho, J. W., Lee, Y. M., Lee, Y. H., Hong, S. J. & Yoon, J. H. Dynamic risk stratification system in post-lobectomy low-risk and intermediate-risk papillary thyroid carcinoma patients. *Clin Endocrinol (Oxf)* **89**, 100-109, doi:10.1111/cen.13721 (2018).
- 87 Park, J. H., Lee, Y. M., Lee, Y. H., Hong, S. J. & Yoon, J. H. The prognostic value of serum thyroid-stimulating hormone level post-lobectomy in low- and intermediate-risk papillary thyroid carcinoma. *J. Surg. Oncol.* **118**, 390-396, doi:10.1002/jso.25164 (2018).
- 88 Rains, S. L., Amaya, C. N. & Bryan, B. A. Beta-adrenergic receptors are expressed across diverse cancers. *Oncoscience* **4**, 95-105, doi:10.18632/oncoscience.357 (2017).
- 89 Ohta, K., Pang, X. P., Berg, L. & Hershman, J. M. Growth inhibition of new human thyroid carcinoma cell lines by activation of adenylate cyclase through the beta-adrenergic receptor. *J Clin Endocrinol Metab* **82**, 2633-2638, doi:10.1210/jcem.82.8.4136 (1997).
- 90 Wei, W. J., Shen, C. T., Song, H. J., Qiu, Z. L. & Luo, Q. Y. Propranolol sensitizes thyroid cancer cells to cytotoxic effect of vemurafenib. *Oncol. Rep.* **36**, 1576-1584, doi:10.3892/or.2016.4918 (2016).
- 91 Yap, A. *et al.* Effect of beta-blockers on cancer recurrence and survival: a meta-analysis of epidemiological and perioperative studies. *Br. J. Anaesth.* **121**, 45-57, doi:10.1016/j.bja.2018.03.024 (2018).
- 92 Na, Z. *et al.* The effects of beta-blocker use on cancer prognosis: a meta-analysis based on 319,006 patients. *Onco Targets Ther.* **11**, 4913-4944, doi:10.2147/OTT.S167422 (2018).
- 93 Drilon, A. *et al.* Safety and Antitumor Activity of the Multitargeted Pan-TRK, ROS1, and ALK Inhibitor Entrectinib: Combined Results from Two Phase I Trials (ALKA-372-001 and STARTRK-1). *Cancer Discov.* **7**, 400-409, doi:10.1158/2159-8290.cd-16-1237 (2017).

- 94 Drilon, A. *et al.* Efficacy of Larotrectinib in TRK Fusion-Positive Cancers in Adults and Children. *N. Engl. J. Med.* **378**, 731-739, doi:10.1056/NEJMoa1714448 (2018).
- 95 Lim, S. M. *et al.* Treatment outcome of patients with anaplastic thyroid cancer: a single center experience. *Yonsei Med. J.* **53**, 352-357, doi:10.3349/ymj.2012.53.2.352 (2012).
- 96 Bannwarth, B. & Kostine, M. Nerve Growth Factor Antagonists: Is the Future of Monoclonal Antibodies Becoming Clearer? *Drugs* **77**, 1377-1387, doi:10.1007/s40265-017-0781-6 (2017).

10 APPENDICES

10.1 Additional publications completed during candidature

The following publications are included in chronological order of publication

- Rowe CW, Murray K, Woods A, Gupta S, Smith R, Wynne K. (2016) **Metastatic Thyroid Cancer in Pregnancy: Risk and Uncertainty**. Endocrinol Diab Metab Case Rep. <https://doi.org/10.1530/EDM-16-0071>
- Rowe CW, Bendinelli C, McGrath S. (2016) **Charting a Course through the CEAs: Diagnosis and Management of Medullary Thyroid Cancer**. Clinical Endocrinology (Oxf). <http://dx.doi.org/10.1016/j.diabres.2017.06.022>
- Rowe CW, Haider AS, Viswanathan D, Jones M, Attia J, Wynne K, Acharya S. (2017) **Insulin resistance correlates with maculopathy and severity of retinopathy in young adults with Type 1 Diabetes Mellitus**. Diabetes Research and Clinical Practice. <https://doi.org/10.1111/cen.13114>
- Gao F, Griffin N, Faulkner S, Rowe CW, Williams L, Roselli S, Thorne R, Ferdoushi A, Jobling P, Walker M and Hondermarck H (2018) **The neurotrophic tyrosine kinase receptor TrkA and its ligand NGF are increased in squamous cell carcinomas of the lung**. Scientific Reports. <https://doi.org/10.1038/s41598-018-26408-2>
- Rowe CW, Arthurs S, O'Neill CJ, Hawthorne J, Carroll R, Wynne K, Bendinelli C. (2018) **High-dose cholecalciferol to prevent post-thyroidectomy hypocalcemia: a randomized double-blind placebo-controlled trial**. Clinical Endocrinology <https://doi.org/10.1111/cen.13897>
- Rowe CW, Putt E, Brentnall O, Allabyrne J, Gebuehr A, Woods A, Wynne K (2018) **An intravenous insulin protocol designed for pregnancy reduces neonatal hypoglycaemia following betamethasone administration in women with gestational diabetes**. Diabetic Medicine <https://doi.org/10.1111/dme.13864>
- Marlow A, Rowe CW, Anderson D, Wynne K, King B, Howley P, Smart C (2019) **Young children, adolescent girls and women with type 1 diabetes are more overweight and obese than reference populations, and this is associated with increased cardiovascular risk factors**. Diabetic Medicine <https://doi.org/10.1111/dme.14133>

Management of metastatic thyroid cancer in pregnancy: risk and uncertainty

Christopher W Rowe^{1,4}, Kirsten Murray¹, Andrew Woods², Sandeep Gupta^{3,5},
Roger Smith^{1,4} and Katie Wynne^{1,4}

¹Departments of Endocrinology and Diabetes and ²Maternity and Gynaecology, John Hunter Hospital, Newcastle, New South Wales, Australia, ³Department of Nuclear Medicine & PET, Hunter New England Imaging, John Hunter and Calvary Mater Hospital, Newcastle, New South Wales, Australia, ⁴Schools of Medicine and Public Health, and ⁵Health Sciences, University of Newcastle, Newcastle, New South Wales, Australia

Correspondence
should be addressed
to C Rowe
Email
Christopher.Rowe@hnehealth.nsw.gov.au

Summary

Metastatic thyroid cancer is an uncommon condition to be present at the time of pregnancy, but presents a challenging paradigm of care. Clinicians must balance the competing interests of long-term maternal health, best achieved by iatrogenic hyperthyroidism, regular radioiodine therapy and avoidance of dietary iodine, against the priority to care for the developing foetus, with inevitable compromise. Additionally, epidemiological and cellular data support the role of oestrogen as a growth factor for benign and malignant thyrocytes, although communicating the magnitude of this risk to patients and caregivers, as well as the uncertain impact of any pregnancy on long-term prognosis, remains challenging. Evidence to support treatment decisions in this uncommon situation is presented in the context of a case of a pregnant teenager with known metastatic papillary thyroid cancer and recent radioiodine therapy.

Learning points:

- Pregnancy is associated with the growth of thyroid nodules due to stimulation from oestrogen receptors on thyrocytes and HCG cross-stimulation of the TSH receptor.
- Thyroid cancer diagnosed during pregnancy has not been shown to be associated with increased rates of persistent or recurrent disease in most studies.
- There is little evidence to guide the management of metastatic thyroid cancer in pregnancy, where both maternal and foetal wellbeing must be carefully balanced.

Background

Thyroid cancer is the most common endocrine malignancy, and the second most common invasive malignancy complicating pregnancy, occurring in 1 of 1000 pregnancies (1). Compared with other solid organ malignancies such as breast cancer, thyroid cancer presents unique management challenges due to its usually slow proliferation rate, the efficacy of surgery and radioiodine as curative first-line treatment and poor response to standard chemotherapy. The majority of thyroid cancer

patients present with localised disease, and widespread metastases are relatively uncommon, especially in women of childbearing age. The published reviews and case series of thyroid cancer in pregnancy focus predominantly on the more common situation of establishing the diagnosis of a suspicious thyroid nodule, and whether definitive therapy can be safely deferred until post-partum (1, 2). Thus, there is a paucity of information to guide clinicians caring for patients with metastatic thyroid cancer during

pregnancy. We present the management of a pregnant patient with known metastatic papillary thyroid cancer (PTC) and recent radioiodine therapy and review the literature regarding risks of disease progression in pregnancy, endocrine management considerations and potential conflicts between maternal and foetal wellbeing.

Case presentation

The patient, a 16-year-old female, presented six weeks pregnant, having self-ceasing prescribed levothyroxine (1250 µg/week) at conception. Serum biochemistry confirmed pregnancy and noted a thyroid-stimulating hormone (TSH) level of 171.6 IU/L (local first trimester reference range 0.4–2.5), undetectable free T4 and thyroglobulin 636 µg/L (reference <30).

Six years prior to this presentation (at age 10), she was diagnosed with sporadic PTC. There was no history suggesting a familial tumour syndrome, and she had no other medical history. Total thyroidectomy revealed a unifocal 35 mm left lobe tumour with extrathyroidal extension and ipsilateral lymph node metastases in the lateral neck. Post-operative I¹²³-whole body scan (WBS) (Fig. 1A) identified residual uptake in the thyroid bed and contralateral lower neck, and she was treated with I¹³¹ (3.01 GBq). Stimulated thyroglobulin was 786 µg/L, and fell to 39 µg/L on levothyroxine (TSH 1.2 IU/L).

Imaging 12 months later (Fig. 1B) revealed iodine-avid lung metastases, treated with four further doses of I¹³¹, with the most recent dosimetry-adjusted dose of 9.9 GBq after TSH withdrawal (Fig. 1E) administered 7 months prior to this presentation with pregnancy (lifetime

cumulative dose 25.2 GBq). Suppressed thyroglobulin level prior to this dose was 19 µg/L.

Treatment

Between 6 and 14 weeks of gestation, extensive discussion occurred between the patient, her partner, her father and a multidisciplinary medical team. Issues discussed included profound hypothyroidism at the time of conception, risk of progression of metastases due to pregnancy and risks to maternal health due to delayed further treatment, risk of premature delivery due to maternal ill health and the guarded long-term prognosis of the patient. The patient decided to continue the pregnancy, supported by her partner and her father.

In addition to standard obstetric care for a high-risk pregnancy, levothyroxine was titrated aiming for TSH suppression (<0.1 IU/L) and a free T4 level close to the upper limit of the reference range for pregnancy. Dose escalation of levothyroxine was required from 1100 µg/week at presentation to 1500 µg/week by delivery. Control of TSH, and relationship with thyroglobulin during and after pregnancy, are summarised in Fig. 2. Maternal iron deficiency was managed with oral iron supplementation; however, a subsequent rise in TSH at this time raised the possibility of malabsorption of levothyroxine due to co-administration. Variable TSH levels despite administration reminders suggested variable adherence.

Due to risk of progression of pulmonary metastases and the potential for underlying pulmonary fibrosis from previous radioiodine ablations, respiratory status

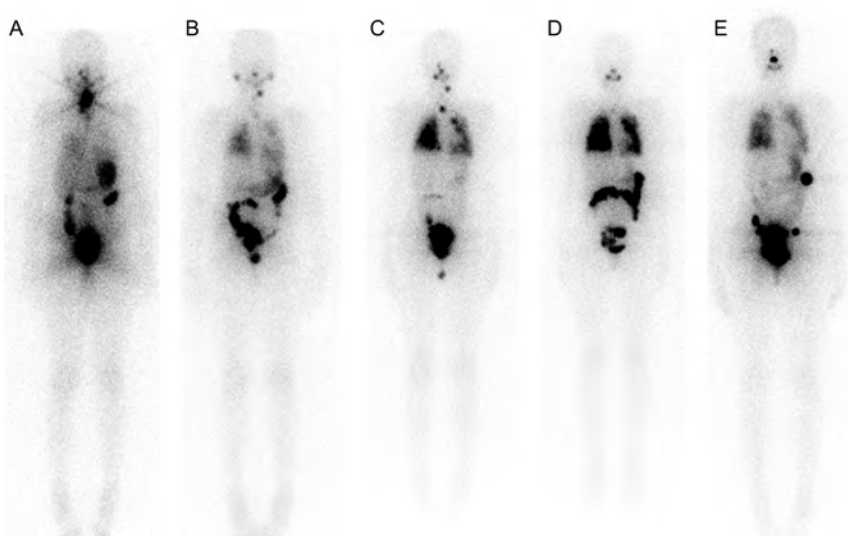
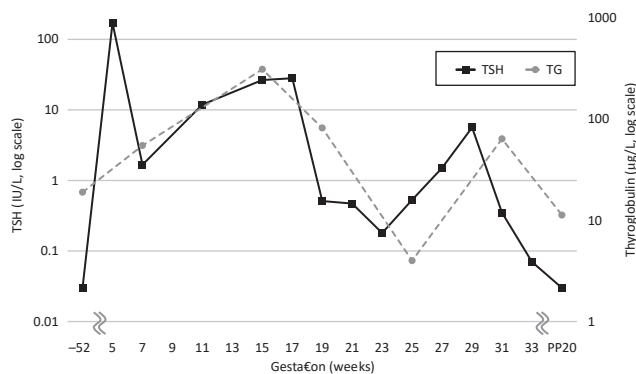


Figure 1

Serial post-I¹³¹ therapy scans (anterior whole body views). (A) Age 10, 3.01 GBq; (B) age 11, 2.95 GBq; (C) age 13, 4.3 GBq; (D) age 14, 5.1 GBq; (E) age 15, 9.9 GBq, 7 months before conception. Neck disease present at age 13 (C) was treated surgically. The final study (E) showed the presence of radioiodine avid bilateral pulmonary metastases (<5 mm maximum diameter on computed tomography) and very small, low-grade lower neck disease. The focal uptake in the left upper abdomen is colonic and is likely physiological in nature.

**Figure 2**

Relationship between serum TSH and thyroglobulin throughout gestation and post-partum. Levothyroxine replacement was adjusted at fortnightly intervals based on blood results. PP, post-partum.

was closely monitored by exercise tolerance, exertional pulse oximetry and formal lung function testing, without abnormality.

Outcome and follow-up

At 34 weeks of gestation, the patient presented in preterm labour, progressing rapidly to a normal birth of a healthy male child weighing 2380 g. Breastfeeding was established on discharge, with an intention to continue for 3 months. The child's TSH was within normal limits. Maternal thyroglobulin 5 months post-partum was 11 µg/L with suppressed TSH. WBS after 3.8 GBq of I^{131} administered 7 months post-partum continued to show radioiodine avid pulmonary metastases. Although there were some areas of increased focal uptake of radioiodine, the overall pulmonary uptake was not significantly different to the pre-pregnancy WBS. There were no new areas of abnormal radioiodine uptake. A concurrent CT chest showed maximum pulmonary nodule size of 3 mm, unchanged from ante-partum.

Discussion

Pregnancy and newly diagnosed thyroid cancer

Thyroid cancer identified during pregnancy most commonly presents as a thyroid nodule, noted either coincidentally or with local symptoms. As the majority of cases are localised to the thyroid (1), the primary management decision is usually the timing of thyroidectomy – either during pregnancy or in the post-partum period – and whether the delay to any planned radioiodine therapy imposed by nursing or breastfeeding is

acceptable. These issues are reviewed in recently published guidelines of the American Thyroid Association (2).

Several observations raise concern that pregnancy may reflect a proliferative environment for differentiated thyroid cancer (DTC). The known three-fold increased incidence of DTC in women of reproductive age suggests the involvement of reproductive hormones as thyroid growth factors, confirmed by cellular studies demonstrating proliferative effects of oestrogen on benign and malignant thyrocytes, mediated by oestrogen receptors (3). Studies of serial thyroid ultrasound in pregnant women demonstrate that pregnancy stimulates the formation and growth of thyroid nodules (4), although the absolute magnitude of nodule growth was small. Additionally, the glycoprotein hormone hCG can cross-stimulate the TSH receptor due to structural homology and a common alpha subunit, which may mediate further stimulatory effects on thyrocytes.

Despite these concerns, most clinical outcome data show no difference in the rate of recurrence or long-term survival of women with well-differentiated thyroid cancer identified during pregnancy (1, 2, 5). Two smaller studies noted DTC diagnosed during pregnancy was associated with higher rates of persistent disease and relapse, although possible confounders have been identified (2).

Pregnancy and established DTC with known distant metastases

DTC with distant metastases present during pregnancy is uncommon, occurring in 2–3% of pregnancies complicated by thyroid cancer (1, 5). To our knowledge, there are no specific guidelines for the prospective management of pregnancy in women with DTC with distant metastases identified prior to pregnancy or at conception. Recently, three large studies retrospectively examined the effect of pregnancy in survivors of thyroid cancer (2). Of 163 women studied, 9 had residual structural disease pre-conception (8 with cervical nodes, 1 with small volume lung metastases), highlighting the uncommon circumstances of our case. Thus, in the remainder of this article, we discuss clinical management principles for such patients, using parallels from the case vignette.

Informed discussion of risk: balancing maternal and foetal wellbeing

Active malignancy during a pregnancy may present a challenging management paradigm, with most decisions either prioritising maternal or foetal wellbeing, sometimes at the expense of the other (6). In pregnancy

complicated by metastatic thyroid cancer, an important unquantifiable risk to maternal health is the potential for accelerated tumour growth due to proliferative effects of oestrogen, hCG and possibly progesterone on metastases, as discussed previously. Additionally, the duration of pregnancy and subsequent breastfeeding may delay planned radioiodine treatment and potentially result in disease progression. Radioiodine uptake is significantly increased in lactating mammary tissue, and subsequent radioiodine treatment should be deferred for at least 3 months after cessation of lactation (2). Conversely, foetal health may be compromised by maternal thyroid status (both hypothyroidism and hyperthyroidism, discussed below), the potential for radiation exposure from residual radioiodine or the need for premature delivery in the case of maternal comorbidity.

This patient's large radioiodine dose 7 months prior to conception raises concern of residual radiation exposure to the foetus. Recent guidelines recommend deferring pregnancy for 6–12 months after radioiodine (2). Shorter time intervals may increase the risk of miscarriage; however, there is a lack of evidence demonstrating adverse pregnancy or foetal outcomes, including congenital abnormality.

Levothyroxine replacement: goals, risks and pitfalls

Physiologic requirements for thyroid hormone rise in early pregnancy due to doubling of thyroid binding globulin by oestrogen and expansion of plasma volume. Hypothyroid women must increase exogenous levothyroxine to compensate, usually by 30% at the time of conception (7), and pre-pregnancy counselling of such patients is mandatory. Monthly monitoring of thyroid function tests to allow early dose titration is recommended.

Maternal hypothyroidism during pregnancy may have deleterious effects on the foetus, particularly neurocognitive development. A study by Haddow (8) found that maternal hypothyroidism during pregnancy was associated with reduced IQ (mean 4 points) in offspring. However, this effect was most pronounced (mean IQ difference 7 points) in the subset of women whose hypothyroidism was untreated for the duration of pregnancy, and it is possible that prompt treatment may ameliorate this effect. Untreated hypothyroidism is also associated with increased risk of early pregnancy loss, and other obstetric complications including gestational hypertension, pre-eclampsia and preterm labour.

Although hyperthyroidism in pregnancy is associated with hypertension, low birth weight and preterm birth, subclinical hyperthyroidism with normal free thyroid

hormones was not associated with an increased rate of adverse pregnancy outcomes in a large cohort study (9). In our patient, a suppressed TSH was targeted to minimise growth stimulus for cancer metastases; however, this may have contributed to premature labour. The strong correlation between TSH and level of thyroglobulin in this pregnancy (Fig. 2) supports the premise of TSH suppression to limit cancer growth in this patient.

Levothyroxine is poorly absorbed from the gut in the presence of iron and calcium supplements that are common components of pregnancy multivitamins. Our practice is to instruct patients to take levothyroxine on an empty stomach in the morning, and vitamins in the evening, to avoid inadvertent hypothyroidism due to malabsorption.

Monitoring for disease progression: methods and endpoints

Progression of metastatic DTC can be determined outside of pregnancy using structural imaging techniques such as computed tomography or functional imaging using radioiodine or ¹⁸F-fluorodeoxyglucose positron emission tomography. However, these modalities are not appropriate in pregnancy due to risk of ionising radiation to the foetus. Serial neck ultrasound is useful for monitoring for growth of any known structural disease in the neck and is safe in pregnancy.

Interpretation of serum thyroglobulin as a surrogate of tumour progression is complicated in pregnancy due to the stimulatory effect of physiologic fluctuations in TSH and thyroid hormone levels, and thus minor changes are unlikely to provide sufficient information to inform major clinical decisions (2). Widely variable TSH levels with corresponding changes in thyroglobulin were present in our patient, which confirmed tumoural TSH responsiveness but hindered meaningful assessment of tumour progression.

With these limitations, there was no objective evidence that this patient's pregnancy resulted in progression or worsening of her thyroid cancer.

Prognosis of metastatic DTC

Despite a variable prognosis, metastatic DTC has a favourable long-term survival compared to other cancers, particularly when diagnosed in childhood. A cohort study of 72 children with DTC (10), including 13 with lung metastases at diagnosis, found that 6 patients (including 2 patients presenting with pulmonary metastases) died over a median 13 years of follow-up, 12–33 years after initial

treatment. The 10-year survival for all patients in this cohort was 98%, falling to 90% at 20 years. Nonetheless, a standardised mortality ratio of 8.1 persists.

Conclusions

Metastatic DTC presents a challenging management paradigm in pregnancy. Ultimately, all decisions reflect an acceptance of the known and unknown risks balanced between mother and foetus, made through comprehensive engagement between clinicians in a multidisciplinary team, centred on the patient and her family. As similar cases are few, data to inform risk must be extrapolated from available evidence and clinician judgement.

Declaration of interest

The authors declare that there is no conflict of interest that could be perceived as prejudicing the impartiality of the research reported.

Funding

This work was supported by the Hunter-New-England Clinical Research Fellowship and the AVANT Doctors-in-Training Research Scholarship Program (to C R).

Patient consent

Written informed consent was obtained from the patient prior to publication.

Author contribution statement

C R, K M, A W, S G and K W cared for the patient. C R drafted the manuscript with K W, with review and revision from K M, A W, S G and R S. All authors have reviewed the final manuscript.

References

- 1 Moosa M & Mazzaferri EL 1997 Outcome of differentiated thyroid cancer diagnosed in pregnant women. *Journal of Clinical Endocrinology and Metabolism* **82** 2862–2866. (doi:10.1210/jcem.82.9.4247)
- 2 Haugen BR, Alexander EK, Bible KC, Doherty GM, Mandel SJ, Nikiforov YE, Pacini F, Randolph GW, Sawka AM, Schlumberger M, *et al.* 2015 American Thyroid Association Management guidelines for adult patients with thyroid nodules and differentiated thyroid cancer: the American Thyroid Association guidelines task force on thyroid nodules and differentiated thyroid cancer. *Thyroid* **26** 1–133. (doi:10.1089/thy.2015.0020)
- 3 Derwahl M & Nicula D 2014 Estrogen and its role in thyroid cancer. *Endocrine-Related Cancer* **21** T273–T283. (doi:10.1530/ERC-14-0053)
- 4 Kung AW, Chau MT, Lao TT, Tam SC & Low LC 2002 The effect of pregnancy on thyroid nodule formation. *Journal of Clinical Endocrinology and Metabolism* **87** 1010–1014. (doi:10.1210/jcem.87.3.8285)
- 5 Yasmeen S, Cress R, Romano PS, Xing G, Berger-Chen S, Danielsen B & Smith LH 2005 Thyroid cancer in pregnancy. *International Journal of Gynaecology and Obstetrics* **91** 15–20. (doi:10.1016/j.ijgo.2005.06.022)
- 6 Oduncu FS, Kimmig R, Hepp H & Emmerich B 2003 Cancer in pregnancy: maternal-fetal conflict. *Journal of Cancer Research and Clinical Oncology* **129** 133–146. (doi:10.1007/s00432-002-0406-6)
- 7 Alexander EK, Marqusee E, Lawrence J, Jarolim P, Fischer GA & Larsen PR 2004 Timing and magnitude of increases in levothyroxine requirements during pregnancy in women with hypothyroidism. *New England Journal of Medicine* **351** 241–249. (doi:10.1056/NEJMoa040079)
- 8 Haddow JE, Palomaki GE, Allan WC, Williams JR, Knight GJ, Gagnon J, O'Heir CE, Mitchell ML, Hermos RJ, Waisbren SE, *et al.* 1999 Maternal thyroid deficiency during pregnancy and subsequent neuropsychological development of the child. *New England Journal of Medicine* **341** 549–555. (doi:10.1056/NEJM199908193410801)
- 9 Casey BM, Dashe JS, Wells CE, McIntire DD, Leveno KJ & Cunningham FG 2006 Subclinical hyperthyroidism and pregnancy outcomes. *Obstetrics and Gynaecology* **107** 337–341. (doi:10.1097/01.AOG.0000197991.64246.9a)
- 10 Schlumberger M, De Vathaire F, Travagli JP, Vassal G, Lemerle J, Parmentier C & Tubiana M 1987 Differentiated thyroid carcinoma in childhood: long term follow-up of 72 patients. *Journal of Clinical Endocrinology and Metabolism* **65** 1088–1094. (doi:10.1210/jcem-65-6-1088)

Received in final form 4 October 2016

Accepted 17 November 2016

CLINICAL QUESTION

Charting a course through the CEAs: diagnosis and management of medullary thyroid cancer

Christopher W. Rowe^{*†}, Cino Bendinelli^{†‡} and Shaun McGrath^{*}

^{*}Department of Endocrinology, John Hunter Hospital, [†]School of Medicine and Public Health, University of Newcastle, and

[‡]Department of Surgery, John Hunter Hospital, Newcastle, Australia

Summary

Medullary thyroid cancer (MTC) is an uncommon thyroid cancer that requires a high index of suspicion to facilitate diagnosis of early-stage disease amenable to surgical cure. The challenges of diagnosis, as well as management in the setting of persistent disease, are explored in the context of a case presenting with the incidental finding of elevated carcinoembryonic antigen (CEA) and an ¹⁸F-fluorodeoxyglucose positron emission tomography (¹⁸F-FDG-PET)-positive thyroid incidentaloma detected following treatment of colorectal cancer. Strategies to individualize prognosis, and emerging PET-based imaging modalities, particularly the potential role of ¹⁸F-DOPA-PET in staging, are reviewed.

(Received 29 February 2016; returned for revision 15 May 2016; accepted 22 May 2016)

Case vignette

A 60-year-old lady presented with an elevated CEA (948 ng/ml, reference <5) performed after resection of Stage IIIb colonic adenocarcinoma. Subsequent evaluation for colorectal metastases revealed an ¹⁸F-FDG-PET-avid 5-cm left thyroid nodule as the only abnormality (Fig. 1a). There was no family history of thyroid cancer or multiple endocrine neoplasia type 2 (MEN-2). She had a background of Hashimoto's hypothyroidism but was otherwise well.

Neck examination confirmed a large, firm left lobe nodule with no palpable lymphadenopathy, corresponding on ultrasound to a 55-mm solid, hypoechoic nodule with irregular margins, increased vascularity and no lymphadenopathy. Fine needle (FNA) biopsy under ultrasound guidance was unusually painful. Cytology demonstrated a hypercellular aspirate, with monomorphic cells, salt-and-pepper chromatin, finely granular cytoplasm and plasmacytic nuclei, typical of MTC. Calcitonin

immunostaining of these cells was strongly positive. Serum calcitonin was elevated at 14 443 pg/ml (reference <10). The cause of the elevated CEA was determined not to be from bowel, but from a large MTC presenting as an ¹⁸F-FDG-PET-avid thyroid incidentaloma. Prior to thyroidectomy, coincident pheochromocytoma and primary hyperparathyroidism were excluded, and it was subsequently confirmed that she did not carry a germline mutation in the REarranged during Transfection (RET) proto-oncogene.

How is MTC diagnosed?

Medullary thyroid cancer, named by the Cleveland Clinic pathologist John 'Beach' Hazard due to its 'solid' appearance,¹ arises from neuroendocrine parafollicular C-cells and represents around 2% of thyroid cancers, now relatively less common due to increased detection of papillary thyroid cancer.² About 80% present sporadically, most commonly as a solitary nodule (75–95%) in middle age, but 20% are associated with germline mutations in *RET* and MEN-2. Differentiated thyroid cancer (DTC) and MTC, based on American Joint Committee on Cancer TNM (AJCC) stage, have a similar prognosis (Fig. 2a). However, whereas 80% of DTC are diagnosed at Stage I or II, with 10 year survival 99% and 85% respectively,³ 60% of MTC are diagnosed at Stage III or IV, with 10 year survival 70% and 20% respectively (Figure 2B).⁴

Early diagnosis with complete surgical resection offers the best chance of cure, so a high index of suspicion is required for timely detection of this uncommon cancer. Clinical clues to MTC include the following: a nodule in the upper third of the thyroid lobe (corresponding to the anatomical distribution of C-cells⁵), a painful solid nodule by palpation or biopsy,⁶ elevation in a serological marker such as calcitonin or CEA or the presence of a secretory syndrome (e.g. flushing, diarrhoea) due to tumoural secretion of vasoactive substances or ACTH. Sonographic appearance is less predictive of malignancy than for DTC,⁷ and FNA biopsy has a lower sensitivity than in DTC due to misreporting as follicular lesions, Hurthle-cell change or nondiagnostic, which can be improved by routine calcitonin immunostaining of FNA samples, or calcitonin assay on FNA needle rinse.^{8–10}

The routine use of serum calcitonin as a screening tool for MTC in the presence of thyroid nodules remains controversial,

Correspondence: Christopher W Rowe, Department of Endocrinology, John Hunter Hospital, Locked Bag 1, HRMC, Newcastle, Australia, 2310. Tel.: +61249214380; E-mail: christopher.rowe@hnehealth.nsw.gov.au

Fig. 1 (a) Prethyroidectomy ^{18}F -FDG-PET demonstrating an avid lesion in the left thyroid lobe. (b) Postthyroidectomy ^{18}F -DOPA-PET demonstrating avidity in a level VII node.

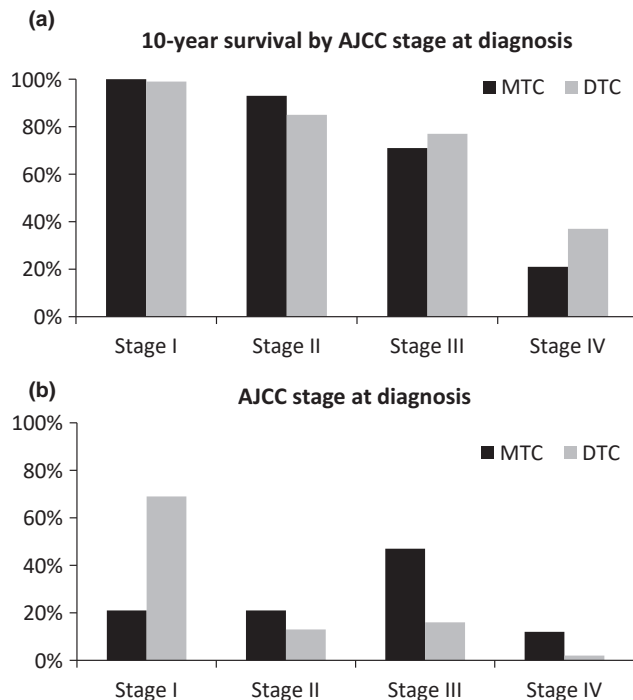
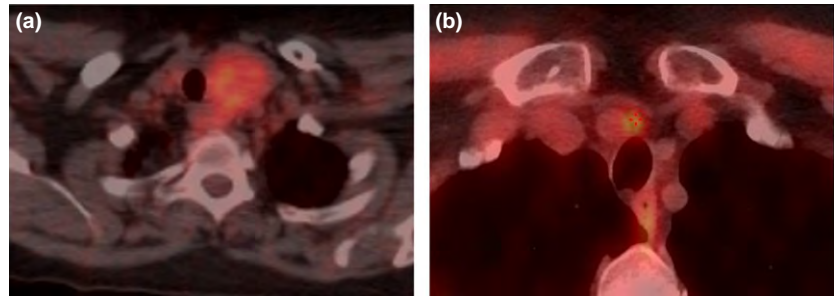


Fig. 2 (a) Prognosis of differentiated thyroid cancer (DTC) and medullary thyroid cancer (MTC) by AJCC stage at diagnosis. (b) AJCC stage at diagnosis for DTC and MTC. Data combined from studies by Sciuto *et al.*³ and Modigliani *et al.*⁴

with guidelines lacking consensus.^{2,11} Calcitonin screening has been shown to improve cure rate compared to unmatched historical controls.¹² However, due to the low incidence of MTC in nodular thyroid disease, most positive screening calcitonin results are false positives, requiring either confirmatory stimulatory testing with pentagastrin or calcium, close follow-up or diagnostic surgery.¹³

Case vignette

At total thyroidectomy, the recurrent laryngeal nerve passed through the tumour and was sacrificed (AJCC Stage IV). Prophylactic bilateral level VI clearance, now a standard of care,² yielded seven ipsilateral nodes positive for micrometastatic disease. Prophylactic compartment-oriented lateral neck dissection in the absence of visible disease remains controversial, and management should be individualized. Both pre-operative calcitonin

level and the primary tumour size correlate positively with the likelihood of lateral neck nodal involvement, but negatively with the chance of biochemical cure following resection, and should be factored into surgical planning.^{14,15} This patient's large primary tumour (55 mm) and high pre-operative calcitonin make lateral neck disease highly likely although there were no abnormal nodes identified on sonography. After discussion, a staged bilateral modified radical neck dissection was performed 6 months after initial thyroidectomy and 3 months after adjuvant chemotherapy for colorectal cancer, yielding two microscopically involved nodes ipsilateral to the primary tumour. Serum calcitonin fell from 14 443 pg/ml to 230 pg/ml after primary surgery, then stabilized at 120 pg/ml 6 months after the second procedure. Restaging with neck ultrasound, computed tomography (CT) neck, chest and abdomen, and ^{18}F -FDG-PET were all negative. She was asymptomatic.

Fluorine-18-dihydroxyphenylalanine (^{18}F -DOPA)-PET showed avidity in two level VII lymph nodes on the right, with no other disease identified (Fig. 1b). On this basis, she proceeded to compartment-oriented redo neck exploration, yielding eight positive lymph nodes containing metastatic deposits, of 13 resected. Calcitonin fell postoperatively to 63 pg/ml.

How should a patient with stage IV disease and detectable calcitonin following initial neck surgery be managed?

Prognostic factors

An initial prognostic category can be assigned following surgery. The group with undetectable calcitonin 6 months post surgery has a 98% 10-year survival and can be followed with annual ultrasound and tumour markers.^{2,4} Detectable calcitonin postoperatively confers 70% 10-year survival. In this group, age greater than 40¹⁶ and increasing AJCC TNM stage¹⁷ confer worse prognosis. However, the current binary classification of involved lymph nodes at surgery (N1a, limited to the central compartment; N1b, involving the lateral neck) has been shown to be less prognostically useful than the total number of involved lymph nodes, which correlates linearly with the risk of distant metastases.¹⁸ The presence of the somatic *RET* codon mutation M918T is associated with more aggressive disease, but may also predict response to tyrosine kinase therapy.¹⁹

Individual tumour growth is highly variable, and the doubling time of calcitonin or CEA (less than 6 months, 6 months to

2 years, greater than 2 years) allows restratification of prognosis over time. Calcitonin doubling time greater than 2 years suggests an indolent tumour with an excellent long-term prognosis.¹⁷

Imaging for residual disease

Serum calcitonin above 150 pg/ml is a suggested threshold to consider imaging for residual or recurrent disease.² Conventional structural imaging has an established role, with comprehensive assessment requiring neck ultrasound, CT of the chest, liver imaging with either ultrasound, CT or magnetic resonance imaging (MRI), and bone assessment with both scintigraphy and axial MRI. Isolated structural disease should be considered for resection if amenable.

There is a growing body of evidence that PET tracers, particularly ¹⁸F-FDG and ¹⁸F-DOPA, may have a complementary role in staging and prognosis of advanced MTC. MTCs, like other neuroendocrine cells, take up the amine precursor DOPA via surface LAT1 transporters, which are often upregulated in neuroendocrine tumours.²⁰ Consequently, Treglia *et al.*²¹ showed ¹⁸F-DOPA-PET to be the most sensitive modality for detecting residual or recurrent MTC in a head-to-head study of 18 patients with detectable calcitonin following thyroidectomy, compared with ¹⁸F-FDG-PET, ⁶⁸Ga-DOTA(NOC/TOC)-PET and conventional imaging.

Despite lower sensitivity, lesions that are ¹⁸F-FDG-PET-avid appear to have prognostic significance. Verbeek *et al.*²² studied 47 patients following thyroidectomy for MTC, followed by ¹⁸F-FDG-PET and ¹⁸F-DOPA-PET. They showed that FDG-avid lesions correlated with shorter calcitonin and CEA doubling time as well as reduced survival, whereas this was not apparent with ¹⁸F-DOPA-PET. Thus, these modalities may have a complementary role, with ¹⁸F-DOPA-PET maximizing sensitivity to exclude additional metastatic disease that would dissuade surgical management and ¹⁸F-FDG-PET conferring prognostic information. However, the routine use of these modalities remains under study.²

Surgery

The decision for re-operation in a patient with identified residual structural disease in the neck must always be individualized. Large series have shown normalization of serum calcitonin in 28–38% of patients,²³ although improved long-term survival has not been shown. Prevention of morbidity from invasion of local structures remains a key indication for surgery. In patients where recurrence is limited to the neck, compartment-oriented resection is recommended,² although there are no randomized trials to validate this approach.

Before embarking on neck surgery with curative intent, it is crucial to exclude the presence of distant metastases. Occult liver lesions are difficult to detect, and if imaging is negative, laparoscopic evaluation and biopsy of the liver should be considered.^{2,23} Further studies examining the utility of ¹⁸F-DOPA-PET in this context are required.

Local or systemic therapies

Adjunctive radioiodine is not indicated in MTC as neuroendocrine cells lack the Na/I symporter. There have been no prospective trials examining the role of external beam radiotherapy in MTC,² and it is usually reserved for patients deemed at high risk of locoregional recurrence. Systemic treatment with small molecule tyrosine kinase inhibitors (vandetanib, cabozatanib) has been shown to slow disease progression but not yet influence overall survival.^{19,24} Treatment is currently reserved for patients with rapidly progressive metastatic disease, or significant symptoms, usually due to hormonally active tumours.^{2,25}

Conclusions

The rarity of MTC and the propensity towards advanced disease at presentation necessitates that clinicians have a high index of suspicion to diagnose MTC at an early stage that is amenable to surgical cure. Clinicians should consider additional screening and diagnostic tests for MTC in patients presenting with suspicious thyroid nodules and utilize clinical clues for aggressive case finding. In the absence of surgical cure, subsequent management decisions including further surgery or systemic therapies must be individualized, best occurring in the context of a multidisciplinary team at an experienced centre. A stepwise approach, guided by established prognostic tools such as stage, postoperative calcitonin and calcitonin doubling time, but also emerging modalities such as ¹⁸F-FDG- and ¹⁸F-DOPA-PET, should be used to guide treatment.

Acknowledgements

Patient consent was obtained for publication of information contained in this case vignette. This work was supported by the Hunter New England Clinical Research Fellowship Scheme and the AVANT Mutual Group Doctors-in-Training Research Scholarship Program (to CR).

References

- 1 Hazard, J.B., Hawk, W.A. & Crile, G. Jr (1959) Medullary (solid) carcinoma of the thyroid; a clinicopathologic entity. *Journal of Clinical Endocrinology and Metabolism*, **19**, 152–161.
- 2 Wells, S.A. Jr, Asa, S.L., Dralle, H. *et al.* (2015) Revised American Thyroid Association guidelines for the management of medullary thyroid carcinoma. *Thyroid*, **25**, 567–610.
- 3 Sciuto, R., Romano, L., Rea, S. *et al.* (2009) Natural history and clinical outcome of differentiated thyroid carcinoma: a retrospective analysis of 1503 patients treated at a single institution. *Annals of Oncology*, **20**, 1728–1735.
- 4 Modigliani, E., Cohen, R., Campos, J.M. *et al.* (1998) Prognostic factors for survival and for biochemical cure in medullary thyroid carcinoma: results in 899 patients. The GETC Study Group. Groupe d'étude des tumeurs a calcitonine. *Clinical Endocrinology (Oxford)*, **48**, 265–273.
- 5 Wolfe, H.J., Voelkel, E.F. & Tashjian, A.H. Jr (1974) Distribution of calcitonin-containing cells in the normal adult human thyroid

- gland: a correlation of morphology with peptide content. *Journal of Clinical Endocrinology and Metabolism*, **38**, 688–694.
- 6 Guerrero, M.A., Lindsay, S., Suh, I. *et al.* (2011) Medullary thyroid cancer: it is a pain in the neck? *Journal of Cancer*, **2**, 200–205.
 - 7 Trimboli, P., Nasrollah, N., Amendola, S. *et al.* (2012) Should we use ultrasound features associated with papillary thyroid cancer in diagnosing medullary thyroid cancer? *Endocrine Journal*, **59**, 503–508.
 - 8 Trimboli, P., Treglia, G., Guidobaldi, L. *et al.* (2015) Detection rate of FNA cytology in medullary thyroid carcinoma: a meta-analysis. *Clinical Endocrinology (Oxford)*, **82**, 280–285.
 - 9 Kudo, T., Miyauchi, A., Ito, Y. *et al.* (2007) Diagnosis of medullary thyroid carcinoma by calcitonin measurement in fine-needle aspiration biopsy specimens. *Thyroid*, **17**, 635–638.
 - 10 Chang, T.C., Wu, S.L. & Hsiao, Y.L. (2005) Medullary thyroid carcinoma: pitfalls in diagnosis by fine needle aspiration cytology and relationship of cytomorphology to RET proto-oncogene mutations. *Acta Cytologica*, **49**, 477–482.
 - 11 Costante, G. & Filetti, S. (2011) Early diagnosis of medullary thyroid carcinoma: is systematic calcitonin screening appropriate in patients with nodular thyroid disease? *The Oncologist*, **16**, 49–52.
 - 12 Elisei, R., Bottici, V., Luchetti, F. *et al.* (2004) Impact of routine measurement of serum calcitonin on the diagnosis and outcome of medullary thyroid cancer: experience in 10,864 patients with nodular thyroid disorders. *Journal of Clinical Endocrinology and Metabolism*, **89**, 163–168.
 - 13 Costante, G., Meringolo, D., Durante, C. *et al.* (2007) Predictive value of serum calcitonin levels for preoperative diagnosis of medullary thyroid carcinoma in a cohort of 5817 consecutive patients with thyroid nodules. *Journal of Clinical Endocrinology and Metabolism*, **92**, 450–455.
 - 14 Machens, A. & Dralle, H. (2010) Biomarker-based risk stratification for previously untreated medullary thyroid cancer. *Journal of Clinical Endocrinology and Metabolism*, **95**, 2655–2663.
 - 15 Moley, J.F. & DeBenedetti, M.K. (1999) Patterns of nodal metastases in palpable medullary thyroid carcinoma: recommendations for extent of node dissection. *Annals of Surgery*, **229**, 880.
 - 16 Saad, M.F., Ordonez, N.G., Rashid, R.K. *et al.* (1984) Medullary carcinoma of the thyroid. A study of the clinical features and prognostic factors in 161 patients. *Medicine (Baltimore)*, **63**, 319–342.
 - 17 Barbet, J., Campion, L., Kraeber-Bodere, F. *et al.* (2005) Prognostic impact of serum calcitonin and carcinoembryonic antigen doubling-times in patients with medullary thyroid carcinoma. *Journal of Clinical Endocrinology and Metabolism*, **90**, 6077–6084.
 - 18 Machens, A. & Dralle, H. (2013) Prognostic impact of N staging in 715 medullary thyroid cancer patients: proposal for a revised staging system. *Annals of Surgery*, **257**, 323–329.
 - 19 Wells, S.A. Jr, Robinson, B.G., Gagel, R.F. *et al.* (2012) Vandetanib in patients with locally advanced or metastatic medullary thyroid cancer: a randomized, double-blind phase III trial. *Journal of Clinical Oncology*, **30**, 134–141.
 - 20 Santhanam, P. & Taieb, D. (2014) Role of (18) F-FDOPA PET/CT imaging in endocrinology. *Clinical Endocrinology (Oxford)*, **81**, 789–798.
 - 21 Treglia, G., Castaldi, P., Villani, M.F. *et al.* (2012) Comparison of 18F-DOPA, 18F-FDG and 68 Ga-somatostatin analogue PET/CT in patients with recurrent medullary thyroid carcinoma. *European Journal of Nuclear Medicine and Molecular Imaging*, **39**, 569–580.
 - 22 Verbeek, H.H., Plukker, J.T., Koopmans, K.P. *et al.* (2012) Clinical relevance of 18F-FDG PET and 18F-DOPA PET in recurrent medullary thyroid carcinoma. *Journal of Nuclear Medicine*, **53**, 1863–1871.
 - 23 Moley, J.F., DeBenedetti, M.K., Dilley, W.G. *et al.* (1998) Surgical management of patients with persistent or recurrent medullary thyroid cancer. *Journal of Internal Medicine*, **243**, 521–526.
 - 24 Elisei, R., Schlumberger, M.J., Muller, S.P. *et al.* (2013) Cabozantinib in progressive medullary thyroid cancer. *Journal of Clinical Oncology*, **31**, 3639–3646.
 - 25 Haddad, R.I. (2013) How to incorporate new tyrosine kinase inhibitors in the treatment of patients with medullary thyroid cancer. *Journal of Clinical Oncology*, **31**, 3618–3620.



Contents available at ScienceDirect

Diabetes Research
and Clinical Practicejournal homepage: www.elsevier.com/locate/diabresInternational
Diabetes
Federation

Insulin resistance correlates with maculopathy and severity of retinopathy in young adults with Type 1 Diabetes Mellitus

C.W. Rowe^{a,b,*}, A.S. Haider^{b,c}, D. Viswanathan^c, M. Jones^d, J. Attia^{b,d}, K. Wynne^{a,b}, S. Acharya^{a,b}

^a Department of Endocrinology and Diabetes, John Hunter Hospital, Newcastle, Australia

^b School of Medicine and Public Health, University of Newcastle, Callaghan, Australia

^c Department of Ophthalmology, John Hunter Hospital, Newcastle, Australia

^d Clinical Research Design, IT, and Statistical Support (CReDITSS) Unit, Hunter Medical Research Institute, Newcastle, Australia

ARTICLE INFO

Article history:

Received 2 March 2017

Received in revised form
19 May 2017

Accepted 15 June 2017

Available online 27 June 2017

Keywords:

Type 1 Diabetes Mellitus

Insulin resistance

Diabetic retinopathy

Diabetic maculopathy

ABSTRACT

Aims: To assess the relationship between insulin resistance (IR), retinopathy and maculopathy in young adults with Type 1 diabetes mellitus.

Methods: A cross-sectional study at a regional Australian tertiary hospital. Retinal pathology, assessed by colour fundus photography, was correlated with two surrogate measures of IR: estimated Glucose Disposal Rate (eGDR) and Insulin Sensitivity Score (ISS), where lower scores reflect greater IR.

Results: 107 patients were recruited, with mean age 24.7 years, 53% male, and mean duration of disease 10.8 years. Mean eGDR scores (5.6 vs 8.0 $p < 0.001$) and ISS (4.7 vs 7.9, $p < 0.001$) were lower in subjects having at least moderate non-proliferative diabetic retinopathy (NPDR; relative to nil/mild-NPDR). Similarly, mean eGDR (4.2 vs 6.2, $p = 0.001$) and ISS (3.8 vs 6.1, $p = 0.003$) were lower in patients with maculopathy. Multivariate logistic regression modelling was used to control for confounding. For retinopathy severity, a unit increase in eGDR or ISS (representing lower IR) was associated with a 50% decrease in odds of moderate-NPDR or worse (eGDR OR 0.5, 95%CI 0.32–0.77, $p = 0.002$; ISS OR 0.49, 95%CI 0.29–0.84, $p = 0.01$). A unit increase in eGDR or ISS was associated with a 46–56% decrease in odds of maculopathy (eGDR OR 0.54, 95%CI 0.37–0.81, $p = 0.003$; ISS OR 0.44, 95%CI 0.22–0.88, $p = 0.02$).

Conclusions: IR correlates with more severe retinopathy in young adults with Type 1 DM. This is the first description of a correlation between IR and maculopathy in Type 1 DM, warranting further evaluation. Prospective studies examining whether reducing IR can improve microvascular complications are required.

© 2017 Elsevier B.V. All rights reserved.

* Corresponding author at: Department of Endocrinology and Diabetes, John Hunter Hospital, Lookout Road, New Lambton Heights, Newcastle, Australia.

E-mail address: Christopher.Rowe@hnehealth.nsw.gov.au (C.W. Rowe).

<http://dx.doi.org/10.1016/j.diabres.2017.06.022>

0168-8227/© 2017 Elsevier B.V. All rights reserved.

1. Introduction

Type 1 Diabetes Mellitus (Type 1 DM) is an autoimmune disease manifesting as hyperglycaemia, due to immune-mediated destruction of insulin-producing pancreatic beta-cells. Increasingly, a subset of patients develop insulin resistance (IR), or 'double diabetes', combining the pathophysiology of insulin deficiency in Type 1 DM and IR, more commonly associated with Type 2 DM [1].

IR in Type 1 DM is common, affecting 26% of children and adolescents with Type 1 DM [2]. Further, obesity in adolescents and adults with Type 1 DM has rapidly increased. A longitudinal study of 589 adults with Type 1 DM in Pittsburgh found the age-specific prevalence of overweight and obesity in 40–49 year olds was 25% in 1986–88, and 68.2% in 2004–07, with a 10-fold increase in the proportion of obese subjects [3]. Intensification of insulin therapy is known to correlate with weight gain and central adiposity [4], with participants in the intensive arm of the Diabetes Control and Complications Trial (DCCT) gaining, on average, 4.6 kg more than patients who received conventional therapy over 5 years [5]. Societal trends towards sedentary behaviors and calorie-dense nutrition are paralleled in patients with Type 1 DM.

HOMA-IR, frequently used in assessment of IR [6], is not well validated for use in subjects treated with insulin, precluding its use in patients with Type 1 DM [7]. The gold standard for assessing IR in Type 1 DM is rate of glucose disposal at euglycaemic-hyperinsulinaemic clamp. Clamp studies in young adults with Type 1 DM have associated IR with increased carotid media intimal thickness [8], and with dyslipidaemia across multiple age-groups [9]. However due to resource utilization and patient tolerability, clamp studies are impractical for large population studies. Regression modelling based on clamp data performed by two groups has independently derived similar formulae for estimating glucose disposal in Type 1 DM: the estimated Glucose Disposal Rate (eGDR) [10], and the Insulin Sensitivity Score (ISS) [11].

IR, as measured by eGDR, has been associated with development of microvascular and macrovascular disease in the Pittsburgh EDC Study [12–14], microvascular disease in a reanalysis of DCCT data [15], and with microvascular disease in cross sectional studies [16–18]. IR, measured by ISS is correlated with risk factors for cardiovascular disease [19].

However, few studies have evaluated the relationship specifically between IR and retinal complications in Type 1 DM [20,21]. Retinopathy (DR) is an important cause of morbidity in Type 1 DM, and strongly correlates with glycaemic control [5]. Further, the relationship between IR and diabetic maculopathy (DMc), referring to retinopathy affecting the macula, has not been examined in Type 1 DM. DMc may occur at any stage of DR and is the leading cause of visual loss in patients with diabetes [22].

This study aimed to explore the relationship between validated surrogate measures of IR (eGDR and ISS) and the presence of DR and DMc in a cohort of adolescents and young adults with Type 1 DM.

2. Subjects

Patients attending a regional tertiary hospital young adult outpatients clinic for routine care of Type 1 DM were recruited. The clinic provides multidisciplinary care for a mixed urban and rural catchment of predominantly Caucasian ethnicity. The Human Research Ethics Committee approved a waiver of consent for retrospective review of an historical cohort. All prospectively enrolled participants provided written informed consent. From August 2015 to March 2016, clinic attendees were invited to participate in a prospective cross-sectional study. Additionally, a medical records database was searched to identify all clinic attendees in the 2014 calendar year aged 18–30 years. The clinical records gave us baseline population characteristics, which were compared to the participants in the cross-sectional study to identify potential selection bias.

3. Materials and methods

Consenting participants had demographic and disease specific information recorded by a study nurse. Waist circumference was measured according to WHO criteria as a measurement taken parallel to the floor at the midpoint between the top of the iliac crest and lower margin of the last palpable rib in the mid-axillary line [23]. Colour fundus (retinal) photography was chosen as the outcome measure for microvascular disease as a simple, reproducible and objective measure of early stage retinal disease. Clinic-based non-dilated fundus photographs were obtained by a trained retinal photographer and qualified orthoptist using a Topcon retinal camera (TRC NW8; Topcon Corporation, Tokyo, Japan). Two single field 45° images centred on the macula and optic disc were taken in each eye, with additional images taken in the presence of significant pathology.

Retinal photographs were graded by two independent and experienced ophthalmology fellows who were blinded to patient characteristics. The eye with the worst grade of disease determined the score. Discordant grading was adjudicated by consensus. Images were classified in two ways: (i) degree of DR and (ii) presence or absence of DMc. The level of DR was graded as no DR; mild, moderate or severe non-proliferative DR (NPDR); and proliferative DR, based on the International Classification of DR (ICDR) Disease Severity Scale [24] (Supplementary Table 1). Mild or minimal DR was defined as microaneurysms only; moderate DR as microaneurysms with additional signs of background retinopathy (i.e. intraretinal haemorrhages or exudates) but to a lesser extent than severe DR; severe DR as any intraretinal vascular abnormalities (IRMA), venous beading and/or extensive intraretinal haemorrhages assessed as more than 20 in each quadrant in the absence of proliferative DR; and proliferative DR as any evidence of new vessel growth.

DMc was graded as absent or present based on the presence of hard exudates within one disc diameter (1500 µm) of the macula in images with DR, a surrogate measure that has been validated in several studies [25].

To estimate IR, two independently derived models of glucose disposal were used. Estimated glucose disposal rate

(eGDR, $\text{mg kg}^{-1} \text{min}^{-1}$), was calculated using the formula validated by Williams in an adult, multi-ethnic population of patients with Type 1 DM [10,18]: $\text{eGDR} = 21.158 + (-0.09 \times \text{WC}) + (-3.407 \times \text{HTN}) + (-0.551 \times \text{HbA1c})$, where WC is waist circumference measured in centimeters; HTN is hypertensive status, defined as systolic blood pressure >140 mmHg or diastolic blood pressure >90 mmHg or treatment with anti-hypertensive pharmacotherapy; and HbA1c is percent glycosylation of haemoglobin (to convert% to mmol/mol, multiply by 10.93 and subtract 23.5). Insulin Sensitivity Score (ISS) was calculated using Dabela's equation, validated in an adolescent, majority non-Hispanic white population of Type 1 DM [2,11]: $\text{ISS} = \exp[4.64725 - (0.02032 \times \text{WC}) - (0.09779 \times \text{HbA1c}) - (0.20815 \times \text{TG})]$, where TG is triglycerides measured in mmol/L (to convert to mg/dL, divide by 88.57396); other parameters are as for eGDR. Lower scores for both parameters reflect increased IR.

3.1. Statistical analysis

To establish that the prospective cohort was not substantively different from the broader group of clinic patients, we compared demographic and clinical characteristics to the historical cohort.

For the outcomes of interest, namely presence of retinopathy ('nil'/'present'), severity of retinopathy ('nil or mild'/'moderate or worse') and diabetic maculopathy ('nil'/'present'), we

provide group level means for eGDR, ISS and other biomarkers of retinal pathology. We compared group means with Student's *t* tests and a Bonferroni correction for multiple comparisons.

We examined the relationship between eGDR and ISS using a generalized linear model (Gaussian family, log link).

To explore the association between DR, DMc, and biomarkers of retinal pathology we fitted separate multivariate logistic regression models for eGDR and ISS with additional covariates for duration of diabetes, age, smoking and gender, but not blood pressure or lipids, as these parameters are included in the eGDR/ISS models. Analyses were based on complete cases.

We assessed the discriminative value of eGDR and ISS for DR and DMc against duration of disease, HbA1c, BMI and hypertension with receiver operating characteristic (ROC) curves. The analyses were performed using Stata (version 14.1, Statacorp, Texas USA).

4. Results

From August 2015 to March 2016, 157 clinic attendees were prospectively enrolled in the cross-sectional study (58% of total clinic attendees over that period), of whom 107 completed the study visit. Demographic characteristics for the prospective cohort and historical retrospective cohort are presented in Table 1. We found no significant differences (at the

Table 1 – Baseline characteristics of entire clinic cohort (historical) and prospectively recruited sample. P values represent the probability of a true difference in the measured parameter between the two populations.

Parameter	Historical Cohort (2014)	Actual Cohort (2015/2016)	p
n	163	107	
Age (mean, SD)	23.5 (3.61)	24.7 (6.0)	0.04
Male:Female Ratio	0.53:0.47	0.54:0.46	0.87
Years since diagnosis (mean, SD)	10.10 (5.9)	10.8 (6.8)	0.37
Subcutaneous insulin pump users (n,%)	38 (23%)	33 (31%)	0.14
Weight, kg (mean, SD)	77.3 (17.3)	78.9 (20.0)	0.48
BMI, kg/m^2 (mean, SD)	26.2 (5.04)	26.8 (5.5)	0.36
Current tobacco use (n,%)	16 (10%)	11 (10%)	0.95
HbA1c, %; mmol/mol (mean, SD)	8.6 (2.0); 70 (21)	8.2 (1.4); 66 (15)	0.07
Systolic BP, mmHg (mean, SD)	118 (14)	126 (15)	< 0.01
Diastolic BP, mmHg (mean, SD)	73 (11)	79 (9)	< 0.01
Cholesterol, mmol/L (mean, SD)	4.9 (1.1)	4.7 (1.1)	0.15
Triglycerides, mmol/L (mean, SD)	1.4 (1.0)	1.13 (0.70)	0.01
Albuminuria (n,%)	17/128 (13%)	13/96 (14%)	0.82
Retinopathy (n,%)			
Nil	97 (60%)	65 (61%)	0.87
NPDR, mild	30 (18%)	16 (15%)	
NPDR, moderate	20 (12%)	9 (8%)	
NPDR, severe	3 (2%)	2 (2%)	
Proliferative DR	2 (1%)	4 (4%)	
Missing data	11 (7%)	11 (10%)	
Other retinal pathology (n,%)			
Diabetic maculopathy	9/152 (6%)	8/96 (8%)	0.54
Prior photocoagulation	1/152 (1%)	3/96 (3%)	0.24

NPDR: Non-proliferative diabetic retinopathy. DR: Diabetic Retinopathy.

* Missing data in actual cohort due to absent images (n = 10) and ungradable images (n = 1). Comparison of parameters in Actual Cohort by 'Missing data' status showed no significant between group differences for all parameters, except lower weight among subjects with missing retinal photographs (p = 0.02).

0.05 level) between the 107 participants used in this study and the historical cohort of 163 clinic attendees in 2014 (duplicate participants were excluded) with respect to important potential confounders of gender ($p = 0.87$), weight ($p = 0.48$), BMI ($p = 0.36$), HbA1c ($p = 0.07$) and duration of disease ($p = 0.37$). Differences were observed in age, blood pressure and triglycerides. While we could compute eGDR for all 107 participants, we were able to compute ISS for only 97 participants due to missing data. Regression modelling demonstrated a high degree of correlation between eGDR and ISS scores (Supplementary Fig. 1).

Table 2 shows the means and standard deviations of established biomarkers by group membership for presence of DR (nil/present), severity of DR (nil or mild/moderate or worse) and DMc (nil/present). Significant differences (at the family-wise 0.05 level = 0.05/18) in the eGDR means were found for the severity of DR (8.0 vs 5.6, $p < 0.001$) and DMc (7.9 vs 4.7, $p < 0.001$) comparisons. We found analogous differences in the ISS means for the severity of DR (6.2 vs 4.2, $p = 0.001$) and DMc (6.1 vs 3.8, $p = 0.003$) comparisons. Differences were also found in the means for HbA1c (8.1% (65 mmol/mol) vs 9.2% (77 mmol/mol), $p = 0.003$) and duration of disease (15.8 vs 9.9 years, $p = 0.002$) for severity of DR and waist circumference (109.9 cm vs 91.9 cm, $p = 0.001$) and duration of disease (17.4 vs 10.2 years, $p = 0.005$) for DMc comparisons.

Table 3 provides the odds-ratios, 95% confidence intervals and p -values from multivariate logistic regression models examining the association between the retinopathy and maculopathy outcomes and the eGDR and ISS biomarkers adjusted for potential confounders of duration of disease, age, gender and smoking status. For retinopathy severity, a unit increase in eGDR (representing lower IR) was associated with a 50% decrease in the odds of moderate NPDR or worse (OR 0.5, 95%CI 0.32–0.77, $p = 0.002$). Similarly a unit increase in ISS was associated with a 51% decrease in the odds of moderate NPDR or worse (OR 0.49, 95%CI 0.29–0.84, $p = 0.01$). For the maculopathy outcome, a unit increase in eGDR was associated with a 46% decrease in the odds of moderate NPDR or worse (OR 0.54, 95%CI 0.37–0.81, $p = 0.003$). Similarly a unit increase in ISS was associated with a 56% decrease in the odds of moderate NPDR or worse (OR 0.44, 95% CI 0.22–0.88, $p = 0.02$). These results were consistent with the comparison of means in Table 2.

The Area Under the ROC curve (AUROC) for eGDR (0.81, 95% CI 0.70–0.92) and ISS (0.78, 95% CI 0.66–0.91) were not significantly different (at the 0.05 level) when compared to the AUROC for duration of disease (0.78, 0.64–0.88, $p = 0.64$). IR also was similar in discrimination of DMc (AUROC 0.84 (0.68–1) and 0.83 (0.70–0.95) for eGDR and ISS respectively, compared to 0.80 (0.64–0.95) for duration of disease ($p = 0.45$) (Table 4, Fig. 1).

5. Discussion

This study identifies a strong association between severity of DR and IR, based on two previously established surrogate markers of IR in a cohort of young adults with Type 1 DM, controlled for potential confounders. This finding is in agreement with other studies, although most studies have defined

Table 2 – Group means and comparison of means for established biomarkers for retinopathy and maculopathy. Lower scores of eGDR and ISS represent increased insulin resistance.

Parameter	eGDR	p	ISS	p	BMI kg/m ²	p	HbA1c %	p	Waist circ. (cm)	p	Duration (years)	p
Presence of Retinopathy		0.07		0.09		0.2		0.03		0.41		0.0001
Nil	7.9 (2.2)		6.2 (2.1)		26.6 (5.2)		8.0 (1.4)		92.5 (15.4)		9.0 (7.0)	
Present	7.0 (2.5)		5.4 (2.2)		28.3 (6.4)		8.7 (1.3)		95.3 (15.9)		14.7 (4.9)	
Severity of Retinopathy		0.0002		0.001		0.21		0.003		0.07		0.002
Nil or Mild NPDR	8.0 (2.2)		6.2 (2.1)		26.7 (5.2)		8.1 (1.4)		92.0 (15.0)		9.9 (6.9)	
Moderate NPDR or worse	5.6 (2.3)		4.2 (1.5)		29.4 (7.6)		9.2 (1.1)		100.9 (16.7)		15.8 (4.6)	
Diabetic Maculopathy		0.0001		0.003		0.11		0.22		0.001		0.005
Nil	7.9 (2.2)		6.1 (2.1)		26.6 (5.1)		8.2 (1.4)		91.9 (6.2)		10.2 (6.7)	
Present	4.7 (2.5)		3.8 (1.3)		32.5 (9.0)		8.9 (0.9)		109.9 (1.5)		17.4 (5.2)	

Data is mean (SD). NPDR: Non-proliferative diabetic retinopathy. PDR: Proliferative diabetic retinopathy. eGDR (estimated glucose disposal rate; mg/kg/min). ISS: Insulin sensitivity score. DM: Diabetes Mellitus. Duration: duration of diabetes. To convert HbA1c to mmol/mol multiply by 10.93 and subtract 23.5.

retinopathy presence/absence as a categorical variable [15–18]. While this study confirmed this trend (borderline significant at the 0.05 level), we noted a stronger relationship between severity of DR and IR in adolescents and young adults, confirming findings from two cross-sectional studies of older adults (mean age 45–46 years) in Romania [20,21]. The reproducibility of these findings across ages and ethnicities supports the generalizability of this association.

A new finding from our study is the association between DMc and IR in Type 1 DM. The presence of DMc was highly associated with IR using both the eGDR and ISS scores, with a 1 unit decrease in IR reducing the odds of maculopathy by 45% and 57% respectively (Table 3). Macular edema in diabetes has a complex pathophysiology, with disruption of the blood-retinal barrier resulting in oxidative stress, inflammation and

vascular dysfunction as the final common pathway [26]. Hypertension and hyperlipidaemia, key features of metabolic syndrome, represent established risk factors for DMc [22], and it is possible that IR contributes to the underlying pathophysiology of this condition. IR has been associated with maculopathy in Type 2 DM [27], and DMc may be more common in Type 2 DM than Type 1 DM [28], supporting a possible causal link between IR and the development of DMc. To our knowledge, this is the first study demonstrating an association between IR and DMc in Type 1 DM.

This study highlights that IR was comparable, and perhaps slightly better, in its discriminative ability (measured by AUROC) for DR and DMc when compared with traditional biomarkers such as duration of diabetes and HbA1c (Fig. 1). This has several implications. First, it suggests a potential role

Table 3 – Crude and adjusted odds ratio estimates from logistic regression models examining the association between retinal pathology and insulin sensitivity. Higher values of eGDR and ISS reflect increased insulin sensitivity.

Outcome	Model	Odds Ratio and 95% CI		p-value (Adjusted OR)
		Crude	Adjusted	
Any Retinopathy	eGDR	0.84 (0.71–1.02)	0.80 (0.64–1.0)	0.05
	ISS	0.83 (0.66–1.03)	0.84 (0.64–1.10)	0.2
Moderate NPDR or worse	eGDR	0.67 (0.54–0.85)	0.50 (0.32–0.77)	0.002
	ISS	0.54 (0.37–0.81)	0.49 (0.29–0.84)	0.01
Diabetic Maculopathy	eGDR	0.61 (0.45–0.82)	0.54 (0.37–0.81)	0.003
	ISS	0.46 (0.26–0.81)	0.44 (0.22–0.88)	0.02

Crude model: IR parameter (eGDR or ISS) only.

Adjusted model accounts for effects of age, gender, duration of disease and smoking status.

Table 4 – AUROC for diagnostic performance of biomarkers for discrimination of retinal pathology.

Biomarker	Any Retinopathy		Moderate NPDR or worse		Diabetic Maculopathy	
	AUROC	95% CI	AUROC	95% CI	AUROC	95% CI
eGDR	0.65	0.52–0.77	0.81	0.70–0.92	0.84	0.68–1.0
ISS	0.62	0.49–0.75	0.78	0.66–0.91	0.83	0.70–0.95
Duration of diabetes (years)	0.75	0.64–0.85	0.78	0.64–0.88	0.8	0.64–0.95
HbA1c	0.68	0.57–0.63	0.74	0.61–0.86	0.67	0.50–0.83
Waist circumference	0.58	0.45–0.71	0.7	0.56–0.83	0.79	0.61–0.96
BMI	0.58	0.44–0.71	0.6	0.41–0.78	0.68	0.41–0.95

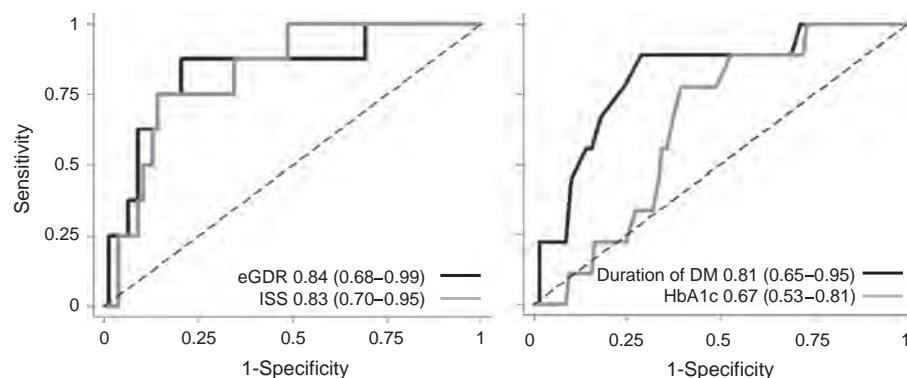


Fig. 1 – ROC Curves for discriminative value of eGDR and ISS (left panel) and conventional risk factors (right panel) in prediction of Diabetic Maculopathy. Legend shows AUROC with 95% CI.

for eGDR or ISS as a biomarker to identify patients appropriate for more intensive macular screening by an ophthalmologist, which may allow for earlier detection and appropriate treatment to prevent visual loss. Second, the possibility of minimising progression of DR and DMC by reducing IR must be considered, and follow up studies addressing this issue prospectively through weight loss or exercise strategies are required.

One strength of this study is the use of two independently derived algorithms for IR. Not only did the study demonstrate consistency of association between DR, DMC and IR using both algorithms, but it was also able to show a high degree of correlation between both measures (Supplementary Fig. 1). Both models were created as a 'best fit' for glucose disposal measured under hyperinsulinaemic-euglycaemic clamp, and were not developed as predictive scores for complications [10,11]. Hence, the observation in this study that both ISS and eGDR are highly correlated with each other is an important confirmation that these scores, which were developed and validated in different populations of Type 1 DM and incorporate different variables, may represent the same underlying biological variable. One previous study has examined this relationship in older adults with Type 1 DM in Brazil; the group did not stratify for hypertension and found a lower degree of correlation between the two scores [29].

Our study has some limitations. First, macular assessment was limited to non-stereoscopic fundus photography without optical coherence tomography. As such, it is possible the number of patients with true DMC were underestimated. Reduced visual acuity is associated with DMC, and is a useful adjunct to retinal examination to help prioritise ophthalmic referral [30], although was not assessed in this study. Second, some enrolled participants did not complete the study visit and were not included in analysis, potentially introducing bias. However, analysis of completers and non-completers showed no important differences in baseline characteristics between these groups. Finally, given the cross-sectional nature of our design, our study is not able to infer a causal link between IR and development of retinal pathology, or to show that reducing IR can modify the progression of DR and DMC over time.

6. Conclusions

This study suggests for the first time that IR may be associated with maculopathy in Type 1 DM, and extends evidence for a correlation between IR and DR into young adults. The relationship between IR and maculopathy must be confirmed in larger prospective studies. Further studies are needed to determine if reducing IR can impact complications.

Funding

This work was funded by a John Hunter Hospital Charitable Trust Grant and the Hunter New England Local Health District Clinical Research Fellowship (to CR).

Conflicts of interest

The authors declare they have no conflicts of interest.

Author contribution

CR conceived and designed the study with SA and KW; and drafted the manuscript. AH and DV interpreted retinal pathology. MJ and JA performed data analysis with CR and assisted with interpretation. All authors critically reviewed the manuscript and have approved the final version.

Acknowledgements

The authors would like to thank Mr Jeff Stormer (Research Nurse); Mr Chris Gialouris (Orthoptist); Dr Kiran Manku (Ophthalmologist and Medical Retinal Subspecialist) and the staff of the John Hunter Hospital Young Persons Clinic for invaluable assistance with this study.

Appendix A. Supplementary material

Supplementary data associated with this article can be found, in the online version, at <http://dx.doi.org/10.1016/j.diabres.2017.06.022>.

REFERENCES

- [1] Cleland SJ, Fisher BM, Colhoun HM, Sattar N, Petrie JR. Insulin resistance in type 1 diabetes: what is 'double diabetes' and what are the risks? *Diabetologia* 2013;56:1462–70.
- [2] Dabelea D, Pihoker C, Talton JW, D'Agostino Jr RB, Fujimoto W, Klingensmith GJ, et al. Etiological approach to characterization of diabetes type: the SEARCH for Diabetes in Youth Study. *Diabetes Care* 2011;34:1628–33.
- [3] Conway B, Miller RG, Costacou T, Fried L, Kelsey S, Evans RW, et al. Temporal patterns in overweight and obesity in Type 1 diabetes. *Diabet Med* 2010;27:398–404.
- [4] Purnell JQ, Zinman B, Brunzell JD. DCCT/EDIC Research Group. The effect of excess weight gain with intensive diabetes mellitus treatment on cardiovascular disease risk factors and atherosclerosis in type 1 diabetes mellitus: results from the Diabetes Control and Complications Trial/Epidemiology of Diabetes Interventions and Complications Study (DCCT/EDIC) study. *Circulation* 2013;127:180–7.
- [5] The Diabetes Control Complications Trial Research Group. The effect of intensive treatment of diabetes on the development and progression of long-term complications in insulin-dependent diabetes mellitus. *N Engl J Med* 1993;329:977–86.
- [6] Matthews DR, Hosker JP, Rudenski AS, Naylor BA, Treacher DF, Turner RC. Homeostasis model assessment: insulin resistance and beta-cell function from fasting plasma glucose and insulin concentrations in man. *Diabetologia* 1985;28:412–9.
- [7] Wallace TM, Levy JC, Matthews DR. Use and abuse of HOMA modeling. *Diabetes Care* 2004;27:1487–95.
- [8] Rathman B, Rosfors S, Sjöholm A, Nystrom T. Early signs of atherosclerosis are associated with insulin resistance in non-obese adolescent and young adults with type 1 diabetes. *Cardiovasc Diabetol* 2012;11:145.

- [9] Maahs DM, Nadeau K, Snell-Bergeon JK, Schauer I, Bergman B, West NA, et al. Association of insulin sensitivity to lipids across the lifespan in people with Type 1 diabetes. *Diabet Med* 2011;28:148–55.
- [10] Williams KV, Erbey JR, Becker D, Arslanian S, Orchard TJ. Can clinical factors estimate insulin resistance in type 1 diabetes? *Diabetes* 2000;49:626–32.
- [11] Dabelea D, D'Agostino Jr RB, Mason CC, West N, Hamman RF, Mayer-Davis EJ, et al. Development, validation and use of an insulin sensitivity score in youths with diabetes: the SEARCH for Diabetes in Youth study. *Diabetologia* 2011;54:78–86.
- [12] Olson JC, Erbey JR, Forrest KYZ, Williams K, Becker DJ, Orchard TJ. Glycemia (or, in women, estimated glucose disposal rate) predict lower extremity arterial disease events in type 1 diabetes. *Metabolism* 2002;51:248–54.
- [13] Orchard TJ, Chang YF, Ferrell RE, Petro N, Ellis DE. Nephropathy in type 1 diabetes: a manifestation of insulin resistance and multiple genetic susceptibilities? Further evidence from the Pittsburgh epidemiology of diabetes complication study. *Kidney Int* 2002;62:963–70.
- [14] Orchard TJ, Olson JC, Erbey JR, Williams K, Forrest KY, Smithline Kinder L, et al. Insulin resistance-related factors, but not glycemia, predict coronary artery disease in type 1 diabetes: 10-year follow-up data from the Pittsburgh Epidemiology of Diabetes Complications Study. *Diabetes Care* 2003;26:1374–9.
- [15] Kilpatrick ES, Rigby AS, Atkin SL. Insulin resistance, the metabolic syndrome, and complication risk in type 1 diabetes: “double diabetes” in the Diabetes Control and Complications Trial. *Diabetes Care* 2007;30:707–12.
- [16] Chillaron JJ, Goday A, Flores-Le-Roux JA, Benaiges D, Carrera MJ, Puig J, et al. Estimated glucose disposal rate in assessment of the metabolic syndrome and microvascular complications in patients with type 1 diabetes. *J Clin Endocrinol Metab* 2009;94:3530–4.
- [17] Girgis CM, Scalley BD, Park KE. Utility of the estimated glucose disposal rate as a marker of microvascular complications in young adults with type 1 diabetes. *Diabetes Res Clin Pract* 2012;96:e70–2.
- [18] Epstein EJ, Osman JL, Cohen HW, Rajpathak SN, Lewis O, Crandall JP. Use of the estimated glucose disposal rate as a measure of insulin resistance in an urban multiethnic population with type 1 diabetes. *Diabetes Care* 2013;36:2280–5.
- [19] Specht BJ, Wadwa RP, Snell-Bergeon JK, Nadeau KJ, Bishop FK, Maahs DM. Estimated insulin sensitivity and cardiovascular disease risk factors in adolescents with and without type 1 diabetes. *J Pediatr* 2013;162:297–301.
- [20] Duta I, Fica S, Ion DA. The association between insulin resistance and proliferative retinopathy in type 1 diabetes. *Rom J Intern Med* 2015;53:261–6.
- [21] Pop A, Clenciu D, Anghel M, Radu S, Socea B, Mota E, et al. Insulin resistance is associated with all chronic complications in type 1 diabetes. *J Diabetes* 2016;8:220–8.
- [22] Das A, McGuire PG, Rangasamy S. Diabetic macular Edema: pathophysiology and novel therapeutic targets. *Ophthalmology* 2015;122:1375–94.
- [23] World Health Organisation. Waist Circumference and Waist: Hip Ratio: Report of a WHO Expert Consultation. Geneva 2008.
- [24] Wong TC. ICO Guidelines for Diabetic Eye Care. <http://www.icoph.org/>: International Council of Ophthalmology 2016.
- [25] Litvin TV, Weissenberg CR, Daskivich LP, Zhou Q, Bresnick GH, Cuadros JA. Improving accuracy of grading and referral of diabetic macular edema using location and extent of hard exudates in retinal photography. *J Diabetes Sci Technol* 2015;10:262–70.
- [26] Romero-Aroca P. Targeting the pathophysiology of diabetic macular Edema. *Diabetes Care* 2010;33:2484–5.
- [27] Zapata MA, Badal J, Fonollosa A, Boixadera A, Garcia-Arumi J. Insulin resistance and diabetic macular oedema in type 2 diabetes mellitus. *Br J Ophthalmol* 2010;94:1230–2.
- [28] Zander E, Herfurth S, Bohl B, Heinke P, Herrmann U, Kohnert K, et al. Maculopathy in patients with diabetes mellitus type 1 and type 2: associations with risk factors. *Br J Ophthalmol* 2000;84:871–6.
- [29] Teixeira MM, Diniz MdFHS, Reis JS, Ferrari TCA, de Castro MGB, Teixeira BP, et al. Insulin resistance and associated factors in patients with Type 1 Diabetes. *Diabetol Metab Syndr* 2014;6:131.
- [30] Ciulla TA, Amador AG, Zinman B. Diabetic retinopathy and diabetic macular Edema. Pathophysiology, screening, and novel therapies 2003;26:2653–64.

SCIENTIFIC REPORTS

OPEN

The neurotrophic tyrosine kinase receptor TrkA and its ligand NGF are increased in squamous cell carcinomas of the lung

Fangfang Gao^{1,2}, Nathan Griffin^{1,2}, Sam Faulkner^{1,2}, Christopher W. Rowe^{2,3}, Lily Williams¹, Severine Roselli^{1,2}, Rick F. Thorne², Aysha Ferdoushi^{1,2}, Phillip Jobling^{1,2}, Marjorie M. Walker^{2,3} & Hubert Hondermarck^{1,2}

The neurotrophic tyrosine kinase receptor TrkA (NTRK1) and its ligand nerve growth factor (NGF) are emerging promoters of tumor progression. In lung cancer, drugs targeting TrkA are in clinical trials, but the clinicopathological significance of TrkA and NGF, as well as that of the precursor proNGF, the neurotrophin co-receptor p75^{NTR} and the proneurotrophin co-receptor sortilin, remains unclear. In the present study, analysis of these proteins was conducted by immunohistochemistry and digital quantification in a series of 204 lung cancers of different histological subtypes *versus* 121 normal lung tissues. TrkA immunoreactivity was increased in squamous cell carcinoma compared with benign and other malignant lung cancer histological subtypes ($p < 0.0001$). NGF and proNGF were also increased in squamous cell carcinoma, as well as in adenocarcinoma ($p < 0.0001$). In contrast, p75^{NTR} was increased across all lung cancer histological subtypes compared to normal lung ($p < 0.0001$). Sortilin was higher in adenocarcinoma and small cell carcinoma ($p < 0.0001$). Nerves in the tumor microenvironment were negative for TrkA, NGF, proNGF, p75^{NTR} and sortilin. In conclusion, these data suggest a preferential therapeutic value of targeting the NGF-TrkA axis in squamous cell carcinomas of the lung.

Lung cancer is the leading cause of cancer related death worldwide and its incidence is increasing¹. Lung cancer histological subtypes are divided into two main categories: small cell lung cancers and non-small cell lung cancers (NSCLC). NSCLC represent the majority of lung cancer cases and include squamous cell carcinomas and adenocarcinomas. Despite extensive research, there are few clinically used biomarkers to help determine diagnosis, prognosis and treatment choice in lung cancer¹. This is particularly problematic for NSCLC where correct identification of histological subtypes is essential to define the appropriate chemotherapeutic regimens. Therefore, the identification of pertinent biomarkers for diagnosis, stratification and therapeutic decision in lung cancer is necessary.

The neurotrophic tyrosine kinase receptor TrkA (NTRK1) and its ligand nerve growth factor (NGF) are essential to the development of the nervous system where they stimulate the outgrowth of sympathetic and sensory neurons². Interestingly, TrkA and NGF are also expressed in several malignancies. In breast cancer, they participate in tumor cell proliferation and spreading *via* the activation of signalling pathways similar to those activated in neurons and including ERK, SRC and AKT³. Recent evidence in gastric⁴ and pancreatic⁵ cancers has shown that the NGF-TrkA signalling pathway is an essential and targetable stimulator of cancer progression. In lung cancer, rearrangements of TrkA have been shown to be oncogenic and are drug-sensitive⁶. TrkA is increasingly regarded as a therapeutic target in lung cancer and clinical trials of drugs against its tyrosine kinase activity are under way⁷. A previous study has shown that the expression of TrkA and NGF is higher in NSCLC⁸, but the distribution of TrkA and NGF in the different subtypes of lung cancer remains unclear. In addition, the expression of the other co-receptors for NGF², the common neurotrophin receptor p75^{NTR} (also called NGFR or CD271), as well as that of the precursor for NGF

¹School of Biomedical Sciences & Pharmacy, Faculty of Health and Medicine, University of Newcastle, Callaghan, NSW, 2308, Australia. ²Hunter Medical Research Institute, University of Newcastle, New Lambton, NSW, 2305, Australia. ³School of Medicine & Public Health, Faculty of Health and Medicine, University of Newcastle, Callaghan, NSW, 2308, Australia. Correspondence and requests for materials should be addressed to H.H. (email: hubert.hondermarck@newcastle.edu.au)

(proNGF) and its receptor sortilin (a member of the Vacuolar Protein Sorting 10 protein - VPS10P - family of receptors) have not been elucidated. Despite early studies showing that neurotrophic growth factors are expressed in lung cancer⁹, the clinicopathological significance warrants clarification.

The present study aimed to clarify the expression and clinicopathological significance of TrkA, NGF, proNGF, p75^{NTR} and sortilin in lung cancer. The expression of these proteins was analysed by immunohistochemistry in a cohort of lung cancers versus normal lung tissues. We report an increased level of TrkA and NGF in squamous cell carcinomas, suggesting that drugs targeting the NGF-TrkA pathway in lung cancer should be used preferentially in this form of the disease.

Results

For all neurotrophins/receptors, representative pictures of immunohistochemical staining are shown in Figs 1–5 and quantification of staining intensities are presented in Table 1. Staining intensities (h-scores) are presented as medians (50th centile value).

TrkA is increased in squamous cell lung carcinoma. Compared with normal lung (Fig. 1A), TrkA labelling was concentrated in cancer epithelial cells (Fig. 1B–F), with an increased staining intensity specifically in squamous cell carcinoma (Fig. 1B–D). Membrane staining was clearly observable. TrkA immunoreactivity was low in normal lung tissue (h-score 18), and lower in adenocarcinoma (h-score 6) ($p < 0.0001$); in squamous cell carcinoma, TrkA intensity (h-score 26) was significantly higher ($p < 0.0001$) (Fig. 1G, Table 1). This increase in h-score was driven by a subpopulation of squamous cell tumours that were strongly positive for TrkA, consistent with a binary receptor expression pattern of TrkA-present (h-score > 50) or TrkA-absent (h-score ≤ 50). When analysed by these parameters (Fig. 1H), 27/96 (28%) of squamous cell carcinomas expressed TrkA, compared to 1/55 (2%) of adenocarcinomas, 0/7 (0%) of small cell cancers and 1/121 normal tissues ($< 1\%$) ($p < 0.0001$), with 12/96 (13%) of squamous cell carcinomas showing very strong TrkA expression (h-score > 100). Multivariate logistic regression modelling confirmed squamous pathology was significantly associated with increased TrkA h-score, when accounting for age and gender (Odds ratio (OR) 1.03, 1.01–1.04, $p < 0.001$). Given that TrkA was not expressed in most adenocarcinomas and small cell lung cancers, the area under the receiver-operating characteristic (AUROC) for the comparison between normal and cancer samples was only 0.39 (95%CI 0.32 to 0.46) (data not shown). No association was found between TrkA expression and age, grade, tumor size, stage, lymph node status.

NGF and proNGF are increased in squamous cell carcinoma and adenocarcinoma. NGF immunoreactivity was observed at low levels in normal tissues (Fig. 2A), and was increased in cancer vs normal samples (Fig. 2B–F). NGF staining intensity (h-score) was significantly increased from 57 in normal to 95 in cancer samples ($p < 0.0001$) (Fig. 2G). Squamous cell carcinoma (Fig. 2B–D) and adenocarcinoma (Fig. 2E) presented with a NGF h-score of 107 and 84 respectively ($p < 0.0001$) (Fig. 2G, Table 1). Small cell cancers (Fig. 2F) displayed a lower level of NGF staining compared to other cancer subtypes (h-score 54) (Fig. 2G, Table 1) ($p < 0.0001$). Multivariate logistic regression modelling confirmed squamous cell carcinoma and adenocarcinoma were significantly associated with increased NGF h-score compared to benign pathology, when accounting for age and gender (OR 1.09 (1.06–1.12) and 1.08 (1.05–1.11) respectively, $p < 0.001$). The AUROC for the comparison between normal and cancer tissue was 0.88 (95%CI 0.84 to 0.92) (Fig. 2H).

ProNGF was also increased in malignant tissue (Fig. 3B–E) compared to normal lung tissue (Fig. 3A), but the differential in median h-score was less than NGF. Multivariate logistic regression modelling confirmed squamous cell carcinoma and adenocarcinoma were significantly associated with increased proNGF h-score compared to benign pathology, when accounting for age and gender (OR 1.04 (1.02–1.05) and OR 1.04 (1.03–1.06) respectively, $p < 0.001$) (Fig. 3G, Table 1). The AUROC for the comparison between normal and cancer samples was 0.70 (95%CI 0.64 to 0.76) (Fig. 3H).

For both NGF and proNGF, there was no association with age, grade, stage, tumor size, or lymph node invasion (Table 1).

p75^{NTR} is increased in all lung cancer subtypes. Immunostaining for p75^{NTR} was observed in both epithelial and stromal cells of normal (Fig. 4A) and cancer samples (Fig. 4B–F). However, p75^{NTR} staining intensity was higher in cancer, with an h-score of 92 in normal compared to 147 in cancer ($p < 0.0001$) (Fig. 4G, Table 1). The increase in p75^{NTR} staining intensity occurred in all histological subtypes of lung cancer (squamous cell, adenocarcinoma, small cell) but was particularly strong in small cell carcinoma (median h-score of 215) (Fig. 4G, Table 1). Multivariate logistic regression modelling confirmed malignant pathology was significantly associated with increased p75^{NTR} h-score for squamous cell carcinoma (OR 1.04 (1.02–1.05), $p < 0.001$), adenocarcinoma (OR 1.07 (1.05–1.10) $p < 0.001$), when compared to benign pathology, when accounting for age and gender ($p < 0.001$). We were unable to fit a logistic regression model for small cell carcinoma vs benign tissue due to perfect separation of h-scores (Fig. 4G). The AUROC for the comparison of cancer vs normal was 0.83 (95%CI 0.79 to 0.88) (Fig. 4H). There was no association between p75^{NTR} staining and tumor size, grade, stage or lymph node status.

Sortilin is increased in adenocarcinoma and small cell lung cancer. Immunostaining for sortilin was weak and found mainly in epithelial cells of both normal (Fig. 5A) and cancer samples (Fig. 5B–F). There was no difference between sortilin staining intensity in benign vs all lung cancer tissues with h-scores of 32 vs 30 respectively ($p = 0.43$). However, there was a higher level of sortilin staining intensity in adenocarcinoma (OR 1.05 (1.03–1.07), $p < 0.001$) and small cell (OR 1.18 (1.06–1.31), $p = 0.002$) when compared to benign pathology in a multivariate logistic regression model. (Fig. 5G, Table 1). The AUROC for comparison of cancer vs normal was 0.46 (95%CI 0.39 to 0.53) (Fig. 5H), confirming that sortilin expression is not significantly modified when comparing all lung cancers to normal tissues. In addition, there were no associations between sortilin expression and age, grade, stage, tumor size or lymph node invasion.

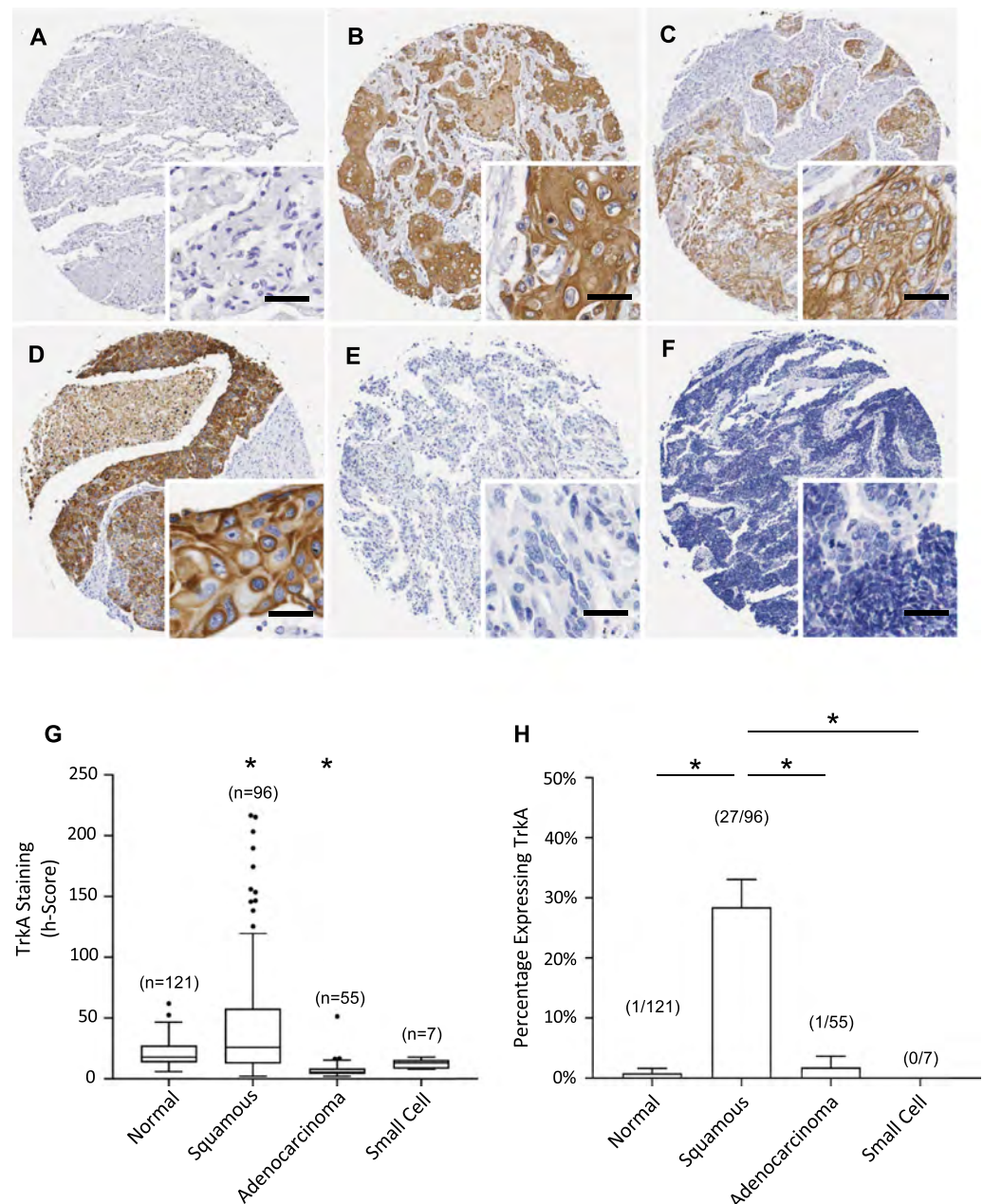


Figure 1. TrkA expression in lung cancers and normal lung tissues. (A–F) Immunohistochemical detection of TrkA, representative pictures are shown for normal tissue (A), squamous cell carcinoma (B–D), adenocarcinoma (E) and small cell cancer (F). Scale = 50 μ m. (G) TrkA staining intensities were significantly higher in squamous cell carcinoma. Corresponding median h-scores are presented in Table 1. The box limits indicate the interquartile range (IQR) with the whiskers extending 1.5 times the IQR from the 25th and 75th percentiles (outliers are represented by dots) (* $p < 0.0001$ in multiple logistic regression model). (H) Proportion of tissues expressing TrkA receptor (binary h-score cutoff of 50) in normal lung tissue vs lung cancer subtypes. Squamous cell carcinoma was significantly higher than all other categories ($p < 0.0001$).

Nerves in the tumor microenvironment of lung cancer do not express NGF, proNGF, TrkA, p75^{NTR} and sortilin. The pan-neuronal marker PGP9.5 was used to detect nerves in the tumor microenvironment. Nerve trunks were occasionally detected in lung cancer (Fig. 6A), based on PGP9.5 positivity as well as typical nerve morphology. Serial sections were used and no labelling for NGF (Fig. 6B), proNGF (Fig. 6C), TrkA (Fig. 6D), p75^{NTR} (Fig. 6E) or sortilin (Fig. 6F) was detected. These data show that there is no expression of NGF, proNGF, TrkA, p75^{NTR} and sortilin in nerves which are present in the tumor microenvironment of lung cancer.

Discussion

ProNGF and sortilin have not been described in lung cancers and there has been limited reports on the expression of NGF and its receptors TrkA and p75^{NTR}^{8,10,11}. Therefore, with only fragmentary data available, the

clinicopathological significance remained unclear. To address this, we undertook a simultaneous investigation of the protein expression of proNGF, NGF, TrkA, p75^{NTR} and sortilin in the same cohort of lung cancers and normal lung tissues. Our results reveal that TrkA, NGF, proNGF, p75^{NTR} and sortilin are differently expressed across lung cancer histological subtypes, with TrkA and NGF most particularly increased in squamous cell carcinomas.

Prior to investigating protein levels by immunohistochemistry, data mining of gene expression in lung datasets available from The Cancer Genome Atlas (TCGA)¹² using cBioportal¹³ was performed. Gene amplification and mRNA upregulation were detected at various frequencies in lung tumors: 6% for NGF, 14% for TrkA, 2% for p75^{NTR} and 4% for sortilin. However, discrepancies between mRNA and protein levels in tumors are now well documented. Global transcriptomic and proteomic analyses estimate that only 30%–60% of changes in protein levels can be explained by corresponding variations in mRNA^{14,15} and proteogenomic investigations in colorectal cancer have revealed that mRNA abundance does not reliably predict differences in tumoral protein abundance¹⁶. This emphasizes the importance of analysing the protein levels directly, in order to define new biomarkers and novel therapeutic targets in oncology.

The participation of TrkA and TrkA fusion proteins in lung cancer progression has been described, with Trk inhibitors undergoing clinical trials⁶. Our data shows a preferential expression of TrkA in squamous cell lung cancer, suggesting that Trk inhibitors should be used more specifically in this histological subtype of lung cancer. A previous investigation has reported an increase in TrkA and NGF in NSCLC and an association with tumor aggressiveness but not histological subtypes⁸. However, in this study staining intensities were visually determined, and no digital quantification assisted by a pathologist (as we have done here) was used, potentially leading to approximation in the quantification of expression levels. In addition, the comparison was done with normal adjacent tissues whereas true normal lung tissues were analysed in our study. Therefore, our study provides a refinement in terms of quantification of TrkA and NGF in lung cancer subtypes, highlighting a significant increase in both TrkA and NGF expression in squamous cell lung cancer. In contrast, as low expression level for TrkA were observed in adenocarcinoma and small cell cancer, it is unlikely that Trk inhibitors will produce any significant clinical impact in these tumors. Interestingly, NGF was also increased in squamous cell lung cancer and to a lesser extent in adenocarcinoma. This concomitant increased expression of both TrkA and its ligand NGF is suggestive of a NGF-mediated autocrine stimulation of squamous cell carcinoma. Similar autocrine stimulation of cancer cell growth via a proNGF/NGF autocrine loop involving TrkA has been described in breast cancer^{17,18} and may also apply to lung cancer. Although further functional investigations are warranted to test this hypothesis, our data reveals that TrkA and its ligand NGF are overexpressed in squamous cell lung cancer. This finding may have clinical ramifications, as humanized NGF blocking antibodies have been developed and are in clinical trials for the treatment of pain¹⁹; they may potentially be repurposed to inhibit the NGF-TrkA signaling axis in lung cancer.

In contrast to NGF, proNGF was only slightly increased in squamous cell lung cancer and adenocarcinoma. ProNGF processing into NGF requires protein convertases, such as furin or metalloproteases, and can occur both intracellularly or after secretion in the extracellular compartment². In the nervous system, proNGF is the predominant protein form of NGF gene expression, with a higher presence of proNGF in comparison to NGF²⁰. The regulatory mechanism that controls proNGF processing is poorly described in cancer, but our data suggest that proNGF is largely processed into NGF in squamous cell carcinomas of the lung. The limited differential in proNGF expression between normal and cancerous lung tissue is in line with the data obtained for its receptor sortilin. Sortilin was expressed at the same low levels in normal lung tissue, squamous cell carcinoma and was only higher in adenocarcinoma and small cell cancer. Sortilin has been reported in various cancer cell lines of different origins and its expression is associated to a poor prognosis in breast cancer where it participates in tumor cell migration and invasion²¹. In the squamous cell line A549, sortilin has been shown to participate in the transfer of exosomes in association with TrkB²², but our data have not highlighted any particular association between sortilin expression and clinicopathological parameters in any histopathological subtypes of lung cancers.

The neurotrophin receptor p75^{NTR} is expressed in a wide range of human tumors and has been shown to be a marker of cancer stem cells of both epithelial and mesenchymal origin²³. However, the mechanism of p75^{NTR} activity in cancer cells is not fully elucidated and some studies in gastric²⁴ and prostatic cancer^{25,26} have reported a tumor suppressor effect associated with p75^{NTR} suppression. In the present study, p75^{NTR} was expressed in normal lung tissues and overexpressed in all investigated lung cancer histological subtypes. The overexpression of p75^{NTR} was observed in epithelial cells as well as stromal cells. Interestingly p75^{NTR} has recently been shown to be a p53 inactivator²⁷, and as such p75^{NTR} could actively participate in lung tumor growth, but further functional investigations are needed to explore this hypothesis.

Emerging evidence indicate the stimulatory role of nerves in tumor progression²⁸. The nerve-cancer cell crosstalk involves the liberation of neurotransmitters and trophic factors to stimulate cancer cell growth and dissemination, while neurotrophic factors are released by cancer cells to attract nerve outgrowth in the tumor microenvironment²⁹. In gastric cancer, NGF has been shown to activate cholinergic nerve-mediated signalling that stimulates the proliferation of stem cells⁴. In prostate cancer, sympathetic and parasympathetic nerves participate in the stimulation of tumor growth and metastasis³⁰ and proNGF released by prostate cancer cells is a driver of neuronal outgrowth³¹. In lung cancer, autonomic nerve infiltration is associated with pathological risk grading and poor patient prognosis³², but the drivers of nerve infiltration have not been identified. Our study showing that there is no expression of the receptors TrkA, p75^{NTR} and sortilin in nerves infiltrated in the tumor microenvironment, suggest that NGF/proNGF are not involved in stimulating the growth of nerves in lung cancer.

Overall, this study highlights the overexpression of NGF, proNGF and their receptors TrkA, p75^{NTR} in lung cancer with a differential expression related to histological subtypes. A similar increased expression of these neurotrophins and receptors has already been observed in breast^{17,18,33} and thyroid^{34,35} cancer, suggesting that the upregulation these proteins is a common molecular feature in these cancers. Pharmacological inhibitors against TrkA⁷ and humanized anti-NGF antibodies¹⁹ have been developed and could therefore be used as therapeutic tools in breast, thyroid and lung cancers. The overexpression of TrkA in squamous cell carcinomas of the lung is

Parameter	NGF Intensity			proNGF Intensity			TrkA Intensity			sortilin Intensity			p75 ^{NTR} Intensity		
	Median h-score	IQR	p-value	Median h-score	IQR	p-value	Median h-score	IQR	p-value	Median h-score	IQR	p-value	Median h-score	IQR	p-value
Normal vs cancer			<0.0001			<0.0001			0.002			0.43			<0.0001
Normal (n = 121)	57	46–70		58	47–70		18	13–26		32	26–41		92	81–110	
Cancer (n = 164)	95	76–112		76	58–96		13	6–33		30	20–48		147	116–176	
Histological Type			0.0001			0.0001			0.0001			0.0001			0.0001
Squamous (n = 98)	107	85–118		73	58–96		26	13–57		25	18–40		132	107–161	
Adenocarcinoma (n = 58)	84	72–98		82	65–98		6	4–9		40	26–66		164	141–184	
Small Cell (n = 8)	54	50–70		52	33–72		13	8–16		56	42–65		215	180–222	
Gender			0.04			0.28			<0.0001			0.002			0.0005
Male (n = 125)	99	80–115		74	58–95		16	7–39		27	19–44		138	112–171	
Female (n = 39)	84	70–108		83	59–109		6	4–13		42	27–58		168	147–189	
Age (yrs)			0.56			0.35			0.31			0.7			0.35
< 50 (n = 40)	94	72–108		72	55–97		16	8–39		30	22–49		154	121–177	
> 50 (n = 124)	96	76–114		76	59–96		11	6–29		31	19–48		141	114–175	
Grade			0.85			0.03			0.24			0.88			0.37
1 (n = 13)	98	84–117		96	89–120		19	10–138		26	18–46		141	82–160	
2 + 3 (n = 135)	97	78–114		74	59–95		14	6–34		29	19–46		142	116–172	
Missing (n = 16)	65	51–89		65	35–83		11	7–15		47	27–58		180	130–215	
T stage			0.88			0.55			0.63			0.71			0.8
T1/T2 (n = 133)	97	75–112		75	58–96		13	6–32		31	20–48		150	115–176	
T3/T4 (n = 31)	95	77–109		76	58–99		13	5–34		27	18–50		142	117–171	
LN Status			0.9			0.78			0.64			0.97			0.48
Negative (n = 70)	96	78–111		76	60–96		13	6–37		31	20–46		149	117–169	
Positive (n = 94)	95	75–112		74	56–96		13	5–31		29	20–49		145	116–178	
Stage			0.38			0.35			0.53			0.93			0.5
I + II (n = 120)	94	75–112		74	58–95		13	6–32		31	20–47		151	116–177	
III + IV (n = 44)	97	79–113		82	58–100		13	5–34		29	20–52		141	114–172	

Table 1. Expression of NGF, proNGF, TrkA, p75^{NTR} and sortilin in lung cancers and association with clinicopathological parameters. Immunohistochemical staining were quantified and h-scores were used to compare protein expression levels. Group-levels medians (IQR, interquartile range) for h-score staining intensities are presented. Family-wise alpha significance level is 0.05/8 = 0.006 using the Wilcoxon Rank-Sum test (pairwise) or Kruskal-Wallis test (multiple comparisons). Statistically significant p-values are shown in bold.

of particular interest, given that TrkA inhibitors have entered clinical trials for the treatment of lung cancer⁷. In the nervous system, neurons responsive to NGF express TrkA and p75^{NTR} and the stimulation of these receptors by NGF induces a cascade of intracellular signalings including SRC, AKT, PI3K, ERK and NFkB. In lung cancer cells, TrkA tyrosine kinase inhibitors induce lung cancer cell growth arrest and apoptosis³⁶. Based on the present findings, the biological effect of targeting TrkA and NGF in lung cancer should be revisited in the context of squamous cell carcinomas with more functional *in vitro* and *in vivo* animal models. From a clinical perspective, our data suggest that anti-TrkA therapies may be more effective in squamous cell lung cancer and could eventually be associated with NGF targeting.

Material and Methods

Lung tissue samples. High-density tumor microarrays (TMA) were obtained from US Biomax Inc. (Maryland, USA). The TMAs used (catalogue numbers: LC2086, LC2087 and BC041115) included a total of 204 lung cancers (of adenocarcinoma, squamous cell carcinoma, small cell carcinoma or other minor subtypes) and 121 normal lung tissues. The following clinicopathological information was available: patient age and sex, histological subtype, tumor size, grade, stage and lymph node status. No information on treatment and patient survival was available. US Biomax Inc. quality controls are described as follows. Each single tissue spot on every array slide was individually examined by pathologists certified according to WHO published standardizations of diagnosis, classification and pathological grade. For each specimen collected, informed consent was obtained from both hospital and individual. Discrete legal consent was obtained and the rights to hold research uses for any purpose or further commercialized uses were waived. The study was approved by the Human Research Ethic Committee of the University of Newcastle and all experiments were performed in accordance with relevant guidelines and regulations.

Immunohistochemistry. Immunohistochemistry (IHC) was performed as previously described³⁴. After deparaffinization and rehydration of the TMA slides following standard procedures, heat induced epitope retrieval was carried out in a low pH, citrate based antigen unmasking solution (Vector Laboratories, California,

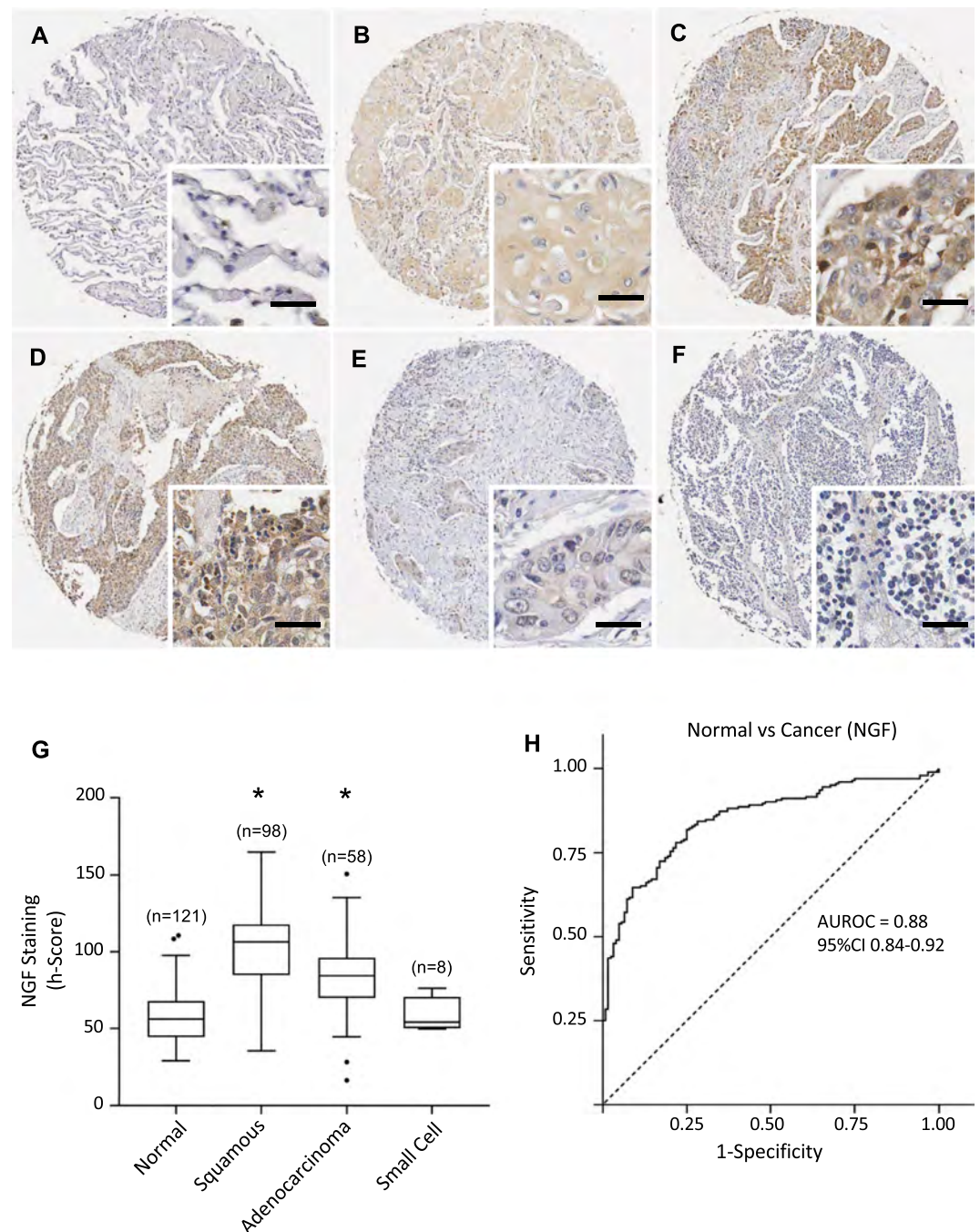


Figure 2. NGF expression in lung cancers and normal lung tissues. (A–F) Immunohistochemical detection of NGF, representative pictures are shown for normal tissue (A), squamous cell carcinoma (B–D), adenocarcinoma (E) and small cell cancer (F). Scale = 50 μ m. (G) NGF staining intensities were significantly higher in squamous cell carcinoma and adenocarcinoma than in normal tissues. Corresponding median h-scores are presented in Table 1. The box limits indicate the interquartile range (IQR) with the whiskers extending 1.5 times the IQR from the 25th and 75th percentiles (outliers are represented by dots) (* $p < 0.0001$ in multiple logistic regression model). (H) ROC curve for NGF staining intensity level in lung cancers versus normal tissues. The area under the curve was 0.88 (95%CI 0.84 to 0.92).

USA, catalogue number H-3300) using a decloaking chamber (Biocare, West Midlands, United Kingdom) at 95 °C for 20 min. IHC was then performed using an ImmPRESSTM HRP IgG (Peroxidase) Polymer Detection Kit (Vector Laboratories, California, USA), as per the manufacturer's recommendations. Briefly, after inactivation of endogenous peroxidases with 0.3% H₂O₂, and blocking with 2.5% horse serum, primary followed by secondary antibodies were applied to the sections and revealed with DAB Peroxidase (HRP) Substrate Kit (Vector Laboratories, California, USA, catalogue number SK-4100). The following primary antibodies were used at 1/500 dilution: anti-proNGF (#AB9040, Merck Millipore), anti-NGF (#ab52918, Abcam), anti-TrkA (#2508,

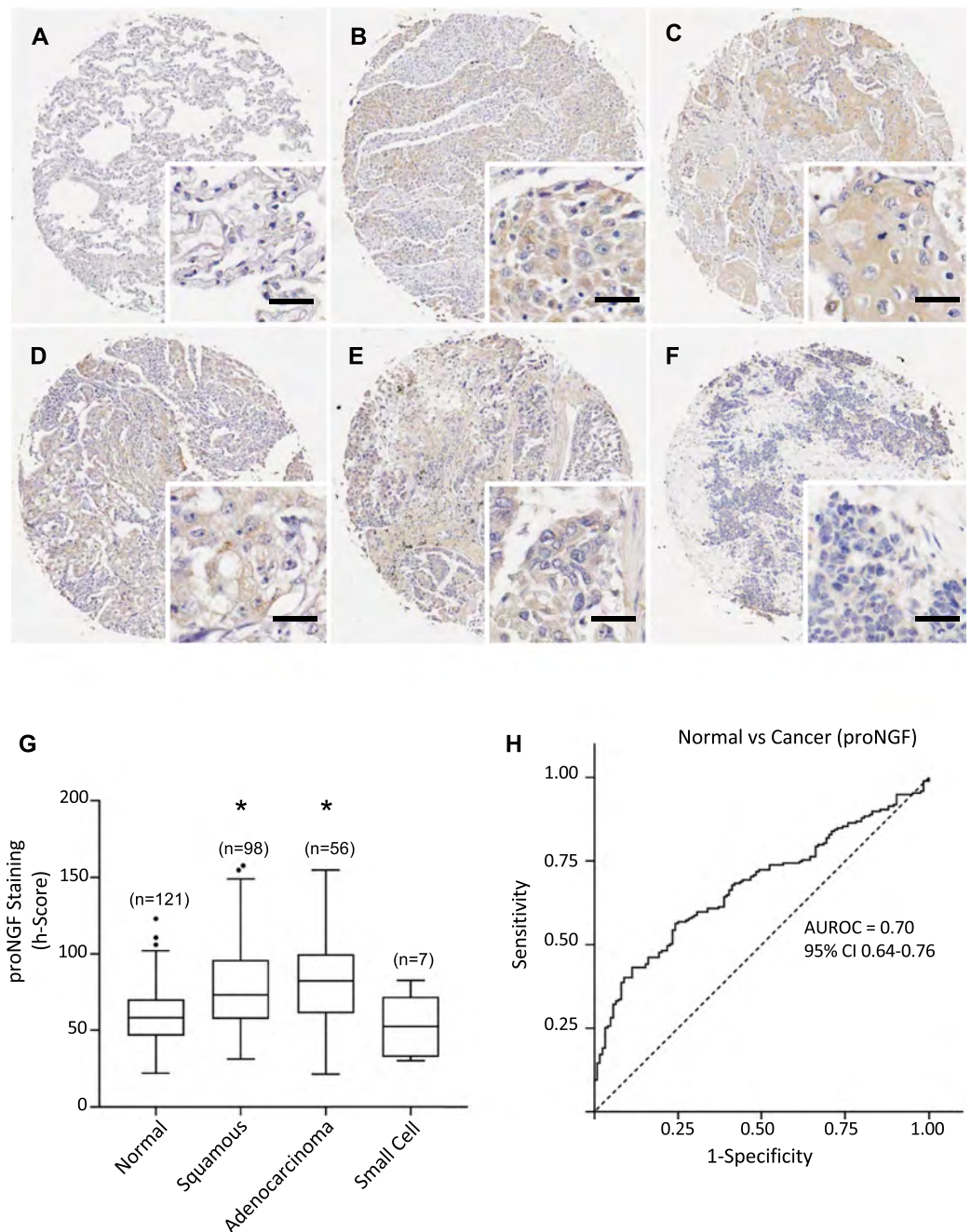


Figure 3. ProNGF expression in lung cancers and normal tissues. **(A–F)** Immunohistochemical detection of proNGF, representative pictures are shown for normal tissue **(A)**, squamous cell carcinoma **(B–D)**, adenocarcinoma **(E)** and small cell cancer **(F)**. Scale = 50 μ m. **(G)** ProNGF staining intensities were significantly higher in squamous cell carcinoma and adenocarcinoma than in normal tissues. Corresponding median h-scores are presented in Table 1. The box limits indicate the interquartile range (IQR) with the whiskers extending 1.5 times the IQR from the 25th and 75th percentiles (outliers are represented by dots) (* $p < 0.0001$ in multiple logistic regression model). **(H)** ROC curve for proNGF staining intensity level in lung cancers versus normal tissues. The area under the curve was 0.70 (95% CI 0.64 to 0.76).

Cell Signaling), anti-p75^{NTR} (#4201, Cell Signaling), anti-sortilin (#ANT-009, Alomone Labs), anti-PGP9.5 (#ab15503, Abcam). Finally, TMA slides were counterstained with hematoxylin (Gill's formulation, Vector Laboratories, California, USA), dehydrated and cleared in xylene before mounting in Ultramount #4 mounting media (Thermo Fisher Scientific, Victoria, Australia). Negative controls, using isotype control antibodies, are shown in Supplementary Fig. 1.

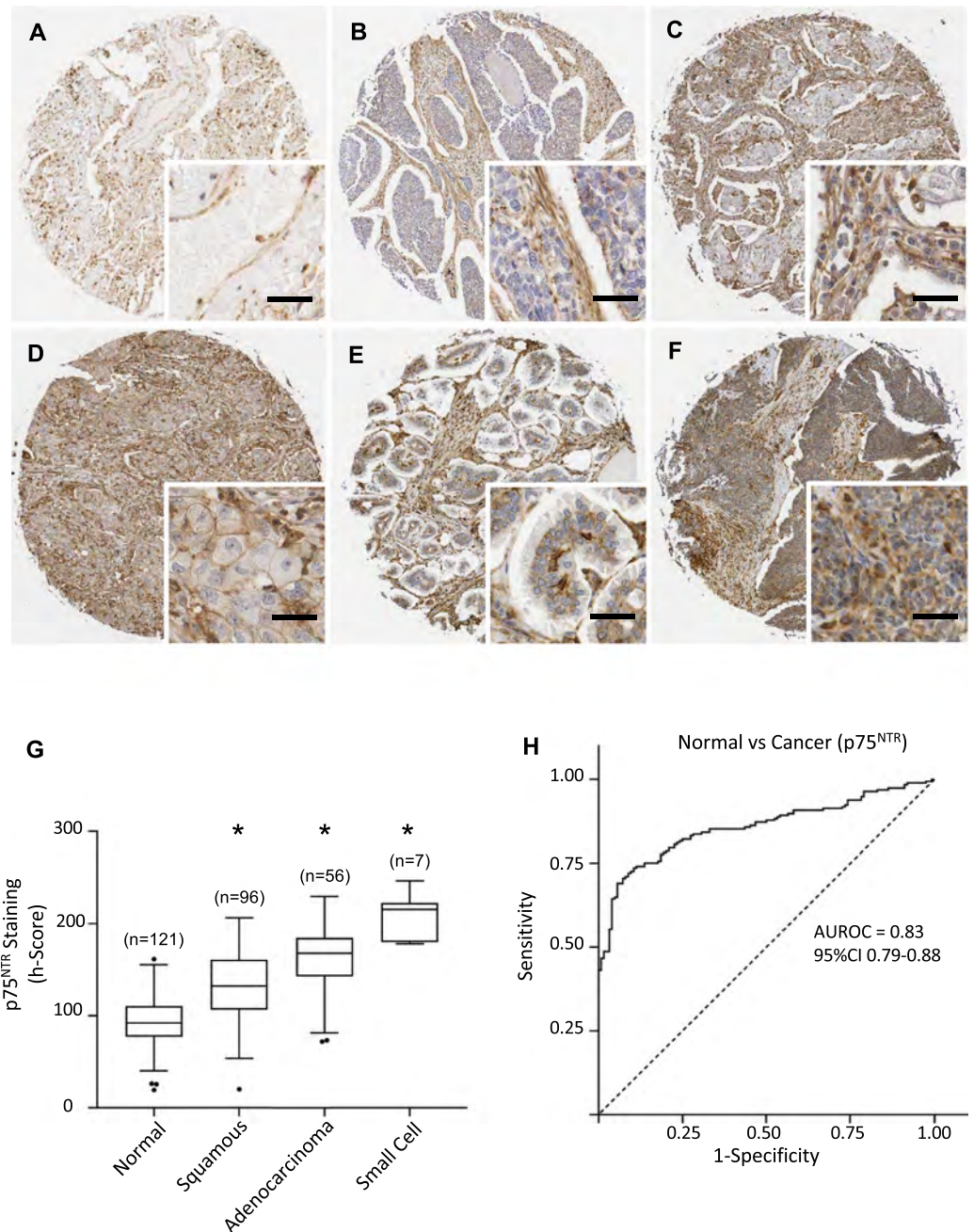


Figure 4. P75^{NTR} expression in lung cancers and normal lung tissues. (A–F) Immunohistochemical detection of p75^{NTR}, representative pictures are shown for normal tissue (A), squamous cell carcinoma (B–D), adenocarcinoma (E) and small cell cancer (F). Scale = 50 μ m. (G) p75^{NTR} staining intensities were significantly higher in squamous cell, adenocarcinoma and small cell cancers. Corresponding median h-scores are presented in Table 1. The box limits indicate the interquartile range (IQR) with the whiskers extending 1.5 times the IQR from the 25th and 75th percentiles (outliers are represented by dots) (* $p < 0.0001$ in multiple logistic regression model). (H) ROC curve for p75^{NTR} staining intensity level in lung cancers versus normal tissues. The area under the curve was 0.83 (95% CI 0.79 to 0.88).

Digital quantification of IHC staining intensities. Quantification of staining intensities was performed as previously described³⁴ using the Aperio AT2 scanner (Leica Biosystems, Victoria, Australia) and the HaloTM image analysis platform (Indica Labs, New Mexico, USA) under the supervision of a pathologist (MMW). Pixel intensity values were used to determine the h-scores for each core (index calculated as the sum of 3x% of pixels with strong staining + 2x% of pixels with intermediate staining + 1x% pixels with weak staining). Each core of the TMAs was investigated and the data were then submitted to statistical analysis.

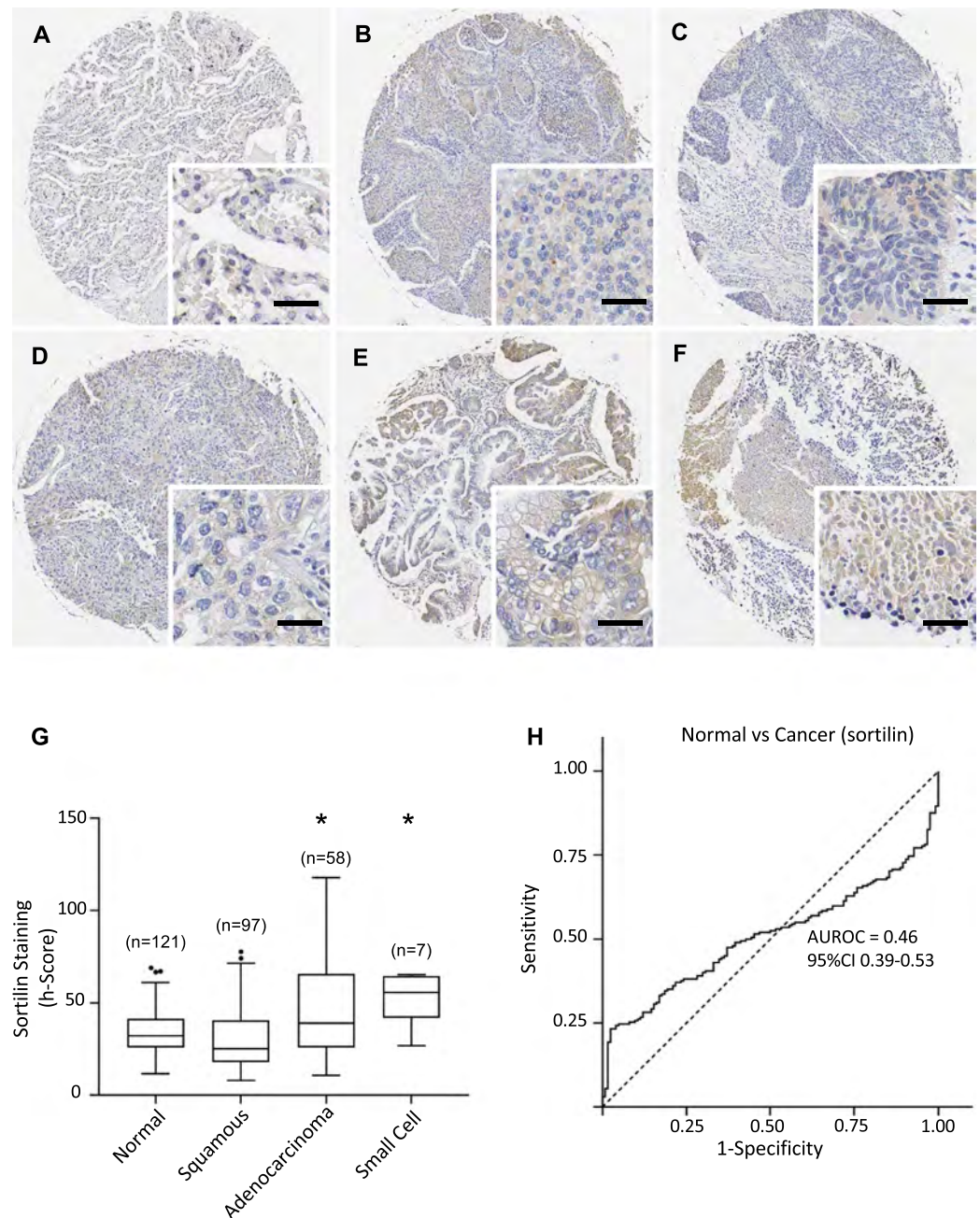


Figure 5. Sortilin expression in lung cancers and normal lung tissues. (A–F) Immunohistochemical detection of sortilin, representative pictures are shown for normal tissue (A), squamous cell carcinoma (B–D), adenocarcinoma (E) and small cell cancer (F). Scale = 50 μ m. (G) Sortilin staining intensities were significantly higher in adenocarcinoma and small cell cancer. Corresponding median h-scores are presented in Table 1. The box limits indicate the interquartile range (IQR) with the whiskers extending 1.5 times the IQR from the 25th and 75th percentiles (outliers are represented by dots) (* $p < 0.0001$ in multiple logistic regression model). (H) ROC curve for sortilin staining intensity level in lung cancers versus normal tissues. The area under the curve was 0.46 (95%CI 0.39 to 0.53).

Statistical analysis. H-scores for NGF, proNGF, sortilin, TrkA and p75^{NTR} were analysed as continuous variables. Major lung cancer subtypes (164 cases of adenocarcinoma, squamous cell carcinoma, small cell cancer) were analysed and are presented in Table 1 and Figures, with other minor subtypes excluded from analysis ($n = 43$). For demographic (age and sex) and disease-specific (histopathology classes of benign, squamous, small cell and adenocarcinoma; tumour size, grade, stage; and nodal status) outcomes of interest, group level medians and interquartile ranges were compared with the Wilcoxon RankSum test, employing a Bonferroni correction for multiple pairwise comparisons (alpha at the family-wise 0.05 level = 0.05/8). All multiple-comparisons used the Kruskal-Wallis test due to unequal variances, with an adjusted multiple-comparison alpha threshold. Analyses were based on complete cases.

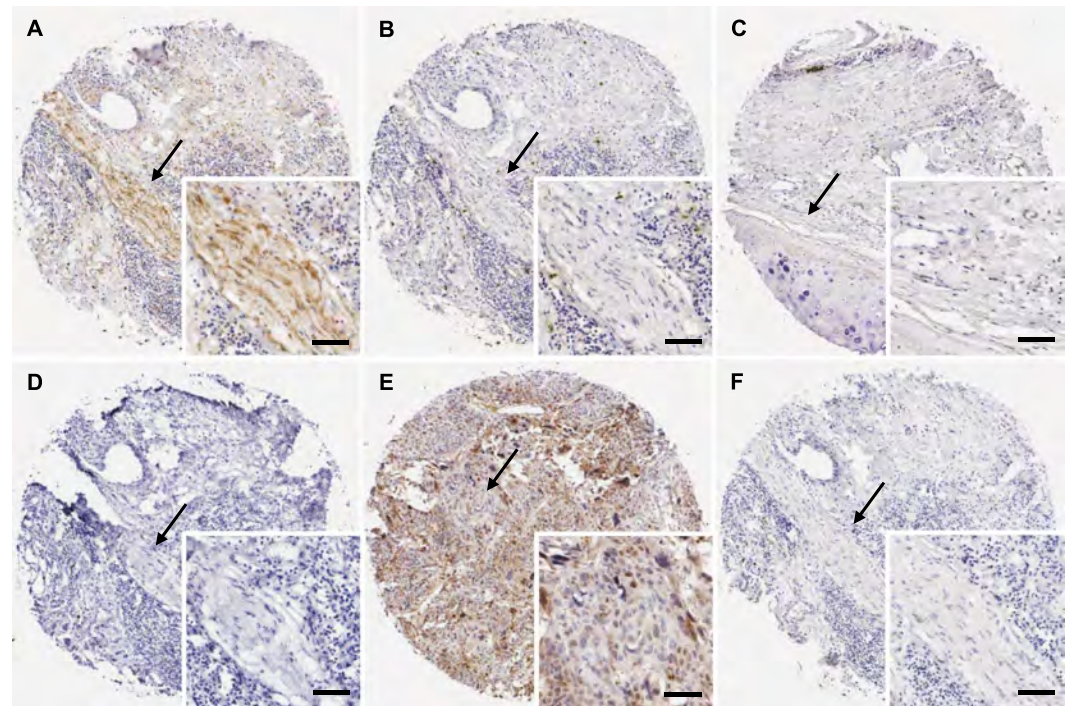


Figure 6. Nerves in the tumor microenvironment of lung cancer do not express NGF, proNGF, TrkA, p75^{NTR} and sortilin. (A) Immunohistochemical detection of the pan-neuronal marker PGP9.5 was used to detect nerves in lung cancers. The expression of NGF (B), proNGF (C), TrkA (D), p75^{NTR} (E) and sortilin (F) was not detected in serial sections. Black arrows indicate a nerve trunk composed of many axons. Scale = 25 μ m.

We explored the association between the subtypes of pathology and neurotrophin h-score by fitting multiple logistic regression models to subsets of the data. We considered each of squamous cell carcinoma, adenocarcinoma and small cell cancer separately, dichotomised against the benign tissue group. All models adjusted for age and gender.

The discriminative value of each neurotrophin or receptor H-score as a biomarker of lung malignancy was assessed with receiver-operating characteristic (ROC) curves, where a value of 0.5 indicates no difference, and a value of 1 signifies perfect discrimination. All analyses were performed using Stata (version 14.1, Statacorp, Texas USA). Additional graphics were created using GraphPad Prism 7 (California, USA).

References

- Herbst, R. S., Heymach, J. V. & Lippman, S. M. Lung cancer. *N Engl J Med* **359**, 1367–1380, <https://doi.org/10.1056/NEJMra0802714> (2008).
- Bradshaw, R. A. *et al.* NGF and ProNGF: Regulation of neuronal and neoplastic responses through receptor signaling. *Adv Biol Regul* **58**, 16–27, <https://doi.org/10.1016/j.bior.2014.11.003> (2015).
- Hondermarck, H. Neurotrophins and their receptors in breast cancer. *Cytokine Growth Factor Rev* **23**, 357–365, <https://doi.org/10.1016/j.cytogfr.2012.06.004> (2012).
- Hayakawa, Y. *et al.* Nerve Growth Factor Promotes Gastric Tumorigenesis through Aberrant Cholinergic Signaling. *Cancer Cell* **31**, 21–34, <https://doi.org/10.1016/j.ccell.2016.11.005> (2017).
- Lei, Y. *et al.* Gold nanoclusters-assisted delivery of NGF siRNA for effective treatment of pancreatic cancer. *Nat Commun* **8**, 15130, <https://doi.org/10.1038/ncomms15130> (2017).
- Vaishnavi, A. *et al.* Oncogenic and drug-sensitive NTRK1 rearrangements in lung cancer. *Nat Med* **19**, 1469–1472, <https://doi.org/10.1038/nm.3352> (2013).
- Vaishnavi, A., Le, A. T. & Doebele, R. C. TRKing down an old oncogene in a new era of targeted therapy. *Cancer Discov* **5**, 25–34, <https://doi.org/10.1158/2159-8290.CD-14-0765> (2015).
- Wang, X. L., Yao, Y. C. & Yang, M. S. Z. Expression of nerve growth factor and tyrosine kinase A in non-small cell lung cancer. *Int J Clin Exp Pathol* **9**, 2153–2158 (2016).
- Ricci, A. *et al.* Neurotrophins and neurotrophin receptors in human lung cancer. *Am J Respir Cell Mol Biol* **25**, 439–446, <https://doi.org/10.1165/ajrcmb.25.4.4470> (2001).
- Missale, C. *et al.* Nerve growth factor abrogates the tumorigenicity of human small cell lung cancer cell lines. *Proc Natl Acad Sci USA* **95**, 5366–5371 (1998).
- Dinh, Q. T. *et al.* Substance P expression in TRPV1 and trkA-positive dorsal root ganglion neurons innervating the mouse lung. *Respir Physiol Neurobiol* **144**, 15–24, <https://doi.org/10.1016/j.resp.2004.08.001> (2004).
- Cancer Genome Atlas, N. Comprehensive molecular portraits of human breast tumours. *Nature* **490**, 61–70, <https://doi.org/10.1038/nature11412> (2012).
- Cerami, E. *et al.* The cBio cancer genomics portal: an open platform for exploring multidimensional cancer genomics data. *Cancer Discov* **2**, 401–404, <https://doi.org/10.1158/2159-8290.CD-12-0095> (2012).
- Gygi, S. P., Rochon, Y., Franza, B. R. & Aebersold, R. Correlation between protein and mRNA abundance in yeast. *Mol Cell Biol* **19**, 1720–1730 (1999).

15. Vogel, C. & Marcotte, E. M. Insights into the regulation of protein abundance from proteomic and transcriptomic analyses. *Nat Rev Genet* **13**, 227–232, <https://doi.org/10.1038/nrg3185> (2012).
16. Zhang, B. *et al.* Proteogenomic characterization of human colon and rectal cancer. *Nature* **513**, 382–387, <https://doi.org/10.1038/nature13438> (2014).
17. Adriaenssens, E. *et al.* Nerve growth factor is a potential therapeutic target in breast cancer. *Cancer Res* **68**, 346–351, <https://doi.org/10.1158/0008-5472.CAN-07-1183> (2008).
18. Demont, Y. *et al.* Pro-nerve growth factor induces autocrine stimulation of breast cancer cell invasion through tropomyosin-related kinase A (TrkA) and sortilin protein. *J Biol Chem* **287**, 1923–1931, <https://doi.org/10.1074/jbc.M110.211714> (2012).
19. Chang, D. S., Hsu, E., Hottinger, D. G. & Cohen, S. P. Anti-nerve growth factor in pain management: current evidence. *J Pain Res* **9**, 373–383, <https://doi.org/10.2147/JPR.S89061> (2016).
20. Fahnstock, M., Michalski, B., Xu, B. & Coughlin, M. D. The precursor pro-nerve growth factor is the predominant form of nerve growth factor in brain and is increased in Alzheimer's disease. *Mol Cell Neurosci* **18**, 210–220, <https://doi.org/10.1006/mcne.2001.1016> (2001).
21. Roselli, S. *et al.* Sortilin is associated with breast cancer aggressiveness and contributes to tumor cell adhesion and invasion. *Oncotarget* **6**, 10473–10486, <https://doi.org/10.18632/oncotarget.3401> (2015).
22. Wilson, C. M. *et al.* Sortilin mediates the release and transfer of exosomes in concert with two tyrosine kinase receptors. *J Cell Sci* **127**, 3983–3997, <https://doi.org/10.1242/jcs.149336> (2014).
23. Chopin, V., Lagadec, C., Toillon, R. A. & Le Bourhis, X. Neurotrophin signaling in cancer stem cells. *Cell Mol Life Sci* **73**, 1859–1870, <https://doi.org/10.1007/s00018-016-2156-7> (2016).
24. Jin, H. *et al.* p75 neurotrophin receptor suppresses the proliferation of human gastric cancer cells. *Neoplasia* **9**, 471–478 (2007).
25. Krygier, S. & Djakiew, D. Neurotrophin receptor p75(NTR) suppresses growth and nerve growth factor-mediated metastasis of human prostate cancer cells. *Int J Cancer* **98**, 1–7 (2002).
26. Khwaja, F., Tabassum, A., Allen, J. & Djakiew, D. The p75(NTR) tumor suppressor induces cell cycle arrest facilitating caspase mediated apoptosis in prostate tumor cells. *Biochem Biophys Res Commun* **341**, 1184–1192, <https://doi.org/10.1016/j.bbrc.2006.01.073> (2006).
27. Zhou, X. *et al.* Nerve growth factor receptor negates the tumor suppressor p53 as a feedback regulator. *Elife* **5**, <https://doi.org/10.7554/eLife.15099> (2016).
28. Boilly, B., Faulkner, S., Jobling, P. & Hondermarck, H. Nerve Dependence: From Regeneration to Cancer. *Cancer Cell* **31**, 342–354, <https://doi.org/10.1016/j.ccell.2017.02.005> (2017).
29. Jobling, P. *et al.* Nerve-Cancer Cell Cross-talk: A Novel Promoter of Tumor Progression. *Cancer Res* **75**, 1777–1781, <https://doi.org/10.1158/0008-5472.CAN-14-3180> (2015).
30. Magnon, C. *et al.* Autonomic nerve development contributes to prostate cancer progression. *Science* **341**, 1236361, <https://doi.org/10.1126/science.1236361> (2013).
31. Pundavela, J. *et al.* ProNGF correlates with Gleason score and is a potential driver of nerve infiltration in prostate cancer. *Am J Pathol* **184**, 3156–3162, <https://doi.org/10.1016/j.ajpath.2014.08.009> (2014).
32. Shao, J. X. *et al.* Autonomic nervous infiltration positively correlates with pathological risk grading and poor prognosis in patients with lung adenocarcinoma. *Thorac Cancer* **7**, 588–598, <https://doi.org/10.1111/1759-7714.12374> (2016).
33. Lagadec, C. *et al.* TrkA overexpression enhances growth and metastasis of breast cancer cells. *Oncogene* **28**, 1960–1970, <https://doi.org/10.1038/nc.2009.61> (2009).
34. Faulkner, S. *et al.* ProNGF is a potential diagnostic biomarker for thyroid cancer. *Oncotarget* **7**, 28488–28497, <https://doi.org/10.18632/oncotarget.8652> (2016).
35. Faulkner, S. *et al.* Neurotrophin Receptors TrkA, p75(NTR), and Sortilin Are Increased and Targetable in Thyroid Cancer. *Am J Pathol* **188**, 229–241, <https://doi.org/10.1016/j.ajpath.2017.09.008> (2018).
36. Perez-Pinera, P. *et al.* The Trk tyrosine kinase inhibitor K252a regulates growth of lung adenocarcinomas. *Mol Cell Biochem* **295**, 19–26, <https://doi.org/10.1007/s11010-006-9267-7> (2007).

Acknowledgements

The authors acknowledge the assistance of the Hunter Cancer Biobank in the execution of this project and Dr Mark Jones (Clinical Research Design and Statistics Unit, Hunter Medical Research Institute) for statistical advice. This research was supported by the University of Newcastle, the Hunter Cancer Research Alliance (HCRA) and the Maitland Cancer Appeal Committee. This work is also supported by China Scholarship Council support to Fangfang Gao.

Author Contributions

M.M.W., P.J., R.F.T. and H.H. designed the study; F.G., N.G., S.F., L.W., S.R., A.F., C.W.R. carried out and analysed the experiments; H.H. wrote the manuscript. All co-authors have edited the manuscript and approved the final version.

Additional Information

Supplementary information accompanies this paper at <https://doi.org/10.1038/s41598-018-26408-2>.

Competing Interests: The authors declare no competing interests.

Publisher's note: Springer Nature remains neutral with regard to jurisdictional claims in published maps and institutional affiliations.



Open Access This article is licensed under a Creative Commons Attribution 4.0 International License, which permits use, sharing, adaptation, distribution and reproduction in any medium or format, as long as you give appropriate credit to the original author(s) and the source, provide a link to the Creative Commons license, and indicate if changes were made. The images or other third party material in this article are included in the article's Creative Commons license, unless indicated otherwise in a credit line to the material. If material is not included in the article's Creative Commons license and your intended use is not permitted by statutory regulation or exceeds the permitted use, you will need to obtain permission directly from the copyright holder. To view a copy of this license, visit <http://creativecommons.org/licenses/by/4.0/>.

© The Author(s) 2018

The neurotrophic tyrosine kinase receptor TrkA and its ligand NGF are increased in squamous cell carcinomas of the lung.

Fangfang Gao^{1,2}, Nathan Griffin^{1,2}, Sam Faulkner^{1,2}, Christopher W. Rowe^{2,3}, Lily Williams¹, Severine Roselli^{1,2}, Rick F. Thorne², Aysha Ferdoushi^{1,2}, Phillip Jobling^{1,2}, Marjorie M. Walker^{2,3}, Hubert Hondermarck^{1,2,*}

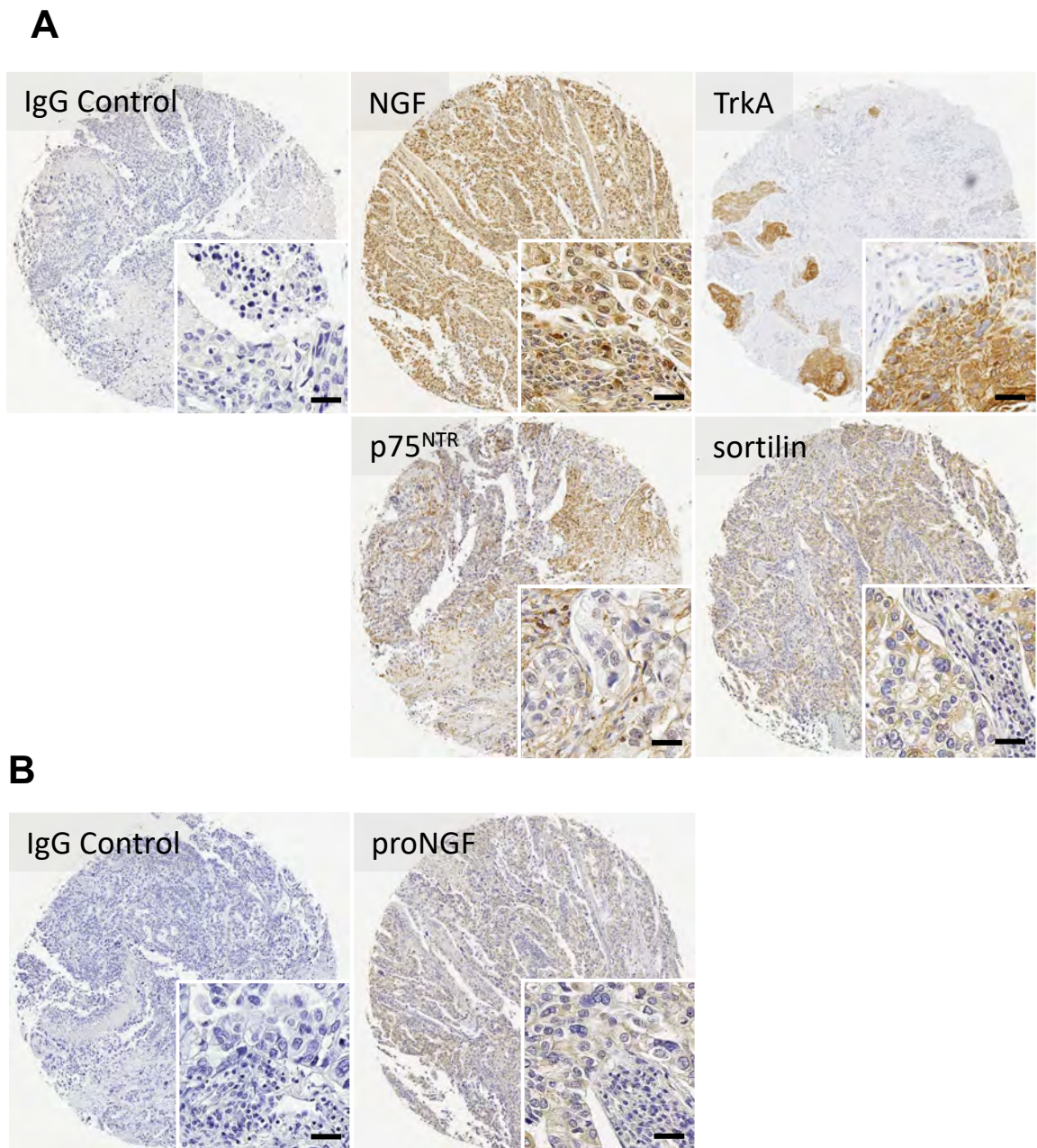
¹School of Biomedical Sciences & Pharmacy, Faculty of Health and Medicine, University of Newcastle, Callaghan NSW 2308, Australia.

²Hunter Medical Research Institute, University of Newcastle, New Lambton NSW 2305, Australia.

³School of Public Health & Medicine, Faculty of Health and Medicine, University of Newcastle, Callaghan NSW 2308, Australia.

Corresponding author: Hubert Hondermarck, School of Biomedical Sciences & Pharmacy, Life Sciences Building (LS3-35), University of Newcastle, Callaghan NSW 2308, Australia. Tel: +61 2492 18830. Email: hubert.hondermarck@newcastle.edu.au

Supplementary Figure 1: Negative controls for immunohistochemistry. A. Rabbit isotype control antibody was used in immunohistochemistry for NGF (ab52918, 1:200), TrkA (cs2508, 1:200), p75^{NTR} (cs4201, 1:400) and sortilin (ANT009,1:500). B. Mouse isotype control antibody was used in immunohistochemistry for proNGF (6E10E7, 2.5µg/ml). Scale=25µm



Supplementary Figure 1: Negative controls for immunohistochemistry. A. Rabbit isotype control antibody was used in immunohistochemistry for NGF (ab52918, 1:200), TrkA (cs2508, 1:200), p75^{NTR} (cs4201, 1:400) and sortilin (ANT009, 1:500). B. Mouse isotype control antibody was used in immunohistochemistry for proNGF (6E10E7, 2.5µg/ml). Scale=25µm



Received: 12 September 2018

Revised: 8 October 2018

Accepted: 29 October 2018

DOI: 10.1111/cen.13897

ORIGINAL ARTICLE

WILEY

High-dose preoperative cholecalciferol to prevent post-thyroidectomy hypocalcaemia: A randomized, double-blinded placebo-controlled trial

Christopher W. Rowe^{1,2} | Sam Arthurs³ | Christine J. O'Neill^{2,4} |
Jacqueline Hawthorne⁴ | Rosemary Carroll⁴ | Katie Wynne^{1,2} | Cino Bendinelli⁴

¹Department of Endocrinology, John Hunter Hospital, Newcastle, New South Wales, Australia

²School of Medicine and Public Health, University of Newcastle, New South Wales, Australia

³Department of Rehabilitation, John Hunter Hospital, Newcastle, New South Wales, Australia

⁴Department of Surgery, John Hunter Hospital, Newcastle, New South Wales, Australia

Correspondence

Cino Bendinelli, Department of Surgery, John Hunter Hospital, New Lambton Heights, NSW, Australia.
Email: cino.bendinelli@hnehealth.nsw.gov.au

Funding information

This study was funded by a John Hunter Hospital Charitable Trust Grant.

Summary

Objective: Post-thyroidectomy hypocalcaemia is a significant cause of morbidity and prolonged hospitalization, usually due to transient parathyroid gland damage, treated with calcium and vitamin D supplementation. We present a randomized, double-blinded placebo-controlled trial of preoperative loading with high-dose cholecalciferol (300 000 IU) to reduce post-thyroidectomy hypocalcaemia.

Patients and Measurements: Patients (n = 160) presenting for thyroidectomy at tertiary hospitals were randomized 1:1 to cholecalciferol (300 000 IU) or placebo 7 days prior to thyroidectomy. Ten patients withdrew prior to surgery. The primary outcome was post-operative hypocalcaemia (corrected calcium <2.1 mmol/L in first 180 days).

Results: The study included 150 patients undergoing thyroidectomy for Graves' disease (31%), malignancy (20%) and goitre (49%). Mean pre-enrolment vitamin D was 72 ± 26 nmol/L. Postoperative hypocalcaemia occurred in 21/72 (29%) assigned to cholecalciferol and 30/78 (38%) participants assigned to placebo ($P = 0.23$). There were no differences in secondary end-points between groups. In pre-specified stratification, baseline vitamin D status did not predict hypocalcaemia, although most individuals were vitamin D replete at baseline. Post-hoc stratification by day 1 parathyroid hormone (PTH) (<10 pg/mL, low vs ≥ 10 pg/mL, normal) was explored due to highly divergent rates of hypocalcaemia in these groups. Using a Cox regression model, the hazard ratio for hypocalcaemia in the cholecalciferol group was 0.56 (95%CI 0.32-0.98, $P = 0.04$) after stratification for Day 1 PTH. Further clinical benefits were observed in these subgroups.

Conclusions: Pre-thyroidectomy treatment with high-dose cholecalciferol did not reduce the overall rate of hypocalcaemia following thyroidectomy. In subgroups stratified by day 1 PTH status, improved clinical outcomes were noted.

KEYWORDS

cholecalciferol, hypocalcaemia, RCT, thyroidectomy, vitamin D

Christopher W. Rowe and Sam Arthurs contributed equally to this publication.

1 | INTRODUCTION

Thyroid surgery is the most common endocrine operation, performed at a rate of 60 operations per 100 000 patients per year.¹ Postoperative hypocalcaemia, due to transient or permanent damage to the parathyroid glands, is a common and significant complication of thyroidectomy.² Postoperative biochemical hypocalcaemia (corrected calcium <2.1 mmol/L on the first post-operative day) occurs in 23% of patients undergoing total thyroidectomy for any indication and in 28%-32% of patients undergoing thyroid cancer surgery,² contributing significantly to morbidity and increased length of hospital stay post-procedure.^{3,4} Common symptoms of hypocalcaemia include perioral tingling or tetany; however, life-threatening arrhythmias or laryngospasm can occur.⁵

Risk factors for post-thyroidectomy hypocalcaemia include older age, female sex, obesity, Graves' disease and extent of intraoperative surgical dissection.⁶⁻⁸ Vitamin D deficiency has been suggested as a risk factor; however, its significance remains uncertain and probably varies with the vitamin D status of the reference population.^{3,9} As it is a potentially modifiable risk factor with a high reported incidence (31% in an Australian population),¹⁰ vitamin D represents an attractive therapeutic target.

Previously, two prospective randomized trials have shown that treatment with activated vitamin D reduces incidence of postoperative hypocalcaemia.^{11,12} However, due to its potency, activated vitamin D presents a risk of hypercalcaemia, which may preclude widespread adoption. In a small study of seven days treatment with calcitriol (1.5 µg daily) plus hydrochlorothiazide prior to thyroidectomy, 3/22 (14%) patients developed hypercalcaemia (range 2.51-2.72 mmol/L).¹¹

To date, no prospective randomized trial has examined the role of vitamin D₃ (cholecalciferol) supplementation in preventing post-thyroidectomy hypocalcaemia. Cholecalciferol is an inexpensive, orally absorbed, lipid-soluble drug with a high volume of distribution and requires endogenous 1-α hydroxylation to achieve full potency, which contributes to its high therapeutic index, low toxicity and extremely long in vivo half-life, permitting high loading doses to be safely administered.¹³ Previous studies have established that single doses of 300 000 international units (IU) of cholecalciferol establish sufficiency in vitamin D-deficient populations and are well tolerated.¹⁴⁻¹⁶

We hypothesized that preoperative supplementation with high-dose oral cholecalciferol would reduce the incidence of postoperative hypocalcaemia following thyroidectomy, compared to placebo.

2 | MATERIALS AND METHODS

We conducted a randomized, parallel-group, double-blinded, placebo-controlled superiority trial comparing the effect of a single oral dose of 300 000 IU of cholecalciferol with placebo on the occurrence of post thyroidectomy hypocalcaemia.

All patients aged 18 years and over scheduled to undergo total or completion thyroidectomy for any cause by one of four specialized thyroid surgeons at John Hunter Hospital or Newcastle Private Hospital were eligible for this trial. Patients were recruited from August 2014 to December 2017.

Specific exclusion criteria were current pharmacotherapy with any form of vitamin D supplementation, chronic kidney disease (eGFR <60 mL/min/1.73m²), pregnancy, current treatment with antiresorptive therapy (bisphosphonates or RANK-L inhibitors), known chronic liver disease or hypercalcaemia (corrected calcium >2.55 mmol/L on screening blood tests).

After written informed consent was obtained, participants were randomized to take the study drug seven days prior to surgery. The study drug was identically presented as 6 gelatin capsules containing 6 x 50 000 IU of cholecalciferol, or 6 capsules of rice flour placebo (supplied at no cost by Biological Therapeutics, Braeside, Victoria), contained in coded bottles labelled in line with good pharmacy manufacturing practice as "C" or "D." Pre-dose (at enrolment) and post-dose vitamin D (day of surgery) results were concealed from clinicians and researchers using coded samples. Blood tests for calcium, phosphate and PTH occurred prior to randomization, on the day of surgery, then at 6 hours, 24 hours, 48 hours, 7 days, 30 days, 90 days and 180 days and were available to clinicians and researchers. At each post-operative blood test, participants were examined for signs or symptoms of hypocalcaemia and responses recorded using a checklist. Postoperative calcium management was standardized according to protocol, where calcium carbonate (1200 mg thrice daily) was commenced if corrected calcium <2.2 mmol/L or symptoms of hypocalcaemia were present; and calcitriol (0.5 µg twice daily) was commenced if PTH was undetectable or if corrected calcium <2.0 mmol/L, with further management at the discretion of the treating surgeon. Magnesium was measured daily and supplemented if low.

A centralized web-based randomization was used, with a 1:1 allocation to placebo or cholecalciferol in computer-generated blocks of 4 (Clinical Research Design and IT Statistical Support Unit, Hunter Medical Research Institute, Newcastle, Australia), stratified by hospital site. A Clinical Trials Pharmacist held the break codes for the trial in the case of a serious adverse event where it was deemed necessary to identify the treatment allocation for clinical care.

Thyroidectomy was conducted through a collar incision and was performed by high-volume thyroid surgeons. Parathyroid glands were visualized after ligation of both the middle thyroid vein and the upper pedicle. In order to preserve parathyroid vascular supply, subcapsular dissection was carried out with blunt and sharp dissection, and the inferior thyroid artery branches were divided as distally as possible. Haemostasis was achieved with a combination of clips, ties and energy devices. If the surgeon considered the parathyroid gland had been devascularized, it was auto-transplanted into the sternocleidomastoid muscle using an injection technique after fine mincing.

The primary outcome was the incidence of any postoperative biochemical hypocalcaemia (corrected serum calcium <2.10 mmol/L)

at any time point during the first 180 post-operative days. Secondary outcomes were incidence of hypocalcaemia in the first 48 post-operative hours, symptomatic hypocalcaemia (any one of: perioral paraesthesia, tetany, positive Chvostek's sign or prolonged QT-interval on ECG associated with biochemical hypocalcaemia), length of hospital stay, permanent hypoparathyroidism (ongoing requirement for calcitriol >90 days postoperative), calcium and calcitriol requirements in the first 48 postoperative hours and need for hospital discharge on calcium/calcitriol supplementation. Pre-specified subgroup analysis stratified participants by baseline (pre - study medication) 25-OH vitamin D levels.

The expected rate of postoperative hypocalcaemia following thyroidectomy for unselected populations with unknown vitamin D status is 23%-32%.^{2,3,17} Prior studies have shown that rates of postoperative hypocalcaemia in populations replete vitamin D is 3%-14% in two studies.^{3,9} To reject the null hypothesis with a two-sided alpha of 0.05 and power 80%, 72 participants in each group were required. Assuming a dropout of rate of 5%-10%, we planned to recruit 160 participants.

Participants were analysed on an intention-to-treat basis, meaning that all patients who were dispensed study medication and underwent thyroidectomy were included. Categorical outcome data were analysed using a chi-square test. Continuous variables were analysed using Student's *t* tests for parametric data and Wilcoxon rank-sum test for non-parametric data. Time-to-hypocalcaemia data were used to fit separate Cox proportional hazard models for the primary outcome, and accounting for baseline vitamin D level as a pre-specified outcome. All models were fitted using Stata v14.2 (Statacorp, Texas, USA).

The trial was prospectively registered with the Australian New Zealand Clinical Trials Registry (ACTRN12614000201673) and was approved by the Hunter New England Human Research Ethics Committee (reference number 14/02/19/3.06).

3 | RESULTS

Between June 2014 and December 2017, 160 of 203 screened patients met inclusion criteria and were randomized (Figure 1). The main reasons to fail screening were pre-existing therapy with vitamin D (29/43 participants), chronic kidney disease (6/43 patients) and declined consent (6/43 patients). Ten patients withdrew from the study between randomization and thyroidectomy, leaving 150 patients who underwent surgery and were included in the final analysis.

The baseline clinical characteristics of study patients are presented in Table 1. Randomization resulted in balanced distribution of demographic and clinical parameters. Overall, mean age was 52 ± 16 years, with 76% female. Most operations (49%) were for multinodular goitre, 31% for Graves' disease and 20% for thyroid cancer. Total thyroidectomy was performed in 90% of participants (34% for Graves' disease, 50% for goitre and 16% for cancer) while 10% had a completion thyroidectomy (all for cancer). Mean baseline 25-OH vitamin D level was 72 ± 26 nmol/L. The mean change in 25-OH vitamin D level following study medication was 1 ± 17 nmol/L in the placebo group and 43 ± 33 nmol/L in the cholecalciferol group. In the cholecalciferol group, 59/67 participants with available post-dose vitamin D measurement had

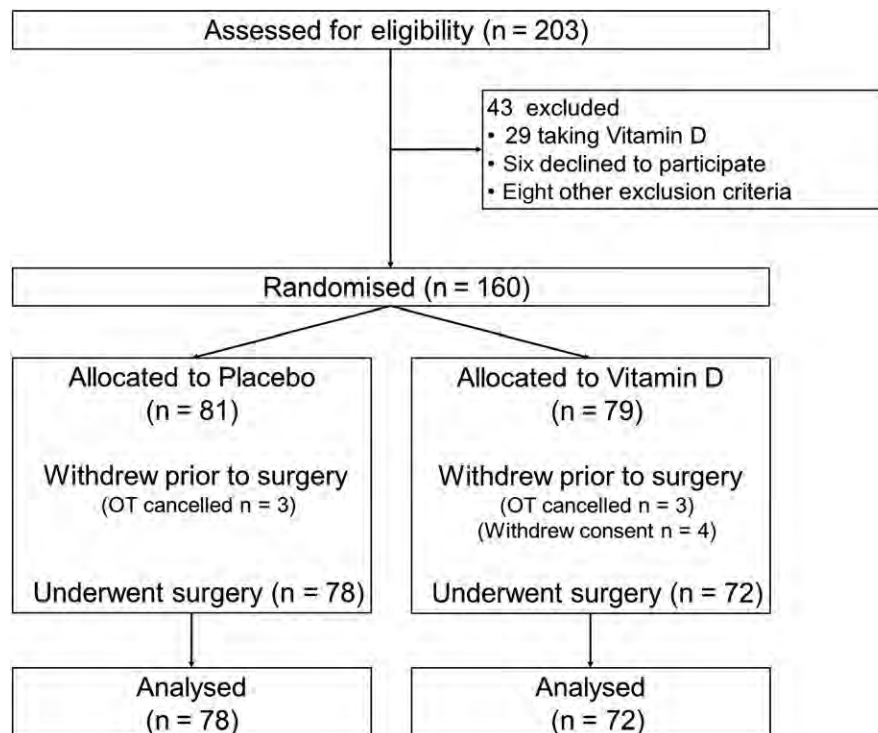


FIGURE 1 Flow diagram of screening, enrolment and dropout

TABLE 1 Demographic and clinical characteristics

	Placebo	Vitamin D
n	78	72
Age (years)	55 (17)	49 (15)
Female gender	61 (78%)	53 (74%)
BMI (kg/m ²) (n = 116)	31.0 (6.6)	29.5 (7.6)
Caucasian ethnicity	73 (94%)	69 (96%)
Indication for thyroidectomy		
Graves' disease	23 (29%)	23 (32%)
Goitre	40 (51%)	34 (47%)
Thyroid cancer	15 (19%)	15 (21%)
Surgical facility		
Public hospital	59 (76%)	57 (79%)
Private hospital	19 (24%)	15 (21%)
Operation type		
Total thyroidectomy	70 (91%)	64 (89%)
Completion thyroidectomy	7 (9%)	8 (11%)
Parathyroid re-implantation	31/78 (40%)	24/72 (33%)
Pre-dose vitamin D ^a		
Pre-dose 25-OH vitamin D (nmol/L)	67 (24)	77 (27)
Pre-dose 25-OH vitamin D < 50 nmol/L	14 (18%)	13 (18%)
Day of surgery biochemistry ^b		
Post-dose 25-OH vitamin D (nmol/L)	69 (20)	119 (41)
Corrected calcium (mmol/L)	2.35 (0.10)	2.32 (0.09)
Phosphate (mmol/L)	1.16 (0.16)	1.13 (0.20)
Magnesium (mmol/L)	0.84 (0.08)	0.84 (0.07)
PTH (pg/mL)	65 (32)	56 (31)

Data are mean (SD) or n (%).

Day of surgery 25-OH vitamin D level is missing for 6 patients in placebo group and 5 patients in vitamin D group. No differences in baseline characteristics were observed between groups.

^a7 days prior to surgery.

^b7 days after study drug and prior to surgery.

a rise in vitamin D level greater than one standard deviation of the placebo group, suggesting a high level of treatment adherence, and that 7 days is sufficient to meaningfully affect serum vitamin D levels.

3.1 | Primary and Secondary End-points

Postoperative hypocalcaemia (corrected calcium <2.10 mmol/L) occurred in 21/72 (29%, 95% CI 19%-40%) participants taking high-dose cholecalciferol and 30/78 (38%, 95% CI 28%-49%) participants taking placebo ($P = 0.23$) (Table 2). In pre-specified secondary end-points, 16/72 (22%, 95% CI 13%-32%) participants assigned to high-dose cholecalciferol developed hypocalcaemia in the first 48 hours, compared to 27/78 (35%, 95% CI 24%-45%) participants assigned

TABLE 2 Primary and secondary outcomes

	Placebo	Vitamin D	P
Primary outcome			
Any postoperative hypocalcaemia	30/78 [38% (28%-49%)]	21/72 [29% (19%-40%)]	0.23
Secondary outcomes			
Inpatient hypocalcaemia	27/78 [35% (24%-45%)]	16/72 [22% (13%-32%)]	0.09
Symptomatic hypocalcaemia	12/78 [15% (7%-23%)]	9/72 [13% (5%-20%)]	ns
Length of hospital stay (days, median (IQR))	2 (2-3)	2 (2-2)	0.16
Permanent hypoparathyroidism	4/78 [5% (0%-10%)]	1/72 [1% (0%-4%)]	0.22
Calcium carbonate required in first 48 h	33/78 [42% (31%-53%)]	24/72 [33% (22%-44%)]	ns
Calcitriol required in first 48 h	19/78 [24% (15%-34%)]	14/72 [19% (10%-29%)]	ns
Discharged on calcium/calcitriol replacement	29/78 [37% (26%-48%)]	20/72 [28% (17%-38%)]	0.22
Safety outcomes			
Any post-dose calcium above 2.55 mmol/L	4/78 (5%)	3/72 (4%)	ns
Any post-dose calcium above 3 mmol/L	1/78 (1%)	1/72 (1%)	ns

Data are % (95% CI) or median (IQR). Hypocalcaemia: corrected calcium <2.1 mmol/L.

to placebo ($P = 0.09$). There were no differences in other secondary end-points (Table 2). The primary outcome was assessed with time-to-hypocalcaemia analysis using Kaplan-Meier curves and a Cox regression analysis for the overall primary outcome (Figure 2A) and for pre-specified subgroup analysis based on pre-operative vitamin D level (continuous variable). In the model including primary outcome and treatment group alone, the hazard ratio favoured high-dose cholecalciferol, but was not significant (HR 0.73 95%CI 0.42-1.27, $P = 0.27$). Baseline Vitamin D status did not predict hypocalcaemia (HR 1.0, 95%CI 0.99-1.01). The study drug was well tolerated, with no increase in the rate of hypercalcaemia between placebo and study drug (Table 2). The three participants in the treatment group with hypercalcaemia all occurred at day 7 post surgery (corrected calcium of 2.56, 2.76 and 3.09 mmol/L) and did not require specific intervention.

3.2 | Subgroup analysis

Highly divergent rates of post-operative hypocalcaemia were noted based on day 1 post-operative PTH status (Figure 2B), which is known to be a reliable predictor of post-operative hypocalcaemia.¹⁸⁻²¹ To investigate for possible masking of an overall treatment effect, we performed post-hoc analysis dichotomized by post-operative day 1

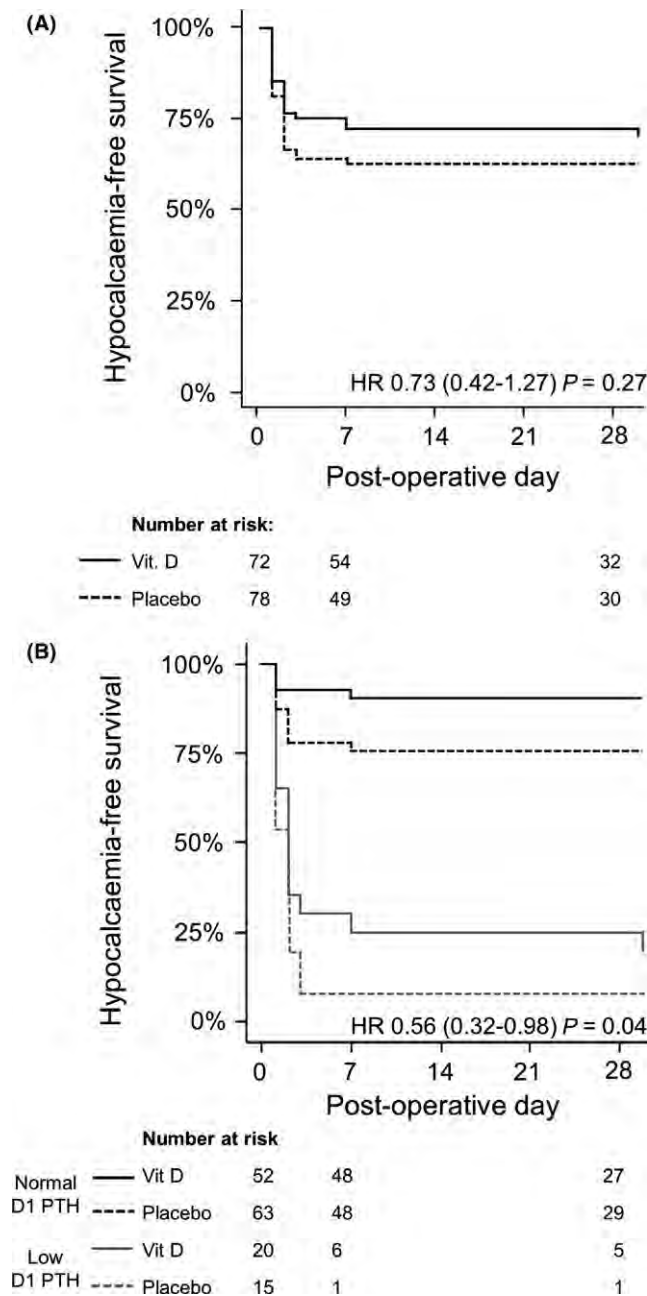


FIGURE 2 Kaplan-Meier curves showing hypocalcaemia-free survival rates for the first 28 post-operative days. A, Overall, stratified by treatment group, Cox proportional hazard ratio for high-dose cholecalciferol 0.73 (95%CI 0.42-1.27, $P = 0.27$) and B) stratified by treatment group and postoperative day 1 PTH levels (<10 vs ≥ 10 pg/mL), hazard ratio for hypocalcaemia-free survival in high-dose cholecalciferol group 0.56 (95% CI 0.31-0.98, $P = 0.04$)

PTH level (<10 pg/mL, below the lower limit of the local reference range; ≥ 10 pg/mL, normal).

Analysis of these subgroups in a Cox proportional hazard model stratified by day 1 post-operative PTH level (below or above the lower limit of the local laboratory reference range, 10 pg/mL) the hazard ratio for postoperative hypocalcaemia was 0.56 (95% CI 0.31-0.98, $P = 0.04$) for the group that received cholecalciferol group compared to placebo (Figure 2B, Table 3). As expected, Day 1

PTH status was strongly predictive of hypocalcaemia (HR 7.44, 95% CI 4.16-13.32, $P < 0.0001$).

Table 3 details the secondary end-points stratified in these groups. In the normal-PTH group, participants that received cholecalciferol had lower requirements for calcium carbonate during hospitalization (12% vs 29% requiring supplementation, $P = 0.03$) and were significantly less likely to require calcium carbonate (8% vs 24%, $P = 0.02$) or calcitriol (0% vs 8%, $P = 0.04$) supplementation on discharge than the placebo group. In the low-PTH subgroup, the rate of inpatient hypocalcaemia was significantly lower in the cholecalciferol group compared to placebo (60% vs 93%, $P = 0.03$), and the median doses of calcium carbonate (3600 vs 7200 mg, $P = 0.01$) and calcitriol 100 vs 200 μ g, $P = 0.05$) were lower in the first 48 hours post-operatively. There was also a significant median reduction in length of stay of 24 hours in the treatment group ($P = 0.04$) (Table 3).

4 | DISCUSSION

Postoperative hypocalcaemia following thyroidectomy is a common complication due to either transient or permanent damage to the parathyroid glands. As well as contributing to patient morbidity, it also increases health care-associated expenditure due to increased monitoring requirements, pharmacotherapy and prolonged hospitalization. Interventions which minimize postoperative hypocalcaemia are needed to improve patient care and improve resource use.

This study tested whether a single preoperative dose of 300 000 IU cholecalciferol was more effective than placebo in reducing the incidence of postoperative hypocalcaemia in an unselected prospective cohort of predominantly Caucasian patients without severe vitamin D deficiency. Although a trend towards improved outcomes was observed in the vitamin D group compared with placebo, in the overall cohort, both primary and secondary end-points did not reach statistical significance.

As expected, post-operative day 1 PTH levels were strongly predictive of hypocalcaemia and identified subgroups with marked differences in incidence of hypocalcaemia and requirements for postoperative therapy (Table 3, Figure 2B).¹⁸ This heterogeneity may have masked the treatment effect of high-dose cholecalciferol in the overall cohort, which was observed when stratified by PTH status. In the subgroup with impaired PTH secretion post surgery ($n = 35$, 23%), the high-dose cholecalciferol group showed an absolute risk reduction of inpatient hypocalcaemia of 33%, with three patients needing treatment to prevent one case of hypocalcaemia; a 50% absolute reduction in the median dose of calcium carbonate and calcitriol required as an inpatient; and a 24-hour median reduction in overall length of stay. Interestingly, these outcomes were observed despite the theoretical reduction in endogenous 1- α hydroxylation of cholecalciferol due to the absence of PTH, suggesting that replete vitamin D reserves may be protective in this setting.

In contrast, in the subgroup with normal PTH on day 1 ($n = 115$, 77%), the treatment group showed a significant reduction in the primary end-point (hypocalcaemia at any postoperative point) with

TABLE 3 Post-hoc subgroup analysis of primary and secondary end-points, stratified by post-operative day 1 parathyroid hormone status

Subgroup: Day 1 PTH	Day 1 PTH <10 pg/mL			Day 1 PTH ≥10 pg/mL		
	Placebo	Vitamin D	P	Placebo	Vitamin D	P
n	15	20		63	52	
Age (y)	53 (18)	49 (17)		56 (17)	50 (15)	
Female gender	80%	75%		78%	73%	
Pre-dose vitamin D (nmol/L)	72 (15)	75 (30)		66 (26)	77 (26)	
Post-dose vitamin D (nmol/L)	72 (15)	125 (54)		68 (21)	117 (34)	
Post-dose calcium (mmol/L)	2.34 (0.12)	2.32 (0.09)		2.35 (0.10)	2.33 (0.09)	
Post-dose PTH (pg/mL)	69 (32)	53 (27)		64 (32)	57 (32)	
Primary outcome						
Any postoperative hypocalcaemia	15/15 (100%)	16/20 (80%)	0.07	15/63 (24%)	5/52 (10%)	0.05
Secondary outcomes						
Inpatient hypocalcaemia	14/15 (93%)	12/20 (60%)	0.03	13/63 (21%)	4/52 (8%)	0.05
Symptomatic Hypocalcaemia	3/15 (20%)	7/20 (35%)	ns	9/63 (14%)	2/52 (4%)	0.06
Length of hospital stay (days)	3 (3-4)	2 (2-3)	0.04	2 (2-2)	2 (2-2)	ns
Calcium carbonate supplementation						
Required in first 48 h (n, %)	15/15 (100%)	18/20 (90%)	ns	18/63 (29%)	6/52 (12%)	0.03
Cumulative dose first 48 h (mg)	7200 (3600-8000)	3600 (1800-4300)	0.01	0 (0-1800)	0 (0-0)	0.03
Required on discharge (n, %)	14/15 (93%)	16/20 (80%)	ns	15/63 (24%)	4/52 (8%)	0.02
Calcitriol supplementation						
Required in first 48 h (n, %)	13/15 (87%)	13/20 (65%)	ns	6/63 (10%)	1/52 (2%)	0.09
Cumulative dose first 48 h (µg)	200 (100-200)	100 (0-175)	0.05	0 (0-0)	0 (0-0)	0.10
Required on discharge (n, %)	12/15 (80%)	13/20 (65%)	ns	5/63 (8%)	0/52 (0%)	0.04

Data are mean (SD); median (IQR) or n (%). ns = non-significant. Hypocalcaemia: corrected calcium <2.1 mmol/L.

seven patients needing treatment to prevent one case of hypocalcaemia and an absolute risk reduction of 14%. Further, there was a 16% absolute reduction in the number of patients discharged on calcium carbonate and calcitriol in this group. These marked improvements in clinically meaningful end-points suggest that pre-treatment with cholecalciferol optimizes inpatient outcomes and facilitates earlier discharge, without an increase in the rate of complications. The rate of post-operative hypercalcaemia was low in both groups, and importantly, there was no signal for higher rates of hypercalcaemia in the cholecalciferol-treated group (4%) compared to placebo (5%). Although it is possible that pre-treatment with cholecalciferol may delay recognition of permanent hypoparathyroidism, this effect was not observed, with the only case of permanent hypoparathyroidism in the cholecalciferol group developing hypocalcaemia within the first 24 post-operative hours.

This study did not demonstrate a correlation between rates of postoperative hypocalcaemia and baseline Vitamin D status. However, in this population, the median 25-OH vitamin D levels were substantially higher than the levels observed in other studies.

This may have been due to the study setting, in which predominantly Caucasian participants were recruited from a low-latitude location.²² Two prior studies showing a strong correlation between preoperative vitamin D status and risk of postoperative hypocalcaemia included higher proportions of patients with severe vitamin D deficiency (<25 nmol/L), with an incidence of severe deficiency of 30% in a Saudi Arabian population⁹ and 29% in a British urban population.³ By contrast, no participant in this present study had a preoperative vitamin D < 25 nmol/L (range in placebo group 28-111 nmol/L). Therefore, although this study does not provide data on response to therapy in a severely vitamin D-deficient group, it does establish that clinical benefits following high-dose cholecalciferol are observed in vitamin D replete populations.

This study builds on results from two previous randomized trials of perioperative activated vitamin D supplementation. Testa and colleagues¹¹ randomized 42 Pre-thyroidectomy Italian patients to pre-operative calcitriol (1.5µg per day) + hydrochlorothiazide for 7 days prior to surgery, or placebo, and found a significant reduction in postoperative hypocalcaemia <2.1 mmol/L

(5% vs 50%, $P < 0.01$) as well as reduced length of stay by 1 day, but at the cost of modest pre-operative hypercalcaemia (calcium 2.55–2.72 mmol/L) in 14% of participants. Baseline vitamin D status was not reported. Genser and colleagues¹² randomized 222 French patients to either placebo or 2 µg alfacalcidol for 9 days, beginning one day prior to surgery. The primary end-point (postoperative calcium <2.0 mmol/L) occurred in 37% of placebo-treated participants compared to 30% of alfacalcidol-treated participants ($P = 0.25$), overall rates that were similar to this present study. Rates of symptomatic hypocalcaemia were lower in the treatment group (11% vs 22%, $P = 0.02$). Mild vitamin D deficiency was noted in the study population (mean vitamin D 54 ± 27 nmol/L, compared to 72 ± 26 nmol/L in this present study).

This study has several key strengths. Firstly, it is a robustly designed and implemented randomized trial with blinding of investigators and participants and evidence of effective randomization. Second, there was a high level of patient participation, when recruited from real-world hospital-based clinics across two sites, suggesting that these results are generalizable to standard hospital settings. Finally, the rate of adherence to study medication is estimated to be high, based on the observed change in vitamin D status in the high-dose cholecalciferol group post-treatment with narrow standard deviation (Table 1), suggesting that the intervention is acceptable to patients.

Our study has some limitations. First, the primary end-point of postoperative hypocalcaemia (<2.1 mmol/L), although robust, was higher than used in some studies and may have been minimized by our proactive, protocolized postoperative care. Secondly, the study may have been underpowered with respect to the primary end-point despite careful literature review, especially with the higher than expected pre-operative vitamin D status in the placebo group.¹⁰ Third, there was reduced study retention after the 7th postoperative day; however, given that the majority of hypocalcaemia occurs within 48 hours of surgery (Figure 2A), the impact of this loss to follow-up is minimal.

In conclusion, Pre-thyroidectomy treatment with high-dose cholecalciferol was not shown to reduce the rate of post-operative hypocalcaemia in the overall group. However, improvements in clinical outcomes were noted when accounting for heterogeneity due to divergence in post-operative PTH status.

ACKNOWLEDGEMENTS

The authors would like to acknowledge Dr Daron Cope and Dr Rob Eisenberg for contributing to study recruitment and the Clinical Research Design IT and Statistical Support Team, Hunter Medical Research Institute for study design advice and online randomization set-up.

CONFLICT OF INTEREST

The authors declare they have no conflict of interest.

AUTHOR CONTRIBUTION

CB conceived the study with KW and designed the protocol with SA, RC and CO. CR analysed the data with CB, KW, SA, CO and JH, and drafted the manuscript, with revision from all authors. All authors were involved in the study and have approved the final manuscript.

ORCID

Christopher W. Rowe  <https://orcid.org/0000-0002-9652-6562>

REFERENCES

- Francis DO, Randolph G, Davies L. Nationwide variation in rates of thyroidectomy among US medicare beneficiaries. *JAMA Otolaryngol Head Neck Surg*. 2017;143:1122–1125.
- Chadwick DR. Hypocalcaemia and permanent hypoparathyroidism after total/bilateral thyroidectomy in the BAETS Registry. *Gland Surg*. 2017;6:S69–S74.
- Kirkby-Bott J, Markogiannakis H, Skandarajah A, Cowan M, Fleming B, Palazzo F. Preoperative vitamin D deficiency predicts postoperative hypocalcemia after total thyroidectomy. *World J Surg*. 2011;35:324–330.
- Alkhalili E, Ehrhart MD, Ayoubieh H, Burge MR. Does Pre-operative vitamin d deficiency predict postoperative hypocalcemia after thyroidectomy? *Endocrine Practice*. 2017;23:5–9.
- Khosla S.(2008)Hypercalcaemia and hypocalcaemia. In Harrison's Principles of Internal Medicine (17th Ed) (ed. E. B. Anthony S Fauci, Dennis L Kasper, Stephen L Hauser, Dan L Longo, J. Larry Jameson, Joseph Loscalzo). McGraw Hill Publishing Inc, United States of America.
- Erbil Y, Ozbey NC, Sari S, et al. Determinants of postoperative hypocalcemia in vitamin D-deficient Graves' patients after total thyroidectomy. *Am J Surg*. 2011;201:685–691.
- Erbil Y, Bozbora A, Ozbey N, et al. Predictive value of age and serum parathormone and vitamin d3 levels for postoperative hypocalcemia after total thyroidectomy for nontoxic multinodular goiter. *Arch Surg*. 2007;142:1182–1187.
- Wingert DJ, Friesen SR, Iliopoulos JI, Pierce GE, Thomas JH, Hermreck AS. Post-thyroidectomy hypocalcemia. Incidence and risk factors. *Am J Surg*. 1986;152:606–610.
- Al-Khatib T, Althubaiti AM, Althubaiti A, Mosli HH, Alwasiah RO, Badawood LM. Severe vitamin D deficiency: a significant predictor of early hypocalcemia after total thyroidectomy. *Otolaryngology and Head and Neck Surgery*. 2015;152:424–431.
- Daly RM, Gagnon C, Lu ZX, et al. Prevalence of vitamin D deficiency and its determinants in Australian adults aged 25 years and older: a national, population-based study. *Clin Endocrinol*. 2012;77:26–35.
- Testa A, Fant V, De Rosa A, et al. Calcitriol plus hydrochlorothiazide prevents transient post-thyroidectomy hypocalcemia. *Horm Metab Res*. 2006;38:821–826.
- Genser L, Tresallet C, Godiris-Petit G, et al. Randomized controlled trial of alfacalcidol supplementation for the reduction of hypocalcemia after total thyroidectomy. *Am J Surg*. 2014;207:39–45.
- Nolin TD, Friedman PA. In: Therapeutics, 13e. Brunton LL, Hilal-Dandan R, Knollmann BC ed. *Agents Affecting Mineral Ion Homeostasis and Bone Turnover*. In Goodman & Gilman's: The Pharmacological Basis of Therapeutics. New York, NY: McGraw-Hill Education; 2017.
- Leventis P, Kiely PD. The tolerability and biochemical effects of high-dose bolus vitamin D2 and D3 supplementation in patients with vitamin D insufficiency. *Scand J Rheumatol*. 2009;38:149–153.

15. Cipriani C, Romagnoli E, Scillitani A, et al. Effect of a single oral dose of 600,000 IU of cholecalciferol on serum calciotropic hormones in young subjects with vitamin D deficiency: a prospective intervention study. *J Clin Endocrinol Metab.* 2010;95:4771-4777.
16. Khan AH, Rohra DK, Saghir SA, Udani SK, Wood R, Jabbar A. Response of a single 'mega intramuscular dose' of vitamin D on serum 25OHD and parathyroid hormone levels. *J Coll Physicians and Surg-Pak.* 2012;22:207-212.
17. Cherian AJ, Ponraj S, Gowri SM, et al. The role of vitamin D in post-thyroidectomy hypocalcemia: Still an enigma. *Surgery.* 2016;159:532-538.
18. Grodski S, Lundgren C, Sidhu S, Sywak M, Delbridge L. Postoperative PTH measurement facilitates day 1 discharge after total thyroidectomy. *Clin Endocrinol.* 2009;70:322-325.
19. Mazotas IG, Wang TS. The role and timing of parathyroid hormone determination after total thyroidectomy. *Gland Surg.* 2017;6:S38-S48.
20. Noureldine SI, Genther DJ, Lopez M, Agrawal N, Tufano RP. Early predictors of Hypocalcemia after total thyroidectomy: an analysis of 304 patients using a short-stay monitoring protocol. *JAMA Otolaryngol Head Neck Surg.* 2014;140:1006-1013.
21. McLeod IK, Arciero C, Noordzij JP, et al. The use of rapid parathyroid hormone assay in predicting postoperative hypocalcemia after total or completion thyroidectomy. *Thyroid.* 2006;16:259-265.
22. Webb AR. Who, what, where and when—influences on cutaneous vitamin D synthesis. *Prog Biophys Mol Biol.* 2006;92:17-25.

How to cite this article: Rowe CW, Arthurs S, O'Neill CJ, et al. High-dose preoperative cholecalciferol to prevent post-thyroidectomy hypocalcaemia: A randomized, double-blinded placebo-controlled trial. *Clin Endocrinol (Oxf).* 2019;90:343–350. <https://doi.org/10.1111/cen.13897>

Research Article: Pregnancy

An intravenous insulin protocol designed for pregnancy reduces neonatal hypoglycaemia following betamethasone administration in women with gestational diabetes

C. W. Rowe^{1,2} , E. Putt¹, O. Brentnall¹, A. Gebuehr¹, J. Allabyrne³, A. Woods^{2,3} and K. Wynne^{1,2}

¹Department of Endocrinology and Diabetes, John Hunter Hospital, ²School of Medicine and Public Health, University of New castle, and ³Department of Maternity and Gynaecology, John Hunter Hospital, Newcastle, Australia

Accepted 14 November 2018

Abstract

Aims Marked hyperglycaemia is common following betamethasone administration in women with gestational diabetes (GDM), and may contribute to neonatal hypoglycaemia. Validated protocols to deliver glycaemic stability following betamethasone are lacking. We hypothesized that an intravenous insulin (IVI) protocol for pregnancy-specific glycaemic targets (Pregnancy-IVI) would achieve greater at-target glycaemic control than a generic adult intravenous insulin protocol (Adult-IVI), and may reduce neonatal hypoglycaemia.

Methods A retrospective cohort study of the performance Adult-IVI and Pregnancy-IVI following betamethasone in GDM, sequentially implemented at a tertiary hospital, without change in indication for IVI. Cases were identified by electronic record search. Primary outcome was percentage of on-IVI time with at-target glycaemia [blood glucose level (BGL) 3.8–7 mmol/l]. Secondary outcomes were time with critical hyperglycaemia (BGL > 10 mmol/l), occurrence of maternal hypoglycaemia (BGL < 3.8 mmol/l), and incidence of neonatal hypoglycaemia (BGL ≤ 2.5 mmol/l) if betamethasone was administered within 48 h of birth.

Results The cohorts comprised 151 women (Adult-IVI $n = 86$; Pregnancy-IVI $n = 65$). The primary outcome was 68% time-at-target [95% confidence interval (CI) 64–71%] for Pregnancy-IVI compared with 55% (95% CI 50–60%) for Adult-IVI ($P = 0.0002$). Critical maternal hyperglycaemia (0% vs. 2%, $P = 0.02$) and hypoglycaemia (2% vs. 12%, $P = 0.02$) were both lower with Pregnancy-IVI than Adult-IVI. Neonatal hypoglycaemia was less common after Pregnancy-IVI (29%) than after Adult-IVI (54%, $P = 0.03$). A multiple logistic regression model adjusting for potential confounders gave an odds ratio for neonatal hypoglycaemia with Pregnancy-IVI of 0.27 (95% CI 0.10–0.76, $P = 0.01$).

Conclusions An IVI protocol designed for pregnancy effectively controlled maternal hyperglycaemia following betamethasone administration in GDM. This is the first intervention to show a reduction in betamethasone-associated neonatal hypoglycaemia, linked with optimum maternal glycaemic control.

Diabet. Med. 00: 1–9 (2018)

Introduction

In women with gestational diabetes (GDM), maintaining glycaemic control within near-physiological parameters throughout gestation is essential for healthy outcomes for mother and child, reducing pre-eclampsia, shoulder

dystocia and macrosomia [1,2]. Additionally, acute maternal hyperglycaemia in the antepartum may be important, disturbing fetal acid–base homeostasis (demonstrated in pre-clinical models [3,4] and human pregnancy [5–9]) and driving neonatal hyperinsulinaemia [10–12]. During labour, maternal hyperglycaemia correlates with neonatal hypoglycaemia [13–18], and it is recommended to maintain maternal glucose between 4 and 7 mmol/l [19], although evidence supporting interventions to achieve these targets is lacking [20].

Correspondence to: Christopher W. Rowe.

E-mail: christopher.rowe@hnehealth.nsw.gov.au

Presented as an abstract to the Society for Endocrinology BES, Glasgow, UK, November 2018.

What's new?

- Antepartum betamethasone causes maternal hyperglycaemia and is associated with neonatal hypoglycaemia. There is no validated protocol to mitigate these risks.
- This is the first large-scale validation of an intravenous insulin protocol for pregnancy that demonstrates high rates of 'at-target' maternal glucose following betamethasone in gestational diabetes, and a low incidence of on-infusion maternal hypoglycaemia, compared with a generic adult intravenous insulin infusion protocol. A reduction in neonatal hypoglycaemia was also demonstrated.
- This effective and safe protocol that delivers clinically relevant endpoints warrants validation in wider settings.

Administration of antenatal steroids, commonly betamethasone, in the setting of preterm labour improves neonatal lung function [21], but induces significant hyperglycaemia in women with and without diabetes mellitus [22]. This maternal hyperglycaemia, resulting in fetal hyperinsulinaemia, may be the mechanism for the observed subsequent neonatal hypoglycaemia. In a randomized trial of 2827 mothers with preterm delivery between 34 and 37 weeks gestation, administration of betamethasone was associated with a 24% incidence of neonatal hypoglycaemia, compared with 15% with placebo [relative risk (RR) 1.6, 1.37–1.87; $P < 0.001$] in women giving birth a median of 33 h after betamethasone [23]. Incidence of GDM in this trial was 11%.

Validated strategies to control maternal hyperglycaemia following betamethasone are lacking, both in terms of large-scale efficacy analysis and precisely defined endpoints. To date, several small uncontrolled trials (recruiting four to eight women each) have evaluated protocols for glycaemic management following glucocorticoids in pregnancy [24–26]. Marked between-trial heterogeneity in setting (early vs. late gestation) and steroid (prednisolone, dexamethasone or betamethasone), and small numbers, preclude significant analysis of efficacy, with no reported data on neonatal hypoglycaemia. Itoh and colleagues [27] demonstrated that intravenous insulin (IVI) infusions can be highly effective for controlling maternal glycaemia following betamethasone (on-IVI glucose 3.9–8.3 mmol/l in 12 women with gestational diabetes), although infusion rates were adjusted individually by attending physicians and no protocol was published. The Joint British Diabetes Societies for Inpatient Care (JBDS-IP) recent guideline proposes a variable rate IVI infusion for the management of glycaemic excursions following betamethasone, and although audit parameters are provided, audit data are not yet available [19].

At our institution prior to June 2017, IVI following betamethasone was administered according to a generic protocol designed for non-pregnant adults (Adult-IVI).

In June 2017, we designed and introduced a pregnancy-specific IVI infusion protocol (Pregnancy-IVI) in response to internal pilot data showing unsatisfactory glycaemic control using the Adult-IVI protocol. Key features of both protocols are highlighted in Table 1 and Fig. 1 (for the full protocol, see Appendices S1 and S2).

We present a cohort study of glycaemic control following betamethasone in women with GDM to assess the efficacy and safety of the Pregnancy-IVI protocol, when compared with an earlier cohort of women using the generic Adult-IVI. We hypothesized that the Pregnancy-IVI protocol would achieve higher at-target glycaemic control than the Adult-IVI, and may reduce neonatal hypoglycaemia.

Methods**Population**

Study approval was granted by the Hunter New England Human Research Ethics Committee (LNR/17/HNE/18), confirming a waiver of consent from participants for data collection from the medical record. The primary cohort was defined as all women diagnosed with GDM (according to the 2014 consensus criteria of the Australasian Diabetes in Pregnancy Society, with fasting glucose 5.1–6.9 mmol/l, or 2-h glucose following 75-g oral glucose 8.5–11.0 mmol/l [28]) receiving antenatal betamethasone (one or two doses of 11.4 mg, 24 h apart) at a regional tertiary hospital in

Table 1 Key features of Pregnancy-IVI protocol, designed to reduce clinical inertia and maintain pregnancy-specific glycaemic targets

Component	Pregnancy-IVI	Adult-IVI
Prescribing	Anticipatory prescribing at time of betamethasone prescription	Reactive prescribing in response to hyperglycaemia
Commencement	Automatic trigger for midwife to commence IVI with any BGL > 6.7 mmol/l	Medical officer review required to commence IVI once any BGL > 6.7 mmol/L
Algorithms	Higher IVI rates within the pregnancy-specific glucose range (3.8–7 mmol/l). Higher IVI rates when glucose > 7 mmol/l	Less-aggressive IVI rates within pregnancy-specific glucose range (3.8–7 mmol/l), as protocol is designed for non-pregnant adults
Treat-to-target	Automatic, midwife-led algorithm escalation if BGL not at target (3.8–7.0 mmol/l)	Medical officer review required to change algorithm if BGL not at target (3.8–7.0 mmol/l)

IVI, intravenous insulin; BGL, blood glucose level.

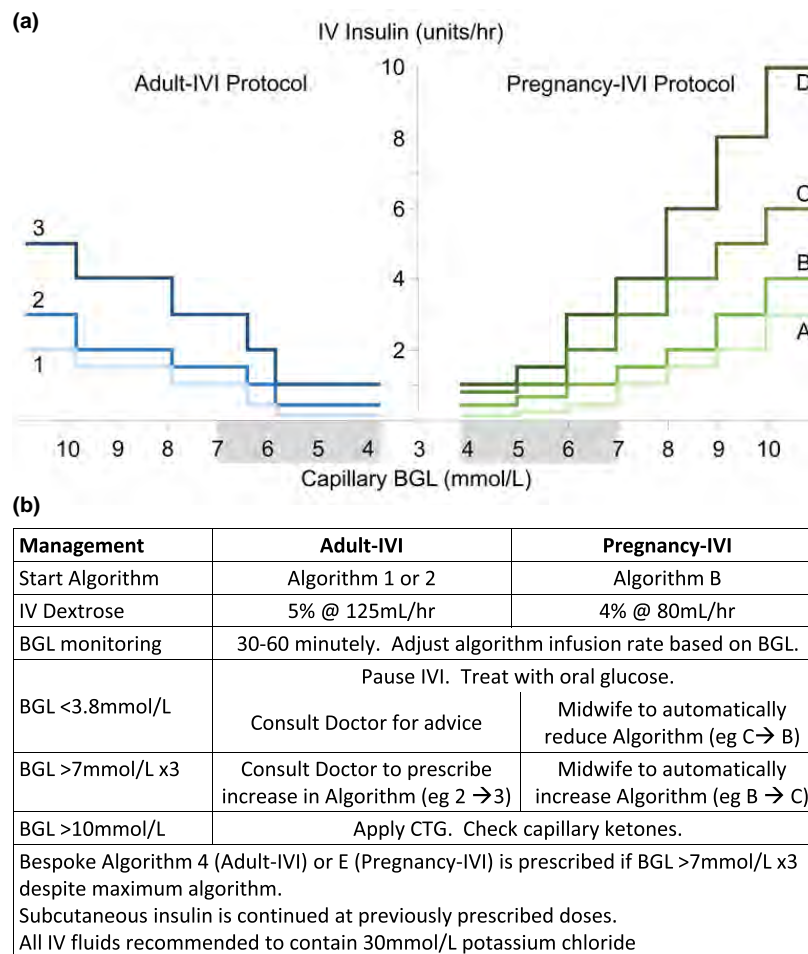


FIGURE 1 Comparison of generic adult intravenous insulin infusion (Adult-IVI) and pregnancy-specific intravenous insulin infusion (Pregnancy-IVI) protocols. (a) Intravenous insulin infusion rates are adjusted every 30–60 min based on capillary blood glucose levels (BGL). (Left) Adult-IVI protocol, algorithms 1–3. (Right) Pregnancy-IVI protocol, algorithms A–D. Grey shading indicates target BGL. (b) Abbreviated management guidelines for use of Adult-IVI and Pregnancy-IVI protocols. For full clinical copies of both protocols, see Appendices S1 and S2.

Australia (John Hunter Hospital) between January 2015 and December 2016 (retrospective arm using Adult-IVI) or June 2017 and May 2018 (prospective arm using Pregnancy-IVI) in whom an IVI was administered according to either protocol. The secondary cohort included a subset of the primary cohort of women in whom birth occurred within 48 h of the first dose of betamethasone (based on prior data [23]). Cases were identified by systematic electronic medical record searching for IVI protocol use (identified from barcode scanning), matched with obstetric birth databases. Ambulatory and inpatient management of women over the entire study period was provided by a consistent group of tertiary endocrinologists and obstetricians without other variation in treatment protocols.

Intervention

All women with GDM requiring betamethasone were admitted to the maternity ward, and had seven-point blood glucose

monitoring according to local standard of care. Local ambulatory glucose targets for GDM are < 5.1 mmol/l in the fasted state and < 6.7 mmol/l at 2 h after a meal [28]. Intravenous insulin with concurrent intravenous dextrose was commenced following any capillary blood glucose level (BGL) > 6.7 mmol/l in the 24 h following betamethasone, and once initiated, continued for 24 h following the last dose of betamethasone. Insulin infusion rate was adjusted by midwives according to a written protocol (Adult-IVI or Pregnancy-IVI, summarized in Fig. 1 and available in full in Appendices S1 and S2), with the ability to change to a more- or less-aggressive regimen based on response to therapy (Fig. 1b). Target on-infusion BGL was 3.8–7 mmol/l. Capillary BGL was measured every 60 min whilst on infusion (or 30 min following an above-target BGL on the Pregnancy-IVI) using an Optium Neo H FreeStyle BGL monitoring system (Abbott Diabetes Care, Doncaster, VIC, Australia).

Data extraction from electronic medical records was performed manually by three investigators using a

standardized electronic template. Maternal capillary BGLs were extracted from the record at 30-min intervals for up to 24 h following the last administration of betamethasone, with missing readings filled with 'last-observation carried back'. Neonatal BGL was reviewed for 48 h after birth. The first neonatal BGL was measured at: clinical signs of hypoglycaemia, or at 3 h of age, or prior to the infant's second feed, whichever was first. Subsequently, BGL was tested before feeds at ~2–3-h intervals depending on feed frequency. After three consecutive BGL measurements > 2.5 mmol/l, testing was repeated every 6–8 h before feeds until the baby was 24 h old. A single reading ≤ 2.5 mmol/l defined neonatal hypoglycaemia (threshold for intervention based on local hospital guidelines).

Outcome

The primary outcome was the percentage of on-IVI time with maternal capillary BGL values within the target range (3.8–7 mmol/l) in the first 48 h following betamethasone. Secondary outcomes included mean on-IVI BGL, percentage of on-IVI time with critical hyperglycaemia (BGL > 10 mmol/l), episodes of on-IVI maternal hypoglycaemia (defined as BGL < 3.8 mmol/l) and incidence of neonatal hypoglycaemia (BGL ≤ 2.5 mmol/l) if betamethasone and IVI were administered within 48 h of birth. Exploratory analyses included measures of glycaemic variability for both protocols, differences in rates of IVI per protocol, and difference in total insulin administered per infusion.

Statistical methods

Based on pilot data, we estimated that the mean on-IVI time-at-target using Adult-IVI was 50%, normally distributed with a standard deviation of 25 percentage points. To demonstrate a minimum difference of 15 percentage points, a sample size of 60 participants in each arm was required with a two-sided alpha of 0.05 and power of 0.9.

Continuous, normally distributed data were analysed using unpaired Student's *t*-tests, with the Wilcoxon Rank Sum test used for non-parametric data. Distribution was assessed using histograms and q-q plots. Categorical data were modelled using Pearson's chi-square. To assess for bias and confounding, multiple logistic regression models were fitted, using protocol (Adult-IVI vs. Pregnancy-IVI) or neonatal hypoglycaemia (absent, present) as the dichotomous variables, and including model variables of gestational age, maternal age, BMI, co-administration of subcutaneous insulin and duration of IVI for the model assessing protocol. For neonatal hypoglycaemia, the additional variables of birthweight and requirement for neonatal intensive care unit admission for any indication, were included. Analysis was performed using Stata v. 14.2 (StataCorp., College Station, TX, USA).

Glucose variability was assessed using the standardized models of CONGA, J-index, GRADE, M-value and MAGE, fitted using EasyGV v. 9.0 (University of Oxford, Oxford, UK) [29]. Standard model parameters were used, with exception of a pregnancy-specific M- reference value of 5.5 mmol/l (100 mg/dl) and a 30-min sampling interval.

Results

Some 151 episodes of IVI protocol use following betamethasone were identified, comprising 86 uses of Adult-IVI and 65 uses of Pregnancy-IVI, with 45 and 27 infusions occurring within 48 h of birth respectively (Table 2). Demographic and clinical characteristics of the two cohorts were well matched with respect to maternal age, gravidity, parity, gestational age at time of betamethasone, rate of multiple gestation, BMI and pre-admission use of subcutaneous insulin ($P \geq 0.05$ for all comparisons). Both Adult-IVI and Pregnancy-IVI cohorts received similar durations of IVI therapy (32 ± 13 h vs. 34 ± 12 h, $P = 0.43$), and glucose levels at initiation of IVI were similar. The subgroup of women who received betamethasone within 48 h of birth showed similarly balanced characteristics (Table 2).

Improved glycaemic control following betamethasone with Pregnancy-IVI

Mean percentage of on-IVI BGL values within target (3.8–7 mmol/l, primary outcome) was 68% [95% confidence intervals (CI) 64–71%] on Pregnancy-IVI, compared with 55% (95% CI 50–60%) using Adult-IVI ($P = 0.0002$; Table 3 and Fig. 2a), with correspondingly lower mean BGL values (6.6 ± 0.4 mmol/l vs. 7.1 ± 0.8 mmol/l, $P = 0.0002$). Median percentage of on-IVI time with critical hyperglycaemia was 0% [interquartile range (IQR) 0–3%] with Pregnancy-IVI compared with 2% (IQR 0–7%) with Adult-IVI ($P = 0.02$; Fig. 2b), which corresponded to fewer women with ≥ 90 min of continuous BGL > 10 mmol/l (20% vs. 38%, $P = 0.02$). Fewer women treated with Pregnancy-IVI had any episodes of hypoglycaemia (2% vs. 12%, $P = 0.02$).

Multiple logistic regression models were used to examine for the presence of confounding, dichotomized by protocol, and including model variables of maternal age, maternal BMI, gestational age, prior use of subcutaneous insulin and duration of IVI. The proportion of on-IVI time with BGL at target remained highly associated with the Pregnancy-IVI protocol ($P < 0.0001$), with no significant change in parameter estimates with the inclusion of additional model variables, suggesting no evidence of confounding from measured variables. None of the model variables were significantly associated with the protocol used.

There was no significant difference in the median rate of IVI between Adult-IVI and Pregnancy-IVI protocols (1.5 vs. 2 units/h respectively, $P = 0.11$). However, the 75th and

Table 2 Demographic and clinical information for women with gestational diabetes receiving betamethasone and intravenous insulin

	Overall			Betamethasone within 48 h of birth		
	Adult-IVI	Pregnancy-IVI	P-value	Adult-IVI	Pregnancy-IVI	P-value
No. of mothers (offspring)	86 (89)	65 (70)		45 (48)	27 (31)	
Maternal age, years	33.0 ± 5.7	31.8 ± 5.7	0.21	34.2 ± 4.8	31.9 ± 4.5	0.05
Gravida (median, IQR)	3 (2–4)	3 (2–5)	0.56	3 (2–4)	3 (2–3)	0.11
Para (median, IQR)	1 (0–2)	1 (0–2)	0.05	1 (0–2)	1 (0–1)	0.07
Gestational age at betamethasone, weeks	34 ± 4	33 ± 4	0.7	36 ± 3	36 ± 2	0.72
Multiple gestation, <i>n</i> (%)	3 of 86 (3)	5 of 65 (8)	0.28	3 of 45 (7)	4 of 27 (15)	0.31
BMI, kg/m ² *	33.9 ± 10.4	31.8 ± 8.2	0.19	34.1 ± 10.2	31.5 ± 8.7	0.28
Subcutaneous insulin treatment, <i>n</i> (%)						
Nil	38 of 86 (44)	35 of 65 (54)	0.29	15 of 45 (33)	15 of 27 (56)	0.06
Basal only	13 of 86 (15)	13 of 65 (20)		7 of 45 (18)	7 of 27 (26)	
Bolus only	6 of 86 (7)	2 of 65 (3)		5 of 45 (11)	0 (0)	
Basal–bolus	29 of 86 (34)	15 of 65 (23)		17 of 45 (38)	5 of 27 (19)	
Blood glucose at commencement of infusion	8.3 ± 1.8	8.0 ± 1.3	0.22	8.3 ± 2.0	8.4 ± 1.3	0.73
Time on infusion, h	32 ± 13	34 ± 12	0.43	28 ± 14	29 ± 12	0.80
Delivery by Caesarean section, <i>n</i> (%)				40 of 48 (83)	24 of 31 (77)	0.51
Birthweight, g				2818 ± 744	2736 ± 751	0.64
NICU admission for any reason				22 of 48 (46)	14 of 31 (45)	0.95

Data are given as mean ± SD (parametric), median (IQR) (non-parametric) or *n* (%) (categorical).

*Data missing for four women in the Adult-IVI group and three women in the Pregnancy-IVI group.

IVI, intravenous insulin protocol; IQR, interquartile range; NICU, neonatal intensive care unit.

Table 3 Outcome data following betamethasone in gestational diabetes, by protocol used

	Overall			Betamethasone within 48 h of birth		
	Adult-IVI	Pregnancy-IVI	P-value	Adult-IVI	Pregnancy-IVI	P-value
Mean on-IVI BGL, mmol/l (mean ± SD)	7.1 ± 0.8	6.6 ± 0.4	0.0002	6.9 ± 0.8	6.7 ± 0.5	
Percentage of total IVI duration						
BGL at study target (3.8–7 mmol/l)*	55 (50–60)	68 (64–71)	0.0002	58 (51–66)	66 (61–71)	
BGL at JBDS target (4–7.8 mmol/l)*	74 (70–78)	84 (82–86)	0.0001	74 (68–80)	84 (80–88)	
Critical hyperglycaemia (> 10mmol/l)†	2 (0–7)	0 (0–3)	0.02	2 (0–6)	0 (0–3)	
Maternal on-IVI critical events‡						
BGL > 10 mmol/l for ≥ 90 min	33 of 86 (38)	13 of 65 (20)	0.02	13 of 48 (27)	3 of 28 (10)	
BGL > 10 mmol/l for two or more 90-min periods	10 of 86 (12)	1 of 65 (2)	0.02	5 of 48 (10)	0 of 31 (0)	
Any BGL < 3.8 mmol/l	10 of 86 (12)	1 of 65 (2)	0.02	5 of 48 (10)	1 of 31 (3)	
IVI rate, units/h†						
50th centile	1.5 (1.0–2.0)	2.0 (1.0–3.0)	0.11	1.5 (1.0–2.0)	2.0 (1.0–3.0)	
75th centile	1.5 (1.0–3.0)	3.0 (1.5–4.0)	0.01	1.8 (1.5–3.0)	3.0 (1.5–4.0)	
90th centile	2.0 (1.5–4)	4.0 (2.0–6.0)	0.001	2.1 (1.5–3.6)	4 (1.5–6.0)	
Total IV insulin per patient, units‡	48 (26–78)	93 (32–143)	< 0.0001	32 (17–65)	93 (47–150)	
Neonatal hypoglycaemia						
BGL ≤ 2.5 mmol/l within first 48 h‡				26 of 48 (54)	9 of 31 (29)	0.03
BGL ≤ 1.8 mmol/l within first 48 h‡				7 of 48 (15)	2 of 31 (6)	n.s.
First neonatal BGL†				2.7 (2.3–3.6)	3.3 (2.6–3.9)	0.07

*95% confidence intervals compared using Student's *t*-test;

†median (IQR) compared using Wilcoxon Rank Sum test;

‡*n* (%) compared using Pearson's chi squared.

IVI, intravenous insulin; JBDS, Joint British Diabetes Society; BGL, capillary blood glucose; n.s., not significant.

90th centile IVI rates were significantly higher with Pregnancy-IVI than with Adult-IVI (Table 3), which resulted in a higher overall median IVI dose administered per patient with Pregnancy-IVI than Adult-IVI (93 vs. 48 units, $P < 0.0001$). Figure 3 demonstrates the mechanism that resulted in the delivery of these higher insulin doses to women with Pregnancy-IVI. While at protocol commencement, similar

proportions of women were commenced on low-intensity IVI algorithms (94% commenced on Algorithm 1 or 2 of Adult-IVI, compared with 98% commenced on Algorithm A or B of Pregnancy-IVI; $P = 0.18$), by 10 h of infusion, low-intensity treatment was continued in only 43% of patients treated with Pregnancy-IVI, compared with 73% with Adult-IVI ($P < 0.001$; Fig. 3b). For patients requiring IVI for > 24 h,

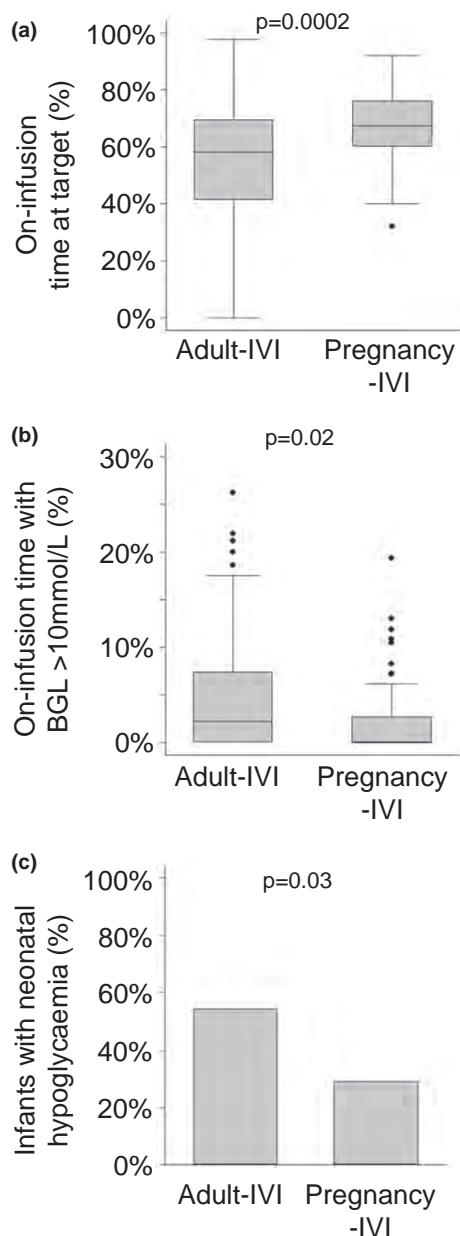


FIGURE 2 Outcomes by protocol used: adult intravenous insulin infusion (Adult-IVI) vs. pregnancy intravenous insulin–glucose infusion (Pregnancy-IVI). (a) Box and whisker plot of proportion of on-IVI time with blood glucose level (BGL) within target range (3.8–7 mmol/L). (b) Box and whisker plot of proportion of on-IVI time with critical hyperglycaemia (BGL > 10 mmol/L). (c) Bar chart of incidence of neonatal hypoglycaemia (BGL ≤ 2.5 mmol/L) in infants born within 48 h of betamethasone. Asterisks denote statistically significant difference ($P < 0.005$) for comparison between proportion of women treated with low-intensity algorithm (Algorithm 1 or 2 for Adult-IVI vs. Algorithm A and B for Pregnancy-IVI) using Pearson's chi-square.

women on Pregnancy-IVI were almost universally on Algorithm C or above (88%), compared with only 48% of patients on Adult-IVI on Algorithm 3 or higher ($P < 0.001$), showing that the built-in automated 'treat-to-target'

escalation of the Pregnancy-IVI infusion algorithms was utilized, and that the greater insulin delivery by these higher intensity algorithms was a key mechanism in the difference between Adult-IVI and Pregnancy-IVI outcomes.

In exploratory analysis of glycaemic variability, four of the five models studied (CONGA, J-index, GRADE and M-value) showed reduced glycaemic variability with Pregnancy-IVI compared with Adult-IVI ($P < 0.001$ for all comparisons; Table S1). No difference in MAGE scores was seen between the two protocols.

Reduced neonatal hypoglycaemia with Pregnancy-IVI when birth occurs within 48 h of betamethasone administration

A subset of both IVI cohorts (Adult-IVI $n = 45$; Pregnancy-IVI $n = 27$; Table 2) in whom betamethasone was administered within 48 h of birth were used to examine the effect of each protocol on the incidence of neonatal hypoglycaemia (Table 3). Median first neonatal BGL was 3.3 mmol/L (IQR 2.6–3.9) for Pregnancy-IVI, compared with 2.7 mmol/L (IQR 2.3–3.6 mmol/L, $P = 0.07$) for Adult-IVI. The rate of neonatal hypoglycaemia (defined as any BGL ≤ 2.5 mmol/L in the first 48 h) for babies born using Pregnancy-IVI was 9 of 31 (29%, 95% CI 13–45%), compared with 26 of 48 (54%, 95% CI 40–68%) with Adult-IVI ($P = 0.03$; Fig. 2c). Multiple logistic regression models were fit to examine for potential confounding of the relationship between neonatal hypoglycaemia (dependent variable) and protocol (Adult-IVI vs. Pregnancy-IVI), and including model variables of maternal age, maternal BMI, gestational age at birth, duration of IVI, co-administration of subcutaneous insulin, neonatal birthweight and requirement for neonatal intensive care unit admission. The model including all potential confounders did not change the parameter estimates compared with the base model including protocol alone, indicating no significant confounding. A final model retaining variables with a significance threshold of 0.2 included protocol, duration of IV infusion and maternal BMI, and gave an odds ratio for neonatal hypoglycaemia using Pregnancy-IVI of 0.27 (95% CI 0.10–0.76, $P = 0.01$).

Discussion

Optimum glycaemic management of women with GDM receiving betamethasone is hampered by an absence of evidence supporting proposed treatments or clinical endpoints.

This study is the first large-scale, real-world validation of an insulin-infusion protocol designed specifically for managing hyperglycaemia following betamethasone in pregnancies complicated by gestational diabetes. The Pregnancy-IVI protocol achieves a higher proportion of time at target for maternal glycaemia than a generic adult IVI, with reduced duration of critical maternal hyperglycaemia and reduced neonatal hypoglycaemia. The coupling of high efficacy and high safety in a robust protocol is an essential component of implementable

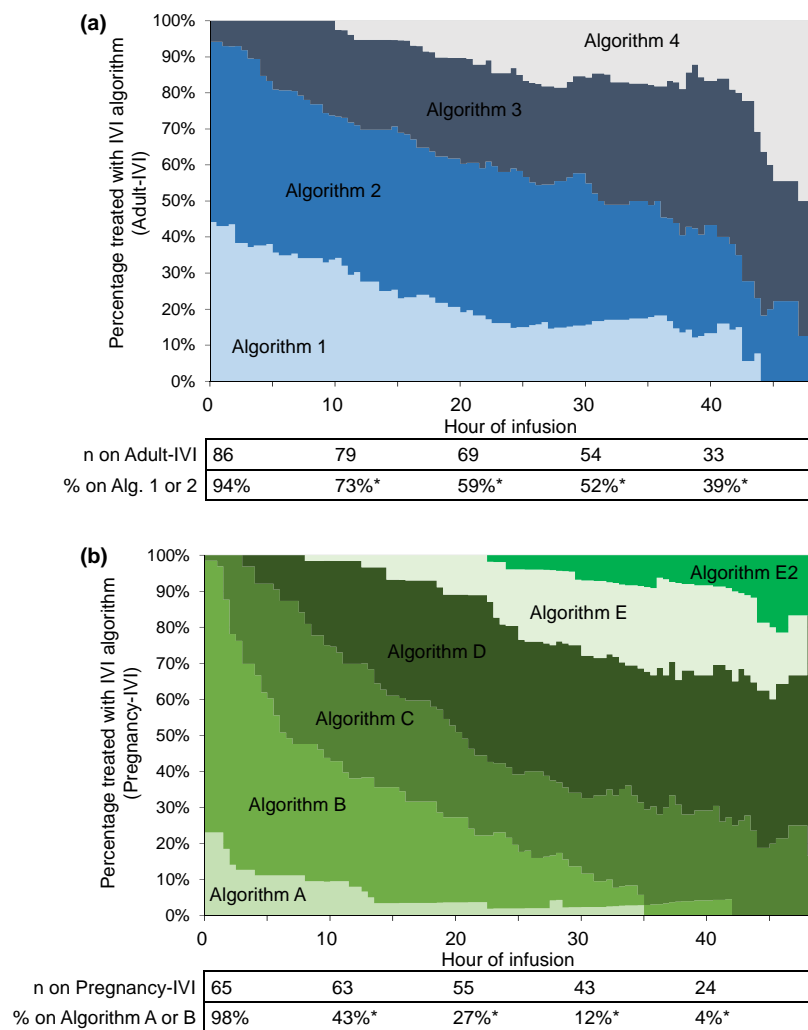


FIGURE 3 Real-world outcome of dynamic adjustment of insulin-dosing algorithms by infusion time point for (a) adult intravenous insulin infusion (Adult-IVI) and (b) pregnancy intravenous insulin–glucose infusion (Pregnancy-IVI). Each 0.5-h increment displays the proportion of women treated with each infusion algorithm as a percentage of all women on IVI at that time point. Algorithm 4 (Adult-IVI) and Algorithms E and E2 (Pregnancy-IVI) are bespoke algorithms charted by the treating clinician with incrementally higher rates of IVI than the previous algorithm. Asterisks denote statistically significant difference ($P < 0.005$) for comparison between proportion of women treated with low-intensity algorithm (Algorithm 1 or 2 for Adult-IVI vs. Algorithm A and B for Pregnancy-IVI) using Pearson's chi-square.

care. Further, this protocol may be less resource-intensive than a comparable generic insulin infusion, because the majority of treatment decisions are protocolized (see online Supporting Information), rather than dependent on senior staff review of each woman. Further, the reduced incidence of critical hyperglycaemia and hypoglycaemia reduces the need for cardiotocography at our institution. Despite at-target control for the majority of women, a small subset of women continue to experience prolonged critical hyperglycaemia despite treatment (outliers in Fig. 2b), suggesting that individualized care may still be beneficial in a subset of cases.

The efficacy of Pregnancy-IVI is likely linked to several interrelated protocolized measures that reduce clinical inertia in insulin administration, and the automatic escalation of IVI algorithms in response to an individual woman's glucose levels, until pregnancy-specific targets are achieved (Table 1

and Fig. 3b). The Pregnancy-IVI protocol delivers a higher rate of infused insulin once the women's glucose levels exceed this target range (Fig. 1a). Importantly, this more aggressive treatment is not at the cost of increased risk of hypoglycaemia. In fact, the opposite was observed, with a decrease in risk of maternal hypoglycaemia with the Pregnancy-IVI protocol (2% vs. 12% of women with any on-IVI hypoglycaemia, $P = 0.02$). At our institution, this protocol is used routinely outside the setting of betamethasone administration (e.g. in labour and intercurrent illness) and in the challenging group of women with pre-gestational diabetes [30] and has demonstrated similar safety data in preliminary analysis.

This study is the first evidence that treatment to improve glycaemic control following betamethasone may reduce the clinically meaningful endpoint of neonatal hypoglycaemia.

There is strong conceptual and observational evidence linking maternal hyperglycaemia in the peripartum with neonatal hypoglycaemia, however to date, no treatment protocol has demonstrated a reduction in this endpoint following betamethasone. The Pregnancy-IVI protocol showed a 25% absolute risk reduction in the incidence of any neonatal hypoglycaemia (one case of neonatal hypoglycaemia prevented for every four women treated). The incidence of severe neonatal hypoglycaemia (≤ 1.8 mmol/l) was numerically lower with Pregnancy-IVI (6% vs. 15%), although this was not statistically significant ($P = 0.27$); however, it should be noted that this study was not powered for the outcome of neonatal hypoglycaemia. Although there is potential for confounding in a retrospective cohort study, cohorts were well matched, and a robustly implemented multiple logistic regression model did not show confounding from a large number of potentially relevant clinical variables.

This study has several strengths. First, it is a real-world implementation study of practice with broad inclusion criteria; hence conclusions are generalizable to routine practice. All protocol violations (e.g. delay in escalating or de-escalating algorithms) were included in the analysis, so the difference in outcomes is representative of typical ward-based care, rather than the highly controlled environment of a clinical trial. Second, although the comparator group (Adult-IVI) is specific to our centre, the Adult-IVI protocol is similar to the recently published JBDS-VR2 for pregnancy (November 2017) which is yet to have outcome data reported [19]. This study establishes quality standards for the management of glycaemic excursions following betamethasone in women with GDM, which can be used as benchmarking for future interventions.

This study has some limitations. First, as an observational study with a retrospective arm, it is possible that unmeasured differences between the study populations may introduce confounding or bias. However, the two cohorts were drawn from the same reference population and showed no difference in key measurable demographics (Table 2), and analysis of primary and secondary endpoints in multivariate models showed no evidence of confounding. In addition, it is unlikely that the Pregnancy-IVI cohort included women with less insulin resistance, because significantly higher IVI doses were required to achieve euglycaemia in this group (Table 3). Second, although the dominant change in the Pregnancy-IVI protocol was to the insulin–glucose infusion algorithms (Fig. 1), protocol implementation may have enhanced staff awareness of GDM, thereby contributing to improved outcomes for the Pregnancy-IVI group. Third, the comparator group for the Pregnancy-IVI infusion was a generic IVI (the prior standard of care at our centre), rather than alternatives used at other obstetric centres (e.g. a subcutaneous outpatient insulin-adjustment protocol or continuation of usual therapy). Thus, we are unable to make direct comparison of Pregnancy-IVI with these other approaches to management. It could be inferred that differences in at-target

glucose control and subsequent neonatal hypoglycaemia may be greater in women receiving less-intensive therapies than Pregnancy-IVI [20]. Finally, this study is underpowered to report differences in the incidence of severe neonatal hypoglycaemia, or neonatal hypoglycaemia requiring neonatal intensive care unit admission, which are important factors in determining the cost-effectiveness of this intervention. However, in women at high risk of imminent birth, hospital admission for close observation is usually required, and the addition of IVI in this setting would be a small incremental cost, which may be offset by reduced resource utilization post-partum. Further larger prospective studies, ideally with randomization to treatment arms, would address these questions.

In conclusion, this study demonstrates that a pregnancy-specific IVI infusion protocol improves time-at-target, and reduces the incidence of neonatal hypoglycaemia, compared with a generic adult IVI infusion following betamethasone in women with gestational diabetes.

Funding sources

None.

Competing interests

None declared.

Acknowledgements

The authors would like to thank the John Hunter Hospital Clinical Information Department for assistance with case-identification, and the John Hunter Hospital Departments of Maternity and Gynecology, and Diabetes and Endocrinology for invaluable support.

References

- 1 HAPO Study Cooperative Research Group, Metzger BE, Lowe LP, Dyer AR, Trimble ER, Chaovarindr U, Coustan DR *et al.* Hyperglycemia and adverse pregnancy outcomes. *N Engl J Med* 2008; 358: 1991–2002.
- 2 Hartling L, Dryden DM, Guthrie A, Muise M, Vandermeer B, Donovan L. Benefits and harms of treating gestational diabetes mellitus: a systematic review and meta-analysis for the U.S. Preventive Services Task Force and the National Institutes of Health Office of Medical Applications of Research. *Ann Intern Med* 2013; 159: 123–129.
- 3 Crandell SS, Fisher DJ, Morriss FH Jr. Effects of ovine maternal hyperglycemia on fetal regional blood flows and metabolism. *Am J Physiol* 1985; 249: E454–E460.
- 4 Smith FG, Lumbers ER. The effect of maternal hyperglycemia on acid base balance and lung liquid production in the fetal sheep. *Pediatr Res* 1987; 22: 355–359.
- 5 Kenepf NB, Kumar S, Shelley WC, Stanley CA, Gabbe SG, Gutsche BB. Fetal and neonatal hazards of maternal hydration with 5% dextrose before caesarean section. *Lancet* 1982; 1: 1150–1152.

- 6 Lawrence GF, Brown VA, Parsons RJ, Cooke ID. Feto-maternal consequences of high-dose glucose infusion during labour. *Br J Obstet Gynaecol* 1982; 89: 27–32.
- 7 Philipson EH, Kalhan SC, Riha MM, Pimentel R. Effects of maternal glucose infusion on fetal acid–base status in human pregnancy. *Am J Obstet Gynecol* 1987; 157: 866–873.
- 8 Nicolini U, Hubinont C, Santolaya J, Fisk NM, Rodeck CH. Effects of fetal intravenous glucose challenge in normal and growth retarded fetuses. *Horm Metab Res* 1990; 22: 426–430.
- 9 Piquard F, Hsiung R, Schaefer A, Haberey P, Dellenbach P. Does fetal acidosis develop with maternal glucose infusion during normal labor? *Obstet Gynecol* 1989; 74: 909–914.
- 10 Tobin JD, Roux JF, Soeldner JS. Human fetal insulin response after acute maternal glucose administration during labor. *Pediatrics* 1969; 44: 668–671.
- 11 Light IJ, Keenan WJ, Sutherland JM. Maternal intravenous glucose administration as a cause of hypoglycemia in the infant of the diabetic mother. *Am J Obstet Gynecol* 1972; 113: 345–350.
- 12 Lucas A, Adrian TE, Aynsley-Green A, Bloom SR. Iatrogenic hyperinsulinism at birth. *Lancet* 1980; 1: 144–145.
- 13 Andersen O, Hertel J, Schmolker L, Kuhl C. Influence of the maternal plasma glucose concentration at delivery on the risk of hypoglycaemia in infants of insulin-dependent diabetic mothers. *Acta Paediatr Scand* 1985; 74: 268–273.
- 14 Miodovnik M, Mimouni F, Tsang RC, Skillman C, Siddiqi TA, Butler JB *et al.* Management of the insulin-dependent diabetic during labor and delivery. Influences on neonatal outcome. *Am J Perinatol* 1987; 4: 106–114.
- 15 Curet LB, Izquierdo LA, Gilson GJ, Schneider JM, Perelman R, Converse J. Relative effects of antepartum and intrapartum maternal blood glucose levels on incidence of neonatal hypoglycemia. *J Perinatol* 1997; 17: 113–115.
- 16 Lean ME, Pearson DW, Sutherland HW. Insulin management during labour and delivery in mothers with diabetes. *Diabet Med* 1990; 7: 162–164.
- 17 Taylor R, Lee C, Kyne-Grzebalski D, Marshall SM, Davison JM. Clinical outcomes of pregnancy in women with type 1 diabetes(1). *Obstet Gynecol* 2002; 99: 537–541.
- 18 Joshi T, Oldmeadow C, Attia J, Wynne K. The duration of intrapartum maternal hyperglycaemia predicts neonatal hypoglycaemia in women with pre-existing diabetes. *Diabet Med* 2017; 34: 725–731.
- 19 Dashora U, Temple R, Murphy H. *JBDS12: Management of Glycaemic Control in Pregnant Women with Diabetes on Obstetric Wards and Delivery Units*. Joint British Diabetes Societies for Inpatient Care Group (JBDS-IP). Available at http://www.diabetologists-abcd.org.uk/JBDS/JBDS_Pregnancy_final_18082017.pdf Last accessed 23 August 2018.
- 20 Barrett HL, Morris J, McElduff A. Watchful waiting: a management protocol for maternal glycaemia in the peripartum period. *Aust N Z J Obstet Gynaecol* 2009; 49: 162–167.
- 21 Crowley PA. Antenatal corticosteroid therapy: a meta-analysis of the randomized trials, 1972 to 1994. *Am J Obstet Gynecol* 1995; 173: 322–335.
- 22 Star J, Hogan J, Sosa ME, Carpenter MW. Glucocorticoid-associated maternal hyperglycemia: a randomized trial of insulin prophylaxis. *J Matern Fetal Med* 2000; 9: 273–277.
- 23 Gyamfi-Bannerman C, Thom EA, Blackwell SC, Tita AT, Reddy UM, Saade GR *et al.* Antenatal betamethasone for women at risk for late preterm delivery. *N Engl J Med* 2016; 374: 1311–1320.
- 24 Dashora UK, Taylor R. Maintaining glycaemic control during high-dose prednisolone administration for hyperemesis gravidarum in Type 1 diabetes. *Diabet Med* 2004; 21: 298–299.
- 25 Mathiesen ER, Christensen AB, Hellmuth E, Hornnes P, Stage E, Damm P. Insulin dose during glucocorticoid treatment for fetal lung maturation in diabetic pregnancy: test of an algorithm [correction of analoritm]. *Acta Obstet Gynecol Scand* 2002; 81: 835–839.
- 26 Kaushal K, Gibson JM, Railton A, Hounsborne B, New JP, Young RJ. A protocol for improved glycaemic control following corticosteroid therapy in diabetic pregnancies. *Diabet Med* 2003; 20: 73–75.
- 27 Itoh A, Saisho Y, Miyakoshi K, Fukutake M, Kasuga Y, Ochiai D *et al.* Time-dependent changes in insulin requirement for maternal glycaemic control during antenatal corticosteroid therapy in women with gestational diabetes: a retrospective study. *Endocr J* 2016; 63: 101–104.
- 28 Abell SK, Boyle JA, Earnest A, England P, Nankervis A, Ranasinha S *et al.* Impact of different glycaemic treatment targets on pregnancy outcomes in gestational diabetes. *Diabet Med* 2018. <https://doi.org/10.1111/dme.13799> [Epub ahead of print].
- 29 Hill NR, Oliver NS, Choudhary P, Levy JC, Hindmarsh P, Matthews DR. Normal reference range for mean tissue glucose and glycemic variability derived from continuous glucose monitoring for subjects without diabetes in different ethnic groups. *Diabetes Technol Ther* 2011; 13: 921–928.
- 30 Murphy HR, Bell R, Dornhorst A, Forde R, Lewis-Barned N. Pregnancy in diabetes: challenges and opportunities for improving pregnancy outcomes. *Diabet Med* 2018; 35: 292–299.

Supporting Information

Additional supporting information may be found online in the Supporting Information section at the end of the article.

Appendix S1. Pregnancy-IVI (A) front (infusion algorithms) and (B) back (automated treat-to-target protocol).

Appendix S2. Front of Adult-IVI. Back (not shown) contains table to record glucose levels and infusion rates without additional information.

Table S1. Exploratory analysis of glycaemic variability, by (A) protocol and (B) neonatal hypoglycaemia.

Research: Epidemiology

Young children, adolescent girls and women with type 1 diabetes are more overweight and obese than reference populations, and this is associated with increased cardiovascular risk factors

A. L. Marlow¹ , C. W. Rowe^{1,3,4} , D. Anderson^{1,3,5}, K. Wynne^{1,3,4} , B. R. King^{1,3,5}, P. Howley² and C. E. Smart^{1,3,5} 

¹School of Medicine and Public Health, ²School of Mathematics and Physical Sciences/Statistics, University of Newcastle, Callaghan, ³Hunter Medical Research Institute, New Lambton, ⁴Department of Diabetes and Endocrinology, John Hunter Hospital, and ⁵Department of Paediatric Diabetes and Endocrinology, John Hunter Children's Hospital, New Lambton Heights, NSW, Australia

Accepted 5 September 2019

Abstract

Aim Overweight and obesity are frequently reported in young persons with type 1 diabetes, however its relative magnitude in comparison to the general population is not well understood. This study compared the prevalence of overweight and obesity in young persons with type 1 diabetes to a reference population and explored possible associated factors, including gender, age, HbA_{1c}, insulin regimen, age at diagnosis, diabetes duration, socio-economic status and cardiovascular disease risk factors.

Methods A cross-sectional review was undertaken of data collected from youth (3–17 years) in 2016 and young adults (18–30 years) in 2015 with a diagnosis of type 1 diabetes for > 3 months attending diabetes centres in Newcastle, Australia. Rates of overweight and obesity were compared with matched population survey results.

Results Data from 308 youth and 283 young adults were included. In girls, significantly higher prevalence of overweight and obesity were seen in the 5–8 (43% vs. 18%), 13–16 (41% vs. 27%), 18–24 (46% vs. 34%) and 25–30 (60% vs. 43%) years age groups; whereas in boys increased prevalence was observed in the 5–8 years age group only (41% vs. 18%). Rates of overweight and obesity increased with age across sexes. In youth, BMI standard deviation score was correlated with socio-economic status, insulin regimen, blood pressure and blood lipids ($P < 0.05$). In adults, BMI was positively associated with blood pressure, and longer diabetes duration ($P < 0.02$).

Conclusions Overweight and obesity are over-represented in young persons with type 1 diabetes, particularly girls. As overweight is associated with other cardiovascular disease markers early intervention is paramount.

Diabet. Med. 36, 1487–1493 (2019)

Introduction

Obesity is one of the most serious public health issues of the 21st century. It is estimated that 27% of Australian youth aged 5–17 years and 45% of young adults aged 18–34 years are overweight or obese [1]. Obesity is an established risk factor for serious health complications including cardiovascular disease and psychological disorders. In addition, evidence indicates that childhood overweight and obesity persist into adulthood [2], and is associated with an increased risk of premature mortality and morbidity [3].

Type 1 diabetes is a common chronic disease affecting people of all ages. Atherosclerotic changes have been shown to appear early in young people with type 1 diabetes [4] and type 1 diabetes has been associated with a tenfold increased risk of cardiovascular disease [5]. Recent findings from a large cohort of adults has found that being diagnosed with type 1 diabetes before the age of 10 years results in a loss of life expectancy of 18 and 14 years in women and men, respectively [6].

The Australasian Diabetes Data Network report from 2017 indicated that one-third of children and adolescents with type 1 diabetes in Australia were overweight or obese [7]. This poses a major concern as obesity is an independent risk factor for cardiovascular disease and further impacts a

Correspondence to: Carmel E. Smart.
E-mail: Carmel.Smart@hnehealth.nsw.gov.au

What's new?

- Overweight and obesity are highly prevalent in young people with type 1 diabetes and are associated with increased cardiovascular disease risk factors.
- This study has shown that across a paediatric and adult service in a single geographic region in Australia, women with type 1 diabetes are significantly more overweight and obese compared with women from age matched groups in the general population.
- Overweight and obesity rates increase with age.
- This research suggests that interventions to prevent excessive weight gain should target girls with type 1 diabetes prior to teenage years.

population already at high risk of cardiovascular disease. In addition, some studies have indicated that rates of people with type 1 diabetes in an unhealthy body weight range may be higher than in the non-diabetic population. In the US SEARCH for diabetes in youth cohort, participants with type 1 diabetes were more overweight, but not more obese, when compared with a US reference sample [8], and individuals from two large clinical registries [the Type 1 Diabetes Exchange, and the Diabetes Prospective Study (DPV) in Europe] had higher median BMI values compared with respective national reference samples [9].

To date, no Australian study has investigated the extent of overweight and obesity in a paediatric and young adult population with type 1 diabetes across clinics in a single geographic location, and compared the findings with age- and sex-matched population samples. Additionally, the key predictive factors of increased BMI in individuals with type 1 diabetes have not been established, and there is no platform for targeted intervention. The primary objectives of this study were to: (1) determine the age-specific prevalence of overweight and obesity in young people aged 3–30 years with type 1 diabetes in the Hunter region of New South Wales (NSW) Australia and compare the prevalence to age-matched populations; (2) undertake an exploratory analysis to identify if demographic or clinical factors were associated with overweight in children or adults including age, gender, diabetes duration, age at diagnosis, glycaemic control, insulin regimen and smoking (young adults only); and (3) explore the association of cardiovascular disease risk factors including blood pressure (BP), total cholesterol and triglycerides with overweight and obesity.

Methods

Study design and participants

Institutional ethics approval was obtained from the Hunter New England Human Research Ethics Committee for the use

of data for research purposes (Reference number: AU201708-10 & 15/06/17/5.01). Using a cross-sectional design, data were collected from a paediatric type 1 diabetes clinic at John Hunter Children's Hospital and the linked young adult type 1 diabetes clinic at the John Hunter Hospital in Newcastle, Australia. These centres are the primary referral centres for all individuals with type 1 diabetes in the Hunter region in these age groups. The John Hunter Children's Hospital cares for all cases of children and adolescents with type 1 diabetes as there are no other clinics in the public or private sector. The John Hunter Hospital looks after the vast majority of young adults due to transition of children from the co-located paediatric centre and the lack of private specialist care for this age group.

Participant data were collected during routine 3-monthly visits for paediatric participants and 3–6-monthly visits for young adult participants. Cross-sectional data were extracted for each individual from the Paediatric Endocrine Database in December 2016 (for visits up to 12 months prior) and from medical files during the period of January to December 2015 for young adults to ensure no participant cross-over. Inclusion criteria were ages 3–30 years old, diagnosed with type 1 diabetes for at least 3 months, where type 1 diabetes diagnosis was defined as the presence of hyperglycaemia and ketosis with a history of polyuria and polydipsia, and at least one positive of a panel of islet antigen-2, insulin and glutamic acid decarboxylase antibodies. Antibody-negative diabetes was excluded because of the possibility of alternative underlying diagnoses. The following variables were extracted for analysis: gender, height, weight, age, insulin therapy type, age at diagnosis, diabetes duration, postcode (as a marker of socio-economic status), Aboriginal or Torres Strait Islander heritage, smoking status (18–30 year group only) and BP. Triglycerides and total cholesterol were extracted from records if measures were performed within 6 months of the review date, as these tests are conducted annually.

Measures

HbA_{1c} measurements were collected using the DCA-Vantage Analyser (paediatric) or the Afinion assay (Abbott) for young adults. Weight and height were measured by trained staff using calibrated scales and stadiometers. Lipids including total cholesterol and triglycerides were measured non-fasting as per the International Society for Paediatric and Adolescent Diabetes guidelines in youth and in line with standards of care across the young adult clinic. Systolic blood pressure (SBP) and diastolic blood pressure (DBP) were measured using a sphygmomanometer after the individual had been seated for at least 5 min. If BP was elevated a repeated measurement was performed and recorded.

BMI (weight in kilograms divided by the square of height in metres) was calculated for youth and young adults. Overweight and obesity was defined for the paediatric cohort using the International Obesity Taskforce's age- and sex-

specific BMI cut-offs for children aged 3–17 years [10]. Sex- and age-specific body mass standard deviation scores (BMI-SDS) were calculated using an international reference population. For the young adults aged 18–30 years, BMI cut-points recommended by the World Health Organization were used to define weight status (underweight < 18.5 kg/m², normal 18.5–24.9 kg/m², overweight 25.0–29.9 kg/m² and obese > 30 kg/m²) [11]. Because formal diagnoses of hypertension could not be obtained, data were categorized for analysis based on current guideline cut-points. A SBP and/or DBP \geq 95th percentile on the basis of age, sex and height percentiles in paediatric participants [12], and a SBP and/or DBP of \geq 130 mmHg and \geq 80 mmHg, respectively, in young adult subjects [13].

The Socio-Economic Indexes for Areas (SEIFA) Index of Disadvantage which enables the ranking and assessment of welfare in Australia was used. Postcodes were aligned with the corresponding SEIFA index and data were broken into deciles 1–10 (1 being most disadvantaged, 10 being most advantaged).

Reference population

To allow for the comparison against state-wide (NSW) population statistics, the prevalence of overweight and obesity were calculated to match five sex- and age-matched reference population groups; 5–8, 9–12, 13–16, 18–24 and 25–34 years. For the paediatric comparison, age groups 5–8, 9–12 and 13–16 years were derived from the Schools Physical Activity and Nutrition Survey (SPANS) 2015 [14] and for the young adult comparison, age groups 18–24 and 25–34 years were derived from the Australian National Health Survey 2014–15 [15]. Reference populations for the Hunter sub-region of the state of NSW were extensively sought after but were not available. Similarly, a reference population for very young children, 3–4 years and adolescents aged 17 years were not available.

Statistical analysis

Statistical analyses were performed using STATA version 15.0 (StataCorp LLC, College Station, TX, USA). Descriptive statistics are reported as mean \pm SD and frequency (%) for categorical variables. BMI weight category was analysed in both two (overweight and obese combined) and three (overweight and obese individually) group form. Pearson's chi-squared and Fisher's exact test for small samples were used to determine if prevalence of overweight and obesity was associated with type 1 diabetes and was stratified by age and sex. Each gender was examined using a Cochran–Mantel–Haenszel test comparing type 1 diabetes with the reference group stratifying by age group. Cochran–Armitage test for trend was used to compare type 1 diabetes vs. the general population counts for healthy BMI, overweight and obesity. Simple linear regression, multiple linear regression, two sample *t*-tests,

simple effects and analysis of variance for multiple groups were used to explore relationships between BMI (adults) and BMI-SDS (youth) and clinical, demographic and cardiovascular disease risk factors. All tests were performed as two-sided and *P* < 0.05 was considered significant.

Results

Participants

The clinical characteristics of the 308 children and adolescents and 283 young adults are shown in Table 1. Blood pressure readings were available for 299 paediatric

Table 1 Characteristics of cross-sectional data of youth and young adults with type 1 diabetes

	Youth <i>n</i> = 308	Young adult <i>n</i> = 283
Mean age (years)	12.9 \pm 3.7	23.7 \pm 3.6
Male	156 (50.6)	151 (53.4)
HbA _{1c} (mmol/mol)	58	70
HbA _{1c} (%)	7.5 \pm 1.4	8.6 \pm 1.8
Mean age at diagnosis (years)	7.4 \pm 3.9	13 \pm 6.3
Mean duration of disease (years)	5.4 \pm 3.7	10.7 \pm 6.2
Aboriginal or Torres Strait Islander	19 (6.2)	17 (6.0)
Insulin regimen		
MDI	163 (52.9)	206 (72.8)
CSII	145 (47.1)	77 (27.2)
BMI-SDS	0.99 \pm 0.97	
BMI (kg/m ²)		26.4 \pm 5.1
Weight category		
Underweight	10 (3.2)	5 (1.8)
Normal weight	183 (59.4)	126 (44.5)
Overweight	84 (27.3)	94 (33.2)
Obese	31 (10.1)	58 (20.5)
Total cholesterol		
Elevated > 4.5 mmol/l* (paediatric)	91 (37.1)	
> 5.5 mmol/l† (adult)		49 (23.4)
Triglycerides		
Elevated > 1.7 mmol/l* (paediatric)	32 (13.1)	
> 2 mmol/l† (adult)		33 (15.8)
Blood pressure		
\geq 95 th percentile‡	34 (11.4)	
> 130 mmHg or 80 mmHg§		57 (20.4)
Smoking status		24 (8.5)

Data are mean \pm SD or frequency (%).

MDI, multiple daily injections; CSII, continuous subcutaneous insulin infusion; BMI-SDS, body mass index standard deviation score. MDI defined as four or more injections per day. Cholesterol, triglycerides and blood pressure values are reported as % above target range.

*American Heart Association Guideline, 2003 [16].

†National Heart Foundation of Australia & Cardiac Society of Australia and New Zealand Target, 2012 [17].

‡Clinical Practice Guideline for Screening and Management of High Blood Pressure in Children and Adolescents, 2017 [12]

§Guideline for the Prevention, Detection, Evaluation, and Management of High Blood Pressure in Adults, 2017 [13].

participants and 280 young adult participants, and lipid measures were available for 170 paediatric participants and 209 young adult participants. Of the children and adolescents, 37% [confidence intervals (CI) 32%, 43%; $n = 115$] were classified as combined overweight and obese. The larger proportion (27%, $n = 84$) of this group were overweight, but a significant proportion (10%, $n = 31$) were obese. Of the young adults, 54% (CI 48%, 60%; $n = 152$) were classified as overweight and obese with a high proportion of overweight (33%, $n = 94$) and obesity (21%, $n = 58$). Those who identified as Aboriginal or Torres Strait Islander had a similar proportion of overweight or obesity as the whole paediatric and young adult cohorts.

Prevalence of overweight and obesity in type 1 diabetes vs. the general population

Two-hundred and fifty youth with type 1 diabetes were age- and sex-matched with the comparison population. Overall the children and adolescents with type 1 diabetes had a significantly greater prevalence of combined overweight and obesity (37%) compared with the reference population (24%, $P < 0.001$). Individual chi-squared tests at each age group and gender combination showed significant differences for the youngest group (aged 5–8 years) in both boys with type 1 diabetes (41%) vs. reference group (18%, $P = 0.008$) and girls with type 1 diabetes (43%) vs. reference group (21%, $P = 0.018$) (Table 2). The proportions of combined overweight and obesity in older male children, adolescent boys and young men were not significantly higher than the reference populations. However, combined overweight and obesity were statistically more prevalent across all age groups for girls ($P = 0.018$), adolescent girls ($P = 0.026$) and young women (18–24 years, $P = 0.029$ and 25–30 years,

$P = 0.021$), except in the 9–12 year group ($P = 0.131$) (Table 2). Furthermore, the paediatric group (5–16) were significantly more overweight ($P = 0.002$) and obese ($P = 0.008$) compared with the reference population. There was no evidence for heterogeneity of odds ratios (OR) between all five age groups in either boys ($\chi^2(4) 5.9$, $P = 0.21$) or girls ($\chi^2(4)=1.12$, $P = 0.89$). For the two genders combined over the five age group strata, ORs were 1.90 (CI 1.46, 2.47) and 1.27 (CI 0.98, 1.65) for girls and boys respectively.

Associations of overweight and obesity with demographic factors, clinical outcomes and cardiovascular disease risk factors

Youth with type 1 diabetes

In the paediatric group, there was a positive linear relationship between BMI-SDS and SBP SD score ($\beta = 0.13$, $P \leq 0.001$), DBP SD score ($\beta = 0.13$, $P = 0.001$), triglyceride levels ($\beta = 0.24$, $P = 0.011$) and total cholesterol levels ($\beta = 0.19$, $P = 0.006$). Of individuals in the overweight and obese categories who had lipid measures recorded ($n = 65$), 42% had elevated total cholesterol and 22% had elevated triglycerides. Some 14% of the overweight and obese paediatric cohort had elevated BP. Regression analysis showed a significant interaction between insulin administration method and SEIFA (as a continuous variable) ($P = 0.02$). Follow-up testing using simple effects at varying SEIFA deciles showed a significantly lower difference in BMI in youth administering continuous subcutaneous insulin infusion (CSII) compared with those on multiple daily injections (MDI), in at SEIFA deciles 1 to 5 [difference (MDI-CSII) (SE)], at decile 1 [−0.73 (0.25), $P = 0.004$], and 3 [−0.47 (0.16), $P = 0.003$] and 5 [0.21 (0.11), $P = 0.05$] only.

Table 2 Prevalence of overweight and obesity among youth and young adults with type 1 diabetes, compared with sex and age-matched comparison populations

Weight category	Combined overweight and obesity									
	Age (years)	Total male	N (%)	P-value	Total females	N (%)	P-value	All	N	P-value
Overweight and obese	3–5	6	1 (17)	†	5	3 (60)	†	–	–	–
	5–8	22	9 (41)	0.008*	21	9 (43)	0.018*	–	–	–
	9–12	38	12 (32)	0.538	49	17 (35)	0.131	–	–	–
	13–16	69	25 (36)	0.147	51	21 (41)	0.026*	–	–	–
	17	21	8 (38)	†	26	10 (38)	†	–	–	–
	18–24	99	47 (47)	0.934	80	37 (46)	0.029*	–	–	–
	25–30	52	37 (71)	0.421	52	31 (60)	0.021*	–	–	–
	5–16	129	46 (36)	0.014*	121	47 (38)	<0.001*	250	93 (37)	<0.001*
Overweight or obesity	18–30	151	84 (56)	0.881	132	68 (52)	<0.001*	283	152 (54)	0.483
	5–16	129	33 (26)	0.060	121	32 (26)	0.014*	250	65 (26)	0.002*
	18–30	151	55 (36)	0.927	132	39 (30)	0.022*	283	94 (33)	0.147
	5–16	129	13 (10)	0.003*	121	15 (12)	0.016*	250	28 (11)	0.008*
	18–30	151	29 (19)	0.195	132	29 (22)	0.063	283	58 (20)	0.212

Data are frequency (percentage).
 *Significant difference between type 1 diabetes and reference sample ($P < 0.05$)
 †Comparison population data unavailable

There was no significant relationship with BMI and gender, age at diagnosis or HbA_{1c}.

Young adults with type 1 diabetes

In the young adult sample, a significantly higher BMI was found in boys in the older 25–30 years age group ($n = 52$) compared with boys in the 18–24 years group ($n = 99$) (27.6 ± 0.7 vs. 25.8 ± 0.5 kg/m², $P = 0.047$). There was a positive linear relationship between BMI and diabetes duration in girls ($\beta = 0.18$, $P = 0.017$). Young adults who were self-reported smokers ($n = 24$) had a significantly lower mean BMI compared with those who reported they did not smoke ($n = 259$) (24.4 ± 1.2 vs. 26.5 ± 0.3 kg/m², $P = 0.049$). There was a positive linear relationship between BMI and SBP ($\beta = 0.09$, $P \leq 0.001$) and DBP ($\beta = 0.13$, $P \leq 0.001$). However, there was no relationship observed between BMI and triglycerides or total cholesterol. Of young adults in the combined overweight and obese category who had lipid measures recorded ($n = 112$), 22% had high total cholesterol and 14% had elevated triglycerides. Some 28% and 29% of the overweight and obese young adult cohort had elevated SBP and DBP, respectively.

There was no significant relationship with BMI and insulin therapy type, gender, age at diagnosis, socio-economic status (SEIFA decile) or HbA_{1c}.

Discussion

This study found that over a third of children and adolescents with type 1 diabetes, and more than half of young adults were overweight and obese with higher rates of overweight and obesity than aged-matched reference samples. Of note, this was most apparent in girls beginning in the teenage years, and a high proportion of youth had additional modifiable cardiovascular risk factors placing them at increased risk of early complications. The degree of excessive weight increased with age group, was associated with MDI therapy in those with lower socio-economic status, and was especially seen in girls with a longer diabetes duration, as shown by another study [18]. In contrast to findings from the SEARCH for diabetes in youth study where young people with type 1 diabetes (< 20 years) had significantly higher prevalence of overweight but not obesity compared with the general US population [8], we found that overweight and obesity were both significantly higher in the type 1 diabetes population aged 5–16 years.

Our results build on and strengthen previous findings in the literature regarding gender-based differences in overweight and obesity. The current study showed that girls were more likely to be overweight and obese than reference populations. The data are limited, but a previous study in the USA [8] showed this was of concern in adolescent girls, and a Canadian study indicated that young women were more likely to be overweight and obese [19]. The reasons for the striking gender-based differential in the rates of child and

adolescent overweight and obesity associated with type 1 diabetes are not understood. Detailed understanding of the mechanisms of this phenomenon is urgently required to guide targeted preventative and therapeutic strategies.

The higher rates of overweight and obesity in teenage and young adult girls compared with population rates might be partially explained by the difficulties encountered in management of type 1 diabetes. The following factors unique to type 1 diabetes have been suggested, some of which are more likely in girls: lower rates of physical activity than peers associated with diabetes-specific barriers to exercise [20], eating disorders are more common in adolescent girls with type 1 diabetes compared with their peers [21] and disordered eating has previously been linked with having a higher BMI in girls with type 1 diabetes [22], and young people with type 1 diabetes consume diets higher in fat, notably saturated fat compared with their peers [23]. Findings from an Australian paediatric centre found that children with type 1 diabetes had higher total daily energy intakes compared with national intake data [24]; however, no difference in energy intake has also been reported [25]. Further research is needed to elaborate the causes of overweight and obesity in young women with type 1 diabetes, and a need for effective intervention to prevent the development of cardiovascular risk factors.

In this study, BMI-SDS was strongly associated with total cholesterol, triglycerides and BP, and a high proportion of overweight and obese youth with type 1 diabetes had other cardiovascular disease risk factors present including elevated total cholesterol (42%) triglycerides (22%) and BP (14%). This is of concern, as multiple cardiovascular disease risk factors put young people at risk of early morbidity and mortality. Similarly, other studies have found that increased BMI in young people with type 1 diabetes is adversely associated with hypertension [25,26] and dyslipidaemia [25]. A concerning 69% of the 27 000 young people with type 1 diabetes in the DPV cohort had one or more cardiovascular disease risk factor [27].

We observed a significantly higher BMI-SDS in youth on MDI therapy from the most disadvantaged socio-economic groups. The association with lower socio-economic indices is synonymous with the findings of a local study in which low socio-economic status was associated with increased prevalence of overweight and obesity in children in the Hunter region of NSW [28]. This effect was not present in those on CSII therapy or in the young adult cohort. One randomized control trial investigating the differences between MDI and CSII therapy in children and adolescents with type 1 diabetes also found a higher BMI-SDS in those on MDI therapy [29]; however, there is no general consensus and further studies are needed in our population to ascertain the difference in weight gain between MDI and CSII.

This study has some limitations. As data were collected retrospectively, dietary intake and physical activity data were unavailable, along with smoking status in teenagers. Further,

fractionated cholesterol readings were not available for all subjects, necessitating the use of total cholesterol measures, and official diagnoses of hypertension were unavailable. We caution against over-interpretation of cardiovascular risk from these summary measures. Additionally, a direct comparison population for the Hunter region of the state of NSW alone was not available. However, local data on secondary age students in the Hunter region show similar outcomes for overweight and obesity (23%) to NSW statistics (21%) [30], offering support that use of state-wide statistics was indeed reflective of this region. The eldest age group in this study (25–30 years) was compared with a reference sample with a larger age range (25–34 years). However, we suggest comparing our data to adults up to 3 years older would only result in a more conservative difference in proportion of combined overweight and obesity, as epidemiological prevalence of overweight and obesity trend upward in the general adult population [31].

Conclusions

In conclusion, this study found a marked prevalence of overweight and obesity in youth with type 1 diabetes, more pronounced in girls, that increases with age. This is accompanied by high rates of at least one other cardiovascular disease risk factor. Our findings that young girls with type 1 diabetes are more overweight and obese compared with the general population, and that a higher risk of overweight is associated with increased diabetes duration, highlight the need for early intervention and further research into the determinants of overweight and obesity in girls with type 1 diabetes.

Funding sources

A.L.M. received a Neville Eric Sansom PhD Scholarship. No other funding sources.

Competing interests

None declared.

Acknowledgements

We would like to thank the children, adolescents and young adults and their families attending the diabetes clinics at John Hunter Children's Hospital and John Hunter Hospital, and the clinical teams for the maintenance of the endocrinology database.

References

- 1 Australian Bureau of Statistics. National Health Survey: First Results, 2014–15. Available at <http://www.abs.gov.au/AUSSTATS/abs@nsf/Lookup/4364.0.55.001Main+Features100012017-18?OpenDocument> Last accessed 12 January 2016.
- 2 Singh AS, Mulder C, Twisk JW, van Mechelen W, Chinapaw MJ. Tracking of childhood overweight into adulthood: a systematic review of the literature. *Obes Rev* 2008; 9: 474–488.
- 3 Reilly JJ, Kelly J. Long-term impact of overweight and obesity in childhood and adolescence on morbidity and premature mortality in adulthood: systematic review. *Int J Obes* 2011; 35: 891–898.
- 4 Jarvisalo MJ, Raitakari M, Toikka JO, Putto-Laurila A, Rontu R, Laine S et al. Endothelial dysfunction and increased arterial intima-media thickness in children with type 1 diabetes. *Circulation* 2004; 109: 1750–1755.
- 5 Laing SP, Swerdlow AJ, Slater SD, Burden AC, Morris A, Waugh NR et al. Mortality from heart disease in a cohort of 23,000 patients with insulin-treated diabetes. *Diabetologia* 2003; 46: 760–765.
- 6 Rawshani A, Sattar N, Franzen S, Rawshani A, Hattersley AT, Svensson AM et al. Excess mortality and cardiovascular disease in young adults with type 1 diabetes in relation to age at onset: a nationwide, register-based cohort study. *Lancet* 2018; 392: 477–486.
- 7 Phelan H, Clapin H, Bruns L, Cameron FJ, Cotterill AM, Couper JJ et al. The Australasian Diabetes Data Network: first national audit of children and adolescents with type 1 diabetes. *Med J Aust* 2017; 206: 121–125.
- 8 Liu LL, Lawrence JM, Davis C, Liese AD, Pettitt DJ, Pihoker C et al. Prevalence of overweight and obesity in youth with diabetes in USA: the SEARCH for Diabetes in Youth study. *Pediatr Diabetes* 2010; 11: 4–11.
- 9 DuBose SN, Hermann JM, Tamborlane WV, Beck RW, Dost A, DiMeglio LA et al. Obesity in youth with type 1 diabetes in Germany, Austria, and the United States. *J Pediatr* 2015; 167: 627–632 e1–4.
- 10 Cole TJ, Lobstein T. Extended international (IOTF) body mass index cut-offs for thinness, overweight and obesity. *Pediatr Obes* 2012; 7: 284–294.
- 11 World Health Organisation. Body Mass Index - BMI 2018. Available at <http://www.euro.who.int/en/health-topics/disease-prevention/nutrition/a-healthy-lifestyle/body-mass-index-bmi> Last accessed 6 February 2019.
- 12 Flynn JT, Kaelber DC, Baker-Smith CM, Blowey D, Carroll AE, Daniels SR et al. Clinical practice guideline for screening and management of high blood pressure in children and adolescents. *Pediatrics* 2017; 140: e20171904.
- 13 Whelton PK, Carey RM, Aronow WS, Casey DE, Collins KJ, Dennison Himmelfarb C et al. Guideline for the prevention, detection, evaluation, and management of high blood pressure in adults. *J Am Coll Cardiol* 2018; 71: e127.
- 14 Hardy LLMS, Drayton BA, Bauman A. NSW Schools Physical Activity and Nutrition Survey (SPANS) 2015: Full Report. Sydney, NSW: NSW Department of Health, 2016.
- 15 Australian Bureau of Statistics. National Health Survey: First Results –Australia, 2014–15. Available at <http://www.abs.gov.au/AUSSTATS/abs@nsf/DetailsPage/4364.0.55.0012014-15?OpenDocument> Last accessed 8 February 2019.
- 16 Kavey RE, Daniels SR, Lauer RM, Atkins DL, Hayman LL, Taubert K. American Heart Association guidelines for primary prevention of atherosclerotic cardiovascular disease beginning in childhood. *Circulation* 2003; 107: 1562–1566.
- 17 National Heart Foundation of Australia and Cardiac Society of Australia and New Zealand. Reducing Risk in Heart Disease An Expert Guide to Clinical Practice of Secondary Prevention of Coronary Heart Disease 2012. Available at https://www.heartfoundation.org.au/images/uploads/publications/Chronic_Heart_Failure_Guidelines_2011.pdf Last accessed 6 February 2019.
- 18 Fröhlich-Reiterer EE, Rosenbauer J, Bechtold-Dalla Pozza S, Hofer SE, Schober E, Holl RW. Predictors of increasing BMI during the

- course of diabetes in children and adolescents with type 1 diabetes: data from the German/Austrian DPV multicentre survey. *Arch Dis Childhood* 2014; **99**: 738–743.
- 19 Szadkowska A, Madej A, Ziolkowska K, Szymanska M, Jeziorny K, Mianowska B *et al.* Gender and age - dependent effect of type 1 diabetes on obesity and altered body composition in young adults. *Ann Agric Environ Med* 2015; **22**: 124–128.
 - 20 Valerio G, Spagnuolo MI, Lombardi F, Spadaro R, Siano M, Franzese A. Physical activity and sports participation in children and adolescents with type 1 diabetes mellitus. *Nutr Metab Cardiovasc Dis* 2007; **17**: 376–382.
 - 21 Young V, Eiser C, Johnson B, Brierley S, Epton T, Elliott J *et al.* Eating problems in adolescents with Type 1 diabetes: a systematic review with meta-analysis. *Diabet Med* 2013; **30**: 189–198.
 - 22 Meltzer LJ, Johnson SB, Prine JM, Banks RA, Desrosiers PM, Silverstein JH. Disordered eating, body mass, and glycemic control in adolescents with type 1 diabetes. *Diabetes Care* 2001; **24**: 678–682.
 - 23 Overby NC, Flaaten V, Veierod MB, Bergstad I, Margeirsdottir HD, Dahl-Jorgensen K *et al.* Children and adolescents with type 1 diabetes eat a more atherosclerosis-prone diet than healthy control subjects. *Diabetologia* 2007; **50**: 307–316.
 - 24 Gilbertson HR, Reed K, Clark S, Francis KL, Cameron FJ. An audit of the dietary intake of Australian children with type 1 diabetes. *Nutr Diabetes* 2018; **8**: 10.
 - 25 Redondo MJ, Foster NC, Libman IM, Mehta SN, Hathway JM, Bethin KE *et al.* Prevalence of cardiovascular risk factors in youth with type 1 diabetes and elevated body mass index. *Acta Diabetol* 2016; **53**: 271–277.
 - 26 van Vliet M, Van der Heyden JC, Diamant M, Von Rosenstiel IA, Schindhelm RK, Aanstoot HJ *et al.* Overweight is highly prevalent in children with type 1 diabetes and associates with cardiometabolic risk. *J Pediatr* 2010; **156**: 923–929.
 - 27 Schwab KO, Doerfer J, Hecker W, Grulich-Henn J, Wiemann D, Kordonouri O *et al.*; DPV Initiative of the German Working Group for Pediatric Diabetology. Spectrum and prevalence of atherogenic risk factors in 27,358 children, adolescents, and young adults with type 1 diabetes. Cross-sectional data from the German diabetes documentation and quality management system (DPV). *Diabetes Care* 2006; **29**: 218–225.
 - 28 Sutherland R, Finch M, Harrison M, Collins C. Higher prevalence of childhood overweight and obesity in association with gender and socioeconomic status in the Hunter region of New South Wales. *Nutr Diet* 2008; **65**: 192–197.
 - 29 Weintrob N, Benzaquen H, Galatzer A, Shalitin S, Lazar L, Fayman G *et al.* Comparison of continuous subcutaneous insulin infusion and multiple daily injection regimens in children with type 1 diabetes: a randomized open crossover trial. *Pediatrics* 2003; **112**: 559–564.
 - 30 Centre for Epidemiology and Evidence. HealthStats NSW. *Overweight and Obesity in Secondary School Students – 2014*. Sydney: NSW Ministry of Health. Available at http://www.healthstats.nsw.gov.au/Indicator/beh_bmi_secstud/beh_bmi_secstud_lhn_snap Last accessed 2 March 2019.
 - 31 Australian Bureau of Statistics. National Health Survey: First Results - Australia, 2014–15. Available at [http://www.ausstats.abs.gov.au/Ausstats/subscriber.nsf/0/CDA852A349B4CEE6CA257F150009FC53/\\$File/national%20health%20survey%20first%20results,%202014-15.pdf](http://www.ausstats.abs.gov.au/Ausstats/subscriber.nsf/0/CDA852A349B4CEE6CA257F150009FC53/$File/national%20health%20survey%20first%20results,%202014-15.pdf) Last accessed 1 March 2019.

10.2 Permissions to include published papers in thesis

Rowe CW, Boelaert K, Smith R. **Thyroid cancer during pregnancy and lactation**. In: Kovacs and Deal [Ed] Maternal-fetal and neonatal endocrinology. Elsevier 2019.

- Elsevier, as publisher of Maternal-Fetal and Neonatal Endocrinology, grants permission for published articles to be included in theses/dissertations for non-commercial purposes. Authors can include their articles in full or in part in a thesis or dissertation for non-commercial purposes. [Accessed 31/01/2019] <https://www.elsevier.com/about/policies/copyright/permissions>

Rowe CW, Faulkner S, Paul JW, Tolosa JM, Gedye C, Bendinelli C, Wynne K, McGrath S, Attia J, Smith R, Hondermarck H. **The precursor for nerve growth factor (proNGF) is not a serum or biopsy-rinse biomarker for thyroid cancer diagnosis** BMC Endocrine Disorders. <https://doi.org/10.1186/s12902-019-0457-1>

- BMC Endocrine Disorders publishes articles under the Creative Commons Attribution License 4.0, which grants the right to unrestricted dissemination and re-use of the work, with only the one proviso that proper attribution is given to authors. <https://www.biomedcentral.com/about/policies/license-agreement> [Accessed 16/08/2019].

Rowe CW, Dill T, Griffin N, Jobling P, Faulkner S, King S, Smith R, Hondermarck H. **Innervation of papillary thyroid cancer and its association with extra-thyroidal invasion**. Scientific Reports. <https://doi.org/10.1038/s41598-020-58425-5>

- *Scientific Reports* does not require authors to assign copyright of their published original research papers to the journal. Articles are published under a [CC BY license](#) (Creative Commons Attribution 4.0 International License). The CC BY license allows for maximum dissemination and re-use of open access materials and is preferred by many research funding bodies. Under this license users are free to share (copy, distribute and transmit) and remix (adapt) the contribution including for commercial purposes, providing they attribute the contribution in the manner specified by the author or licensor.

Rowe CW, Dill T, Faulkner S, Gedye C, Paul JW, Tolosa JM, Jones M, King S, Smith R, Hondermarck H. **The precursor for nerve growth factor (proNGF) in thyroid cancer lymph node metastases: correlation with primary tumour and pathological variables.** Int J Mol Sci. <https://doi.org/10.3390/ijms20235924>

- MDPI, publisher of International Journal of Molecular Sciences, applies the CC BY license to published papers, which permits authors to copy and redistribute the material in any medium or format.
<https://creativecommons.org/licenses/by/4.0/>

Faulkner S, Jobling P, Rowe CW, Rodriguez-Oliveira S, Roselli S, Thorne R, Oldmeadow C, Attia Jiang J, Zhang X, Walker M, Hondermarck H. (2017) **Neurotrophin Receptors TrkA, p75NTR and Sortilin are Increased and Targetable in Thyroid Cancer.** American Journal of Pathology <https://doi.org/10.1016/j.ajpath.2017.09.008>

- Elsevier, as publisher of American Journal of Pathology, grants permission for published articles to be included in theses/dissertations for non-commercial purposes. Authors can include their articles in full or in part in a thesis or dissertation for non-commercial purposes. [Accessed 31/01/2019]
<https://www.elsevier.com/about/policies/copyright/permissions>

Rowe CW, Paul J, Gedye C, Tolosa J, Bendinelli C, McGrath S & Smith, R. (2017) **Targeting the TSH receptor in thyroid cancer.** Endocrine-Related Cancer. <https://doi.org/10.1530/ERC-17-0010>

- Bioscientifica Ltd. grants permission for the article to be reproduced as part of this dissertation/thesis. The License agreement is included below.

2/8/2019 RightsLink® by Copyright Clearance Center




[Account Info](#)
[Help](#)

Title: Endocrine-related cancer

Article ID: 1479-6821

Publication: Publication 1

Publisher: CCC Reproduction

Date: Jan 1, 1998

Copyright © 1998, CCC Reproduction

Logged in as:
Christopher Rowe
UNIVERSITY OF NEWCASTLE
Account #1:
3001084853

[LOGOUT](#)

Order Completed

Thank you for your order.

This Agreement between Christopher Rowe ("You") and Bioscientifica Limited ("Bioscientifica Limited") consists of your order details and the terms and conditions provided by Bioscientifica Limited and Copyright Clearance Center.

License number	Reference confirmation email for license number
License date	Feb, 07 2019
Licensed content publisher	Bioscientifica Limited
Licensed content title	Endocrine-related cancer
Licensed content date	Jan 1, 1998
Type of use	Thesis/Dissertation
Requestor type	Academic institution
Format	Electronic
Portion	chapter/article
The requesting person/organization	Christopher Rowe
Title or numeric reference of the portion(s)	Targeting the TSH receptor in thyroid cancer
Title of the article or chapter the portion is from	Endocrine-Related Cancer
Editor of portion(s)	N/A
Author of portion(s)	C.W Rowe et al
Volume of serial or monograph	24
Page range of portion	
Publication date of portion	2017
Rights for	Main product
Duration of use	Life of current and all future editions
Creation of copies for the disabled	no
With minor editing privileges	no
For distribution to	Worldwide
In the following language(s)	Original language of publication
With incidental promotional use	no
Lifetime unit quantity of new product	Up to 499
Title	PhD Thesis (Dissertation)
Institution name	University of Newcastle, Australia
Expected presentation date	May 2019
Requestor Location	UNIVERSITY OF NEWCASTLE F04M, MEDICINE-SMPH-MBRC UNIVERSITY DRIVE CALLAGHAN Newcastle, NSW NA

<https://e100.copyright.com/AppDispatchServlet> 1/2

Rowe CW, Murray K, Woods A, Gupta S, Smith R, Wynne K. (2016) **Metastatic Thyroid Cancer in Pregnancy: Risk and Uncertainty**. Endocrinol Diab Metab Case Rep. <https://doi.org/10.1530/EDM-16-0071>

- The article is reproduced in this thesis under the terms of the CC-BY CC BY-NC-ND license, allowing free sharing, copying and redistribution of the material in any medium or format

Rowe CW, Bendinelli C, McGrath S. (2016) **Charting a Course through the CEAs: Diagnosis and Management of Medullary Thyroid Cancer**. Clinical Endocrinology (Oxf). <http://dx.doi.org/10.1016/j.diabres.2017.06.022>

**JOHN WILEY AND SONS LICENSE
TERMS AND CONDITIONS**

Jun 27, 2019

This Agreement between UNIVERSITY OF NEWCASTLE -- Christopher Rowe ("You") and John Wiley and Sons ("John Wiley and Sons") consists of your license details and the terms and conditions provided by John Wiley and Sons and Copyright Clearance Center.

License Number	4616861327796
License date	Jun 27, 2019
Licensed Content Publisher	John Wiley and Sons
Licensed Content Publication	Clinical Endocrinology
Licensed Content Title	Charting a course through the CEAs: diagnosis and management of medullary thyroid cancer
Licensed Content Author	Christopher W. Rowe, Cino Bendinelli, Shaun McGrath
Licensed Content Date	Jun 29, 2016
Licensed Content Volume	85
Licensed Content Issue	3
Licensed Content Pages	4
Type of use	Dissertation/Thesis
Requestor type	Author of this Wiley article
Format	Electronic
Portion	Full article
Will you be translating?	No
Title of your thesis / dissertation	PhD Thesis (Dissertation)
Expected completion date	Oct 2019
Expected size (number of pages)	1
Requestor Location	UNIVERSITY OF NEWCASTLE FoHM, MEDICINE-SMPH-MBRC UNIVERSITY DRIVE CALLAGHAN Newcastle, NSW NA Australia Attn: Christopher Rowe
Publisher Tax ID	EU826007151
Total	0.00 AUD

Rowe CW, Haider AS, Viswanathan D, Jones M, Attia J, Wynne K, Acharya S. (2017). **Insulin resistance correlates with maculopathy and severity of retinopathy in young adults with Type 1 Diabetes Mellitus.** Diabetes Research and Clinical Practice. <https://doi.org/10.1016/j.diabres.2017.06.022>

- Elsevier, as publisher of Diabetes Research and Clinical Practice, grants permission for published articles to be included in theses/dissertations for non-commercial purposes. Authors can include their articles in full or in part in a thesis or dissertation for non-commercial purposes. [Accessed 31/01/2019] <https://www.elsevier.com/about/policies/copyright/permissions>



Title: Insulin resistance correlates with maculopathy and severity of retinopathy in young adults with Type 1 Diabetes Mellitus

Author: C.W. Rowe, A.S. Haider, D. Viswanathan, M. Jones, J. Attia, K. Wynne, S. Acharya

Publication: Diabetes Research and Clinical Practice

Publisher: Elsevier

Date: September 2017

© 2017 Elsevier B.V. All rights reserved.

Logged in as:
Christopher Rowe
UNIVERSITY OF NEWCASTLE
Account #:
3001084853
[LOGOUT](#)

Please note that, as the author of this Elsevier article, you retain the right to include it in a thesis or dissertation, provided it is not published commercially. Permission is not required, but please ensure that you reference the journal as the original source. For more information on this and on your other retained rights, please visit: <https://www.elsevier.com/about/our-business/policies/copyright#Author-rights>

Gao F, Griffin N, Faulkner S, Rowe CW, Williams L, Roselli S, Thorne R, Ferdoushi A, Jobling P, Walker M and Hondermarck H (2018) **The neurotrophic tyrosine kinase receptor TrkA and its ligand NGF are increased in squamous cell carcinomas of the lung.** Scientific Reports. <https://doi.org/10.1038/s41598-018-26408-2>

- *Scientific Reports* does not require authors to assign copyright of their published original research papers to the journal. Articles are published under a [CC BY license](#) (Creative Commons Attribution 4.0 International License). The CC BY license allows for maximum dissemination and re-use of open access materials and is preferred by many research funding bodies. Under this license users are free to share (copy, distribute and transmit) and remix (adapt) the contribution including for commercial purposes, providing they attribute the contribution in the manner specified by the author or licensor

Rowe CW, Arthurs S, O'Neill CJ, Hawthorne J, Carroll R, Wynne K, Bendinelli C. (2018) **High-dose cholecalciferol to prevent post-thyroidectomy hypocalcaemia: a randomized double-blind placebo-controlled trial.** Clinical Endocrinology <https://doi.org/10.1111/cen.13897>

- John Wiley and Sons grants permission for the article to be reproduced as part of this dissertation/thesis. The License agreement is included below.

**JOHN WILEY AND SONS LICENSE
TERMS AND CONDITIONS**

Jun 27, 2019

This Agreement between UNIVERSITY OF NEWCASTLE -- Christopher Rowe ("You") and John Wiley and Sons ("John Wiley and Sons") consists of your license details and the terms and conditions provided by John Wiley and Sons and Copyright Clearance Center.

License Number	4616861456260
License date	Jun 27, 2019
Licensed Content Publisher	John Wiley and Sons
Licensed Content Publication	Clinical Endocrinology
Licensed Content Title	High-dose preoperative cholecalciferol to prevent post-thyroidectomy hypocalcaemia: A randomized, double-blinded placebo-controlled trial
Licensed Content Author	Christopher W. Rowe, Sam Arthurs, Christine J. O'Neill, et al
Licensed Content Date	Dec 10, 2018
Licensed Content Volume	90
Licensed Content Issue	2
Licensed Content Pages	8
Type of use	Dissertation/Thesis
Requestor type	Author of this Wiley article
Format	Electronic
Portion	Full article
Will you be translating?	No
Title of your thesis / dissertation	PhD Thesis (Dissertation)
Expected completion date	Oct 2019
Expected size (number of pages)	1
Requestor Location	UNIVERSITY OF NEWCASTLE FoHM, MEDICINE-SMPH-MBRC UNIVERSITY DRIVE CALLAGHAN Newcastle, NSW NA Australia Attn: Christopher Rowe
Publisher Tax ID	EU826007151
Total	0.00 AUD

Rowe CW, Putt E, Brentnall O, Allabyrne J, Gebuehr A, Woods A, Wynne K (2018) **An intravenous insulin protocol designed for pregnancy reduces neonatal hypoglycaemia following betamethasone administration in women with gestational diabetes.** Diabetic Medicine <https://doi.org/10.1111/dme.13864>

- John Wiley and Sons grants permission for the article to be reproduced as part of this dissertation/thesis. The License agreement is included below.

**JOHN WILEY AND SONS LICENSE
TERMS AND CONDITIONS**

Jun 27, 2019



This Agreement between UNIVERSITY OF NEWCASTLE -- Christopher Rowe ("You") and John Wiley and Sons ("John Wiley and Sons") consists of your license details and the terms and conditions provided by John Wiley and Sons and Copyright Clearance Center.



License Number	4616870078149
License date	Jun 27, 2019
Licensed Content Publisher	John Wiley and Sons
Licensed Content Publication	Diabetic Medicine
Licensed Content Title	An intravenous insulin protocol designed for pregnancy reduces neonatal hypoglycaemia following betamethasone administration in women with gestational diabetes
Licensed Content Author	C. W. Rowe, E. Putt, O. Brentnall, et al
Licensed Content Date	Dec 10, 2018
Licensed Content Volume	36
Licensed Content Issue	2
Licensed Content Pages	9
Type of use	Dissertation/Thesis
Requestor type	Author of this Wiley article
Format	Electronic
Portion	Full article
Will you be translating?	No
Title of your thesis / dissertation	PhD Thesis (Dissertation)
Expected completion date	Oct 2019
Expected size (number of pages)	1
Requestor Location	UNIVERSITY OF NEWCASTLE FoHM, MEDICINE-SMPH-MBRC UNIVERSITY DRIVE CALLAGHAN Newcastle, NSW NA Australia Attn: Christopher Rowe
Publisher Tax ID	EU826007151
Total	0.00 AUD



Marlow A, Rowe CW, Anderson D, Wynne K, King B, Howley P, Smart C (2019). **Young children, adolescent girls and women with type 1 diabetes are more overweight and obese than reference populations, and this is associated with increased cardiovascular risk factors.** Diabetic Medicine <https://doi.org/10.1111/dme.14133>

- John Wiley and Sons grants permission for the article to be reproduced as part of this dissertation/thesis. The License agreement is included below.

License Number	4703881167195
License date	Nov 07, 2019

 Licensed Content		 Order Details	
Licensed Content Publisher	John Wiley and Sons	Type of use	Dissertation/Thesis
Licensed Content Publication	Diabetic Medicine	Requestor type	Author of this Wiley article
Licensed Content Title	Young children, adolescent girls and women with type 1 diabetes are more overweight and obese than reference populations, and this is associated with increased cardiovascular risk factors	Format	Print and electronic
Licensed Content Author	A. L. Marlow, C. W. Rowe, D. Anderson, et al	Portion	Full article
Licensed Content Date	Sep 20, 2019	Will you be translating?	No
Licensed Content Volume	36		
Licensed Content Issue	11		
Licensed Content Pages	7		

 About Your Work		 Additional Data	
Title of your thesis / dissertation	PhD Thesis (Dissertation)		
Expected completion date	Oct 2019		
Expected size (number of pages)	1		



 Requestor Location		 Tax Details	
Requestor Location	UNIVERSITY OF NEWCASTLE FoHM, MEDICINE-SMPH-MBRC UNIVERSITY DRIVE CALLAGHAN Newcastle, NSW NA Australia Attn: Christopher Rowe	Publisher Tax ID	EU826007151

10.3 Permissions to reproduce figures in thesis


Every effort has been made to appropriately acknowledge sources and obtain appropriate permissions prior to use of figures. In cases where figures reproduced within this thesis were granted general permission for reuse without the need for a specific license (based on a statement on the publisher's website), this has been acknowledged in the figure caption. Any figure that required a specific licence to reproduce is acknowledged in the sections below.

Acknowledgement is also made to Kayla Friedman and Malcolm Morgan of the Centre for Sustainable Development, University of Cambridge, UK whose thesis template was used as a guide for the formatting of this thesis.

- Figure 1

[Home](#)
[Account Info](#)
[Help](#)



Chapter: Chapter 28 Thyroid Hormones

Book: Netter's Essential Physiology

Author: Susan E. Mulrone,Adam K. Myers

Publisher: Elsevier

Date: 2016

Copyright © 2016 Elsevier Inc. All rights reserved.

Logged in as:
Christopher Rowe
UNIVERSITY OF NEWCASTLE
Account #:
3001084853

[LOGOUT](#)

Order Completed

Thank you for your order.

This Agreement between UNIVERSITY OF NEWCASTLE -- Christopher Rowe ("You") and Elsevier ("Elsevier") consists of your license details and the terms and conditions provided by Elsevier and Copyright Clearance Center.

Your confirmation email will contain your order number for future reference.

[printable details](#)

License Number	4657960130165
License date	Aug 28, 2019
Licensed Content Publisher	Elsevier
Licensed Content Publication	Elsevier Books
Licensed Content Title	Netter's Essential Physiology
Licensed Content Author	Susan E. Mulrone,Adam K. Myers
Licensed Content Date	Jan 1, 2016
Licensed Content Pages	7
Type of Use	reuse in a thesis/dissertation
Portion	figures/tables/illustrations
Number of figures/tables/illustrations	2
Format	both print and electronic
Are you the author of this Elsevier chapter?	No
Will you be translating?	No
Original figure numbers	Figure 28.1 and 28.2
Title of your thesis/dissertation	PhD Thesis (Dissertation)
Publisher of new work	University of Newcastle, Australia
Expected completion date	Oct 2019
Estimated size (number of pages)	1
Requestor Location	UNIVERSITY OF NEWCASTLE FoHM, MEDICINE-SMPH-MBRC UNIVERSITY DRIVE CALLAGHAN Newcastle, NSW NA Australia Attn: Christopher Rowe
Publisher Tax ID	GB 494 6272 12
Total	0.00 AUD

- Figure 4

ELSEVIER LICENSE TERMS AND CONDITIONS	
Apr 10, 2019	
This Agreement between UNIVERSITY OF NEWCASTLE – Christopher Rowe ("You") and Elsevier ("Elsevier") consists of your license details and the terms and conditions provided by Elsevier and Copyright Clearance Center.	
License Number	4565640968849
License date	Apr 10, 2019
Licensed Content Publisher	Elsevier
Licensed Content Publication	Elsevier Books
Licensed Content Title	Netters Clinical Anatomy
Licensed Content Author	John T. Hansen
Licensed Content Date	Jan 1, 2019
Licensed Content Pages	119
Start Page	437
End Page	555
Type of Use	reuse in a thesis/dissertation
Portion	figures/tables/illustrations
Number of figures/tables/illustrations	1
Format	electronic
Are you the author of this Elsevier chapter?	No
Will you be translating?	No
Original figure numbers	Figure 8.68
Title of your thesis/dissertation	PhD Thesis (Dissertation)
Publisher of new work	University of Newcastle, Australia
Expected completion date	May 2019
Estimated size (number of pages)	1
Requestor Location	UNIVERSITY OF NEWCASTLE F0HM, MEDICINE-SMPH-MBRC UNIVERSITY DRIVE CALLAGHAN Newcastle, NSW NA Australia Attn: Christopher Rowe
Publisher Tax ID	GB 494 6272 12
Total	0.00 AUD